NAT'L INST OF STAND & TECH
A11106 033815
Reference
NBS Publi-cations

NBSIR 84-3007

# THERMAL CONDUCTIVITY OF ALUMINUM, COPPER, IRON, AND TUNGSTEN FOR TEMPERATURES FROM 1 K TO THE MELTING POINT

National Bureau of Standards
U.S. Department of Commerce
Boulder, Colorado 80303

June 1984

QC
100
.U56
84-3007
1984

NATIONAL BUREAU
OF STANDARDS
LIBRARY

NBSIR 84-3007

# THERMAL CONDUCTIVITY OF ALUMINUM, COPPER, IRON, AND TUNGSTEN FOR TEMPERATURES FROM 1 K TO THE MELTING POINT

J. G. Hust
A. B. Lankford

Chemical Engineering Science Division
National Engineering Laboratory
National Bureau of Standards
U.S. Department of Commerce
Boulder, Colorado 80303

June 1984

U.S. DEPARTMENT OF COMMERCE, Malcolm Baldrige, Secretary

NATIONAL BUREAU OF STANDARDS, Ernest Ambler, Director

CONTENTS


| | Page |
|---|---|
| Abstract | 1 |
| 1. Introduction | 1 |
| 1.1 Thermal Conductivity | 4 |
| 1.2 Electrical Resistivity | 7 |
| 1.3 Wiedemann-Franz-Lorenz (WFL) Law | 8 |
| 1.4 Literature Review | 10 |
| 1.5 Analysis | 11 |
| 1.6 Thermal Expansion Corrections | 13 |
| 1.7 Acknowledgments | 13 |
| 1.8 References | 14 |
| 2. Copper | 15 |
| 2.1 General | 15 |
| 2.2 Deviations From Recommended Equation | 16 |
| 2.2.1 Physical Defect Effects | 17 |
| 2.2.2 Size Effects | 20 |
| 2.2.3 Magnetic Field Effects | 21 |
| 2.3 Electrical Resistivity and Lorenz Ratio | 21 |
| 2.4 Summary for Copper | 23 |
| 2.5 Format for Annotated Bibliography for Copper | 62 |
| 3. Aluminum | 87 |
| 3.1 General | 87 |
| 3.2 Deviations From Recommended Equation | 88 |
| 3.2.1 Physical Defect Effects | 89 |
| 3.2.2 Size Effects | 90 |
| 3.2.3 Magnetic Field Effects | 90 |

Page

3.3 Electrical Resistivity and Lorenz Ratio . . . . . 91

3.4 Summary for Aluminum . . . . . 93

3.5 Format for Annotated Bibliography for Aluminum . . . . . 122

4. Iron . . . . . 141

4.1 General . . . . . 141

4.2 Deviations From Recommended Equation . . . . . 142

4.2.1 Physical Defect Effects . . . . . 143

4.2.2 Size Effects . . . . . 144

4.2.3 Magnetic Field Effects . . . . . 144

4.3 Electrical Resistivity and Lorenz Ratio . . . . . 145

4.4 Summary for Iron . . . . . 146

4.5 Format for Annotated Bibliography for Iron . . . . . 176

5. Tungsten . . . . . 199

5.1 General . . . . . 199

5.2 Deviations From Recommended Equation . . . . . 200

5.2.1 Physical Defect Effects . . . . . 201

5.2.2 Size Effects . . . . . 202

5.2.3 Magnetic Field Effects . . . . . 203

5.3 Electrical Resistivity and Lorenz Ratio . . . . . 204

5.4 Summary for Tungsten . . . . . 205

5.5 Format for Annotated Bibliography for Tungsten . . . . . 235

# THERMAL CONDUCTIVITY OF ALUMINUM, COPPER, IRON, AND TUNGSTEN FOR TEMPERATURES FROM 1 K TO THE MELTING POINT

J. G. Hust and A. R. Lankford

Chemical Engineering Science Division
National Bureau of Standards
Boulder, Colorado 80303

Literature data on the thermal conductivity of commercially pure aluminum, copper, iron, and tungsten specimens have been collected, coded, critically analyzed, and correlated with analytical techniques based on theoretical and empirical equations. The resulting functions are presented and used to generate tables and graphs of thermal conductivity as a function of temperature and residual resistivity ratio (RRR). An annotated bibliography of references is included. Discussions are included on the variations in thermal conductivity caused by chemical impurities, physical defects, size effects, and magnetic fields. Smoothed values are presented for temperatures from 1 K to near the melting point and for a large range of RRR values.

Key words: aluminum; copper; electrical resistivity; iron; Lorenz ratio; residual resistivity ratio; thermal conductivity; tungsten

## 1. Introduction

The growth of modern technology has increased the need for and use of thermophysical properties reference data on materials, often by engineers not totally familiar with the physical phenomena that influence the properties or the conditions under which the data are valid. Such a lack of understanding can lead to serious design errors, especially for low-temperature transport properties, such as thermal conductivity, that are strongly dependent on detailed material characteristics as well as environmental conditions. The data explosion appearing in the literature may be a drawback rather than an asset to the non-specialist, who needs ready access to critically evaluated, correlated, and smoothed data with a clear indication of their range of application. Center for Information and Numerical Data Analysis and Synthesis (CINDAS) (at Purdue University), the editors of Landolt-Bornstein, the Office of Standard Reference Data of the National Bureau of Standards, and others have made efforts to perform this service. These

efforts generally encompass such a wide range of materials and properties that the results are lacking in detail desirable for reference data. For example, example, when recommended values are presented, it is not always clear how well they agree with the original data. In cases where recommended values are not given, the user must exercise considerable effort to obtain such values. This paper presents both the literature thermal conductivity data as well as recommended values for a few metals (aluminum, copper, iron, and tungsten) along with a clear indication of the agreement of the recommended values and the experimental data.

The objective of this work is to present reference data for selected metals including the most pure research materials and the more commonly produced commercially pure materials. Generally speaking this includes impurities up to about the 1% level. The reference data are based on a critical analysis and correlation of the best experimental data. Only two variables (temperature and residual electrical resistivity) are used to correlate the selected experimental data. There are numerous factors that complicate the establishment of the uncertainty of this correlation. First, there is the direct thermal conductivity measurement uncertainty. It has been found that 5-10% uncertainties are common and occasionally data are found in error by as much as 50%. Second, literature data are frequently found for inadequately characterized specimens, i.e., the investigator did not report such factors as residual resistivity, purity, anneal condition, and specimen size. In addition, these factors are frequently not determined for the exact specimen measured. Third, there are uncertainties introduced by extracting literature data by reading small graphs and sometimes from extrapolated equations. Finally, the uncertainty of the reference data is dependent on the validity of the correlation equation used. Therefore, the reference data presented here, for a wide range of purities, are probably not as accurate as those that can be obtained from the accurate measurement of a single specimen; but they

do represent the best available data for the entire family of specimens considered.

The reference data are most accurate for all specimens measured at high temperatures where impurity effects are small and for the most pure specimens measured at low temperatures where the impurity effects are dramatic. A secondary objective was to include as wide a range of impurities as possible with a single equation. Because of this the uncertainty tends to increase at the higher impurity levels. However, specimen size effects and increased experimental uncertainties tend to increase at low temperatures and low impurity levels, therefore the total uncertainty at low temperatures is considerably larger than at high temperatures. Each major section of this report discusses details of the deviations.

This work was performed under the auspices of the Committee on DATA for Science and Technology of the International Council of Scientific Unions (CODATA) which seeks to ".... improve the quality, reliability, and accessibility of data of importance to science and technology ....". Therefore, its Task Group on Thermophysical Properties has embarked on preparation of critically evaluated and recommended values of a limited set of properties on materials often used for calibration or reference. The properties are thermal conductivity, electrical resistivity, heat capacity, thermal diffusivity, absolute thermopower, and thermal expansion. Materials include aluminum, alumina, copper, iron, silicon, and tungsten.

The above properties are similar in that at temperatures, T, well below the Debye characteristic temperature, $\Theta_D$, they vary rapidly with T in a complex manner according to the degree of excitation of the thermal vibrations (phonons) and the electrons in some cases. The properties are dissimilar as far as their dependence on purity is concerned. The transport properties (thermal conductivity, thermal diffusivity, and electrical resistivity) are dominated by host

lattice imperfections as temperature approaches absolute zero, whereas specific heat and thermal expansion depend primarily on the host lattice characteristics and are practically insensitive to lattice imperfections.

Thermal conductivity and electrical resistivity of pure metals are closely associated with the same conduction source and limiting (scattering) mechanisms. This correlation is expressed by the Wiedemann-Franz-Lorenz Ratio. Because of this correlation between thermal and electrical resistivity and because the impurity effect is primarily additive in resistivity, the residual resistivity (or the residual resistivity ratio) is a useful parameter to characterize these properties for a given specimen. A brief discussion of these properties is given below.

## 1.1. Thermal Conductivity

The thermal conductivity, $\lambda$, of a metal or alloy usually is considered to be the sum of the electronic, $\lambda_e$, and lattice, $\lambda_g$, components:

$$\lambda = \lambda_e + \lambda_g \qquad (1.1.1)$$

There are other mechanisms of heat transport; however, they generally are not applicable for metals. The electronic term designates the thermal energy carried by the electrons, while the lattice term designates the energy carried by the quantized lattice vibrations (phonons). In pure metals the lattice term is small (frequently less than 5 and almost always less than 20 percent). Although theory provides a guide for the dependencies of the lattice conductivity and its order of magnitude, it is generally not sufficient for reference data purposes. Theory does provide an adequate formulation for the low-temperature electronic term. For these reasons, the formulation provided here is based on the theoretical form of the electronic term. Modifications of this form to account for the lattice contribution and higher temperature dependencies are based on the experimental data.

Theory shows that at low temperatures the electronic thermal conductivity component is limited mainly by two mechanisms, a) the interaction of the electrons with phonons, and b) the interaction of the electrons with physical and chemical imperfections. The interaction of electrons with phonons leads to a resistive term approximately proportional to $T^2$. The proportionality constant, $\alpha$, is characteristic of the generic type of metal, i.e., it is an intrinsic property of the base metal. The interaction of electrons with lattice defects leads to a thermal resistivity which is inversely proportional to temperature. The proportionality constant, $\beta$, is determined by the type and concentration of the lattice imperfections. This approximation of low-temperature electronic thermal conductivity is written as

$$\lambda = (W_o + W_i)^{-1} = (\beta/T + \alpha T^n)^{-1} \text{ where } n = 2 \qquad (1.1.2)$$

and where $W_o$ represents the electron-defect interaction and $W_i$ is the electron-phonon interaction. Cezairliyan and Touloukian [1]* presented a revised form of this theoretical equation to account for observed deviations. This revised form, reviewed in reference [2], is based on experimental data that show a) n is usually larger than 2, and b) $\alpha$ is weakly dependent on lattice imperfections. The modified equation is valid only for temperatures up to about 1.5 times the temperature at which the maximum in thermal conductivity occurs. For the metals of interest here, this limit occurs at about 40 K. At higher temperatures, thermal conductivity decreases more slowly with increasing temperature than predicted by this equation. Theory predicts that at high temperatures, thermal conductivity of metals should approach a constant. To account for this high temperature behavior, the form presented by Cezairliyan and Touloukian [1] has been further modified. Finally, evidence has been presented that indicates

*The references shown in [ ] are listed in Section 1.8.

the presence of an interaction term between $W_o$ and $W_i$. It is denoted by $W_{io}$. The base equation selected to represent the predominant thermal conductivity behavior of these metals is therefore,

$$\lambda_b = (W_o + W_i + W_{io})^{-1} \tag{1.1.3}$$

where

$$W_o = \beta/T \tag{1.1.4}$$

$$W_i = P_1 T^{P_2}/(1 + P_1 P_3 T^{(P_2+P_4)} \exp(-(P_5/T)^{P_6})) + W_c \tag{1.1.5}$$

$$W_{io} = P_7 W_i W_o/(W_i + W_o) \tag{1.1.6}$$

where the $P_i$'s are parameters determined by least squares fit of the experimental data. The quantity $W_c$ is a temperature dependent term (defined later for each metal) that accounts for mathematical residual deviations in $W_i$. This equation is intended to describe the thermal conductivity of annealed bulk specimens of these metals. Thus it describes the intrinsic thermal conductivity and the limiting effect of the presence of chemical impurities in each metal. The reader should be aware, however, of the existence of other limiting mechanisms, such as physical defects, size effects, and magnetic field effects. Brief discussions of these effects are presented for each metal.

Both thermal conductivity and electrical resistivity of a pure metal are strongly dependent on the concentration of lattice imperfections. Indeed, they are both influenced to the same degree by the imperfections at very low temperatures. The resulting correlation is referred to as the Wiedemann-Franz-Lorenz Law, discussed in Section 1.3. Since electrical resistivity is much easier to measure accurately than thermal conductivity, it is often used to determine imperfection concentrations, and therefore thermal conductivity. The following discussions on electrical resistivity and the Wiedemann-Franz-Lorenz Law are included for that reason.

1.2. Electrical Resistivity

For discussion purposes the electrical resistivity is described adequately by Matthiessen's rule (MR). This rule, (1.2.1) states that the electrical resistivity, $\rho$, of a metal is the sum of two parts: the intrinsic resistivity, $\rho_i$, which is characterized by electrons interacting with phonons only, and the residual resistivity, $\rho_o$, which is characterized by electrons interacting with the chemical and physical imperfections of the metal.

$$\rho(T) = \rho_o + \rho_i(T) \tag{1.2.1}$$

The residual resistivity is temperature independent, while the intrinsic resistivity increases rapidly with temperature. The specific temperature dependence varies widely both with temperature and base material. Nevertheless, $\rho_i$ is not dependent significantly upon composition changes for a given base metal. Thus, if one knows $\rho_i(T)$ for a given base metal, $\rho(T)$ for any composition of that metal can be approximated from (1.2.1) after measuring only $\rho_o$. The value of $\rho_o$ is obtained by measuring $\rho$ at low temperatures, where $\rho_i$ is negligible (liquid helium temperatures generally are adequate). For several reasons, the ratio of the resistivity at the ice point to the residual resistivity is frequently used to characterize the purity of a metal. This ratio is called the residual resistivity ratio and is denoted by RRR.

Within the limitations of MR, RRR can be written as,

$$RRR = \frac{\rho_{i273\ K}}{\rho_o} + 1 \tag{1.2.2}$$

Although, deviations from MR cause (1.2.2) to be slightly in error, we have adopted it for conversion between $\rho_o$ and RRR in this report. This conversion is necessary because some authors use $\rho_o$ for characterization while others use

RRR. In either case, the authors frequently do not report the value of $\rho_{273\ K}$. It was convenient in this study of thermal conductivity to develop a simple analytical approximation for electrical resistivity. The base function chosen and fitted to selected resistivity data for each metal is

$$\rho = \rho_o + \rho_i + \rho_{io} \tag{1.2.3}$$

where $\rho_o$ = residual electrical resistivity (1.2.4)

$$\rho_i = P_1 T^{P_2}/(1 + P_1 P_3 T^{(P_2+P_4)} \exp(-(P_5/T)^{P_6})) + \rho_c \tag{1.2.5}$$

$$\rho_{io} = P_7 \rho_i \rho_o/(\rho_i + \rho_o) \tag{1.2.6}$$

Note the similarity to Eqs. 1.1.3 through 1.1.6. The $\rho_{io}$ term accounts for observed deviations from MR. The quantity $\rho_c$ is designed to account for the mathematical residual deviations in $\rho_i$. It should be noted that Eq. 1.2.3 does not assume the validity of MR as does Eq. 1.2.2. Section 1.5 describes how this apparent contradiction was circumvented.

1.3 Wiedemann-Franz-Lorenz (WFL) Law

In 1853 Wiedemann and Franz formulated an empirical law relating the thermal and electrical conductivities of metals, namely, that the ratio of the electrical and thermal conductivities (WF ratio) at a given temperature is the same for all metals. In 1872 Lorenz discovered that the WF ratio is proportional to temperature. The result was the Wiedemann-Franz-Lorenz (WFL) law:

$$\frac{\lambda}{\sigma} = \lambda\rho = LT \tag{1.3.1}$$

where $\sigma$ = electrical conductivity, L = Lorenz number, and T = absolute temperature.

data evaluation process. Graphical illustrations of the dependencies of $\lambda$, $\rho$, and L are given in the latter section of this report.

1.4. Literature Review

The existing principal compilations and reviews [2,3] were used as a starting point for this compilation. The resulting list of references was updated by searching current literature, abstracting services, and computerized data banks, as well as the reference lists of the most recent publications. The initial emphasis was directed toward temperatures below 300 K. Later the scope was extended to include temperatures up to near the melting point of each metal. The high temperature compilation was directed toward obtaining the most significant publications rather than a complete listing.

Since the principal interest is the dependence of thermal conductivity on temperature and electrical resistivity for relatively pure metals, not all of the literature data for a given base metal is referenced here. For example, numerous publications on the measurement of thermal conductivity at a single temperature have been excluded. Also, all measurements on specimens with more than 1% total impurity concentration were excluded.

Each of the selected sources was coded for content, and the data were extracted for computer analysis. When the literature data were presented in graphical form, the graphs were enlarged and read as accurately as possible. The resulting data were then smoothed to reproduce the original curves. Each set of data for a given measured specimen was characterized with values of residual resistivity, RRR, chemical impurity concentrations, and thermal/mechanical history. Other details regarding the experimental procedure, purpose of the work, and analysis of data are also coded in the annotated bibliography for the convenience of the reader.

Drude gave a theoretical derivation of the WFL law in 1900 and obtained a value of $2.228 \times 10^{-8} V^2/K^2$ for L. Sommerfeld calculated the first order approximation of L from the free electron theory of metals. His value, $2.443 \times 10^{-8} V^2/K^2$ commonly is designated $L_o$. It should be pointed out that the theoretically calculated value of L is based on the electron component of thermal conductivity, $\lambda_e$. Electron Lorenz numbers, $\rho\lambda_e/T$, other than the Sommerfeld value are designated by $L_e$ to distinguish them from total Lorenz numbers, $L = \rho\lambda/T$.

For many pure metals the experimentally determined values of L fall between 2.2 and $3.0 \times 10^{-8} V^2/K^2$ at room temperature and only slightly higher at 100 °C. At very low temperatures (liquid helium) the experimental values are near the Sommerfeld value. Thus $\beta$ as defined in Eq. 1.1.4 is equal to $\rho_o/L_o$. For intermediate temperatures the agreement of L and $L_o$ vanishes. At intermediate temperatures, $L_e$ and L are strong functions of purity and temperature, with the decrease from $L_o$ greatest for the most pure metals and at about 15 K to 40 K.

Deviations of L from $L_o$ at high temperatures are often attributed to the presence of lattice conductivity; however, as pointed out by Touloukian, Powell, Ho, and Klemens [2], the actual electronic Lorenz number may also deviate from $L_o$, even in the absence of lattice conductivity.

For the interested reader, detailed theoretical treatments can be found in numerous sources. A few of these are listed in the references [2-13].

The principal reason for consideration of the WFL law in this report is because of its utility in examining experimental data for unusual behavior. The functions used to represent $\lambda$ and $\rho$ were used to calculate the Lorenz ratio as a function of temperature and RRR. The resulting plots were examined to aid the

establish values of $\rho_0$ and RRR for each reported thermal conductivity measurement in the literature:

1. The value of $\rho_0$ that produces the best agreement of Eq. 1.1.3 and the reported thermal conductivity data at low temperatures was selected. The corresponding residual resistivity ratio, RRR, was calculated from Eq. 1.2.2. In addition, at this stage of the analysis, the Sommerfeld value of the Lorenz ratio, $L_0 = 2.443 \times 10^{-8}$, was assumed to be valid to obtain the corresponding value of $\beta = \rho_0/L_0$.

The values of $\rho_{i273}$ used in Eq. 1.2.2 for the four metals investigated are given below.

| Metal | $\rho_{i273}$ (n$\Omega$·m) |
|---|---|
| Copper | 15.4 |
| Aluminum | 24.8 |
| Iron | 87.0 |
| Tungsten | 48.4 |

The values listed in this table are our best estimates based on literature values and a variety of published and unpublished measurements performed at this laboratory over a period of 25 years.

2. Upon completion of the data fits and comparisons, plots were made of RRR (selected) versus RRR (reported) for each metal. These plots were used to determine the Lorenz ratio adjustment necessary for each metal and the range of RRR for which Eq. 1.1.3 is valid. Recommended values as a function of T and RRR are given in the form of equations, tables, and graphs for each metal.

1.5. Analysis

Selected data sets (primary data) were used to establish best values over the entire range of temperature and $\rho_0$ or RRR. The primary data were chosen on the basis of proven laboratory techniques, as applied to pure and annealed specimens. These data are believed to be accurate to within 5 to 10%. The primary data were then used to optimize the parameters in the selected equation for each metal. The $\rho_0$ or RRR value assigned to each data set was not necessarily that reported by the author. The values were selected to minimize the thermal conductivity deviations in the low temperature range, i.e., the range below the peak in the curve. If data did not exist below the peak in the $\lambda$ vs. T curve, the author's value of RRR (or $\rho_0$) was used. If a value of RRR (or $\rho_0$) was not reported for a high temperature data set, it was estimated by considering purity and anneal conditions. The relationship of the selected values of RRR (or $\rho_0$) and reported values are shown in each of the following major sections. The fitted equation was then compared to other data sets, including those for the less pure and unannealed specimens. The comparisons were examined for deviations varying systematically with RRR and temperature. The results of this analysis are described in the section for each metal (Sections 2 through 5).

As briefly discussed in Section 1.2, the relationship between RRR and $\rho_0$ is not uniquely defined for a given specimen in the absence of other measurements. For very pure metals RRR is frequently reported because the determination of RRR can be done without a knowledge of the form factor, $\ell/A$, i.e., the length to cross-sectional area ratio of the specimen. Such specimens are frequently very thin; and consequently, the accurate determination of $\ell/A$ and $\rho_0$ is difficult. In the absence of MR deviations, Eq. 1.2.2 may be used to define the relationship between $\rho_0$ and RRR. However, MR deviations are known to exist and, thus Eq. 1.2.2 is also inexact. We have chosen the following procedure to

## 1.6 Thermal Expansion Corrections

It would be desirable to specify that the recommended values in this report are based on the actual dimensions of the specimens at any given temperature, i.e., they are corrected for thermal expansion. However, only a small fraction of the authors indicated whether their reported data are corrected or uncorrected for thermal expansion. Therefore, the reported data were not modified for thermal expansion effects. This, although an undesirable situation, is not serious in view of the relatively large measurement uncertainties. It is also noted that, although a linear correction is usually appropriate, the proper correction depends on the nature of the measurement method employed.

For the convenience of the reader, estimates of the magnitude of the thermal expansion correction are given here. Room temperature is used as the basis for this correction since specimen dimensions are normally determined at room temperature. The four metals discussed have positive thermal expansion coefficients, thus the thermal conductivity values corrected for thermal expansion are smaller than the uncorrected values at temperatures above room temperature, and larger at temperatures below room temperature.

## 1.7 Acknowledgments

This work began several years ago and has progressed at a low level of effort. It was funded in part by the Air Force Office of Scientific Research. During these several years numerous NBS staff members have contributed to the tasks involved. In particular, we wish to acknowledge the assistance of Dr. Nancy Simon, Mr. Bruce Howry, and Mr. Jeff Wood. We also express appreciation to Dr. M. L. Minges (USAF-AFML), Dr. G. K. White (CSIRO-Australia) and other members of the CODATA Task Group on Thermophysical Properties for their helpful suggestions and reviews of this manuscript.

## 1.8 References


1. Cezairliyan, A. and Touloukian, Y. S., Correlation and prediction of thermal conductivity of metals through the application of the principle of corresponding states, in Advances in Thermophysical Properties at Extreme Temperatures and Pressures, Third Symposium on Thermophysical Properties, ASME (1965), 301-313.

2. Touloukian, Y. S., Powell, R. W., Ho, C. Y., and Klemens, P. G., Thermophysical properties of matter, Vol. 1, Thermal Conductivity (Metallic elements and alloys), Plenum Press, N.Y. (1970), 1469 pp.

3. Childs, G. E., Ericks, L. J., and Powell, R. L., Thermal conductivity of solids at room temperature and below (A review and compilation of the literature), National Bureau of Standards, Monograph No. 131 (1973), 608 pp.

4. Parrott, J. E. and Stukes, A. D., Thermal conductivity of solids, J. W. Arrowsmith Ltd., Bristol, England (1975), 157 pp.

5. Berman, R., Thermal conduction in solids, Clarendon Press, Oxford, England (1976), 193 pp.

6. Klemens, P. D., Theory of the thermal conductivity of solids, in Thermal Conductivity, Vol. 1, R. P. Tye, Editor, Academic Press, N.Y. (1969), 1-68.

7. Ziman, J. M., Electrons and Phonons (The theory of transport phenomena in solids), Clarendon Press, Oxford, England (1960), 554 pp.

8. Wilson, A. H., The theory of metals, Cambridge Press, England (1958), 346 pp.

9. Klemens, P. G., Thermal conductivity of solids at low temperatures, in Handbuch der Physik, S. Flugge, Editor, Vol. 14, Springer-Verlag, Berlin (1956), 198-281.

10. Klemens, P. G., Thermal conductivity and lattice vibrational modes, in Solid State Physics, Vol. 7, Academic Press, N.Y. (1958), 1-99.

11. Mendelssohn, K. and Rosenberg, H. M., The thermal conductivity of metals at low temperatures, in Solid State Physics, Vol. 12, Academic Press, N.Y. (1961), 223-274.

12. Mott, N. F. and Jones, H., Theory of the properties of metals and alloys, Clarendon Press, Oxford, England (1936), 326 pp.

13. Peierls, R. E., Quantum theory of solids, Clarendon Press, Oxford, England (1955), 229 pp.

## 2. Copper

### 2.1 General

Copper is discussed first because it is the most extensively measured metal. A total of 44 references were selected for inclusion in the annotated bibliography. The following references from the annotated bibliography (Section 2.5) represent the primary data sets: 4, 7, 8, 14, 16, 18, 19, 21, 23, 24, 26, 27, 28, 29, 30, 33, 34, 35, 38, 41, 42, and 43.

The primary data cover a range of temperatures from 0.2 to 1250 K, and a range of RRR from 20 to 1800. These data are illustrated in Figs. 2.1.1 through 2.1.6. These data are illustrated seven sets to a figure to avoid figures that are overly crowded and to aid in identifying the source of each data set. For additional convenience a composite of all data is also given, Fig. 2.1.6, but without source identification. For comparison, the electrically purest copper ever produced has an RRR of about 50,000. These high RRR values are not indicative of the actual impurity content. They were produced by oxygen anneal of high purity copper. The impurity content under these conditions remains unchanged, but the impurities (especially iron) chemically combine with oxygen to form less effective scattering centers. The RRR of typical commercially pure copper wire is in the range of 50 to 500. Very high purity copper, produced routinely, may have an RRR as high as 2000.

Equation 1.1.3 was fitted to represent the primary copper data over the entire temperature range.

The values of the parameters, $P_i, i = 1, 2, \ldots, 7$, obtained by nonlinear least squares fit are

$P_1 = 1.754 \times 10^{-8}$ $P_5 = 70$

$P_2 = 2.763$ $P_6 = 1.765$

$P_3 = 1102$ $P_7 = 0.838/\beta_r^{0.1661}$

$P_4 = -0.165$

where $\beta_r = \beta/0.0003$. All units are SI.

The data at high RRR were examined for systematic residuals as a function of temperature. These residuals were represented by the $W_c$ term in Eq. 1.1.5. The result is

$$W_c = -0.00012\ \ell n(T/420)\ \exp(-(\ell n(T/470)/0.7)^2)$$

$$-0.00016\ \ell n(T/73)\ \exp(-(\ell n(T/87/0.45)^2)$$

$$-0.00002\ \ell n(T/18)\ \exp(-(\ell n(T/21)/0.5)^2)$$

where $W_c$ and T are in SI units.

2.2 Deviations From Recommended Equation

The deviations of the primary data from Eq. 1.1.3 are illustrated in Figs. 2.2.1 through 2.2.6. Figure 2.2.6 is a composite of all deviations without data source identification. Five data sets exhibit differences of greater than $\pm$10%. In most of these cases, the deviations are significantly higher than the stated or implied uncertainty of the source document. It is not clear if these deviations are the result of underestimated uncertainties or the result of real differences between specimens. Although temperature dependent deviations do exist for individual data sets, the overall pattern is random in nature. No systematic trends with RRR were identified.

The primary data were selected from the literature data on relatively large, well annealed specimens. Therefore, the deviations exhibited in Figs. 2.2.1

through 2.2.6 are indicative of the combined effect of (a) experimental measurement errors and (b) the inability of Eq. 1.1.3 to account for the effects of chemical impurity variations. The effects of physical defect variations, small specimen size variations, and magnetic fields are exhibited, in part, by the deviations of the secondary data. The thermal conductivity variations, caused by other than chemical impurity variations, are not expected to be represented as well by Eq. 1.1.3. However, the RRR (or $\rho_0$) correlating parameter does account for an appreciable part of these variations. Some users may find this to be an adequate representation and, therefore, discussions of these comparisons are included for completeness.

The deviations of the secondary data sets (other than the primary sets) are illustrated in Figs. 2.2.7 through 2.2.16. These plots are divided into two groups, according to the magnitudes of the deviations. Figures 2.2.7 through 2.2.12 and Figs. 2.2.13 through 2.2.16. Figures 2.2.12 and 2.2.16 are composite graphs for each group, respectively.

Finally, it was of interest to compare the values calculated from Eq. 1.1.3 to the most widely used references (13,39) of recommended thermal conductivity values. Figure 2.2.17 shows this comparison. Within the combined uncertainties of this work and references 13,39 the differences are not significant. It should be noted however that references 13,39 give values only for a single value of RRR (approximately 1800), while Eq. 1.1.3 covers a wide range of RRR.

### 2.2.1 Physical Defect Effects

Investigations of physical defects in copper have produced several noteworthy references 5,10,12,15,22,26,33,41,44. We shall discuss each of them below.

Reference 10 shows the effects of mechanical deformation. The peak value of the thermal conductivity of the unstrained specimen was 2750 $W \cdot m^{-1} \cdot K^{-1}$. After

a 30.8% elongation, the value at the peak was 1050 $W \cdot m^{-1} \cdot K^{-1}$. The deviations from Eq. 1.1.3 for the unstrained condition were within $\pm$4%.

Reference 22 reports the effects of mechanical deformation on two specimens of different purities. For the 99.9% pure Cu specimen, the unstrained peak value of the thermal conductivity was 2700 $W \cdot m^{-1} \cdot K^{-1}$, and after a 30.8% elongation, the peak value was 1100 $W \cdot m^{-1} \cdot K^{-1}$. For the 99.99% Cu specimen, the unstrained peak value was 5800 $W \cdot m^{-1} \cdot K^{-1}$, and after a 28.4% elongation, the peak value was 1300 $W \cdot m^{-1} \cdot K^{-1}$. The deviations from Eq. 1.1.3 for the 99.9% copper specimen are within $\pm$12% (unstrained condition). Similarly, the deviations for the 99.99% copper specimen are within $\pm$3% (unstrained condition). The strained conditions were not compared.

Another study of the effect of mechanical deformation is given in reference 15 in which a specimen was torsionally deformed ($nd/\ell = 1.29$, where n is the number of turns on the specimen). The specimen was 99.55% copper and had strained thermal conductivity values of 24 $W \cdot m^{-1} \cdot K^{-1}$ at 20 K, and 50 $W \cdot m^{-1} \cdot K^{-1}$ at 40 K. After these measurements were taken, the specimen was annealed in helium at 450 °C for three hours and measurements were taken again. After the anneal, the values were 36 $W \cdot m^{-1} \cdot K^{-1}$ at 20 K and 60 $W \cdot m^{-1} \cdot K^{-1}$ at 40 K. The thermal conductivities of a control specimen were also measured. The deviations from Eq. 1.1.3 for the control specimen were within $\pm$16%. The deviations for the deformed specimen were within $\pm$26%, while for the annealed specimen, the deviations were within $\pm$20%. A possible explanation for these large deviations may be that the specimen's RRR is close to the lower validity limit of Eq. 1.1.3.

References 26 and 33 demonstrate the effect on thermal conductivity of annealing a specimen, then drawing it. The specimen was annealed in vacuum and the thermal conductivity was determined. A similar specimen was cold-drawn 26%

and its thermal conductivity was measured. The maximum thermal conductivity for the annealed specimen was 14000 $W \cdot m^{-1} \cdot K^{-1}$, while for the drawn specimen it was 2500 $W \cdot m^{-1} \cdot K^{-1}$. The deviations from Eq. 1.1.3 for the annealed specimen were within $\pm$9%, while for the cold-drawn specimen, the deviations were within $\pm$6%.

Reference 41 reports the differences in thermal conductivity of a specimen in the "as-drawn" state and in the annealed state. The peak value of the thermal conductivity for the drawn condition was 1540 $W \cdot m^{-1} \cdot K^{-1}$, and that for the annealed condition was 5300 $W \cdot m^{-1} \cdot K^{-1}$. The deviations from Eq. 1.1.3 for the as-drawn state were within $\pm$7%, while for the annealed state, they were within $\pm$10%.

Reference 12 investigated the effects on thermal conductivity of different annealing conditions and sizes. For an oxygen anneal, the peak conductivity was found to be 56500 $W \cdot m^{-1} \cdot K^{-1}$ for a specimen of 12.5 μm thickness, and 55300 $W \cdot m^{-1} \cdot K^{-1}$ for a specimen of 125 μm. After a high vacuum anneal, these peaks are 15500 $W \cdot m^{-1} \cdot K^{-1}$ and 5000 $W \cdot m^{-1} \cdot K^{-1}$, respectively. The deviations from Eq. 1.1.3 for the smaller specimen were within $\pm$30% for the oxygen anneal, $\pm$35% for the high vacuum anneal. Those for the larger specimen were within $\pm$30% for the oxygen anneal, +120% for the high vacuum anneal. A possible explanation for these very large deviations may be that size corrections applied to the data were too large.

Reference 44 showed the effect on thermal conductivity of a specimen in an unannealed (as fabricated) state and in an annealed state. The peak conductivity in the unannealed state was 390 $W \cdot m^{-1} \cdot K^{-1}$, while for the annealed state, it was 570 $W \cdot m^{-1} \cdot K^{-1}$. The deviations from Eq. 1.1.3 for both the unannealed and annealed specimens were within $\pm$5%.

Reference 5 reported the effect of neutron irradiation on thermal conductivity. Neutron irradiation produces physical defects within the lattice. The neutrons had energies up to $10^7$ eV while the specimens had a maximum exposure of $6.5 \times 10^{23}$ neutrons per square meter. The damage, as measured by thermal resistivity, was linear with neutron exposure. The maximum thermal conductivity for the unirradiated specimen was 16700 $W \cdot m^{-1} \cdot K^{-1}$, while for the maximum exposure specimen, it was 1700 $W \cdot m^{-1} \cdot K^{-1}$. The deviations from Eq. 1.1.3 for the unirradiated specimen were within $\pm$35%, while those for the maximum exposure were within $\pm$20%. The nature of the deviations for these specimens are not understood.

Although the temperature dependence of physical defect scattering mechanism is different from that due to impurity scattering, Eq. 1.1.3 generally represents the unannealed specimen data quite well (within $\pm$20%). This indicates that the residual electrical resistivity characterizes both types of scattering for the range of RRR included here.

### 2.2.2 Size Effects

Nath[1] showed that the thermal conductivity was a strong function of specimen thickness below about 0.1 μm while it is nearly independent of thickness for specimens larger than 0.4 μm. The variation of the thermal conductivity with thickness was studied for temperatures above 80 K and was found to be significant even at 500 K. A 50% reduction in thermal conductivity below that of bulk copper was observed for a film of 0.01 μm thickness.

Reference 12 contains thermal conductivity data that has already been corrected for size effects on two copper crystals of 12.5, 125 μm thickness.

---

[1]Nath, P. and Chopra, K. L., Thermal Conductivity of Copper Films, Thin Solid Films, 20, 53-62 (1974).

### 2.2.3 Magnetic Field Effects

Although magnetic field effects on thermal conductivity were not studied explicitly, reference 24 showed that a 6 T field increases the thermal resistivity by 33% at 3 K, decreasing to 18% at 31 K for the same field. The increase in thermal resistivity changes linearly with the field while the slope decreases with increasing temperature.

Sparks[2] measured the effect of magnetic fields up to 8 T on two specimens of copper of differing purities. The magnetothermal resistivity introduced into the high conductivity specimen exhibited a strong temperature dependence below a field of 2 T. Above this value, the temperature dependence was much less. The value of the magnetothermal resistivity at high fields was about $0.0004\ m \cdot K \cdot W^{-1}$ near 4 K. Up to 8 T, the lower conductivity specimen exhibited a more uniform behavior, and the magnetothermal resistivity introduced near 4 K was appreciably higher, $0.002\ m \cdot K \cdot W^{-1}$. The relative change in thermal resistivity, however, is greater for the high purity specimen at a given field. Fevrier and Morize[3] reported measurement on two specimens of pure copper at fields up to 5 T at 4.2 K. The maximum field induced a factor of four increase in resistivity. Nevertheless, the ratio of the thermal and electrical conductivities was reported to be a constant for both longitudinal and transverse magnetic fields.

## 2.3 Electrical Resistivity and Lorenz Ratio

During this investigation it was frequently helpful to examine the Lorenz ratio as a function of temperature and RRR. However, to do this we needed values

---

[2]Sparks, L. L., Magnetothermal Conductivity of Selected Pure Metals and Alloys, Semi-Annual Technical Report on Materials Research in Support of Superconducting Machinery-IV, NBSIR 75-828 (1975).

[3]Fevrier, A. and Morize, D., The effect of Magnetic Field on the Thermal Conductivity and Electrical Resistivity of Different Materials, Cryogenics, 13, 603-6 (1973.

of electrical resistivity. Therefore, we selected those data sources from the primary data set that contained electrical resistivity data. The electrical resistivity data used is shown in Figs. 2.3.1 through 2.3.3. Figure 2.3.3 is a composite of all data. The parameters for Eq. 1.2.3 are:

$$P_1 = 0.1171 \times 10^{-16}$$

$$P_2 = 4.49$$

$$P_3 = 3.841 \times 10^{10}$$

$$P_4 = 1.14$$

$$P_5 = 50$$

$$P_6 = 6.428$$

$$P_7 = 0.4531$$

All units are SI.

The deviations of the experimental data from this equation are illustrated in Figs. 2.3.4 through 2.3.6. It is clear that in the midrange of the $\ell nT$ plots (10 to 100 K) there is a fairly large uncertainty in the representation ($\pm$10 to 15%). Smooth curves of $\rho$ vs. T at selected RRR values are plotted in Fig. 2.3.7. From the $\rho(T,RRR)$ and $\lambda(T,RRR)$ equations values of $L(T,RRR)$ were calculated and plotted in Fig. 2.3.8. Irregularities are greatly magnified on this plot ($\pm$10% equals about 1 cm on the L scale). It is noted that the bumps in the curves in the vicinity of 30 to 80 K correspond to the region of greatest uncertainty in both the $\rho(T,RRR)$ and $\lambda(T,RRR)$ representations. However, it is also noted that the bumps correspond to less than $\pm$10% irregularity in L from what is normally expected and this corresponds to the combined irregularity of the $\rho$ and $\lambda$ representations.

In Section 1.5 we discuss the procedure for selecting values of $\rho_0$ and calculating RRR for each thermal conductivity data set. These values of $\rho_0$

along with the Sommerfeld value of Lorenz ratio were used to best fit each low temperature data set. The resulting values of RRR obtained by this procedure are compared to the values reported in the references in Fig. 2.3.9 and are listed in Table 2.3.1. Figure 2.3.9 shows values of RRR (calc), those values from the above procedure, versus RRR (obs), those values reported in the references listed in the annotated bibliography. Also shown in this figure is the line that represents RRR (calc) = RRR (obs). Systematic deviations from this line indicate ranges in which the derived Eq. 1.1.3 is invalid. Figure 2.3.9 indicates that the fitted equation becomes progressively less valid below RRR values of 20. Four points in the region 200 to 1600 lie appreciably (20%) from the line. Discussions with these authors suggest that large uncertainties were present in the $\rho_0$ measurements for these specimens. In addition, the data listed in Table 2.3.1 confirm the validity of using the Sommerfeld value of the Lorenz ratio for copper.

## 2.4 Summary for Copper

Equation 1.1.3 represents the primary copper data to within $\pm$15% of the experimental values. Deviations for unannealed specimens (i.e., those containing physical defects) are within 20%.

Based on the deviations illustrated in Figs. 2.2.1 through 2.2.16 and the large changes that occur in thermal conductivity due to the introduction of chemical defects, physical defects, size effect, and magnetic fields, it is clear that a large proportion of these effects is reflected by the residual electrical resistivity. The incorporation of RRR (or $\rho_0$) in Eq. 1.1.3 produces an equation that represents the data for a wide range of copper specimens and environments.

Equation 1.1.3 with the parameters listed here was used to generate thermal conductivity values for selected temperatures and values of RRR. These values are listed in Table 2.4.1 and plotted in Fig. 2.4.1.

List of Tables and Figures for Copper

Tables


| | | Page |
|---|---|---|
| Table 2.3.1 | Comparison of Calculated and Observed RRR Values for Copper | 27 |
| Table 2.4.1 | Thermal Conductivity Values for Copper Calculated From Eq. 1.1.3 at Selected Temperatures and RRR Values | 28 |


Figures


| | | Page |
|---|---|---|
| Figure 2.1.1 | Experimental thermal conductivity data selected from the following primary references in the copper annotated bibliography: (4,7,8,14,16,18) | 29 |
| Figure 2.1.2 | Experimental thermal conductivity data selected from the following primary references in the copper annotated bibliography: (19,20,21,23,24,27) | 30 |
| Figure 2.1.3 | Experimental thermal conductivity data selected from the following primary references in the copper annotated bibliography: (26,27,28,29,30,33) | 31 |
| Figure 2.1.4 | Experimental thermal conductivity data selected from the following primary references in the copper annotated bibliography: (35,38,41,43) | 32 |
| Figure 2.1.5 | Experimental thermal conductivity data selected from the following primary reference in the copper annotated bibliography: (42) | 33 |
| Figure 2.1.6 | Composite of the data in Figs. 2.1.1 through 2.1.5 | 34 |
| Figure 2.2.1 | Thermal conductivity deviations of the copper data from the following primary references compared to Eq. 1.1.3: (4,7,8,14,16,18) | 35 |
| Figure 2.2.2 | Thermal conductivity deviations of the copper data from the following primary references compared to Eq. 1.1.3: (19,20,21,23,24,27) | 36 |
| Figure 2.2.3 | Thermal conductivity deviations of the copper data from the following primary references compared to Eq. 1.1.3: (26,27,28,29,30,33) | 37 |
| Figure 2.2.4 | Thermal conductivity deviations of the copper data from the following primary references compared to Eq. 1.1.3: (35,38,41,43) | 38 |

Page

Figure 2.2.5 Thermal conductivity deviations of the copper data from the following primary reference compared to Eq. 1.1.3: (42) . . . . . 39

Figure 2.2.6 - Composite of the deviations in Figs. 2.2.1 through 2.2.5 . . . . . 40

Figure 2.2.7 Thermal conductivity deviations of the copper data from the following secondary references compared to Eq. 1.1.3: (1,2,3,6,9) . . . . . 41

Figure 2.2.8 Thermal conductivity deviations of the copper data from the following secondary references compared to Eq. 1.1.3: (10,15,17,22,25) . . . . . 42

Figure 2.2.9 Thermal conductivity deviations of the copper data from the following secondary references compared to Eq. 1.1.3: (26,31,32,33,37) . . . . . 43

Figure 2.2.10 Thermal conductivity deviations of the copper data from the following secondary reference compared to Eq. 1.1.3: (37) . . . . . 44

Figure 2.2.11 Thermal conductivity deviations of the copper data from the following secondary references compared to Eq. 1.1.3: (40,43,44) . . . . . 45

Figure 2.2.12 Composite of the deviations in Figs. 2.2.7 through 2.2.11 . . . . . 46

Figure 2.2.13 Thermal conductivity deviations of the copper data from the following secondary references compared to Eq. 1.1.3: (5,7,12) . . . . . 47

Figure 2.2.14 Thermal conductivity deviations of the copper data from the following secondary references compared to Eq. 1.1.3: (11,12,15,27,36) . . . . . 48

Figure 2.2.15 Thermal conductivity deviations of the copper data from the following secondary references compared to Eq. 1.1.3: (36,44) . . . . . 49

Figure 2.2.16 Composite of the deviations in Figs. 2.2.13 through 2.2.15 . . . . . 50

Figure 2.2.17 Comparison of Eq. 1.1.3 to the values recommended for copper in the following references: (13,39) . . . . . 51

Figure 2.3.1 Experimental electrical resistivity data for copper selected from the following references in the copper annotated bibliography: (4,14,21,23,24,26,29) . . . . . 52

Page

Figure 2.3.2 Experimental electrical resistivity data for copper selected from the following references in the copper annotated bibliography: (33,38,43) . . . . . 53

Figure 2.3.3 Composite of the electrical resistivity data in Figs. 2.3.1 and 2.3.2 . . . . . 54

Figure 2.3.4 Electrical resistivity deviations of the copper data from the following references compared to Eq. 1.2.3: (4,14,21,23,24,26,29) . . . . . 55

Figure 2.3.5 Electrical resistivity deviations of the copper data from the following references compared to Eq. 1.2.3: (33,38,43) . . . . . 56

Figure 2.3.6 Composite of the electrical resistivity deviations shown in Figs. 2.3.4 and 2.3.5 . . . . . 57

Figure 2.3.7 Electrical resistivity for copper as a function of temperature calculated from Eq. 1.2.3 at selected values of RRR . . . . . 58

Figure 2.3.8 Lorenz ratio for copper as a function of temperature calculated from Eq. 1.2.3 and Eq. 1.1.3 at selected values of RRR . . . . . 59

Figure 2.3.9 RRR values calculated as per Section 1.5, RRR(CALC) versus reported RRR values, RRR(OBS), for copper . . . . . 60

Figure 2.4.1 Thermal conductivity for copper as a function of temperature calculated from Eq. 1.1.3 at selected values of RRR . . . . . 61

Table 2.3.1. Comparison of Calculated and Observed RRR Values for Copper.

| Reference | RRR (obs.) | RRR (calc.) |
|---|---|---|
| | Primary Data | |
| 4 | 274.0 | 271.0 |
| 8 | 45.5 | 44.3 |
| 14 | 214.0 | 216.0 |
| 16 | 900.0 | 900.0 |
| 18 | 270.0 | 190.0 |
| 23 | 900.0 | 900.0 |
| 24 | 49.2 | 51.5 |
| 26 | 1530.0 | 1070.0 |
| 33 | 1450.0 | 1060.0 |
| 33 | 400.0 | 306.0 |
| 42 | 1780.0 | 1800.0 |
| 43 | 19.5 | 20.5 |
| 43 | 38.8 | 42.8 |
| | Secondary Data | |
| 1 | 29.0 | 38.0 |
| 9 | 2.5 | 3.4 |
| 10 | 140.0 | 120.0 |
| 15 | 1.6 | 2.0 |
| 15 | 1.6 | 1.9 |
| 15 | 1.6 | 1.6 |
| 26 | 115.0 | 102.0 |
| 33 | 350.0 | 102.0 |
| 36 | 870.0 | 880.0 |
| 36 | 1390.0 | 1350.0 |
| 36 | 2680.0 | 2630.0 |
| 37 | 1.9 | 2.6 |
| 37 | 2.1 | 3.0 |
| 37 | 2.5 | 3.1 |
| 37 | 2.5 | 3.3 |
| 37 | 3.2 | 4.0 |
| 37 | 3.1 | 4.4 |
| 37 | 3.9 | 4.5 |
| 37 | 3.6 | 4.6 |
| 37 | 3.8 | 5.0 |
| 37 | 4.2 | 5.5 |
| 37 | 4.5 | 5.9 |

Table 2.4.1. Thermal Conductivity Values for Copper Calculated from Eq. 1.1.3 at Selected Temperatures and RRR Values.

| T (K) | $\lambda(W \cdot m^{-1} \cdot K^{-1})$ | | | | |
|---|---|---|---|---|---|
| | RRR = 30 | RRR = 100 | RRR = 300 | RRR = 1000 | RRR = 3000 |
| 1 | 46 | 156 | 471 | 1574 | 4726 |
| 2 | 91 | 312 | 942 | 3147 | 9434 |
| 3 | 137 | 468 | 1413 | 4710 | 14044 |
| 4 | 183 | 624 | 1880 | 6243 | 18380 |
| 5 | 228 | 779 | 2343 | 7715 | 22170 |
| 6 | 274 | 933 | 2796 | 9075 | 25084 |
| 7 | 319 | 1085 | 3232 | 10260 | 26834 |
| 8 | 365 | 1235 | 3642 | 11197 | 27328 |
| 9 | 409 | 1380 | 4015 | 11836 | 26756 |
| 10 | 454 | 1520 | 4343 | 12172 | 25496 |
| 12 | 541 | 1778 | 4844 | 12127 | 22264 |
| 14 | 624 | 2002 | 5144 | 11544 | 19150 |
| 16 | 703 | 2186 | 5267 | 10725 | 16398 |
| 18 | 777 | 2324 | 5231 | 9771 | 13924 |
| 20 | 843 | 2408 | 5054 | 8727 | 11683 |
| 25 | 960 | 2381 | 4215 | 6135 | 7271 |
| 30 | 999 | 2119 | 3245 | 4151 | 4573 |
| 35 | 970 | 1784 | 2436 | 2859 | 3028 |
| 40 | 900 | 1467 | 1841 | 2047 | 2122 |
| 45 | 814 | 1205 | 1423 | 1531 | 1568 |
| 50 | 731 | 1002 | 1135 | 1196 | 1216 |
| 60 | 597 | 740 | 799 | 824 | 832 |
| 70 | 513 | 601 | 634 | 647 | 651 |
| 80 | 465 | 526 | 549 | 557 | 560 |
| 90 | 437 | 485 | 502 | 508 | 510 |
| 100 | 421 | 461 | 475 | 480 | 482 |
| 150 | 396 | 419 | 426 | 429 | 430 |
| 200 | 391 | 407 | 413 | 414 | 415 |
| 250 | 388 | 401 | 405 | 407 | 407 |
| 300 | 386 | 397 | 400 | 401 | 402 |
| 400 | 383 | 391 | 393 | 394 | 394 |
| 500 | 379 | 385 | 387 | 388 | 388 |
| 600 | 374 | 379 | 381 | 381 | 381 |
| 700 | 368 | 372 | 374 | 374 | 374 |
| 800 | 362 | 365 | 367 | 367 | 367 |
| 900 | 356 | 359 | 360 | 360 | 360 |
| 1000 | 350 | 352 | 353 | 353 | 354 |
| 1100 | 344 | 347 | 347 | 348 | 348 |
| 1200 | 339 | 341 | 342 | 342 | 342 |
| 1300 | 335 | 337 | 337 | 338 | 338 |

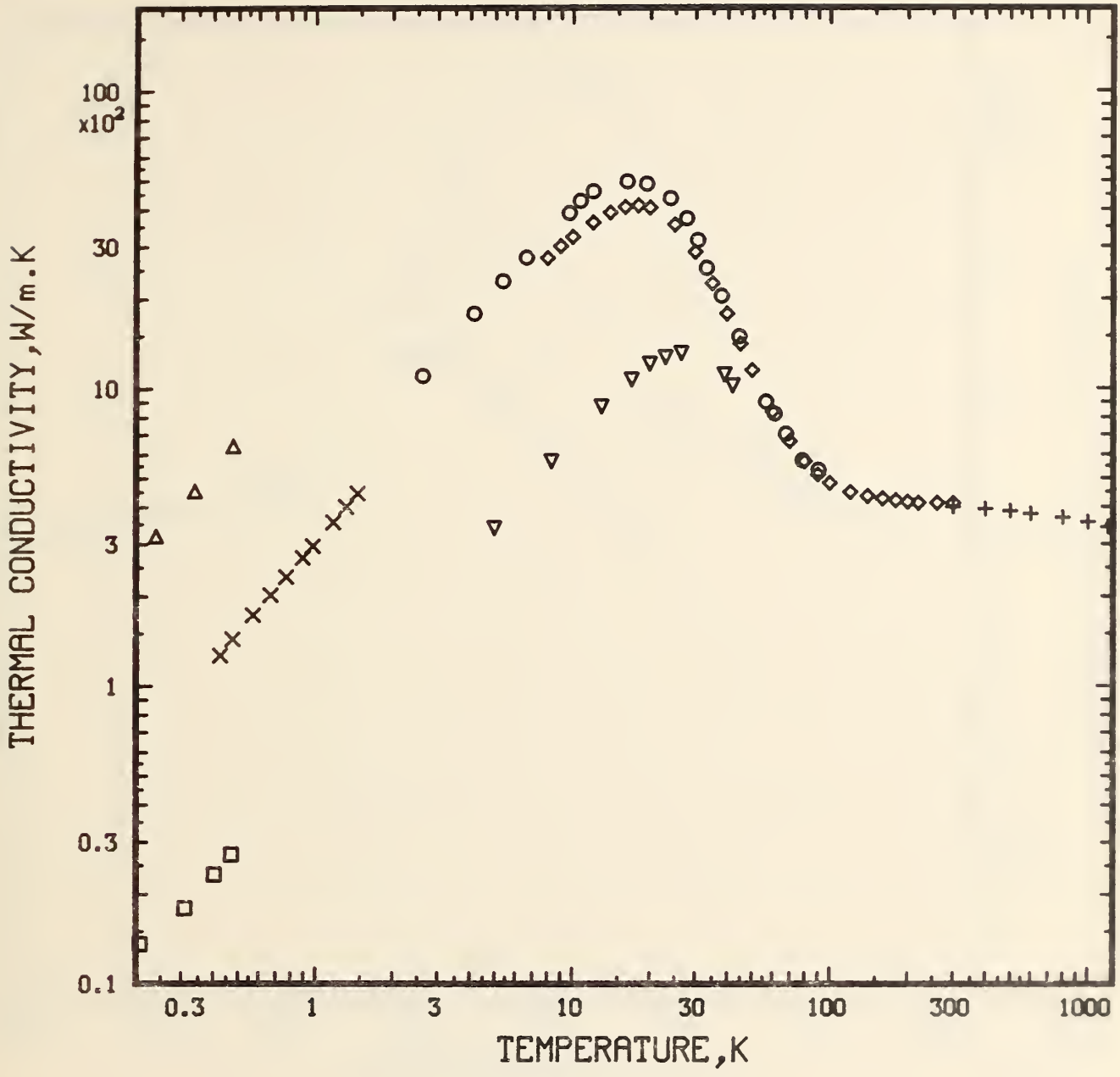


Figure 2.1.1 Experimental thermal conductivity data selected from the following primary references in the copper annotated bibliography:(4,7,8,14,16,18)

○ - (4), △ - (7), □ - (7), ▽ - (8),
◇ - (14), + - (16), × - (18)

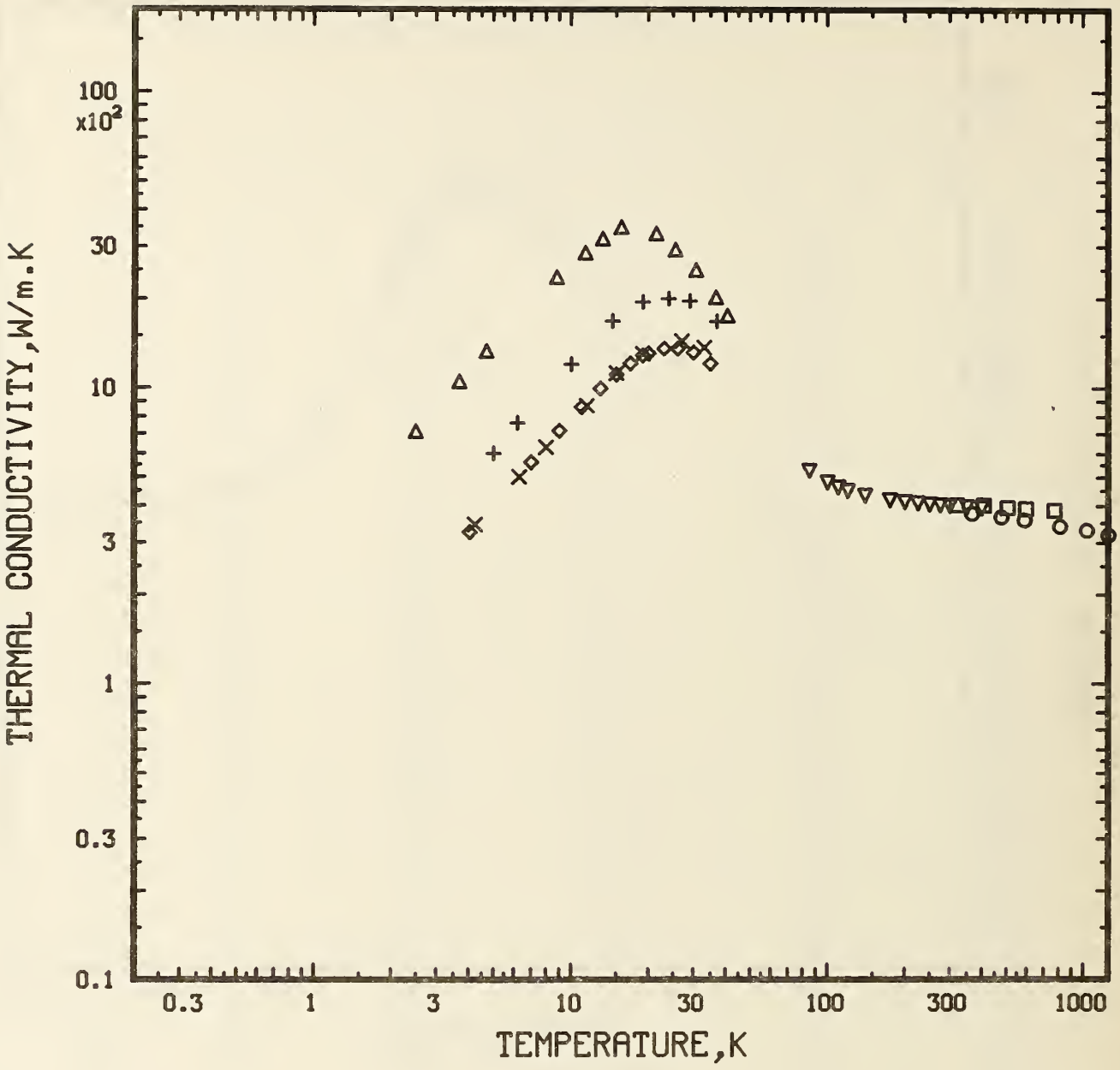


Figure 2.1.2 Experimental thermal conductivity data selected from the following primary references in the copper annotated bibliography:(19,20,21,23,24,27)

○ - (19), △ - (20), □ - (21), ▽ - (23),
◇ - (24), + - (27), × - (27)

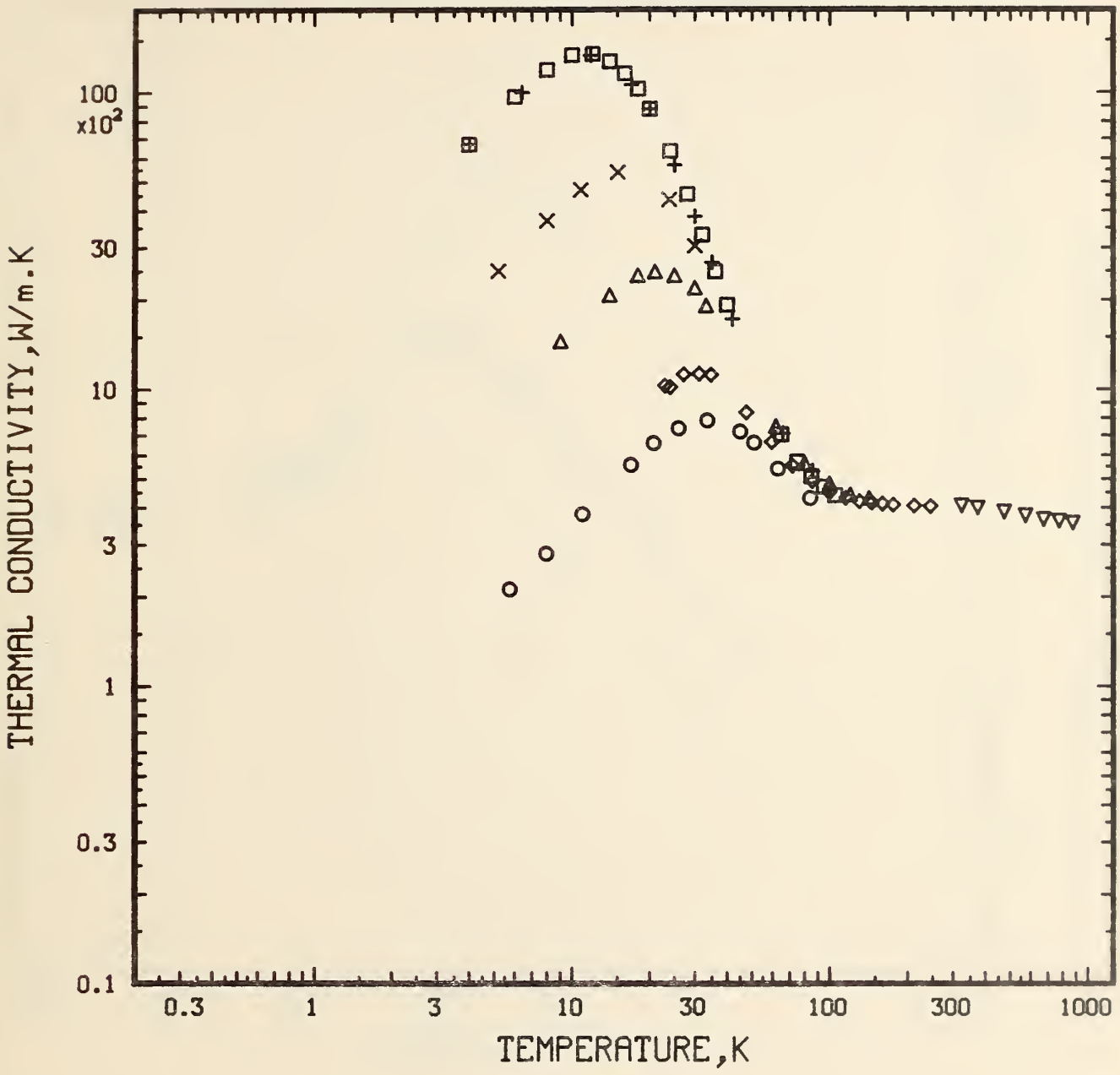


Figure 2.1.3 Experimental thermal conductivity data selected from the following primary references in the copper annotated bibliography:(26,27,28,29,30,33)

○ - (27), △ - (28), □ - (26), ▽ - (29),
◇ - (30), + - (33), × - (33)

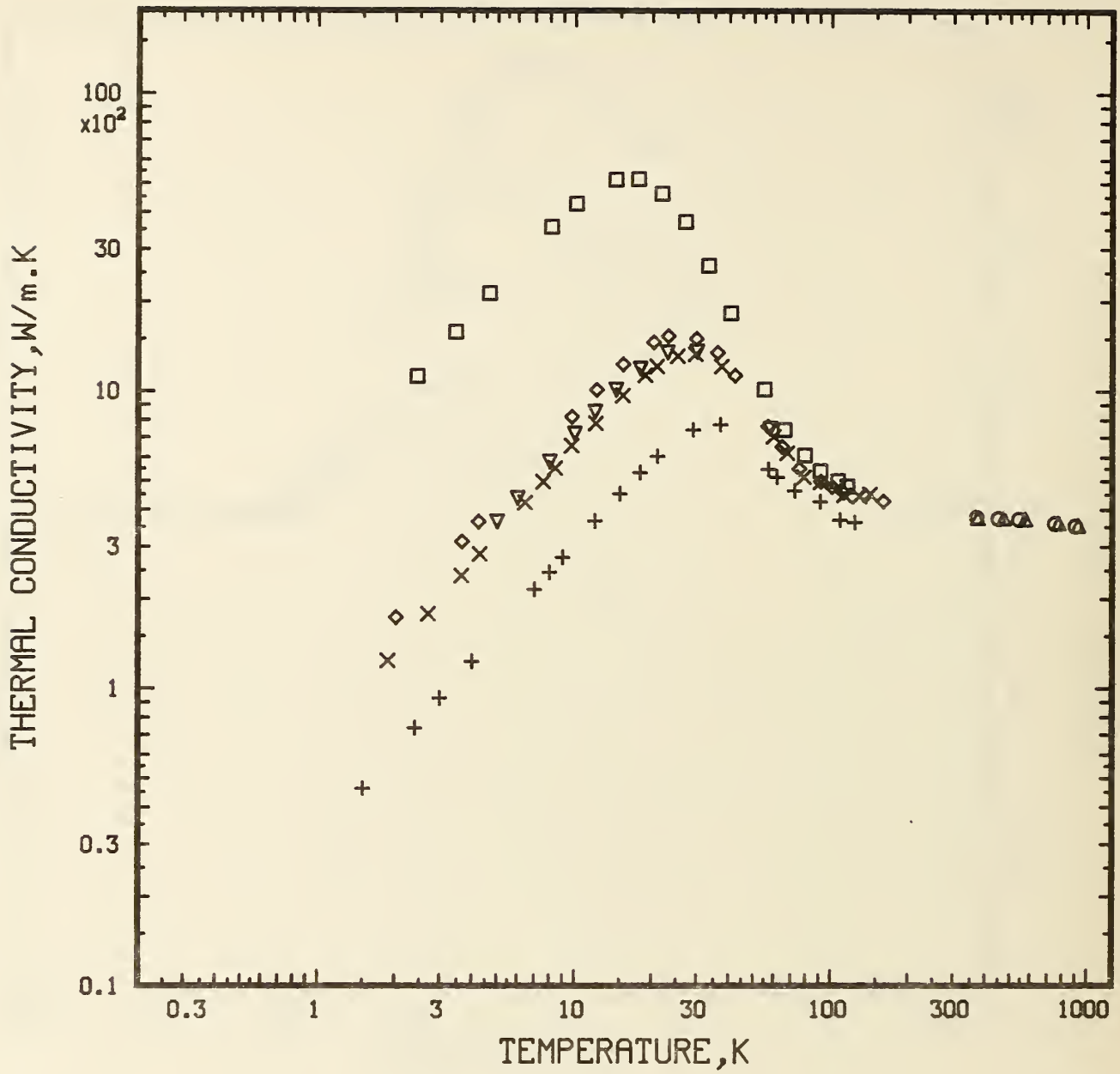


Figure 2.1.4 Experimental thermal conductivity data selected from the following primary references in the copper annotated bibliography:(35,38,41,43)

○ - (35), △ - (38), □ - (41), ▽ - (41),
◇ - (41), + - (43), × - (43)

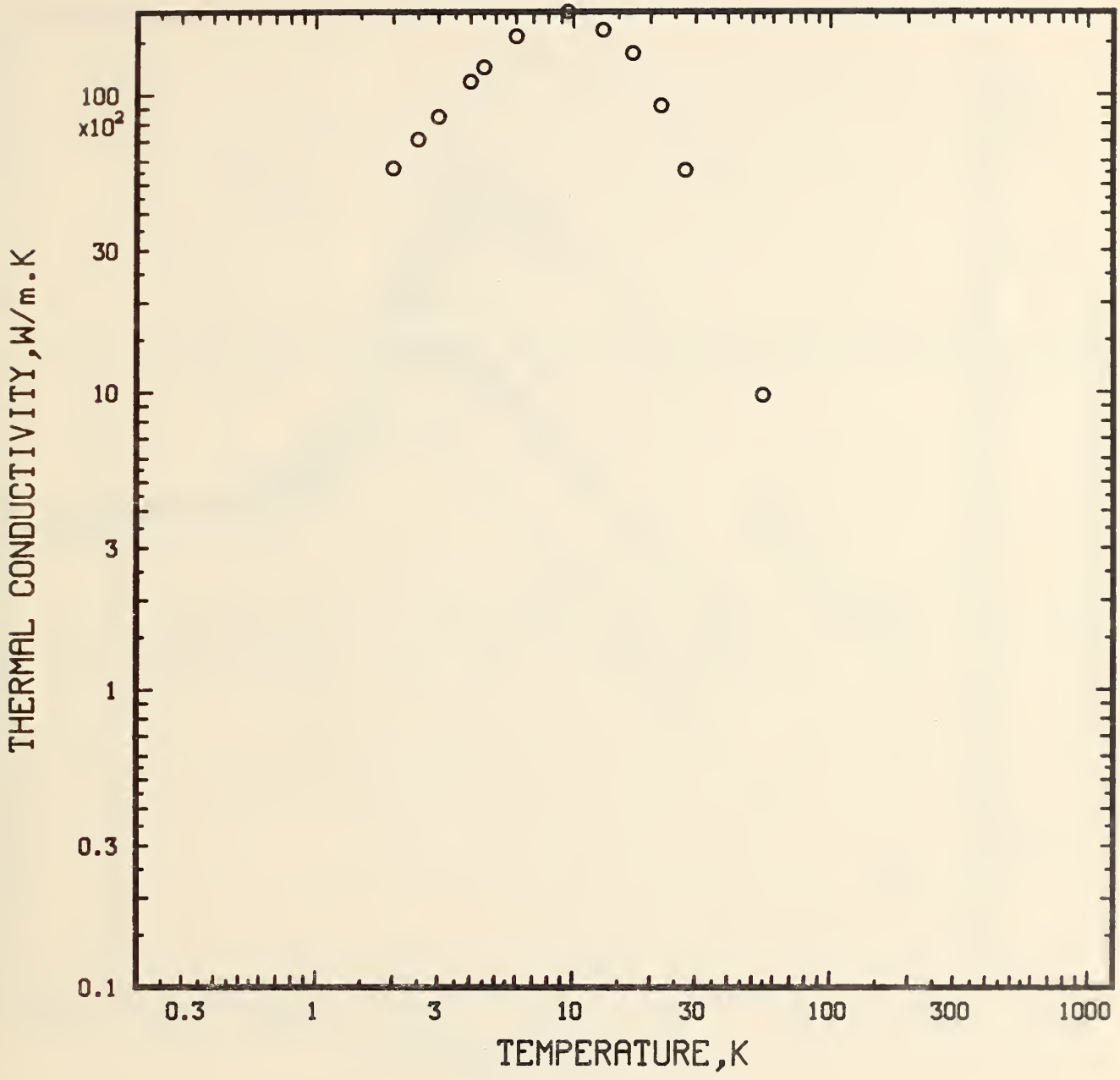


Figure 2.1.5 Experimental thermal conductivity data selected from the following primary reference in the copper annotated bibliography:(42)

O - (42)

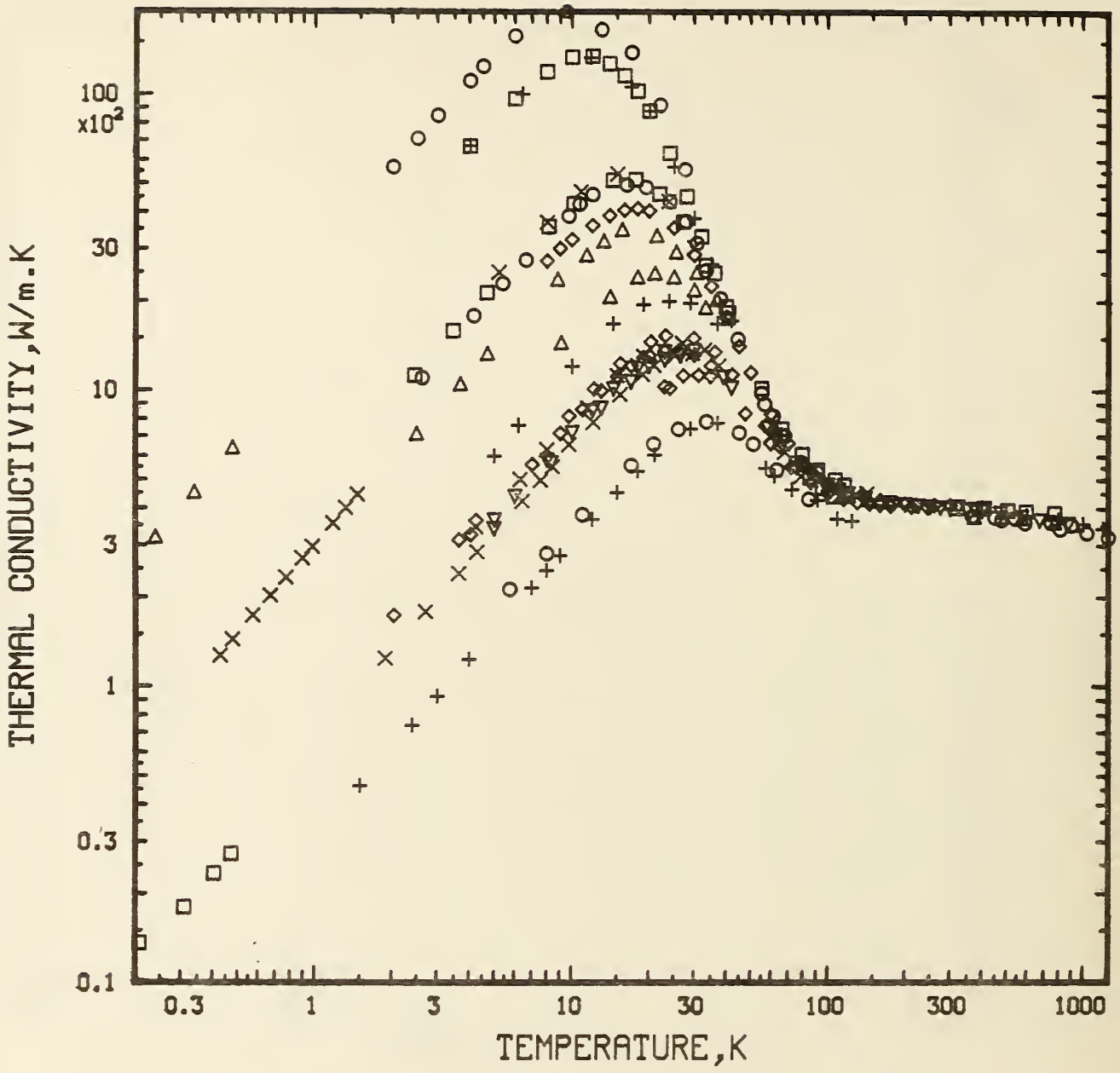


Figure 2.1.6 Composite of the data in figs. 2.1.1 through 2.1.5

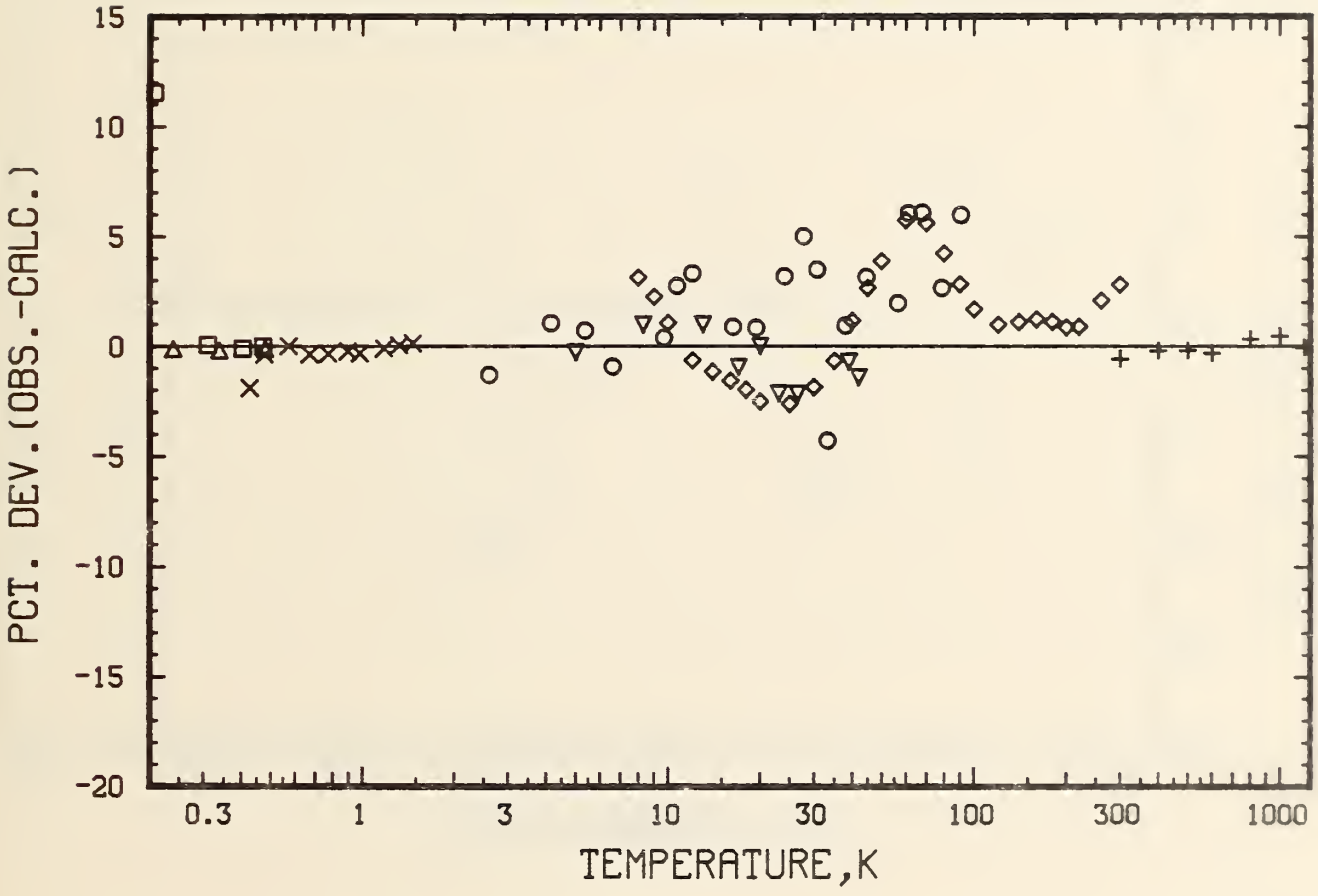


Figure 2.2.1 Thermal conductivity deviations of the copper data from the following primary references compared to eq. (1.1.3): (4,7,8,14,16,18)

○ - (4), △ - (7), □ - (7), ▽ - (8),
◇ - (14), + - (16), × - (18)

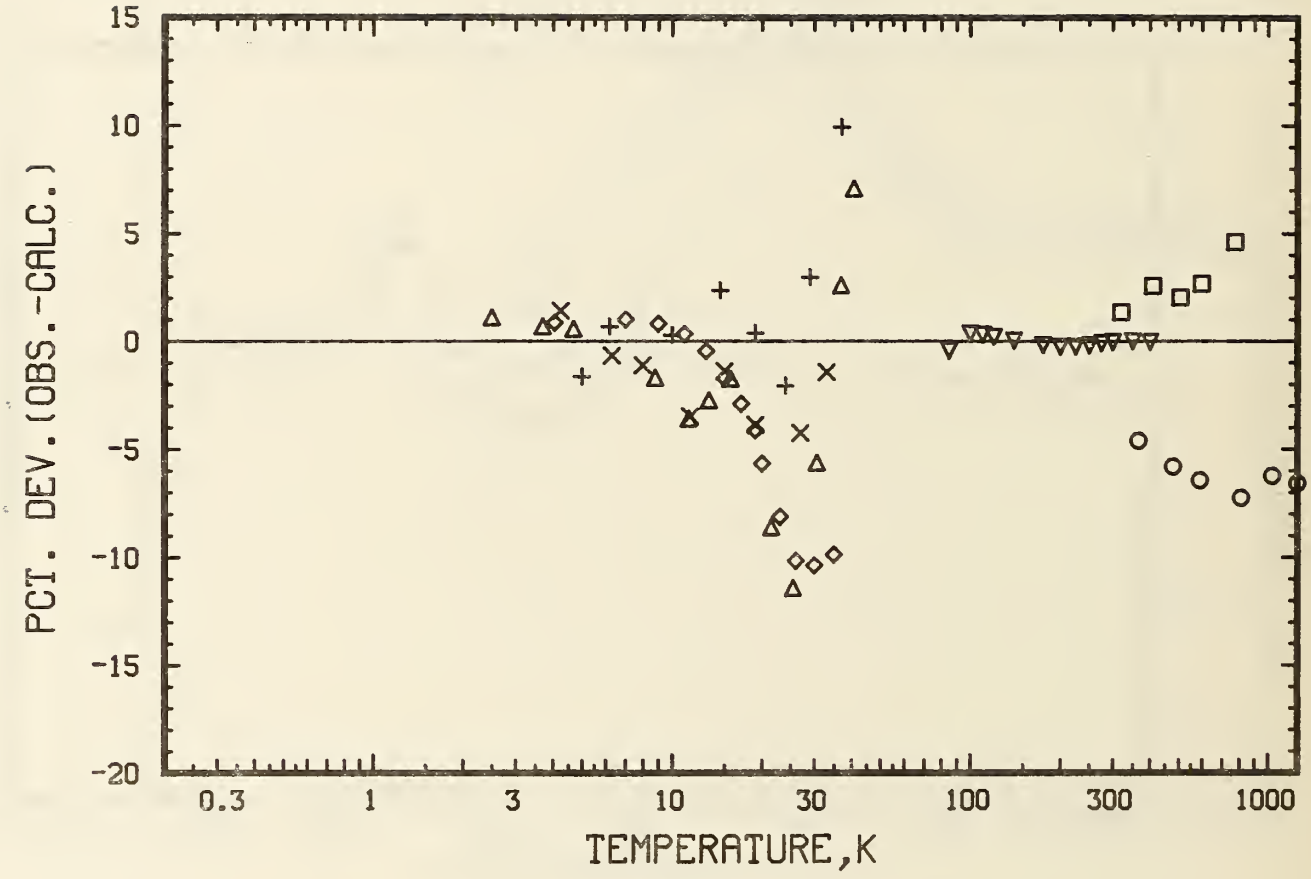


Figure 2.2.2 Thermal conductivity deviations of the copper data from the following primary references compared to eq. (1.1.3): (19,20,21,23,24,27)

○ - (19), △ - (20), □ - (21), ▽ - (23),
◇ - (24), + - (27), × - (27)

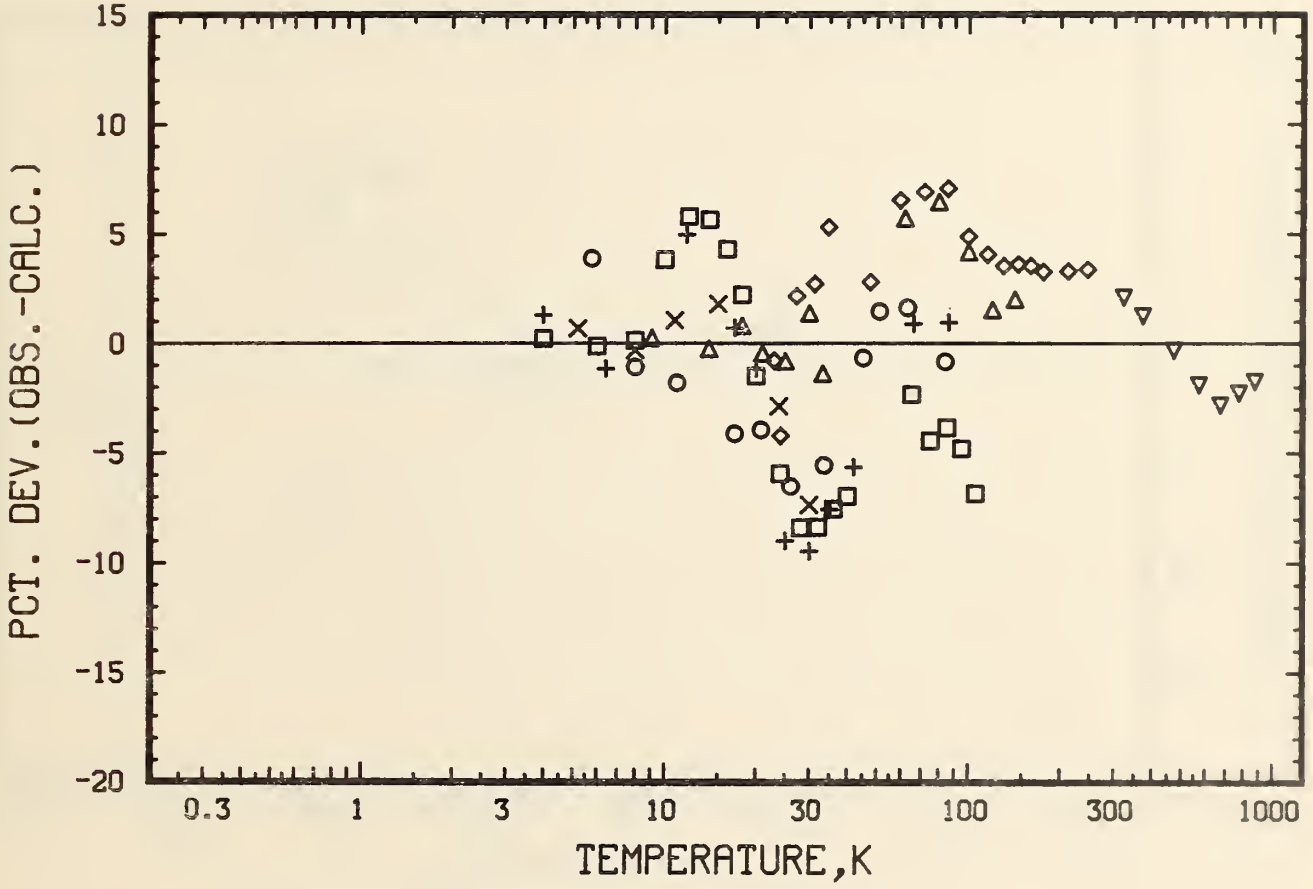


Figure 2.2.3 Thermal conductivity deviations of the copper data from the following primary references compared to eq. (1.1.3): (26,27,28,29,30,33)

○ - (27), △ - (28), □ - (26), ▽ - (29),
◇ - (30), + - (33), × - (33)

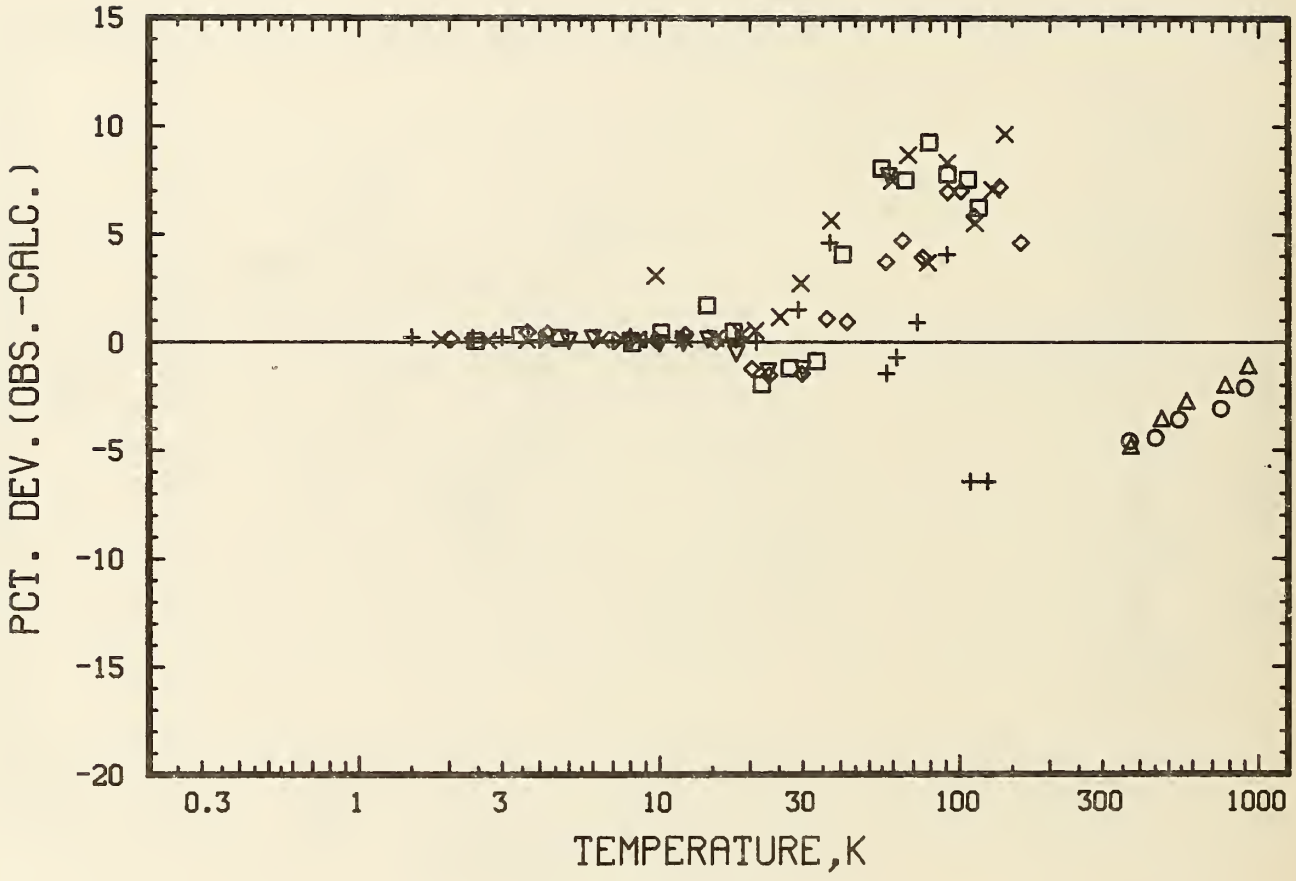


Figure 2.2.4 Thermal conductivity deviations of the copper data from the following primary references compared to eq. (1.1.3): (35,38,41,43)

○ - (35), △ - (38), □ - (41), ▽ - (41),
◇ - (41), + - (43), × - (43)

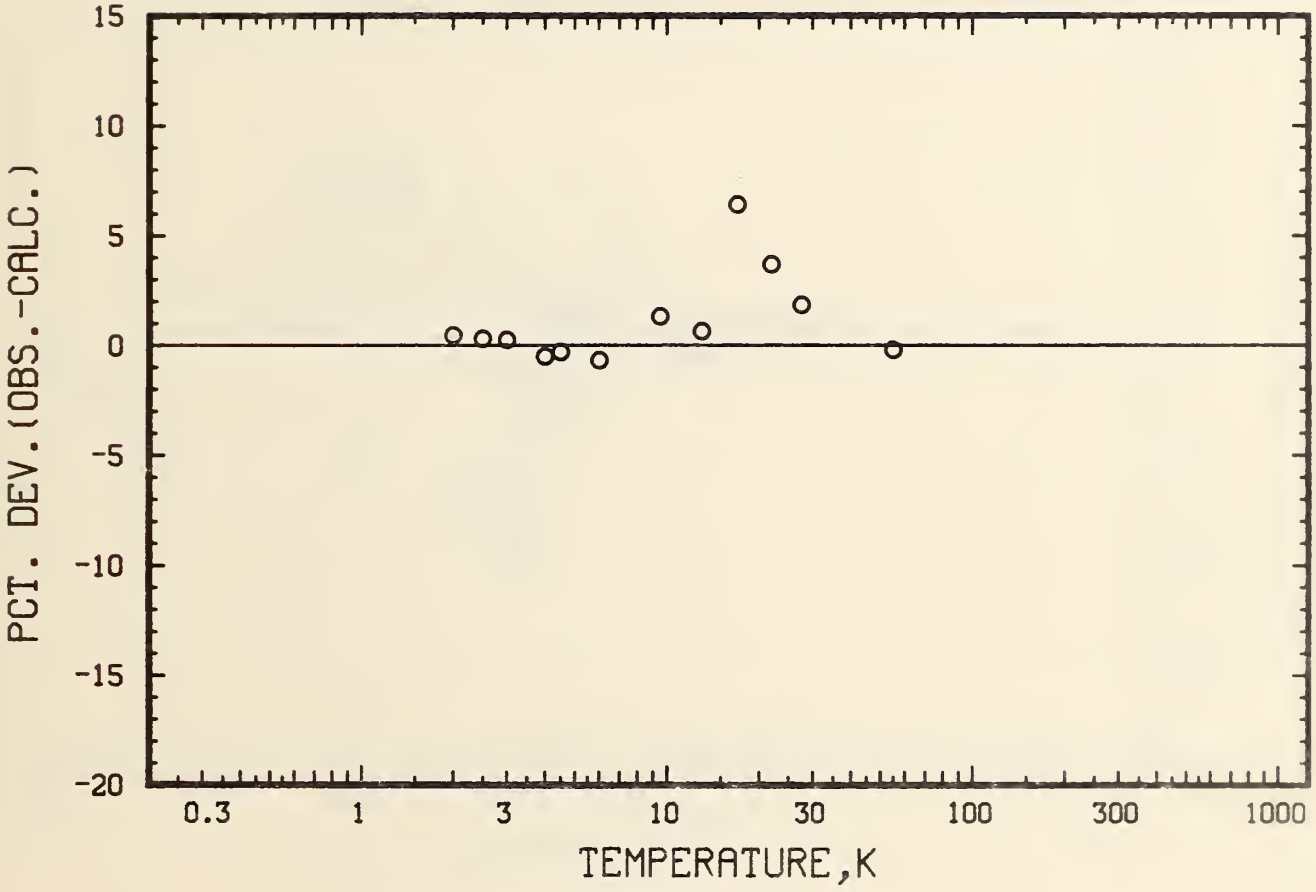


Figure 2.2.5 Thermal conductivity deviations of the copper data from the following primary reference compared to eq. (1.1.3): (42)

O - (42)

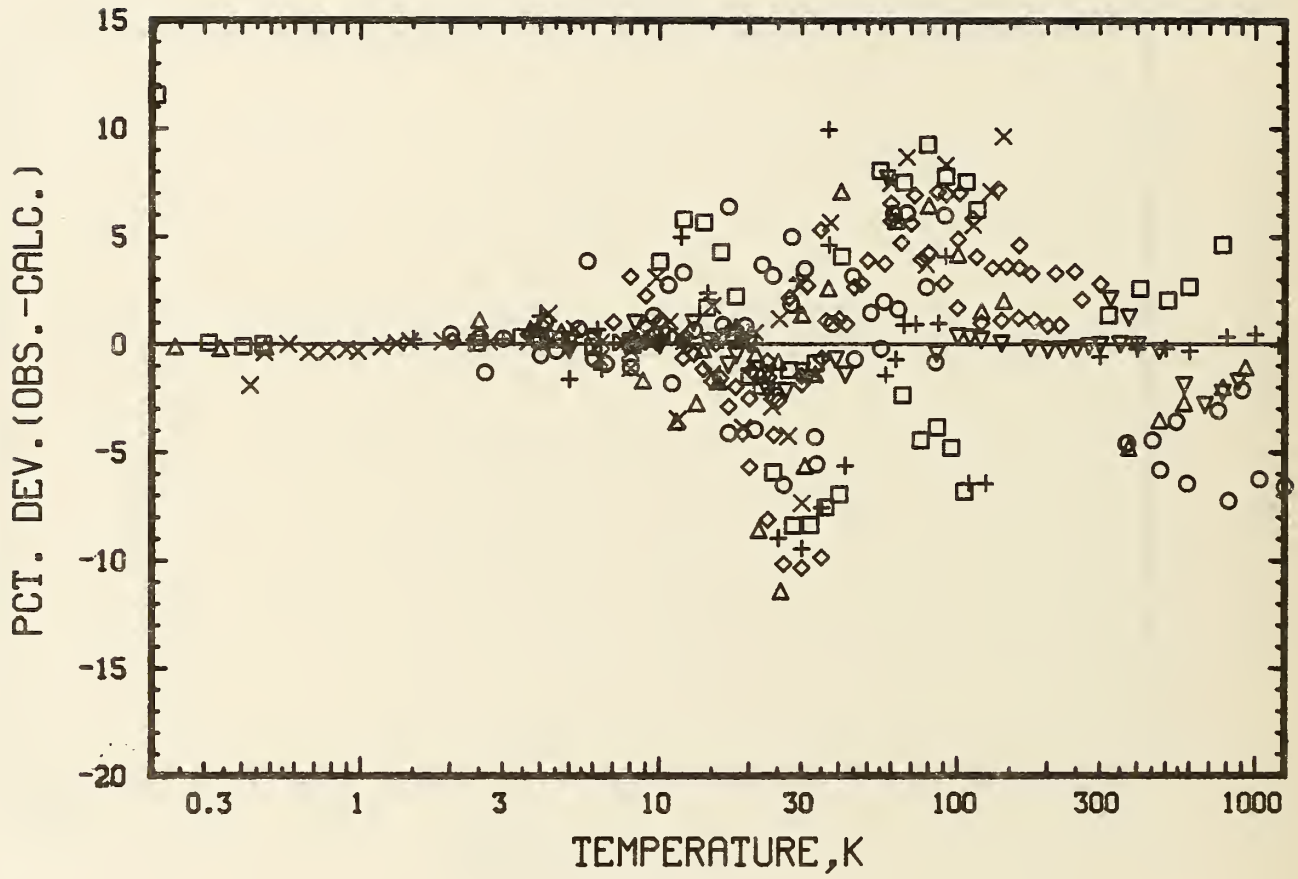


Figure 2.2.6 Composite of the deviations in figs. 2.2.1 through 2.2.5

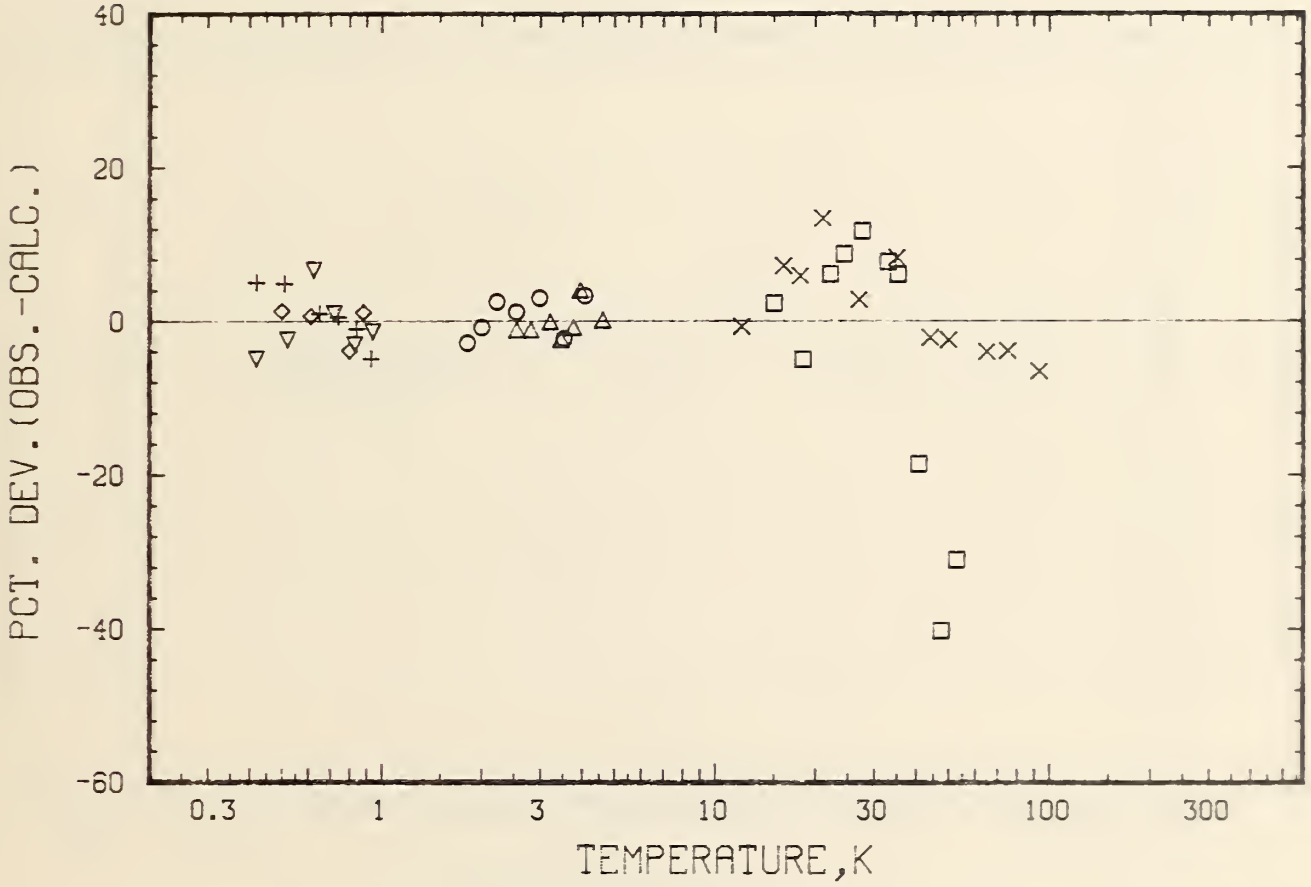


Figure 2.2.7 Thermal conductivity deviations of the copper data from the following secondary references compared to eq. (1.1.3):(1,2,3,6,9)

○ - (1), △ - (2), □ - (3), ▽ - (6),
◇ - (6), + - (6), × - (9)

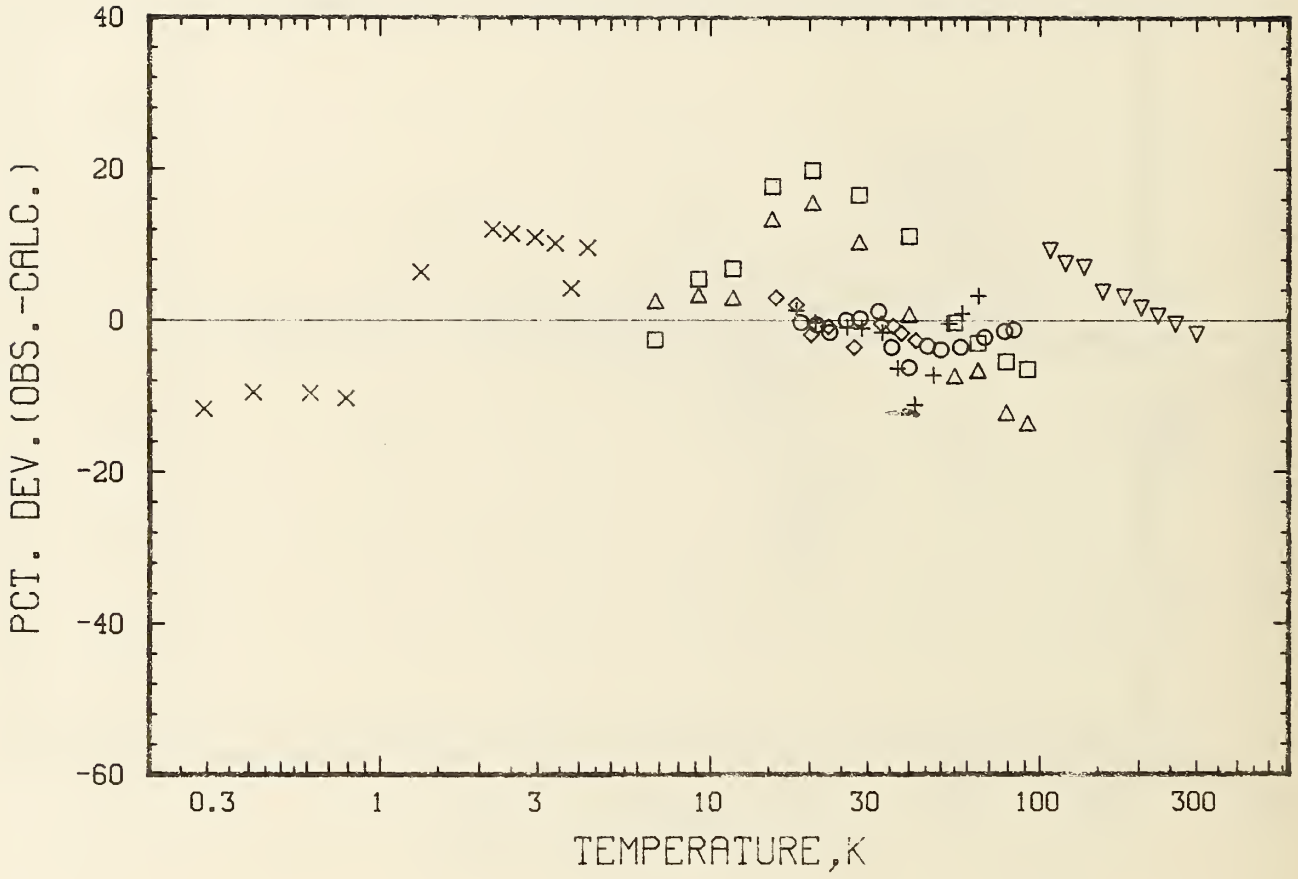


Figure 2.2.8 Thermal conductivity deviations of the copper data from the following secondary references compared to eq. (1.1.3):(10,15,17,22,25)

○ - (10), △ - (15), □ - (15), ▽ - (17),
◇ - (22), + - (22), × - (25)

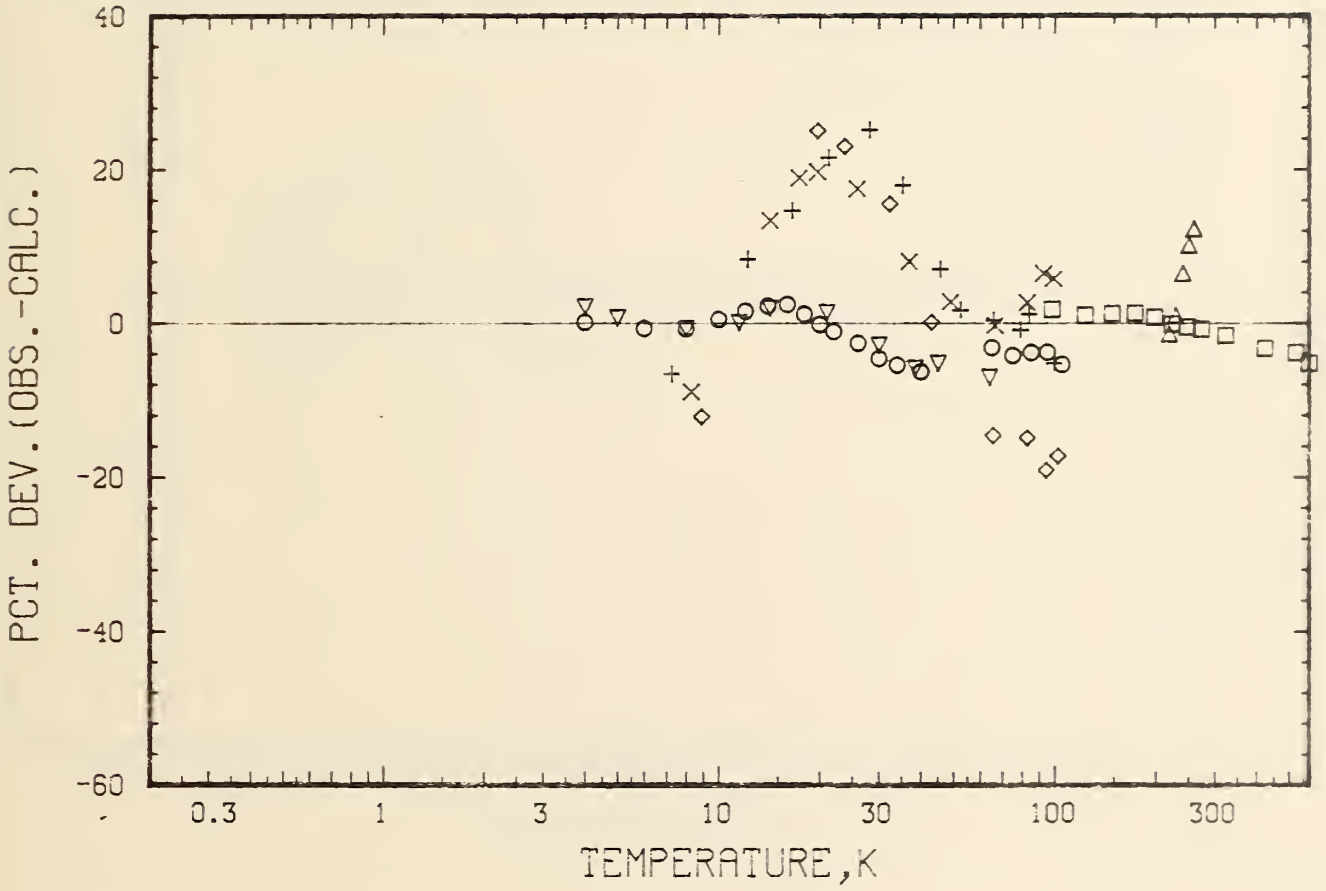


Figure 2.2.9 Thermal conductivity deviations of the copper data from the following secondary references compared to eq. (1.1.3):(26,31,32,33,37)

○ - (26), △ - (31), □ - (32), ▽ - (33),
◇ - (37), + - (37), × - (37)

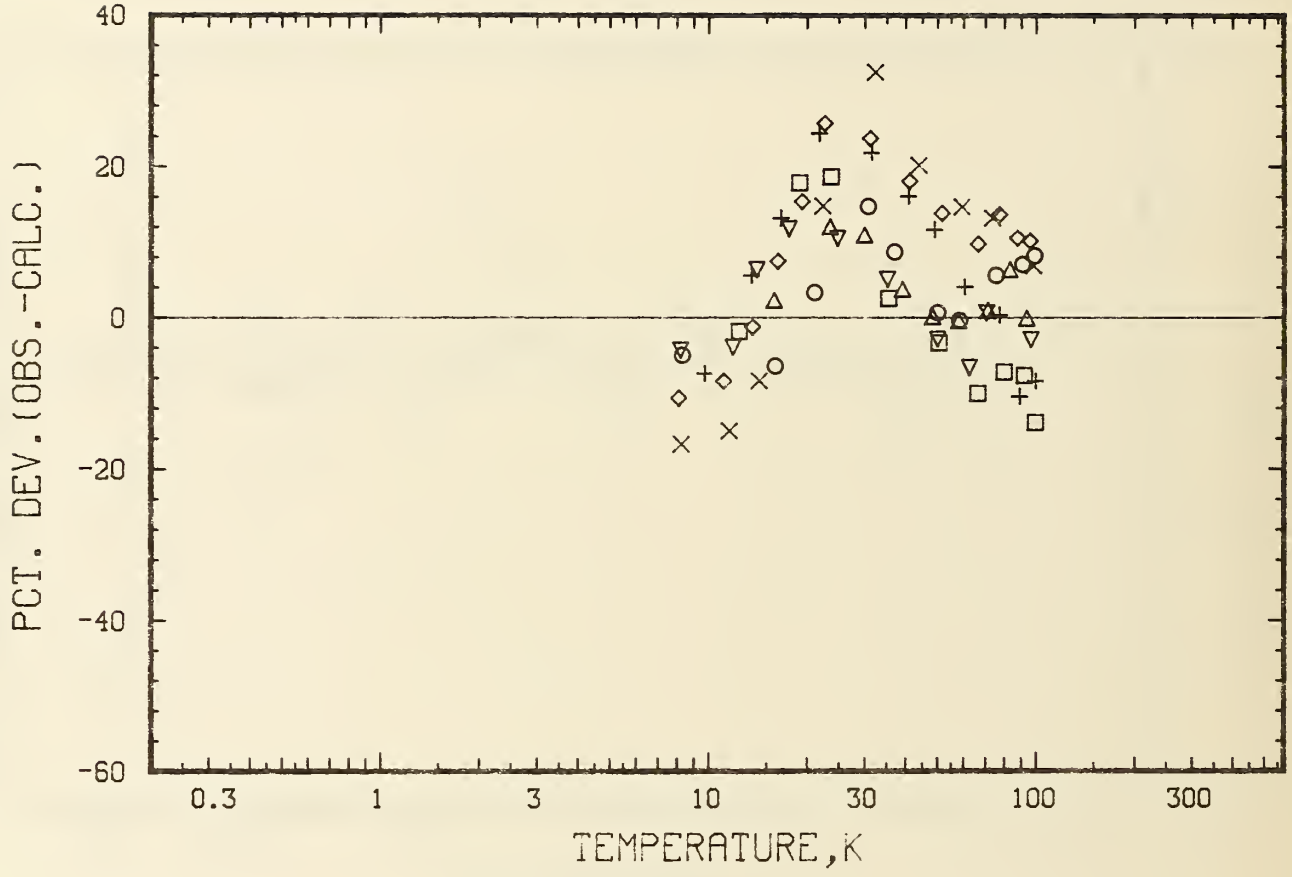


Figure 2.2.10 Thermal conductivity deviations of the copper data from the following secondary reference compared to eq. (1.1.3):(37)

○ - (37), △ - (37), □ - (37), ▽ - (37),
◇ - (37), + - (37), × - (37)

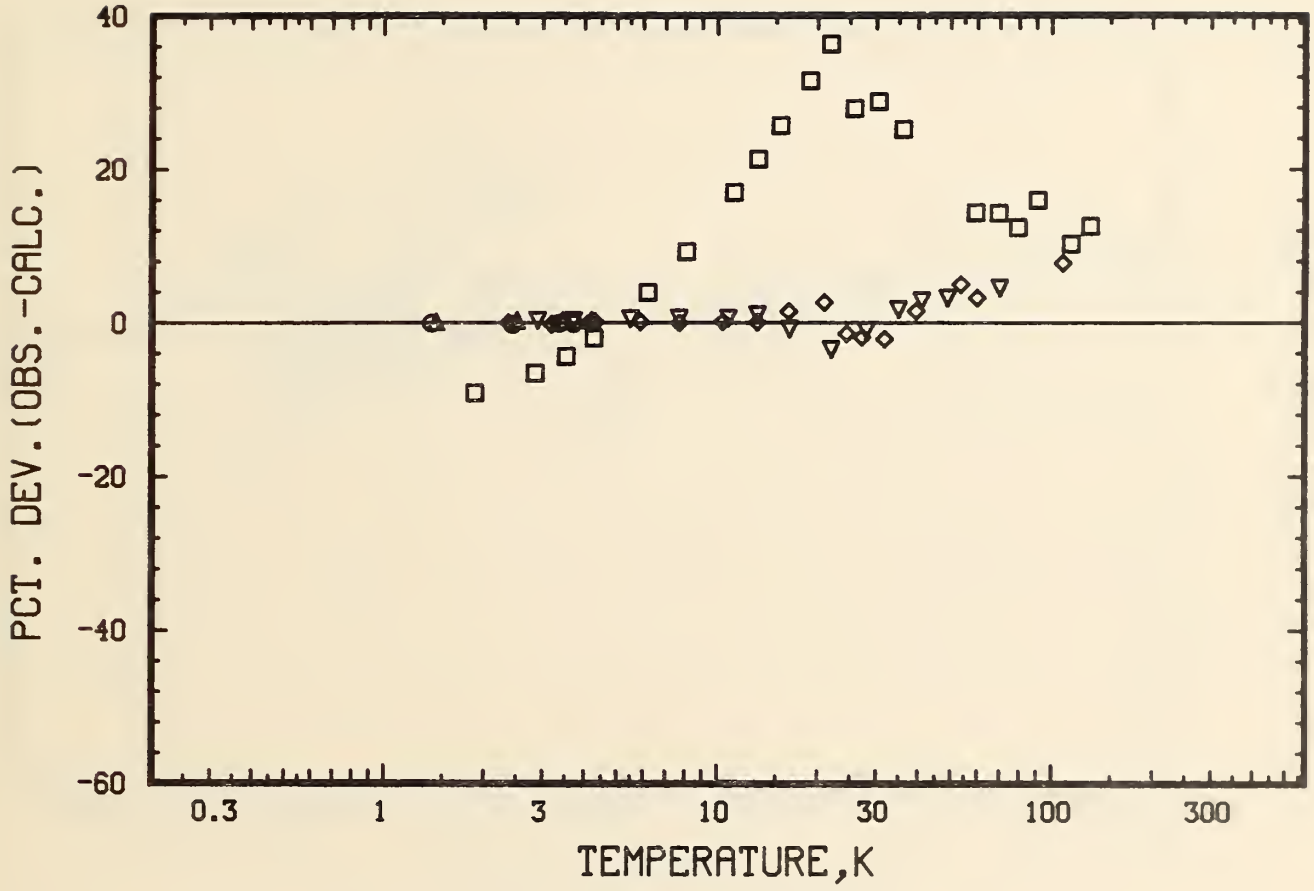


Figure 2.2.11 Thermal conductivity deviations of the copper data from the following secondary references compared to eq. (1.1.3):(40,43,44)

○ - (40), △ - (40), □ - (43), ▽ - (44), ◇ - (44)

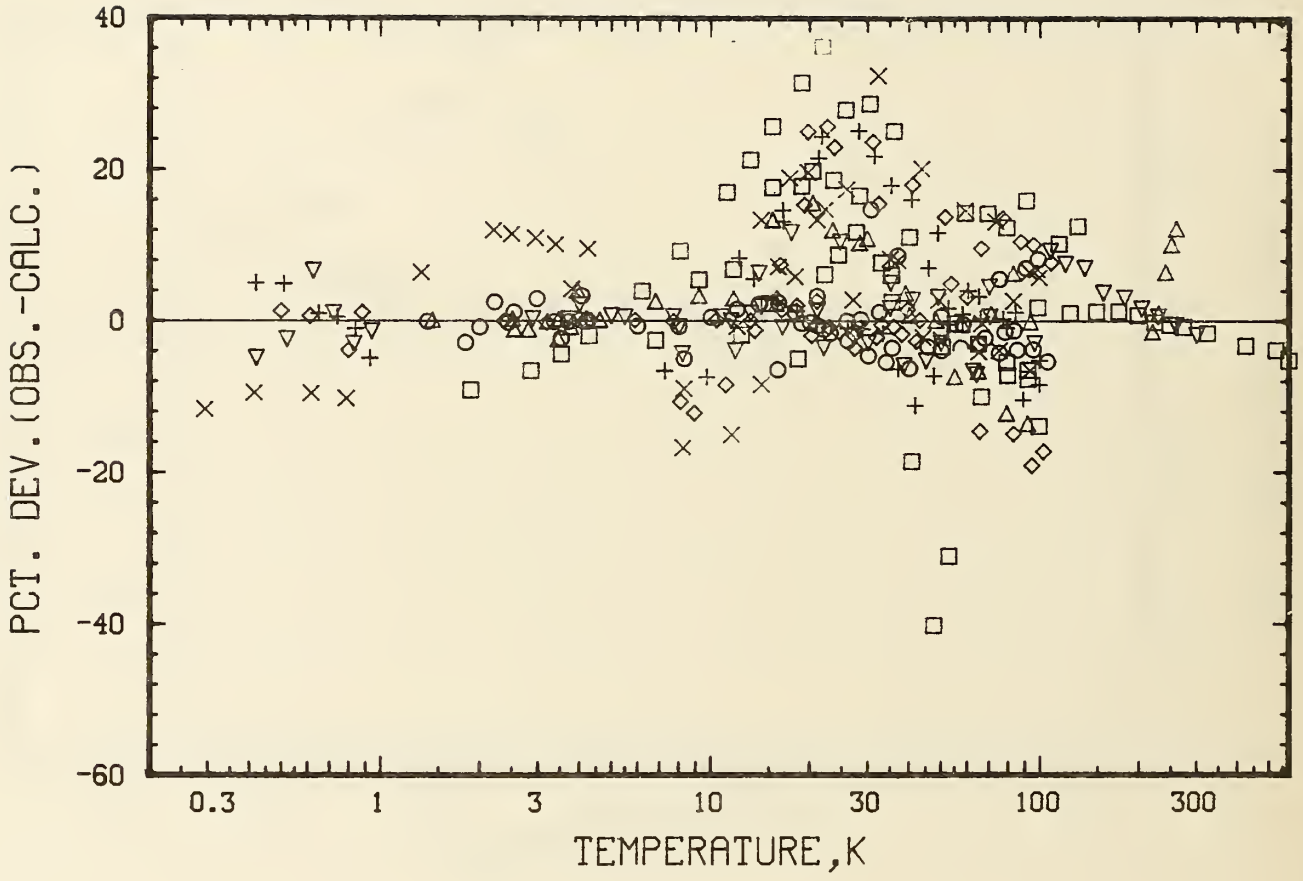


Figure 2.2.12 Composite of the deviations in figs.2.2.7 through 2.2.11

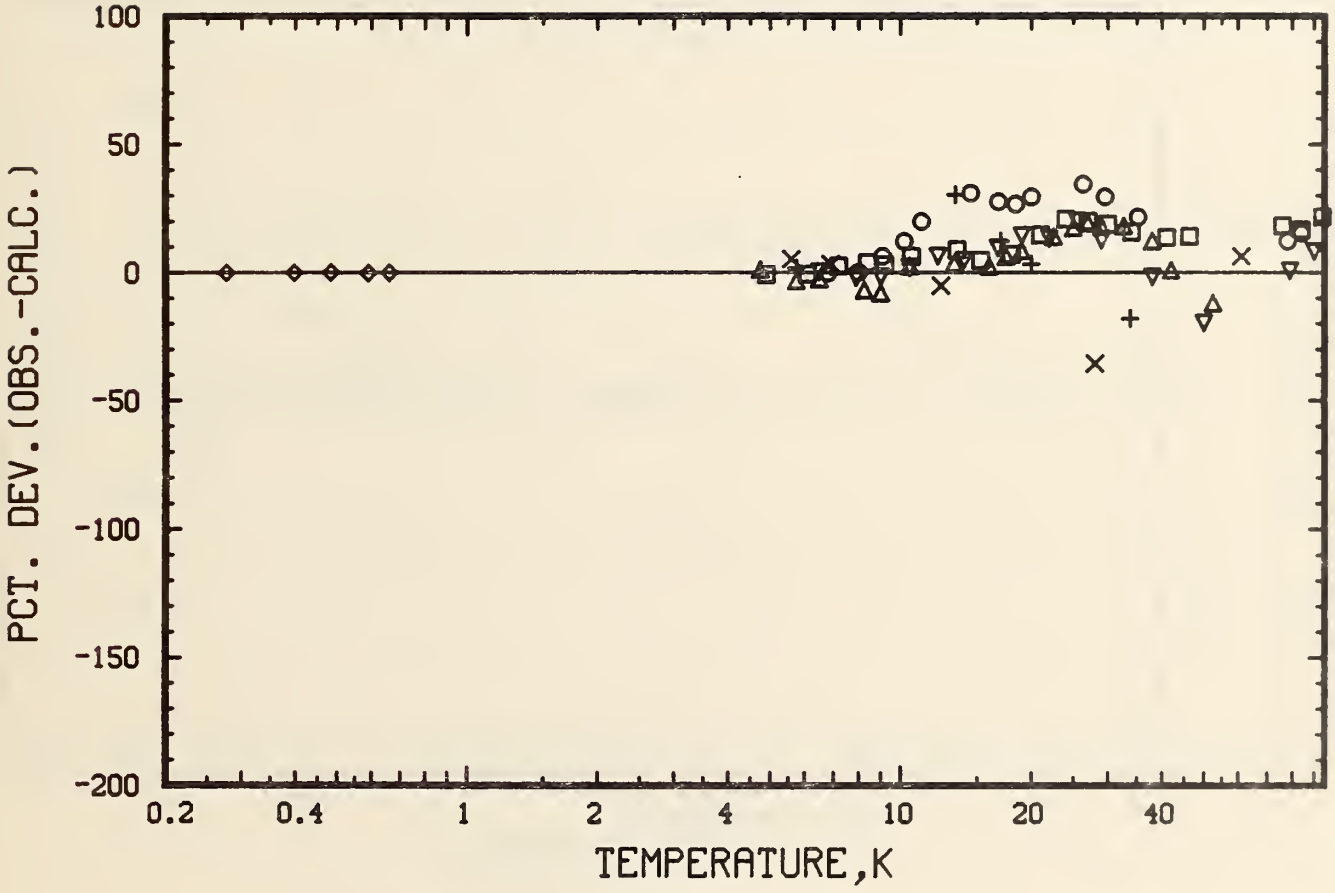


Figure 2.2.13 Thermal conductivity deviations of the copper data from the following secondary references compared to eq. (1.1.3):(5,7,12)

○ - (5), △ - (5), □ - (5), ▽ - (5),
◇ - (7), + - (12), × - (12)

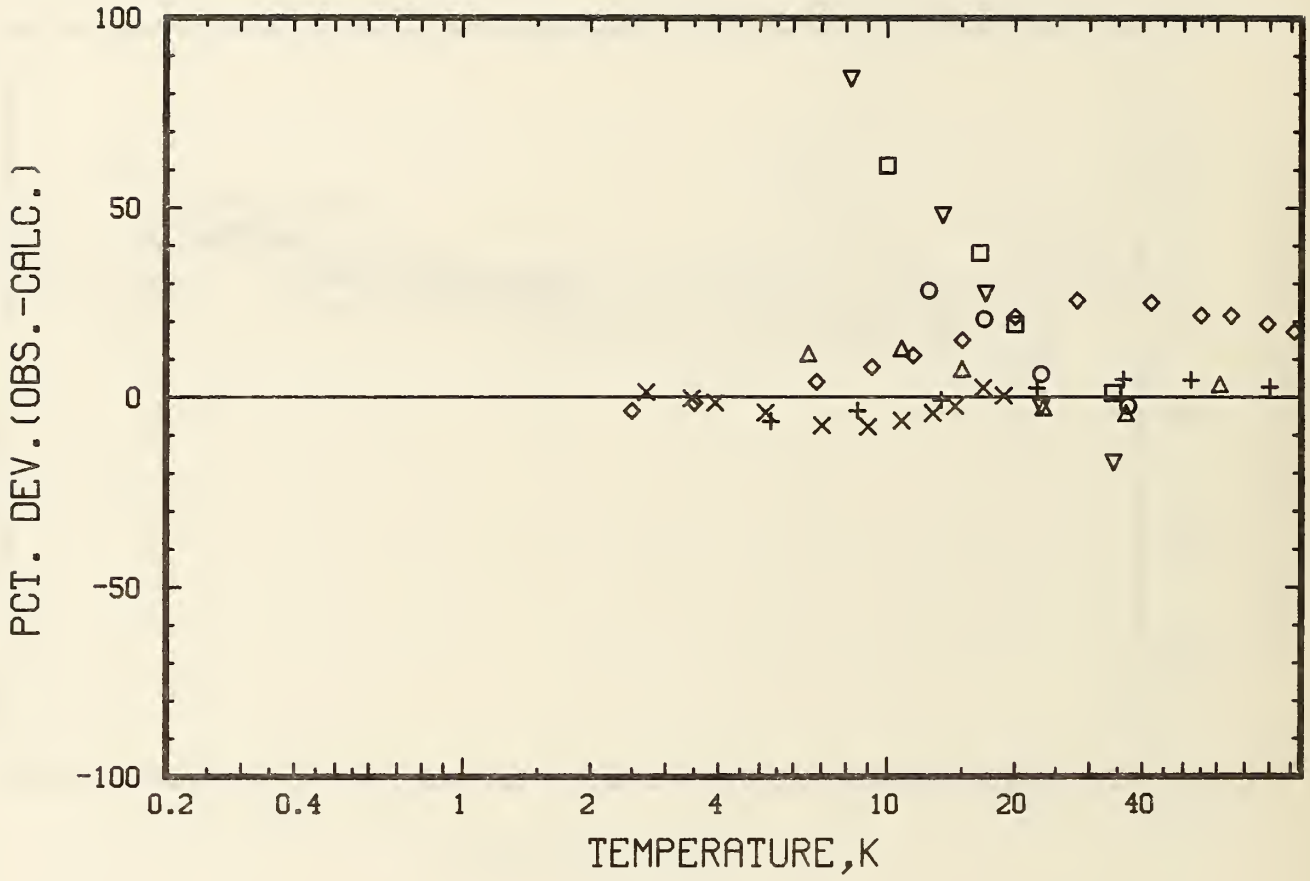


Figure 2.2.14 Thermal conductivity deviations of the copper data from the following secondary references compared to eq. (1.1.3):(11,12,15,27,36)

○ - (12), △ - (12), □ - (11), ▽ - (11),
◇ - (15), + - (27), × - (36)

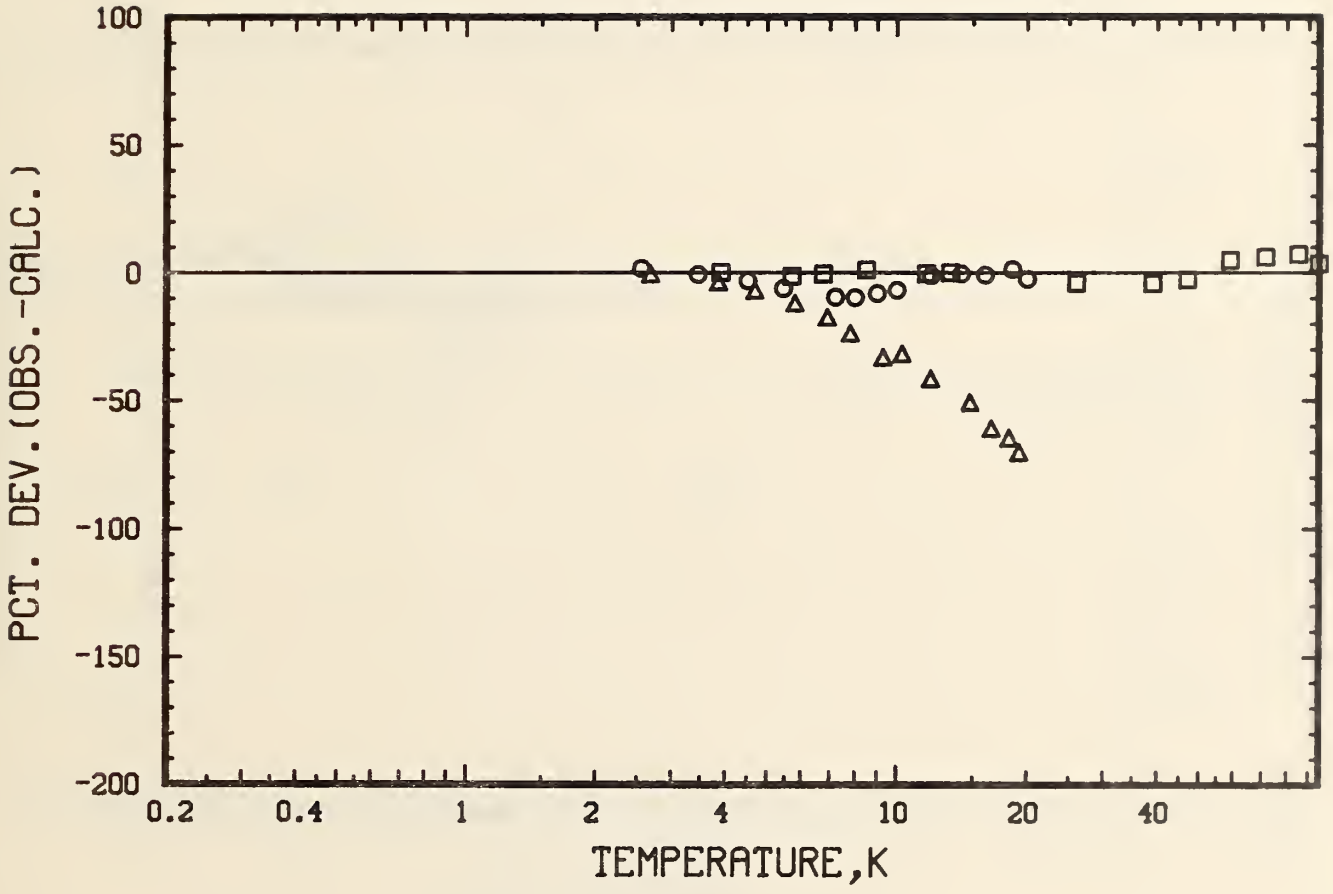


Figure 2.2.15 Thermal conductivity deviations of the copper data from the following secondary references compared to eq. (1.1.3):(36,44)

○ - (36), △ - (36), □ - (44)

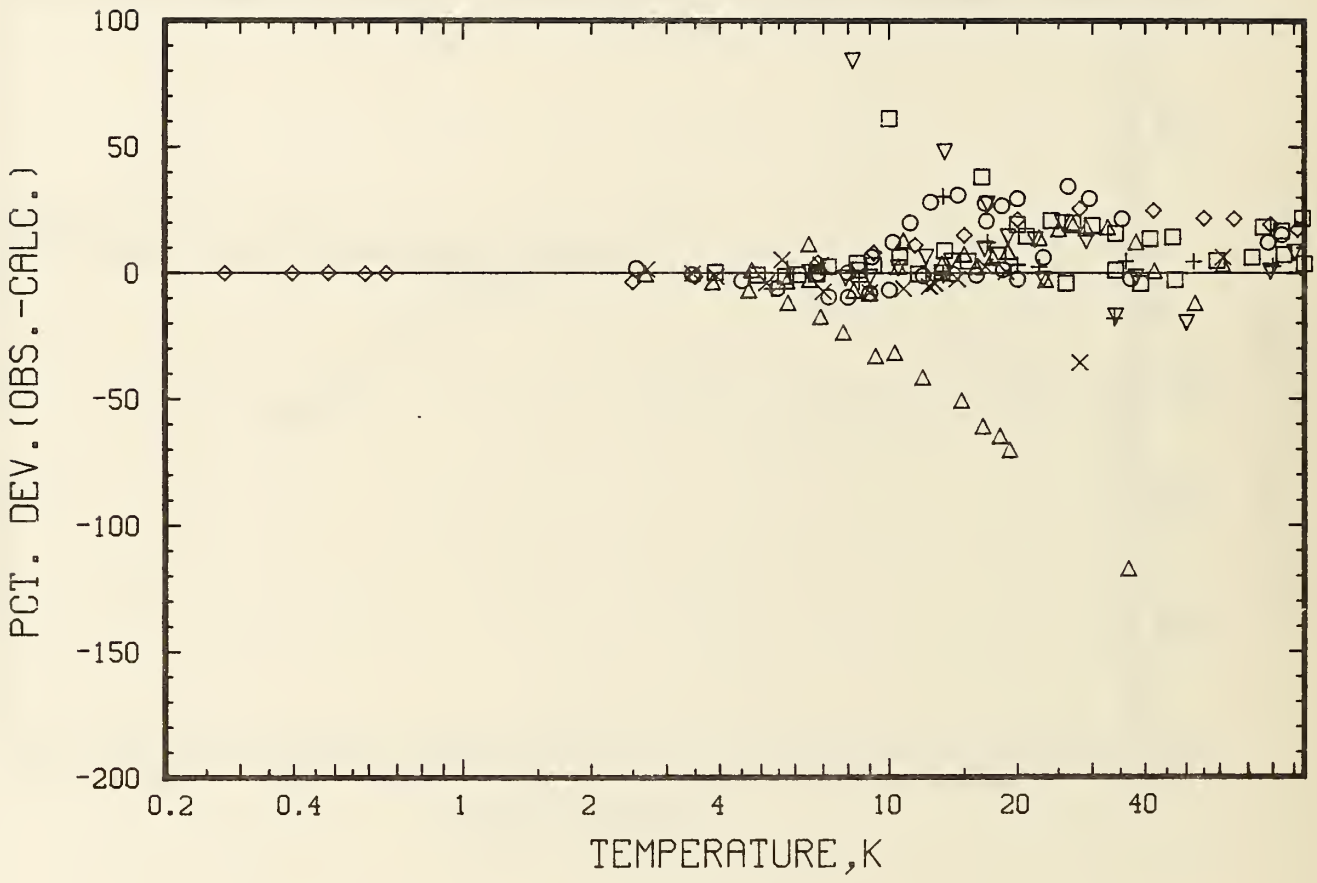


Figure 2.2.16 Composite of the deviations in figs. 2.2.13 through 2.2.15

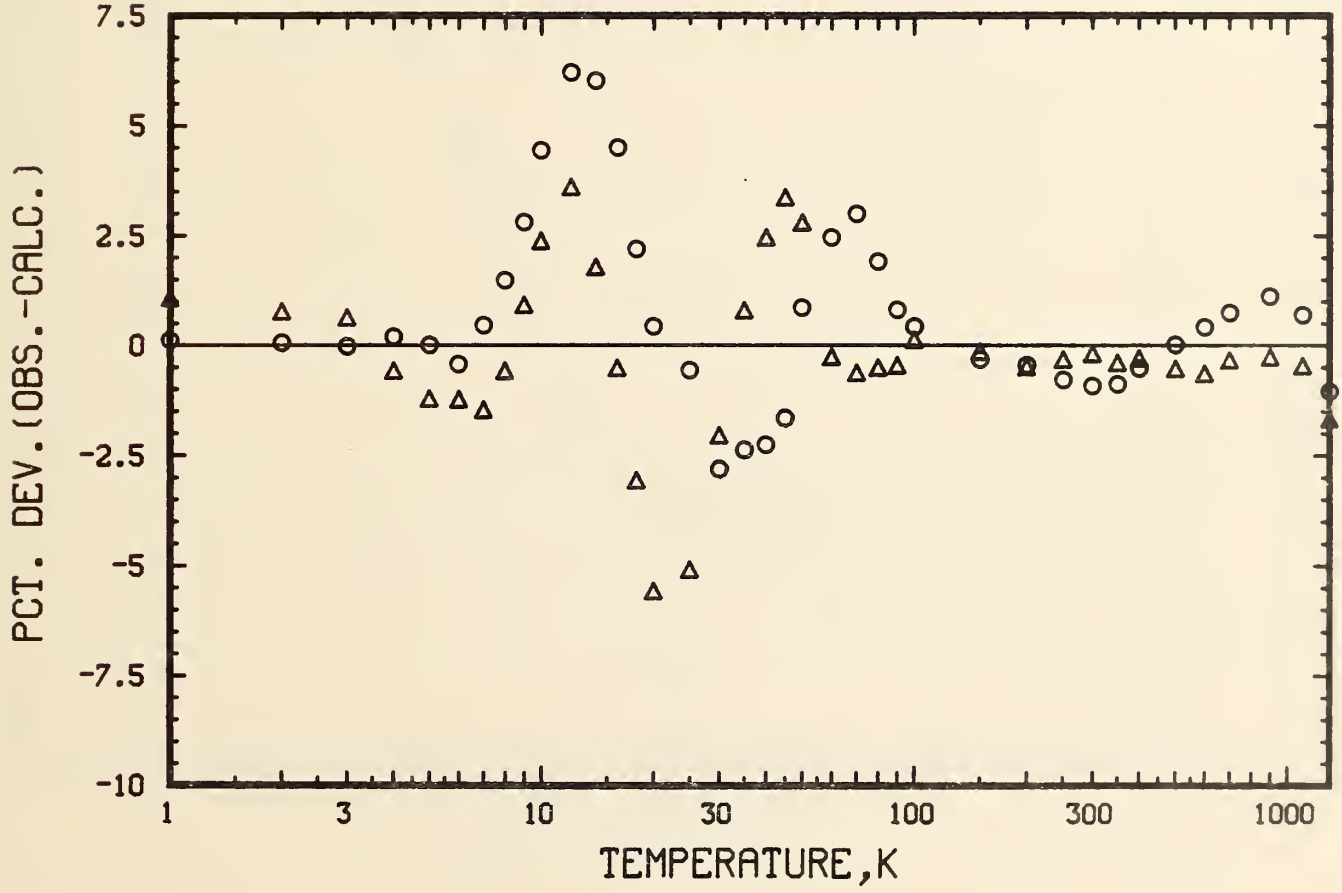


Figure 2.2.17 Comparison of eq.(1.1.3) to the values recommended for copper in the following references:(13,39)

O - (39), Δ - (13)

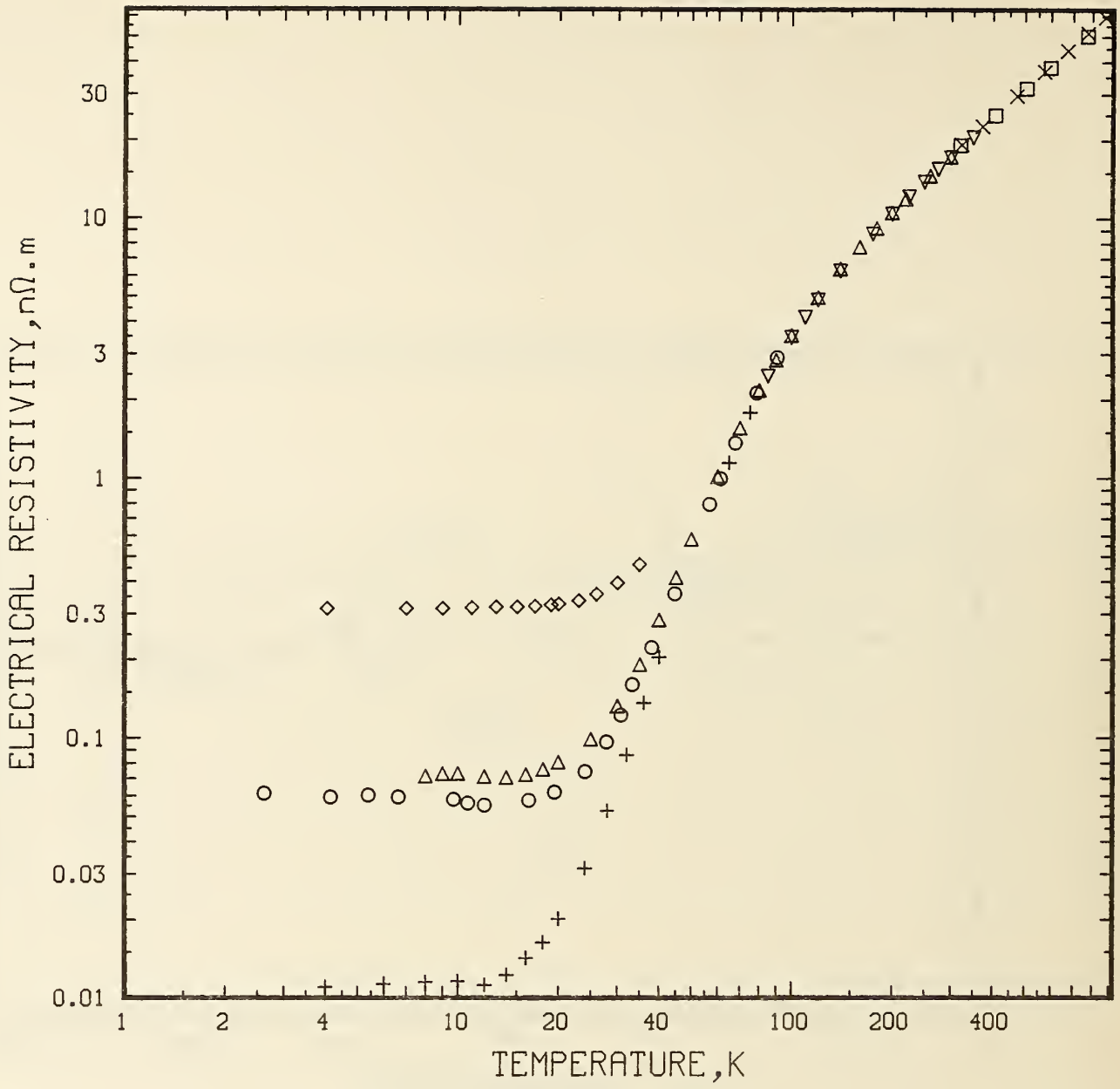


Figure 2.3.1 Experimental electrical resistivity data for copper selected from the following references in the copper annotated bibliography: (4,14,21,23,24,26,29)

○ - (4), △ - (14), □ - (21), ▽ - (23),
◇ - (24), + - (26), × - (29)

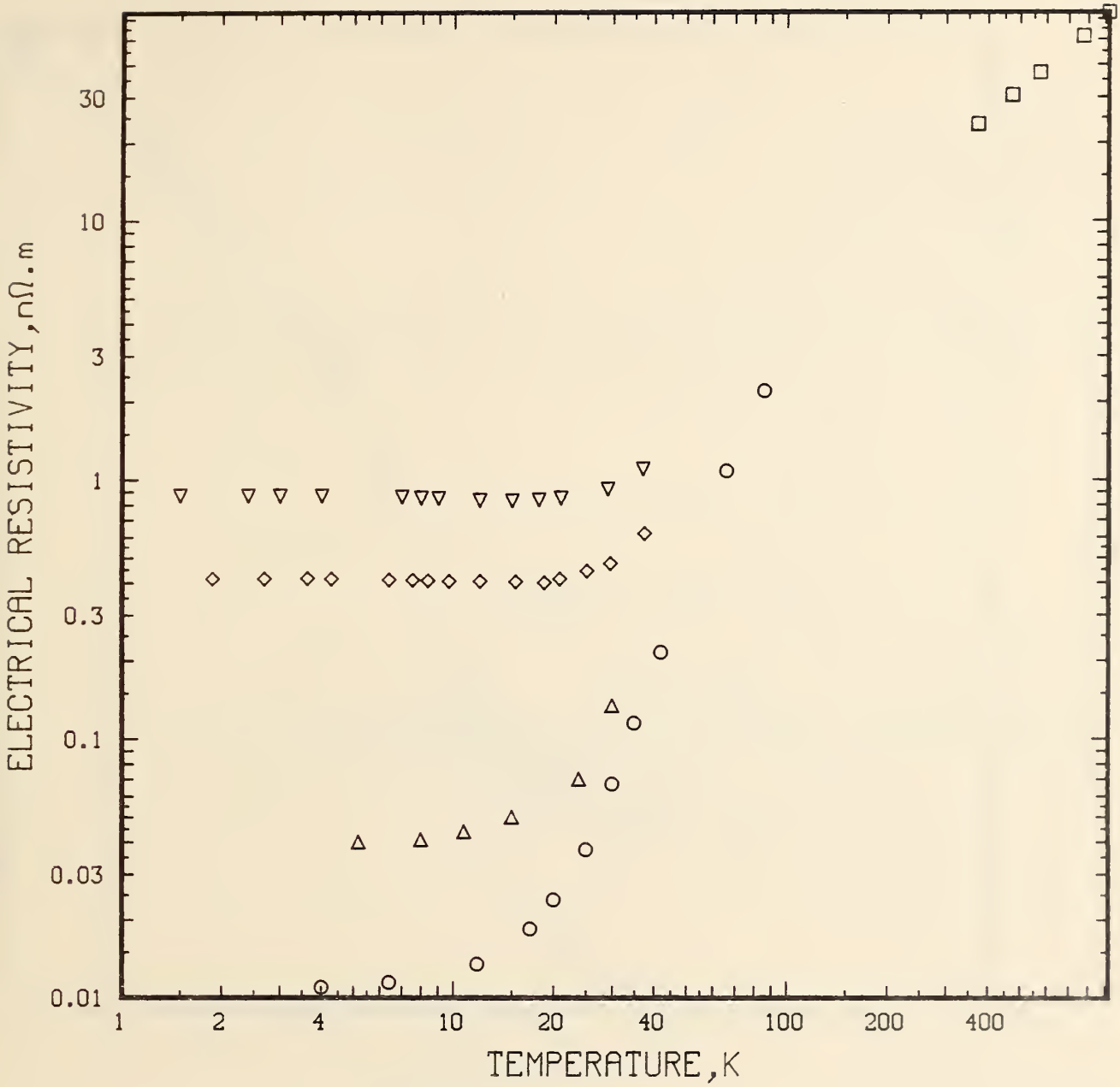


Figure 2.3.2 Experimental electrical resistivity data for copper selected from the following references in the copper annotated bibliography: (33,38,43)

○ - (33), △ - (33), □ - (38), ▽ - (43), ◇ - (43)

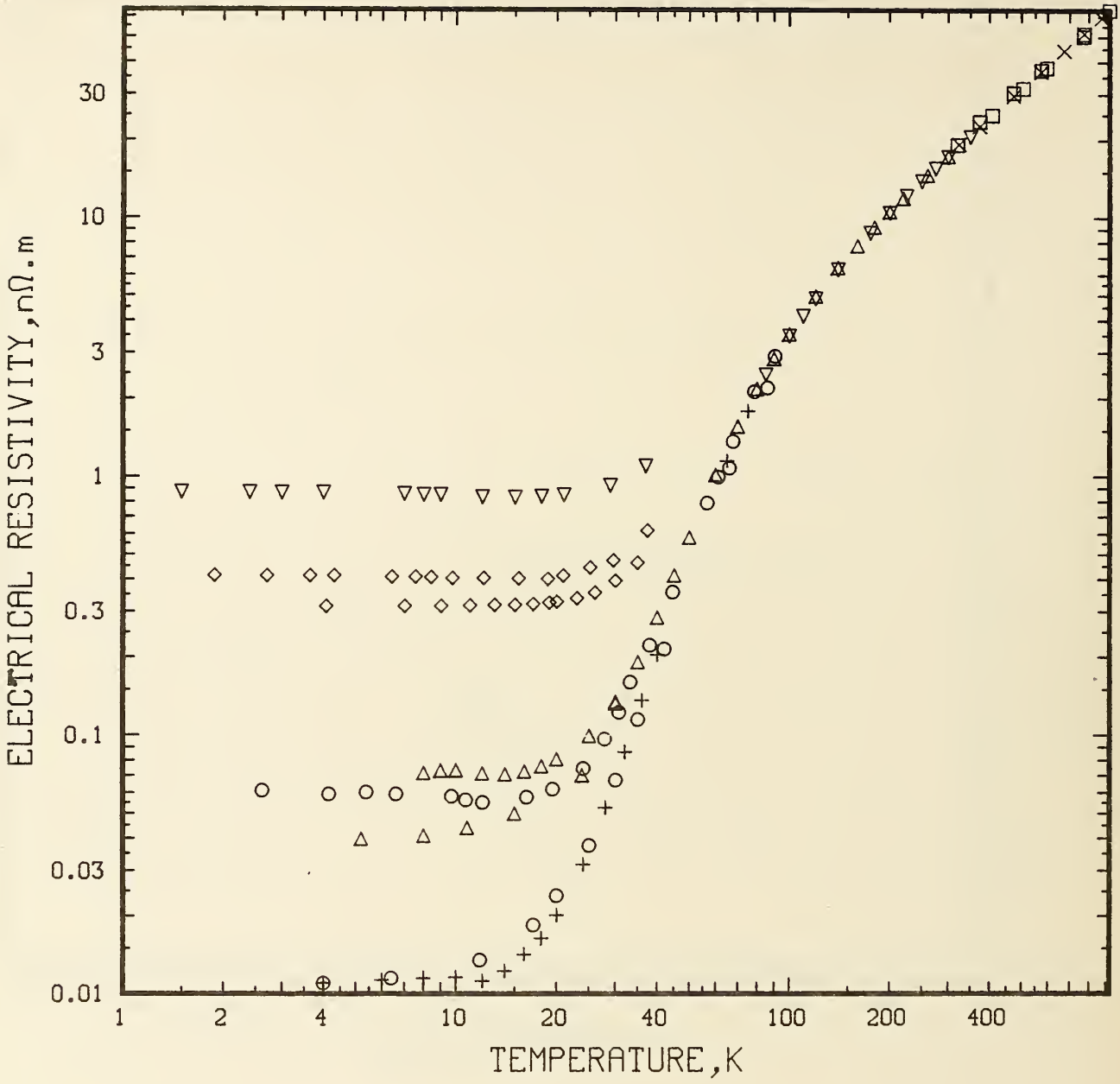


Figure 2.3.3 Composite of the electrical resistivity data in figs. 2.3.1 and 2.3.2

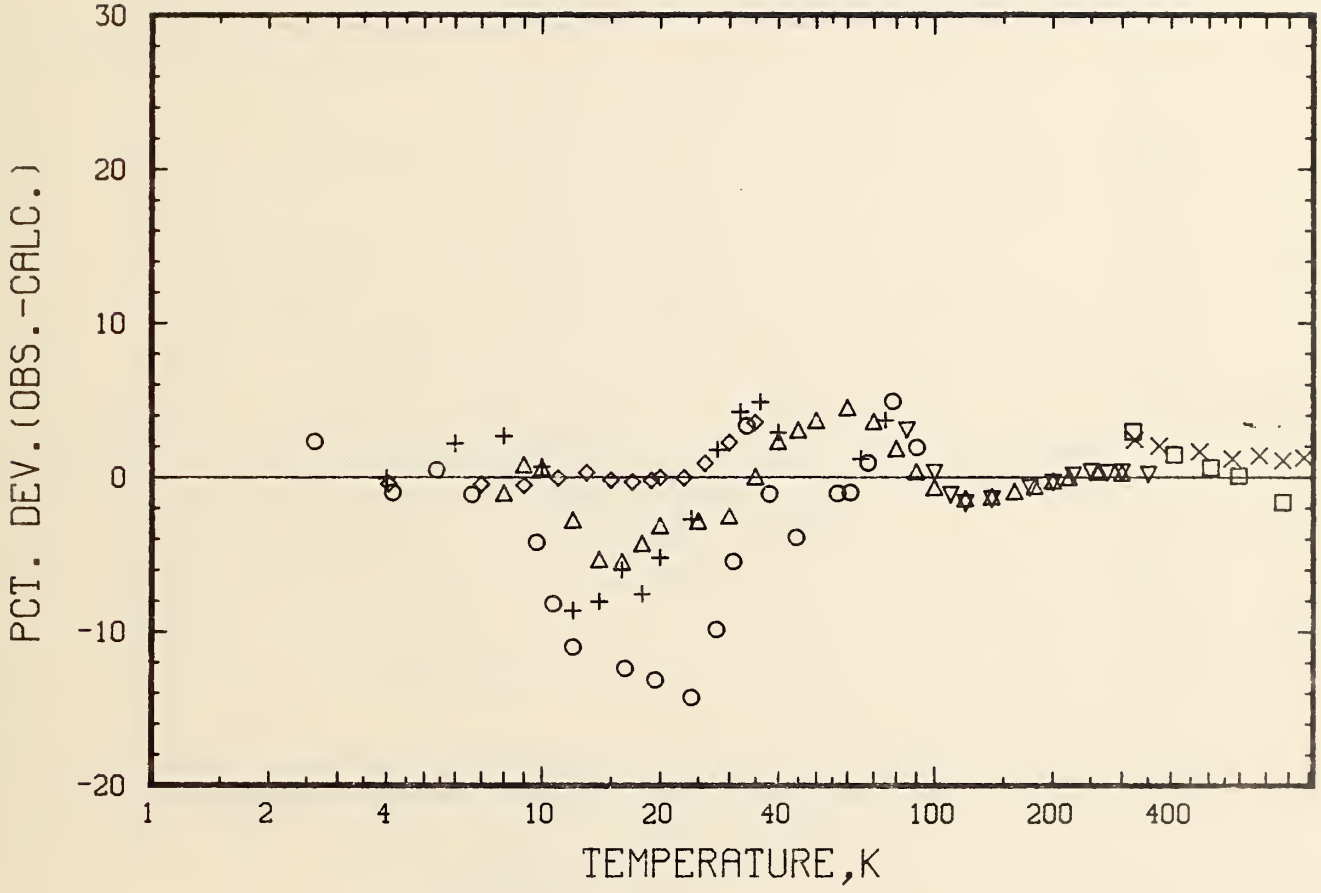


Figure 2.3.4 Electrical resistivity deviations of the copper data from the following references compared to eq. (1.2.3):(4,14,21,23,24,26,29)

○ - (4), △ - (14), □ - (21), ▽ - (23),
◇ - (24), + - (26), × - (29)

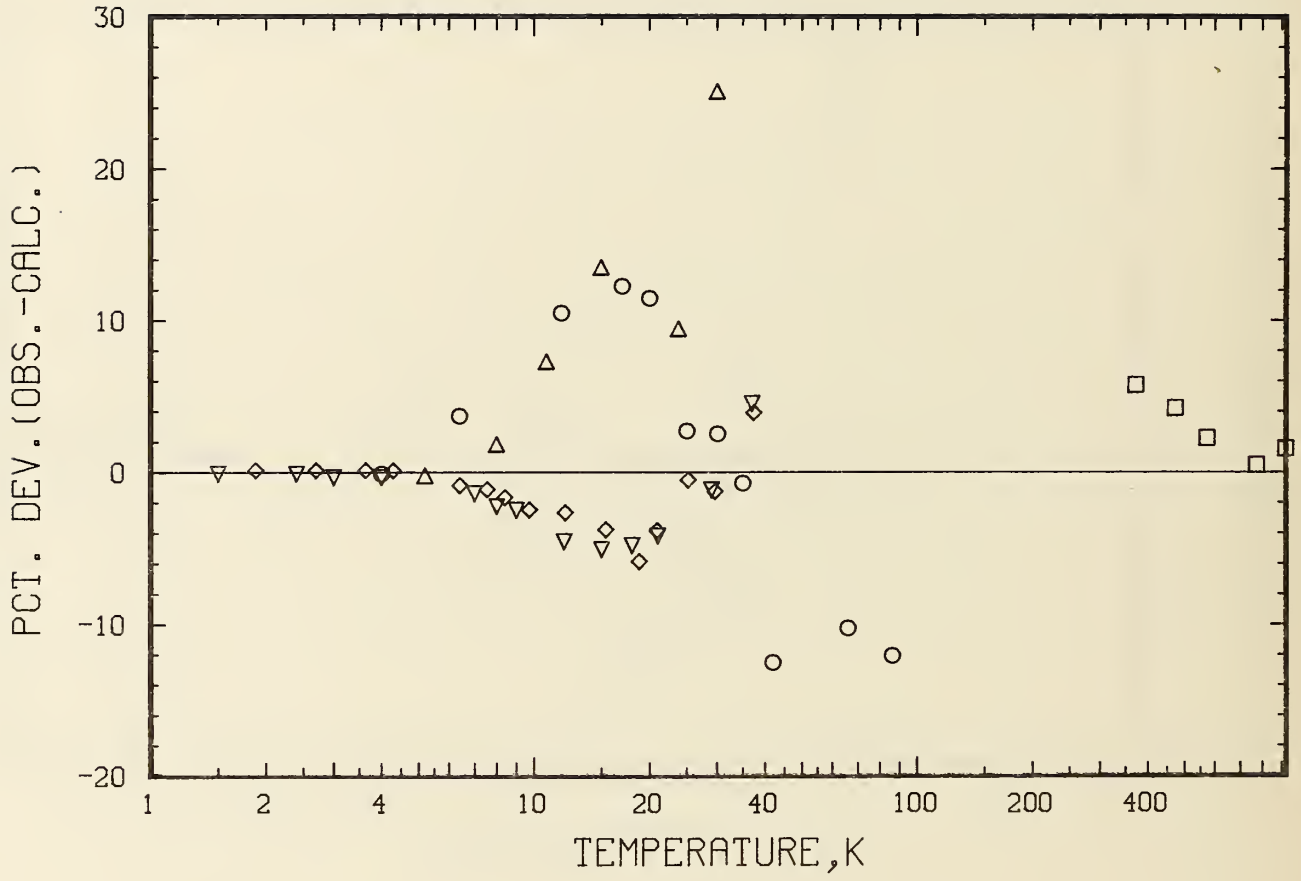


Figure 2.3.5 Electrical resistivity deviations of the copper data from the following references compared to eq. (1.2.3):(33,38,43)

○ - (33), △ - (33), □ - (38), ▽ - (43), ◇ - (43)

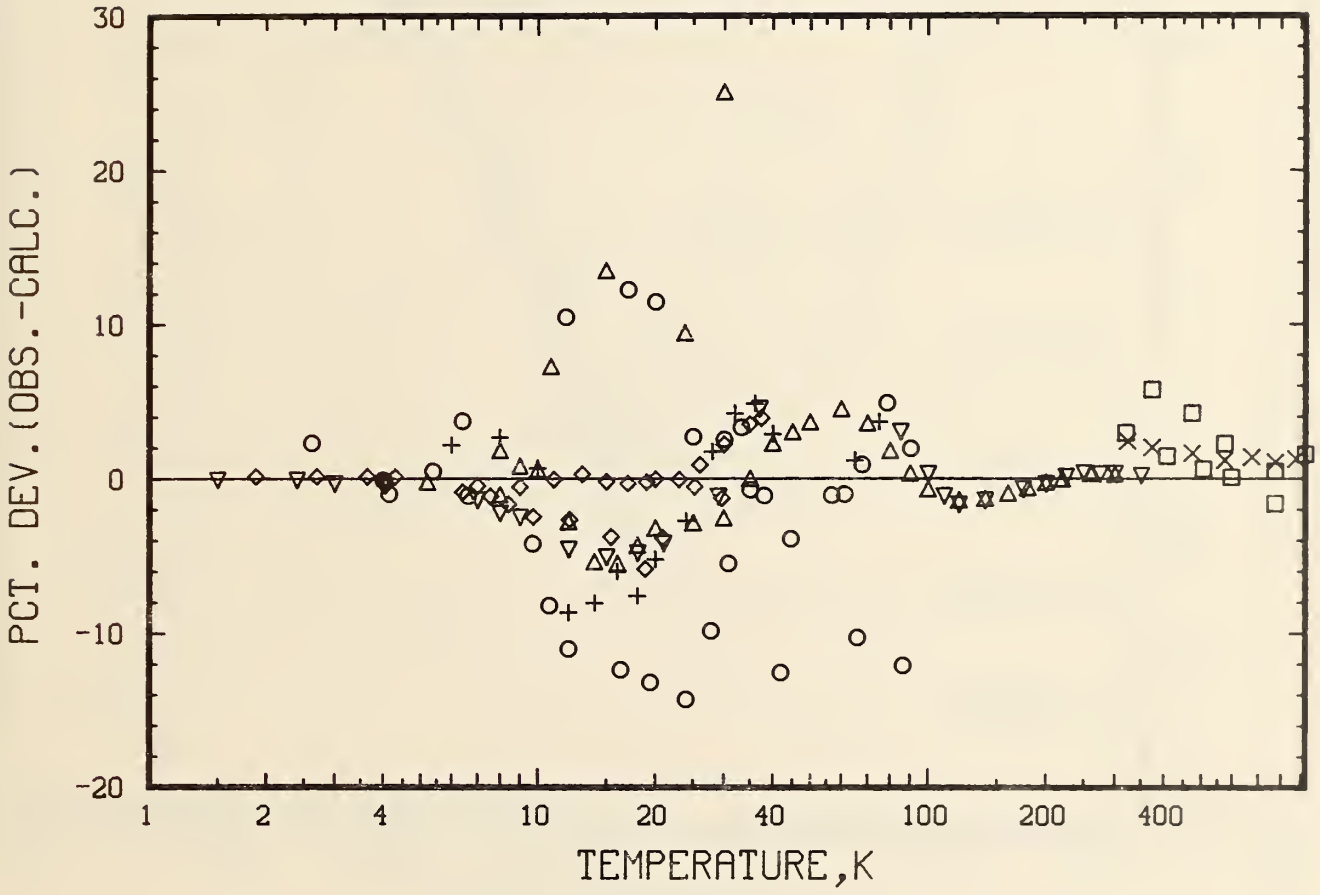


Figure 2.3.6 Composite of the electrical resistivity deviations shown in figs. 2.3.4 and 2.3.5

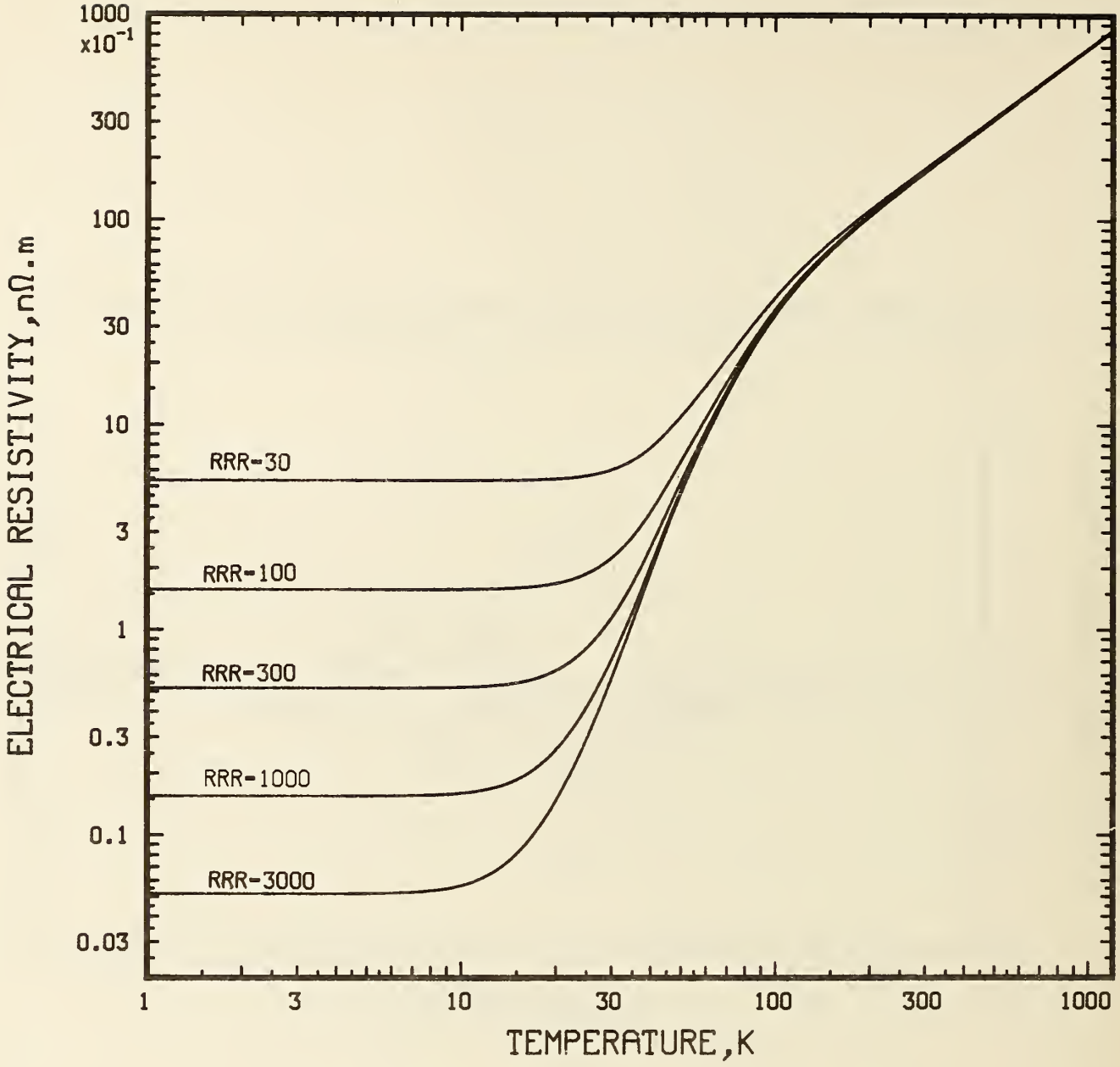


Figure 2.3.7 Electrical resistivity for copper as a function of temperature calculated from eq.(1.2.3) at selected values of RRR.

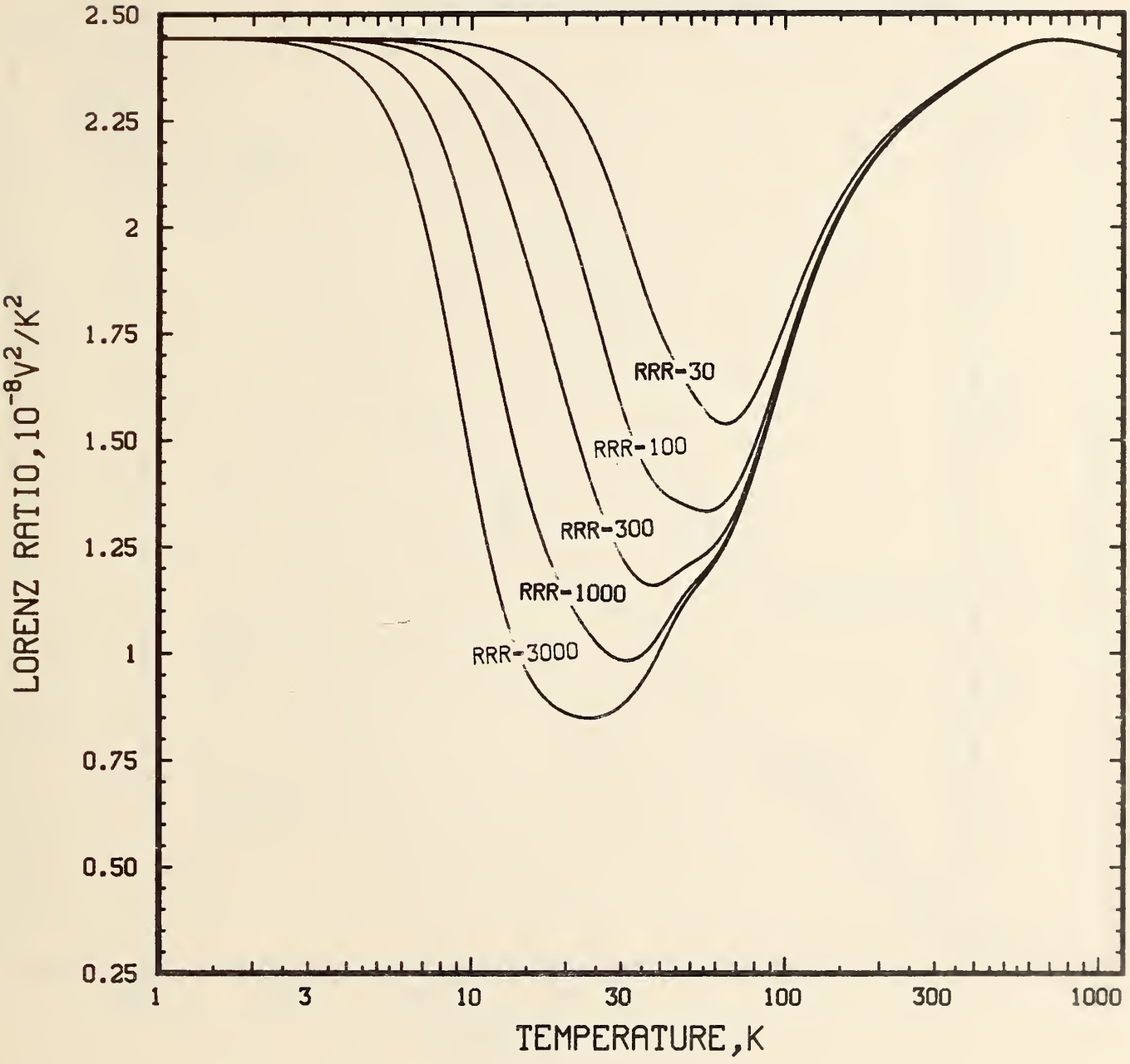


Figure 2.3.8 Lorenz ratio for copper as a function of temperature calculated from eq.(1.2.3) and eq.(1.1.3) at selected values of RRR.

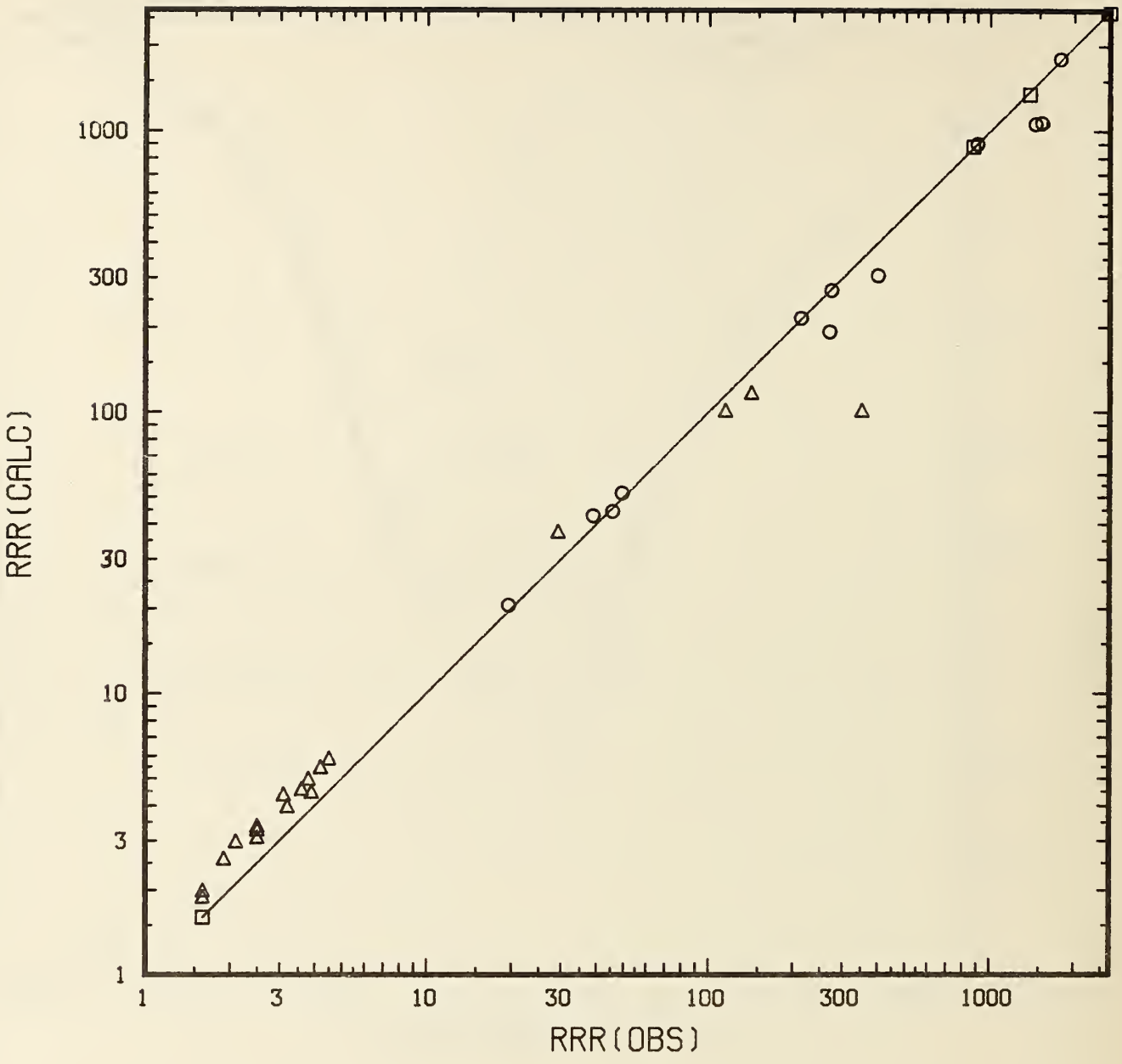


Figure 2.3.9 RRR values calculated as per Section 1.5, RRR(CALC), versus reported RRR values, RRR(OBS), for copper.

○ = Primary, △ = Secondary,
□ = Secondary

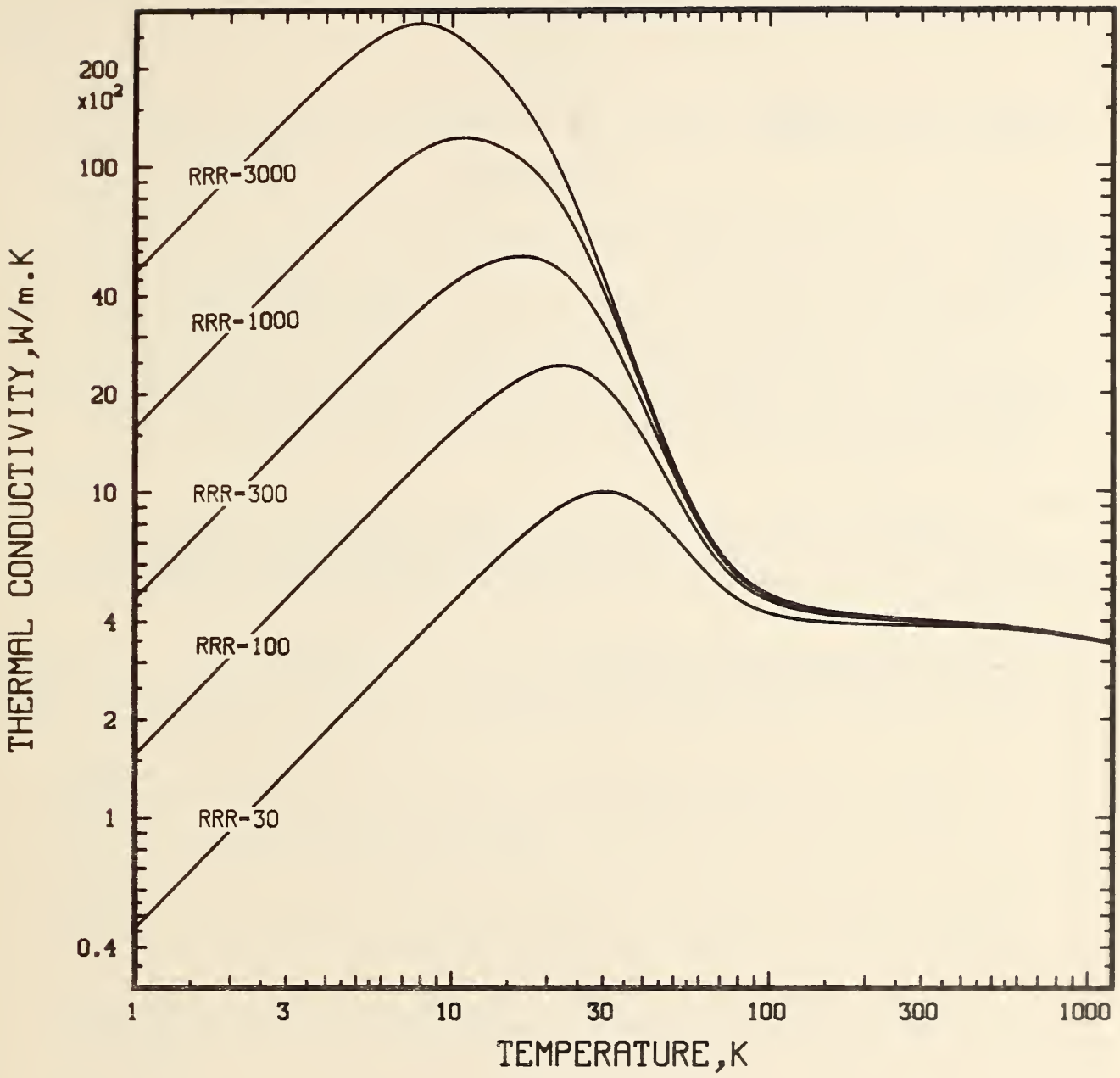


Figure 2.4.1 Thermal conductivity for copper as a function of temperature calculated from eq.(1.1.3) at selected values of RRR.

## 2.5 FORMAT FOR ANNOTATED BIBLIOGRAPHY OF COPPER

### REFERENCE

AUTHOR, TITLE, CITATION

### ANNOTATION

PURPOSE

SPECIMEN
a) Dimensions/Shape; b) Crystal Status; c) Thermal/Mech. History; d) Purity Specification; e) RRR; f) $\rho_0$; g) Other Characterization Data

APPARATUS
a) Type; b) Thermometry/Calibration/Anchoring; c) Thermal Isolation; d) Other (Q meas.)

DATA
a) Temperature Range/Difference; b) Content of Tables, Figures and Equations/Data Extraction; c) Uncertainty/Imprecision; d) Disputable Corrections to Measurements by Authors; e) Errata (by Author or Reviewer)

ANALYSIS
a) Comparisons; b) Conclusions

[1] Allen, J. F. and Mendoza, E., Thermal Conductivity of Copper and German Silver at Liquid Helium Temperatures, Proc. Cambridge Philos. Soc., 44, 280-8 (1948)

PURPOSE
To describe a longitudinal apparatus and perform $\lambda$ measurements on copper and German silver.

SPECIMEN
a) /rod; c) annealed in air/machined before and after annealing; d) 0.003% Ag, 0.003% Ni, 0.003% Pb, 02 free; f) $\rho o = 5.5 \times 10^{-8}$ $\Omega \cdot cm$; g) source: Johnson, Matthey and Co., No. 1562.

APPARATUS
a) longitudinal; b) phosphor-bronze thermometers/calibrated in terms of vapor pressure of He bath using 1932 scale/thermometer leads thermally grounded to can; c) radiation shield, vacuum insulation.

DATA
a) 1.8 to 4.1 K/0.01 K maximum; b) figure 2 - $\lambda$; c) uncertainty: ±2%.

ANALYSIS
b) in agreement with Makinson's theory.

[2] Andrews, F. A., Webber, R. T., and Spohr, D. A., Thermal Conductivity of Copper, Aluminum and Tin at Helium Temperatures, ASTIA AD No. 147716; Contract No. AF 33(616)-56-8

PURPOSE
To measure $\lambda$ for Cu, Al, Sn and for Sn in low magnetic field, and determine an emperical relationship.

SPECIMEN
a) /rod; b) polycrystalline; d) 99.998% Cu; g) source: Johnson, Matthey and Co.

APPARATUS
a) longitudinal; b) gas thermometers; c) radiation shield, vacuum insulation.

DATA
a) 2.5 to 4.6 K; b) figure 2 - $\lambda$; c) uncertainty: ±4% at $T < 4.5$ K, > 4% at $T > 4.5$ K; d) corrections for second virial coefficient and oil volume change for gas thermometry.

ANALYSIS
b) results in agreement with Allen, J. F. and Mendoza, E., Proc. Cambridge Philos. Soc., 44, 280 (1948).

[3] Balcerek, K., Lipinski, L., Mucha, J., Rafalowicz, J., Wlosewicz, D., Grosse, G. and Hegenbarth, E., Thermal Conductivity of Copper in Temperature Range 15 to 60 K, Acta Phys. Pol. A, 49, 417-20 (1976)

PURPOSE
To verify the CINDAS $\lambda$ equation for pure polycrystalline Cu.

SPECIMEN
a) 3.05 mm dia./rod; b) polycrystalline; c) /mechanically worked; d) 99.999% Al; g) $\beta = 1.33$ cm·$K^2$ $W^{-1}$.

APPARATUS
a) longitudinal; b) Cu-Au + 0.03 at. % Fe low temperature thermocouples of alloy and Cu wires//thermocouples glued to specimen surface.

DATA
a) 14.5 to 58 K; b) figure 1 - $\lambda$/data points taken from private communication with Rafalowicz, J.; c) uncertainty: larger than ±10%.

ANALYSIS
b) $K_e = (\alpha' T^n + \beta/T)^{-1}$, $n = 2.21$, $m = 2.63$, $\beta = 0.0237$ cm·$K^2$·$W^{-1}$, $\alpha''$ = 0.0423 x $10^{-4}$ cm·$K^{(n-m-mn+1)/(n+1)}$·$W^{-1}$; CINDAS equation verified in the range of maximum $\lambda$.

[4] Berman, R., MacDonald, D. K. C., The Thermal and Electrical Conductivity of Copper at Low Temperatures, Proc. Roy. Soc. London, Ser. A, 211, 122-8 (1952)

PURPOSE
To measure $\lambda$ and $\rho$ at low temperatures for Cu.

SPECIMEN
a) 1.12 mm, 0.45 mm dia./rods; c) drawn, annealed 6 h in He at 450 °C; d) 0.0005% Ag, < 0.0003% Ni, < 0.0004% Pb; f) $\rho_{4.2} = 5.5$ nΩ·cm; g) source: Johnson, Matthey and Co., No. 4234.

APPARATUS
a) longitudinal; b) gas thermometers; c) radiation shield.

DATA
a) 3 to 90 K; b) figure 1 - $\lambda$, figure 2 - $\rho$; c) uncertainty: ±2%; d) data corrected for conduction through glass thermometers.

ANALYSIS
b) $W(\text{cm K } W^{-1}) = 0.212/T + 2.55 \times 10^{-5} T^2$ for $12 < T < 30$ K, $1/\rho$ ($10^{-6}$ Ω·cm) = $1/189.6 + 2.64 \times 10^{-10} T^5$ for $30 > T > 12$; the Weidemann Franz Law is not strictly obeyed at temperatures < 4 K, minimum of $\lambda$ given in Makinson's theory not found.

[5] Bowman, H. F., Ziebold, T. D., Smith, J. L., Jr., Low Temperature Thermal Conductivity of Copper Irradiated with Reactor Neutrons, Proceedings of the Eighth Thermal Conductivity Conf., 175-84 (Oct 7-10, 1968)

PURPOSE
To measure $\lambda$ for radiated and irradiated Cu samples.

SPECIMEN
a) 2.00 in. (5.08 cm) long, 0.120 in. (0.305 cm) square/bar;
d) 99.999 + % Cu.

APPARATUS
a) longitudinal; b) precision Ge thermometers/instrument leads thermally anchored to reference heat sink, Ge sensors anchored to pick-up shoes.

DATA
a) 5 to 100 K/0.4 K at 5 K, 4 K at 100 K; b) figure 4 - $\lambda$; c) uncertainty: ±3%.

ANALYSIS
b) the influence of each neutron collision is roughly 10 to 30 times greater than the influence of each impurity atom.

[6] Davey, G. and Mendelssohn, K., Heat Conductivity of Pure Metals Below 1 K, Phys. Lett., 1(3), 183-4 (1963)

PURPOSE
To measure $\lambda$ for Cu, Au, Ti, Fe below 1 K.

SPECIMEN
a) /wire; b) polycrystalline; c) Cu 3 annealed for 3 h at 625 °C; d) Cu 1: commercial wire, Cu 2, Cu 3: 99.999% Cu.

APPARATUS
a) not given.

DATA
a) 0.4 to 1.0 K; b) figure 1 - $\lambda$.

ANALYSIS
a) Phillips, N., Phys. Rev., 100, 1719 (1955), Jericho, M. H., Thesis, Cambridge (1963); b) anomalous deviations from $T^1$ for $\lambda$.

[7] Dupre, A., Van Itterbeek, A., and Michiels, L., Heat Conductivity of Copper Below 1 K, Phys. Lett., 8(2), 99-100 (1964)

PURPOSE
To measure $\lambda$ of Cu samples from 0.2 K to 0.7 K.

SPECIMEN
a) 3 mm dia./rods; d) Cu 1: < 10 ppm; Cu 3: 1 ppm Co, 2 ppm Fe, 0.5 ppm Mn, 1 ppm Ni, 2 ppm Si; Cu 5: 97 ppm Co, 110 ppm Fe, 130 ppm Mn, 140 ppm Ni, 160 ppm Si; g) sources: Cu 1: Metallurgical Society of Hoboken (Belgium); Cu 3: Johnson, Matthey and Co., CB 8; Cu 5: Johnson, Matthey and Co. CB 2; Cu 1: $\beta = 0.075$ cm$\cdot K^2 W^{-1}$; Cu 3: $\beta = 1.73$ cm$\cdot K^2 W^{-1}$; Cu 5: $\beta = 17.3$ cm$\cdot K^2 W^{-1}$.

APPARATUS
a) not given.

DATA
a) 0.2 to 0.7 K; b) figure 1 - $\lambda$(Cu 1), figure 2 - $\lambda$(Cu 3, Cu 5).

ANALYSIS
a) Davey, G. and Mendelssohn, K., Phys. Lett., 7, 183 (1963); b) results verify $\lambda = T/\beta$; no anomalies found as in Davey, G. and Mendelssohn, K.

[8] Fletcher, R., The Nernst-Ettinghausen Coefficient and the Kondo Effect in Copper and Gold, Philos. Mag., 25(1), 87-95 (1972)

PURPOSE
To measure the isothermal Nernst-Ettinghausen coefficient over a wide temperature range.

SPECIMEN
a) cut from 7 x 5 x 0.025 cm/plate; c) annealed for 6 hr. at 950 °C; d) spectroscopically pure; e) RRR = 45.5; g) source: Johnson, Matthey and Co.

APPARATUS
a) longitudinal; d) $Q^i$ measured.

DATA
a) 5 to 42 K; b) figure 2 - $\lambda$ (zero field).

[9] Garber, M., Scott, B. W., and Blatt, F. J., Thermal Conductivity of Dilute Copper Alloys, Phys. Rev., 130(6), 2188-92 (1963)

PURPOSE
To measure $\lambda$ of Cu and find its lattice component.

SPECIMEN
a) 0.25 cm dia., 5-10 cm long/rod; c) annealed at 600 °C for 3 h, then swaged; d) specimen 14 = 0.23% Cd, 0.76% In; f) $\rho_0$ = 1.06 $\mu\Omega\cdot$cm; g) Cu for specimen supplied by American Smelting and Refining Co.

APPARATUS
a) longitudinal; b) 2 Au 2.1% Co vs. Ag 37% Au thermocouples/calibrated against Pt resistance thermometer/soldered to small Cu fittings placed along specimen circumference.

DATA
a) 12.5 to 93 K; b) figure 2 - $\lambda$ (total).

ANALYSIS
b) below 20 K, the lattice component is reduced relative to the residual electrical resistivity, in agreement with Pippard's theory.

[10] Gladun, C. H. R. and Holzhauser, W., Work on Thermal Conductivity at Low Temperatures, Monatsber. Dtsch. Akad. Wiss. Berlin, 6(1), 311-3 (1961)

PURPOSE
To measure $\lambda$ and $\rho$ of metal specimens from 17 to 100 K.

SPECIMEN
a) rod; d) electrolytic Cu; f) $\rho_0$ = 1.1 x $10^{-8}$ $\Omega\cdot$cm; g) mechanical deformation ranges from 0 to 30.8%.

APPARATUS
a) longitudinal; b) Pb resistance thermometers; c) radiation shield, vacuum insulation.

DATA
a) 19 to 83 K; b) figure 1 - $\lambda$ (no deformation).

ANALYSIS
b) measurements show a strong lowering of the maximum $\lambda$ and a corresponding increase in residual resistance for increasing deformation.

[11] Gröger, V. and Stangler, F., Der Warmewiderstand infolge Elektron - Phonon-streuung in Ideal-Reinem Kupfer, Acta Phys. Austriaca, 40, 145-9 (1974)

PURPOSE
To determine $W_i$ of high purity Cu due to electron-phonon interactions.

SPECIMEN
a) specimen 1: 12.5 μm thick, specimen 2: 125. μm thick/foil; c) annealed for 4 h at 950 °C; d) specimen 1 = 3 ppm Fe, specimen 2 = 99.999% Cu.

APPARATUS
a) longitudinal; b) carbon resistance thermometer.

DATA
a) 8 to 37 K; b) figure 1 - λ; c) uncertainty: less than ±5%.

ANALYSIS
b) $W_i = \alpha T^{2.98}$.

[12] Gröger, V. and Stangler, F., Verbesserung der Warmeleitfahigkeit von Reinstkupfer durch Gluhbehandlung unter geringem sauerstoffpartialdruck, Z. Metallkd., 65(5), 333-6 (1974)

PURPOSE
To investigate the effect of different annealing conditions on λ of high purity Cu.

SPECIMEN
a) specimen 1: 12.5 μm thick, specimen 2: 0.125 μm thick/foil; c) three states of anneal for each specimen: $O_2$ anneal, high vacuum anneal, unannealed; d) ultrahigh purity (see Table 3).

APPARATUS
a) longitudinal; b) carbon resistance thermometers.

DATA
a) 5 to 70 K; b) figure 1 - λ (specimen 1), figure 2 - λ (specimen 2); c) uncertainty: less than ±5%; d) size effect, lattice conductivity corrections.

ANALYSIS
a) Anderson, H. H. and Nielsen, M., Riso, Rep. No. 77; b) Lorenz number 15% higher after high vacuum anneal than Lo for small Fe content; for large Fe content, L is 22% higher than Lo.

[13] Ho, C. Y., Powell, R. W., Liley, P. E., Thermal Conductivity of the Elements: A Comprehensive Review, J. Phys. Chem. Ref. Data, 3, Supplement No. 1, 242-257 (1974)

PURPOSE
To provide a comprehensive listing of data on λ of the elements.

SPECIMEN
d) high purity; f) $\rho_o$ = 5.79 x $10^{-10}$ Ω·cm for T below 100 K.

APPARATUS
a) not given.

DATA
a) 0 to 8500 K; b) Table 48 - λ, recommended values; c) uncertainty: ±2% near room temperatue, ±4% at low and high temperatures, and ±15% for the molten phase up to 2000 K. The values above 2000 K are provisional.

[14] Hust, J. G. and Giarratano, P. J., Semi-Annual Report on Materials Research in Support of Superconducting Machinery: Thermal Conductivity, NBSIR 74-393, 1-35 (1974)

PURPOSE
To measure λ for materials for use in superconducting machinery.

SPECIMEN
a) 23 cm long, 3.26 mm dia./rod; c) swaged, vacuum annealed at 650 °C for 1 h; e) RRR = 14; g) OFHC.

APPARATUS
a) longitudinal; b) thermocouples/calibrated by Pt + Ge resistance thermometers; c) sample surrounded by insulation and radiation shield.

DATA
a) 8 to 300 K; b) Table 2 - λ, ρ, L; c) uncertainty in λ: from 4 to 20 K: ±2%; from 20 to 200 K: ±1%; from 200 to 300: ±2%; uncertainty in ρ: ±0.2%.

ANALYSIS
a) data within 10% of predicted values found in previous report (NBSIR 74-359).

[15] Kemp, W. R. G., Klemens, P. G., and Tainsh, R. J., The Thermal Conductivity of Copper Alloys: Effect of Plastic Deformation and Annealing, Philos. Mag., 4(43), 845-57 (1959)

PURPOSE
To study the lattice component of $\lambda$ as a function of torsional deformation.

SPECIMEN
a) 8 cm long, 3.25 mm dia./rods; c) drawn, annealed at 450 °C; No. 0: control specimen, No. 1: torsionally deformed to 1.29 with no anneal, No. 4: No. 1 annealed at 450 °C in He; d) 99.55% Cu, 0.35% As, 0.05% P; f) No. 0 ($\rho_0$ = 2.71 μΩ·cm), No. 1 ($\rho_0$ = 2.79 μΩ·cm), No. 4 ($\rho_0$ = 2.77 μΩ·cm).

APPARATUS
a) longitudinal; b) He thermometers; c) radiation shield, insulation.

DATA
a) 7 to 92 K; b) figure 1 - $\lambda$, Table 1 - $\rho_0$.

ANALYSIS
b) the observed change in $\lambda_g$ due to removal of dislocations during recrystallization.

[16] Laubitz, M. J., Transport Properties of Pure Metals at High Temperatures, Can. J. Phys., 45, 3677-96 (1967)

PURPOSE
To report measurements of high-temperature properties of monovalent metals.

SPECIMEN
a) 1.9 cm dia., 20 cm long/rod; c) annealed for 2 h at 700 K/machined from 1 in. dia. x 15 in. bar; d) 99.999 + % Cu; e) RRR = 900.

APPARATUS
a) modified Forbes Bar method; b) Pt/Pt-10% Rh thermocouples/calibrated at NRC/peened into specimen; c) several radiation shields, argon atmosphere of 10-25 cm Hg.

DATA
a) 300 to 1200 K; b) equation 4 - $\lambda$; c) uncertainty: ±0.9% at 300 K to ±1.5% at 1200 K.

ANALYSIS
a) Schofield, F. H., Proc. Roy. Soc. London, Ser. A, 107, 206 (1925), Midryukov, V. E., Vestn. Mosk. Univ., Ser. Mat., Mekh., Astron., Fiz., Khim., 12, 57 (1957); b) $\lambda = 4.182(7) - 0.631(6) \times 10^{-3}$ T; results agree with Mikryukov to within combined experimental error.

[17] Lees, C. H., the Effects of Temperature and Pressure on the Thermal Conductivities of Solids - Part II: The Effects of Low Temperatures on the Thermal and Electrical Conductivities of Certain Approximately Pure Metals and Alloys, Philos. Trans. Roy. Soc. London, Ser. A, 208, 381-443 (1908)

PURPOSE
To measure $\lambda$ and $\rho$ of several materials from 107 to 299 K.

SPECIMEN
a) 7 cm long, 0.585 cm dia./rod; c) /soft-drawn, turned.

APPARATUS
a) longitudinal; b) Pt resistance thermometer.

DATA
a) 107 to 299 K; b) Table (pp. 406-7) - $\lambda$, Table (p. 432) - $\rho$; c) uncertainty: less than ±5%; d) corrections for heat leaks.

ANALYSIS
b) $\lambda$ increases with increasing temperature.

[18] Lindenfeld, P., Lynton, E. A., and Soulen, R., Metallic Heat Conductivity Below 1 K, Phys. Lett., 19(4), 265 (1965)

PURPOSE
To measure $\lambda$ of Cu below 1 K.

SPECIMEN
a) 0.05 cm thick/foil; c) annealed for 3 h at 530 °C; e) RRR = 270; g) electrolytic tough pitch from Chase Brass and Copper Co.

APPARATUS
a) longitudinal; b) carbon resistors/calibrated against the vapor pressure (above 1.2 K), susceptibility of ruby probe, germanium resistance thermometers (below 1.2 K).

DATA
a) 0.4 to 1.5 K; b) figure 1 - $\lambda/T$ vs. T; c) uncertainty: less than ±1%.

ANALYSIS
b) no anomaly found as in Davey, G. and Mendelssohn, K., Phys. Lett., 7 (1963).

[19] Lucks, C. F. and Deem, H. W., Thermal Properties of Thirteen Metals, Am. Soc. Test. Mater., Spec. Tech. Publ., No. 227, 1-29 (1958)

PURPOSE
To report high temperature data on several metals.

SPECIMEN
a) 3/4 in. dia. x 6 in./rod; c) cold drawn/electrolytic tough pitch; g) federal specification QQ-C-502; source: Revere Copper and Brass, Inc.

APPARATUS
a) longitudinal; b) specimen soldered to heater block, Fe standard; c) guard tubes, insulation.

DATA
a) 366 to 1255 K; b) Table VI - $\lambda$.

ANALYSIS
b) Smith, C. S. and Palmer, E. W., Am. Inst. Min. Metall. Pet. Eng., 124 (1937); Schofield, F. H., Proc. Roy. Soc. London, Ser. A, 107 (1925).

[20] Mendelssohn, K. and Rosenberg, H. M., The Thermal Conductivity of Metals at Low Temperatures. I. The Elements of Groups 1, 2, and 3, Proc. Phys. Soc., London, Sect. A, 65, 385 (1952); see Rosenberg, H. M., The Thermal Conductivity of Metals at Low Temperatures, Philos. Trans. Roy. Soc. London, 247, 441-497 (Mar 1955)

[21] Mikryukov, V. E., Vestn. Mosk. Univ., Ser. Mat., Mekh., Astron., Fiz., Khim., 11(2), 53-70 (1956)

PURPOSE

To measure $\lambda$ and $\rho$ of Cu.

SPECIMEN
b) polycrystalline; d) 99.99% Cu.

APPARATUS
a) not given.

DATA
a) 320 to 773 K; b) Table 1 - $\lambda$, $\rho$; c) uncertainty: ±3%.

[22] Misiorek, H., Zakrzewski, T., and Rafalowicz, J., Influence of Plastic Deformation on the Thermal Conductivity Maximum of Copper and Aluminum in the Temperature Range 4.2 to 70 K, Phys. Status Solidi A, 47, K137 (1978)

PURPOSE
To determine the effect of increasing deformation on the thermal conductivity maximum.

SPECIMEN
a) /rod; c) deformed, undeformed specimens; d) 99.9%, 99.99% Cu.

APPARATUS
a) longitudinal.

DATA
a) 15 to 65 K (undeformed); b) figures 3,4; e) captions for all figures switched: figure 1 should be labeled as 4, figure 2 as 3, figure 3 as 1, figure 4 as 2.

ANALYSIS
b) with increasing deformation, the maximum decreases in value and is shifted toward higher temperatures.

[23] Moore, J. P., McElroy, D. L., and Graves, R. S., Thermal Conductivity and Electrical Resistivity of High-Purity Copper from 78 to 400 K, Can. J. Phys., 45, 3849-65 (1967)

PURPOSE
To compare measurements of a guarded longitudinal technique with other data.

SPECIMEN
a) /rods; b) polycrystalline; d) 99.999% Cu; e) RRR = 900; g) average grain size: 574 μm, hardness of 40 (DPH) with 0.1 kg load.

APPARATUS
a) longitudinal; b) Chromel-P, constantan thermocouples/calibrated spools/electrically insulating epoxy; c) Au plated radiation shield, spun $Al_2O_3$ placed between polished specimen and shield.

DATA
a) 85 to 400 K; b) Table 2 - $\lambda$, $\rho$ (both smoothed); c) uncertainty: ±1.86%; d) $\lambda$, $\rho$ uncorrected for thermal expansion.

ANALYSIS
a) Laubitz, M. J., Can. J. Phys., 45, 3677 (1967); b) $\lambda(W\ cm^{-1}K^{-1}) = 4.1631 - 5.904 \times 10^{-4}\ T + 7.0872 \times 10^{5}\ T^{-3}$ $300 < T < 1200$.

[24] Nelson, W. E. and Hoffman, A. R., Measurements of Temperatures and Magnetic Field Dependence of Electrical Resistivity and Thermal Conductivity in OFHC Copper, Proceedings of the Fourteenth Thermal Conductivity Conf., 73-80 (Jun 2-4, 1975)

PURPOSE
To measure $\lambda$ and $\rho$ on Cu in a longitudinal magnetic field.

SPECIMEN
a) 2.5 cm long; c) soldered at T = 160 °C/machined from 0.5 in. rod; d) commercial grade OFHC, 3 ppm P, 1 ppm Zn, 10 ppm each Pb, O, Te, 10 ppm total As, Bi, Mn, Sb, Sn; f) ($\rho_o$ = 3.15 x $10^{-8}$ $\Omega$·cm); g) source: Admiral Brass and Copper Co., Alloy 101.

APPARATUS
a) longitudinal; b) carbon resistor thermocouples/calibrated against commercial Ge resistance thermometer and fit to a modified resistance vs. temperature expression (Clemment, J. R. and Quinnell, E. H., Rev. Sci. Instr., 24 (1952) 213).

DATA
a) 4.05 to 34.9 K; b) Table 1 - $\lambda$, $\rho$, L; c) uncertainty in $\lambda$: ±5%, uncertainty in $\rho$: ±1.5%.

ANALYSIS
b) $\lambda^{-1}$ (Ø field) = $\alpha T^2 + \beta T^{-1}$, $\rho$ (Ø field) = $a + bT^{4.42}$.

[25] Nicol, J. and Tseng, T. P., Thermal Conductivity of Copper between 0.25 and 4.2 K, Phys. Rev., 92(4), 1062-3 (Nov 15, 1953)

PURPOSE
To measure low temperature $\lambda$ for Cu.

SPECIMEN
a) 27.2 cm long, 0.025 cm dia./wire; b) polycrystalline; d) commercial grade high-purity magnet wire; g) source: General Electric Co.

APPARATUS
a) longitudinal; b) T < 1 K: Cr-K-alum paramagnetic thermometry, ac bridge. T > 1 K: carbon thermometers//T < 1 K: contact between salts and mounting by high pressure salt molding.

DATA
a) 0.25 to 4.2 K; b) figure 1 - $\lambda$.

ANALYSIS
b) $\lambda = \alpha T$: $\alpha(W \cdot cm^{-1} \cdot K^{-2})$ = 1.76; the observed linear dependence of $\lambda$ on temperature indicates $\lambda$ is electronic in character.

[26] Powell, R. L., Roder, H. M., and Hall, W. J., Low-Temperature Transport Properties of Copper and Its Dilute Alloys: Pure Copper, Annealed and Cold-Drawn, Phys. Rev., 115(2), 314-23 (Jul 15, 1959)

PURPOSE
To measure $\lambda$, $\rho$ and thermoelectric power of two high purity Cu specimens.

SPECIMEN
a) specimen 1: 0.07 in. (0.18 cm) dia., specimen 2: 0.0816 in. (0.207 cm) dia./rod; c) specimens 1,2 swaged and drawn from 3/8 in. (0.95 cm) rod/specimens 1,2: annealed in vacuum at 400 °C, 2 h, after swaging and before drawing. Specimen 1 annealed at 400 °C, 2 h, after drawing; d) specimens 1,2: 99.999% Cu; e) specimen 1 (RRR = 1530), specimen 2 (RRR = 115); f) specimen 1 ($\rho_0$ = 1.01 x $10^{-9}$ $\Omega$·cm), specimen 2 ($\rho_0$ = 1.30 x $10^{-8}$ $\Omega$·cm); g) source: CRL of American Smelting and Refining Co.

APPARATUS
a) longitudinal; b) Au-Co vs. Cu thermocouples, Pt resistance thermometer.

DATA
a) 4 to 105 K; b) Table 1 - $\lambda$, Table 2 - $\rho_0$ and RRR, figure 4 - $\rho$, figure 8 - L.

ANALYSIS
a) experimental results agree qualitatively with theory and previous work; b) observed $\rho$ deviation from Matthiessen's rule; L curve flattens out considerably below Sommerfeld valve when extrapolated to 0 K.

[27] Powell, R. L., Roder, H. M., and Rogers, W. M., Low Temperature Thermal Conductivity of Some Commercial Copper, J. Appl. Phys., 28(11), 1282-8 (Nov 1957)

PURPOSE
To measure $\lambda$ for some commercial coppers.

SPECIMEN
a) all specimens 0.144 in. (0.366 cm) dia./rod; c) all specimens ground from 0.25 in. (0.64 cm) to 0.144 in. (0.366 cm); d) coalesced: 99.98% Cu; Electrolytic Tough Pitch: 99.98% Cu; Tellurium Cu: 99.4% Cu; Phosphorus Deoxidized Cu: 99.62% Cu; g) more detailed characterization given in Table 1.

APPARATUS
a) longitudinal; b) 8 Au-Co vs. Cu thermocouples/calibrated from 4 to 300 K in separate apparatus; c) temperature controlled radiation shield and vacuum insulation.

DATA
a) 5 to 37 K, 4 to 33 K, 6 to 84 K, 5 to 80 K for coalesced, electrolytic, free cutting, phosphorized respectively/1 to 60 K; b) figure 2 - $\lambda$.

ANALYSIS
b) $K/T = (1/B) + (T/D)$, $B(cm \cdot K^2 \cdot w^{-1})$ = 54(±2), 190(±10), $D(cm \cdot K^3 \cdot w^{-1})$ = 7(±1) x $10^3$, 2.2(±0.5) x $10^4$ for phosphorized and free cutting respectively; $\lambda$ of work hardened Cu-alloys is predominantly electronic thermal conduction as limited by the imperfection scattering.

[28] Powell, R. L., Rogers, W. M., and Coffin, D. O., An Apparatus for Measurement of Thermal Conductivity of Solids at Low Temperatures, J. Res. Nat. Bur. Stand., 59(5), 349-55 (Nov 1957)

PURPOSE
To describe an apparatus for $\lambda$ measurements of solids between 4 and 300 K.

SPECIMEN
a) 23.2 cm long, 0.367 cm dia./rod; c) annealed in He for 4 h, 400 °C, cooled to 200 °C for 8 h; d) 13 ppm $O_2$, 8 ppm Pb, 7 ppm Ni, Fe < 5 ppm; g) density = 8.90 g/cm$^3$, hardness on Vickers diamond point with 10 kg weight: 54.1 - longitudinal, 48.8 - transverse, source: Phelps Dodge Copper Products Corp.

APPARATUS
a) longitudinal; b) Au-Co vs. Cu thermocouples, Pt resistance reference thermometer/Pt resistance thermometer calibrated down to 12 K by Temperature Measurements Section of NBS; c) vacuum insulation.

DATA
a) 9 to 142 K; b) figure 8 - $\lambda$; c) uncertainty: ±5% (maximum).

[29] Powell, R. W. and Tye, R. P., New Measurements on Thermal Conductivity Reference Materials, Internat. J. Heat and Mass Transfer, 10(5), 581-96 (1967)

PURPOSE
To provide information on $\lambda$ and $\rho$ of possible reference materials.

SPECIMEN
a) 15 cm long, 7 mm dia./rod; c) heat treated to 900 °C; d) OFHC; g) source: Johnson, Matthey and Co. No. 4351.

APPARATUS
a) longitudinal.

DATA
a) 293 to 1173 K; b) Table 1 - $\lambda$; c) uncertainty: not given.

ANALYSIS
a) see Table 2 for data comparison at 50 °C; b) present data agree well with the two highest values of Kannuluik, W. G. and Laby, T. H., Proc. Roy. Soc., A121, 640 (1928); Mikryukov, V. E., Mosk. Gos. Univ., Ser. Mat., Mekh. Astron. Fiz. i Khim. 11(2), 53 (1956).

[30] Powers, R. W., Schwartz, D., and Johnston, H. L., The Thermal Conductivity of Metals and Alloys at Low Temperatures. I. Apparatus for Measurements Between 25 and 300 K, USAF TR-264-5, Cryogenic Lab., Dept. of Chem., O.S.U., Columbus, Ohio (1950)

PURPOSE
To describe an apparatus for measuring $\lambda$ for metals from 25 to 300 K in small temperature increments.

SPECIMEN
a) 20 in. (51 cm) long, 0.5 in. (1.3 cm) dia./rod; d) OFHC; g) source: American Brass Co.

APPARATUS
a) longitudinal; b) Cu-constantan thermocoules/calibrated against a He gas thermometer; c) 3 monel radiation shields.

DATA
a) 23 to 245 K; b) Table 4 - $\lambda$; c) uncertainty: ±0.7% from 100 to 250 K, ±1.9% at 30 K.

[31] Quick, R. W., Child, C. D., and Lanphear, B. S., Thermal Conductivity of Copper. II. Conductivity at Low Temperatures, Phys. Rev., 3(1), 1-20 (1895)

PURPOSE
To extend observations of $\lambda$ from 219 to 260 K.

SPECIMEN
d) electrolytic Cu.

APPARATUS
a) Forbes bar method.

DATA
a) 219 to 260 K; b) Table 10 - $\lambda$.

ANALYSIS
b) An increase in T corresponds to an increase in $\lambda$ over the temperature range measured.

[32] Rhodes, B. L., Moeller, C. E., and Saver, H. J., An Apparatus for Determining Thermal Conductivity of Solids From 20 to 600 K, Cryogenics, 5(1), 17-20 (1965)

PURPOSE
To discuss a $\lambda$ apparatus with which a large temperature gradient is not required over the specimen.

SPECIMEN
a) 10 cm long, 6 mm dia./rod; d) 99.999% Cu.

APPARATUS
a) longitudinal; b) Cu-constantan thermocouples; c) radiation shield, $2 \times 10^{-5}$ mm ($3 \times 10^{-3}$ Pa) insulation.

DATA
a) 98 to 573 K; b) Table 2 - average $\lambda$; c) uncertainty: ±3% (maximum) for $T > 48$, ±12% at 20 K.

ANALYSIS
a) Roder, Powell, and Hall, Phys. Rev., 115, 314 (1959); White, Aust. J. Phys., 6, 397 (1953); Berman and MacDonald, Proc. Roy. Soc. London, Ser. A, 211, 122 (1952); b) data agree to within ±6% of reference data.

[33] Roder, H. M., Powell, R. L., and Hall, W. J., Thermal and Electrical Conductivity of Pure Copper, Low Temperature Physics and Chemistry, 364-6 (Aug 1958)

PURPOSE
To measure $\lambda$ and $\rho$ for pure Cu.

SPECIMEN
a)./rod; c) specimens 1,2: annealed, specimen 3: not annealed/ specimen 3: drawn to 25% less cross sectional area; d) specimens 1,3: 99.999% Cu, specimen 2: 343 ppm Ag; e) specimen 1 (RRR = 1450), specimen 2 (RRR = 400), specimen 3 (RRR > 350); g) source: American Smelting and Refining Co.

APPARATUS
a) not given, but probably longitudinal.

DATA
a) specimen 1: 4 to 86 K, specimen 2: 4 to 64 K, specimen 3: 5 to 30 K; b) figure 1 - $\lambda$, figure 2 - $\rho$, figure 3 - L.

ANALYSIS
b) $W = AT^n + B/T$.

[34] Rosenberg, H. M., The Thermal Conductivity of Metals at Low Temperatures, Philos. Trans. Roy. Soc. London, 247, 441-97 (Mar 1955); see also Mendelssohn, K., and Rosenberg, H. M., Proc. Phys. Soc., London, Sect. A, 65, 385 (1952)

PURPOSE
To measure $\lambda$ for many metals at low temperatures.

SPECIMEN
a) 2.99 cm long, 2.99 mm dia./rod; b) polycrystalline; c) vacuum annealed, 800 °C for several h/turned down from 3.02 mm dia.; d) 99.999% Cu; g) $\rho_{293}/\rho_{20}$ = 85.3, source: Johnson, Matthey and Co., No. 4234.

APPARATUS
a) longitudinal; b) gas thermometers/calibrated at liquid He and $H_2$ temperatures/thermometer capillaries anchored to liquefier top and vacuum jacket; c) Cu radiation shield, vacuum insulation.

DATA
a) 2.5 to 41 K; b) figure 4 - $\lambda$; c) uncertainty: ±3% (maximum).

ANALYSIS
a) Berman and MacDonald (1952) curve of Cu from same batch agrees for temperatures above the maximum and $\alpha = 2.5 \times 10^{-5}$ also agrees;
b) Matthiessen's rule is not strictly valid in the region of $\lambda$ maximum; $1/\lambda = \alpha T^2 - \beta/T$.

[35] Schofield, F. H., The Thermal and Electrical Conductivities of Some Pure Metals, Proc. Roy. Soc. (London), 107, 206-27 (1924)

PURPOSE
To measure $\lambda$ and $\rho$ of several metals.

SPECIMEN
a) 3/4 in. (1.905 cm) dia./rod; c) hot rolled to 1 in. dia., drawn to 7/8 in. dia., machined and polished to 3/4 in. dia., then annealed; d) 99.9%; g) source: T. Bolton and Sons, Ltd., Oakmoor.

APPARATUS
a) Forbes bar method; b) Pt/10%Ir-Pt thermocouples; c) insulation between specimen and guard ring.

DATA
a) 369 to 898 K; b) Appendix II - $\lambda$, $\rho$; c) uncertainty: not given.

ANALYSIS
a) Lees (1908); Jaeger and Diesselhorst (1900).

[36] Schriempf, J. T., Deviations from Matthiessen's Rule in the Low Temperature Thermal and Electrical Resistivities of Very Pure Copper, Proceedings of the Seventh Thermal Conductivity Conf., 249-52 (Nov 13-16, 1967)

PURPOSE
To use $\lambda$ and $\rho$ data to show the deviation of Matthiessen's rule at low temperatures.

SPECIMEN
a) Cu 1: 0.119 in. (0.302 cm) dia., Cu 2 and Cu 2-O: 0.076 in. (0.19 cm) dia./rods; c) Cu 1: annealed 12 h at 1000 °C in air, $10^{-3}$ mm (0.1 Pa), Cu 2: annealed 3 h at 530 °C, $10^{-6}$ mm ($10^{-4}$ Pa), Cu 2-O: Cu 2 annealed 22 h at 1000 °C in air, $5 \times 10^{-4}$ mm ($7 \times 10^{-2}$ Pa)/Cu 1: swaged from 3/8 (0.95 cm) to 0.125 in. (0.318 cm) dia., annealed, etched, Cu 2: swaged to 0.080 in. (0.20 cm) dia., etched, annealed; d) Cu 1: 100 ppm Mn, Cu 2 and Cu 2-O: Mn < 10 ppm; f) Cu 1 ($\rho_0 = 1.73 \times 10^{-11}$ $\Omega \cdot m$), Cu 2 ($\rho_0 = 0.579 \times 10^{-11}$ $\Omega \cdot m$), Cu 2-O ($\rho_0 = 1.12 \times 10^{-11}$ $\Omega \cdot m$); g) source: American Smelting and Refining Co.

APPARATUS
a) longitudinal; b) thermocouple difference thermometer/referenced by Ge thermometer.

DATA
a) 2 to 20 K; b) figure 1 - $\lambda$; c) uncertainty: ±3%.

ANALYSIS
b) results agree with White, G. K. and Tainsh, R. J., Phys. Rev., 119, 1869 (1960), but disagree with Powell, R. L., Roder, H. M., and Hall, W. J., Phys. Rev., 115, 314 (1959).

[37] Scott, B. W., Transport Properties of Dilute Copper Alloys, Ph.D. Thesis, Michigan State Univ. (1962), University Microfilms Inc., Ann Arbor, Michigan

PURPOSE
To measure $\lambda$, $\rho$ and thermoelectric power of dilute Cu alloys and compare with existing theory.

SPECIMEN
a) all specimens 5 to 10 cm long, 0.25 cm dia./rods; c) all specimens cast into 3/16 x 2 in. (0.48 x 5 cm) slugs from 99.999% Cu, homogenized at 600 °C for six days and annealed in sealed vycor capsules, each step in 2/3 atm. ($6.8 \times 10^4$ Pa) He (specimen 8 high vacuum). Specimen 8 annealed at 600 °C for 5 h, 750 °C for 1 h, specimens 14, 15, 17 annealed at 600 °C for 3 h, remaining annealed at 750 °C for 2 h/all swaged between homogenization and annealing, and given acid etch before casting and annealing; d) specimen 8: 0.61% Sn, specimen 14: 0.225% Cd, 0.762% In, specimen 15: 0.104% Cd, 0.389% In, specimen 17: 0.477% Cd, 0.294% In, specimen 101: 0.47% Zn, 0.294% In, specimen 102: 0.49% Zn, 0.77% In, specimen 103: 0.416% In, 0.995% Zn, specimen 104: 0.331% Zn, 0.35% Ga, specimen 105: 0.34% Zn, 0.805% Ga, specimen 106: 0.856% Zn, 0.37% Ga; f) specimen 8 ($\rho_0 = 1.75 \times 10^{-6}$ $\Omega$·cm), specimen 14 ($\rho_0 = 1.061 \times 10^{-6}$ $\Omega$·cm), specimen 15 ($\rho_0 = 0.549 \times 10^{-6}$ $\Omega$·cm), specimen 101 ($\rho_0 = 0.481 \times 10^{-6}$ $\Omega$·cm), specimen 102 ($\rho_0 = 1.03 \times 10^{-6}$ $\Omega$·cm), specimen 103 ($\rho_0 = 0.73 \times 10^{-6}$ $\Omega$·cm), specimen 104 ($\rho_0 = 0.585 \times 10^{-6}$ $\Omega$·cm), specimen 105 ($\rho_0 = 1.418 \times 10^{-6}$ $\Omega$·cm), specimen 106 ($\rho_0 = 0.718 \times 10^{-6}$ $\Omega$·cm); g) source: American Smelting and Refining Co.

APPARATUS
a) longitudinal; b) Au - 2.1 at. % Cu vs. Ag - 37 at. % Au thermocouples/ calibrated against Pt resistance thermometer certified by NBS; c) vacuum insulation.

DATA
a) 7 to 100 K/1 to 5 K; b) Tables on pp. 142-149, 162-164, 166-170 - $\lambda$ and $\rho$, all specimens; c) uncertainty: ±3% at 20 K, ±7% at 50 K.

ANALYSIS
b) low temperature lattice conductivity of dilute alloys is explained by Pippard's theory. At higher temperatures the anisobaric effect is apparently masked by scattering.

[38] Siu, M. C. I., Carroll, W. L., and Watson, T. W., Thermal Conductivity and Electrical Resistivity of Six Copper-Base Alloys, NBSIR 76-1003, 1-18 (1976)

PURPOSE
To measure $\lambda$ and $\rho$ at high temperatures.

SPECIMEN
a) 37 cm long, 0.64 cm dia./rod; c) extruded at 1233 K and aged at 693 K in cracked natural gas atmosphere; d) 0.002% Fe, 0.662% Ni, 0.20% Zr.

APPARATUS
a) longitudinal; b) Pt/Pt - 10% Rh; c) heaterguard, vacuum, alumina powder surrounds specimen and guard.

DATA
a) 373 to 923 K; b) Table 4 - $\lambda$, Table 5 - $\rho$; c) uncertainty: ±2%.

ANALYSIS
b) the measured values of $\lambda$, $\rho$ conform to the Smith-Palmer equation to within 10%.

[39] Touloukian, Y. S., Powell, R. W., Ho, C. Y., and Klemens, P. G., Thermophysical Properties of Matter, Volume 1: Thermal Conductivity, Metallic Elements and Alloys, 68-81 (1970)

PURPOSE
To provide an extensive list of data for $\lambda$ of the metallic elements and alloys.

SPECIMEN
d) 99.999%; f) $\rho_0 = 8.51 \times 10^{-10}$ $\Omega \cdot$cm.

APPARATUS
a) not given.

DATA
a) 0 to 1356 K; b) Figure and Table 12R - $\lambda$, recommended values; c) uncertainty: ±3% near room temperature, ±3 to 5% at other temperatures; e) the values below 1.5 Tm are calculated to fit the experimental data by using $n = 2.40$, $a = 0.19$, $m = 2.59$, $\alpha'' = 4.16 \times 10^{-6}$, and $\beta = 0.0348$.

[40] Tseng, Tse-Pei, Properties of Matter at Very Low Temperatures, Ph.D. Thesis, Ohio State Univ. (1954)

PURPOSE
To provide λ data on commercial grade Cu.

SPECIMEN
a) 0.025 cm dia./wire; d) commercial grade; g) source: General Electric Co.

APPARATUS
a) longitudinal; b) C resistance thermometers/resistance extrapolated to zero power of measuring current for calibration; c) $10^{-6}$ mm ($10^{-4}$ Pa) insulation.

DATA
a) 1.4 to 4.2 K; b) Table 2 - λ; d) corrections for thermometer and heater lead conduction.

ANALYSIS
b) results are comparable to Mendelssohn, K. and Rosenberg, H. M., Proc. Phys. Soc., London, Sect. A, 65, 385 (1952).

[41] White, G. K., The Thermal and Electrical Conductivity of Copper at Low Temperatures, Aust. J. Phys., 6(4), 397-404 (1953)

PURPOSE
To measure λ and ρ for pure Cu.

SPECIMEN
a) Cu 1, 2: 2 mm dia., Cu 3: 1 mm dia., all 5 cm long/rods; c) Cu 2 is Cu 1 after vacuum annealing at 550 °C for 3 h/Cu 1, 3 in "as drawn" condition; d) all specimens, 0.0005% Ag, < 0.0003% Ni, 0.0004% Pb, trace of Ga, Fe; e) Cu 1 ($\rho_0$ = 0.051 μΩ·cm); Cu 2 ($\rho_0$ = 0.0576 μΩ·cm); Cu 3 ($\rho_0$ = 0.00458 μΩ·cm); g) source: Johnson, Matthey and Co., No. JM4272.

APPARATUS
a) longitudinal; b) gas thermometers; c) vacuum insulation.

DATA
a) Cu 1: 2.5 to 116 K, Cu 2: 5 to 58 K, Cu 3: 2.03 to 160 K;
b) figure 2 - λ; c) uncertainty: ±4% from 5 to 15 K, ±1% for all others;
d) correction for radiative heat loss at higher temperatures.

ANALYSIS
b) results in agreement with Berman, R. and MacDonald, D. K. C., sample of pure annealed Cu; measurements support theory of non-additivity of impurity and ideal resistances.

[42] White, G. K. and Tainsh, R. J., Lorenz Number for High Purity Copper, Phys. Rev., 119(6), 1869-71 (Sep 1960)

PURPOSE
To investigate L for very pure copper.

SPECIMEN
a) 0.03 in. (0.08 cm) dia., 8 cm long/wire; c) annealed at 530 °C in vacuo/ rolled and drawn from 0.75 in. (1.9 cm) dia.; d) < 0.0001% Fe, Sb, Se each, < 0.0002% Te, As each; f) $\rho_0$ = 0.87 x $10^{-9}$ Ω·cm; g) source: American Smelting and Refining Co.

APPARATUS
a) longitudinal; b) He gas thermometers.

DATA
a) 2 to 55 K; b) figure 1 - λ; c) uncertainty: ±4% for 2 < T < 15; ±1% T > 15.

ANALYSIS
b) $\lambda = A/T + BT^n$: A = 0.035 cm·K $W^{-1}$ compared to 0.059 for Powell, R. L., Roder, H. M., and Hall, W. J., Phys. Rev., 115, 314 (1959).

[43] White, G. K. and Woods, S. B., Thermal and Electrical Conductivities of Solids at Low Temperatures, Can. J. Phys., 33, 58-73 (1955); The Lattice Thermal Conductivity of Dilute Copper Alloys, Philos. Mag., 45, 1343-5 (1954)

PURPOSE
To describe an apparatus for measuring λ and ρ of solids between 2 and 300 K.

SPECIMEN
a) 1 to 2 mm dia., 6 cm long/rods; c) Cu 1, 2, 3 annealed at 700 °C for 2 h/drawn; d) Cu 1: 0.02% Ge, Cu 2: 0.056% Fe, Cu 3: 0.0043% Fe; f) Cu 1 ($\rho_0$ = 0.084 x $10^{-6}$ Ω·cm), Cu 2 ($\rho_0$ = 0.53 x $10^{-6}$ Ω·cm), Cu 3 ($\rho_0$ = 0.041 x $10^{-6}$ Ω·cm).

APPARATUS
a) longitudinal; b) gas thermometers//all leads to specimen are anchored to Cu pillars; c) temperature controlled radiation shield.

DATA
a) 1.5 to 142 K; b) figure 2 - ρ, figure 3 - λ, Table 1 - $\rho_0$; c) uncertainty: ±5% for high λ specimens from 4 to 15 K, all others: ±1%; d) correction for radiation.

ANALYSIS
b) $\lambda = AT^{-1} + B\,T^{2.4}$.

[44] Zavaritskii, N. V. and Zel'dovich, A. G., Thermal Conductivity of Technical Materials at Low Temperatures, Sov. Phys. Tech. Phys., 1, 1970-4 (1956)

PURPOSE
To describe an apparatus for measuring $\lambda$ for solid materials.

SPECIMEN
a) 20 and 6 mm long, 10 and 6 mm dia./rods; c) M-3-annealed: annealed at 800 °C/M-3-annealed: cut from tube; d) M-3-annealed and unannealed: Bi $<$ 0.003, Sb $\leq$ 0.05, As $\leq$ 0.05, Fe $\leq$ 0.05, Ni $\leq$ 0.20, Pb $\leq$ 0.05, Sn $\leq$ 0.05, S $\leq$ 0.01, O $\leq$ 0.1%, Cupalloy: 0.61% Cr, 0.18% Ag.

APPARATUS
a) longitudinal; b) carbon resistance thermometers/calibrated from 2 to 4.2 K and from 14 to 20 K from vapor pressures of He and $H_2$ respectively and from 20 to 110 K from standard Pt resistance thermometer; c) radiation shield and vacuum insulation.

DATA
a) 2 to 100 K; b) figure 2 - $\lambda$; c) uncertainty: ±5%.

ANALYSIS
b) results agree with White, G. K. and Woods, S. B., Can. J. Phys., 33, 58 (1955).

## 3. Aluminum

### 3.1 General

Aluminum has also been measured extensively but not as completely as copper. A total of 35 publications are included in the annotated bibliography (Section 3.5). The following of these data sets were selected as primary data: 1, 9, 11, 12, 17, 25, 26, 29, and 33.

The primary data contain only annealed specimens, and covers a range of temperature from 2 to 873 K, and a range of RRR from 13 to 16800. Thermal conductivity values from these sources are shown in Figs. 3.1.1 through 3.1.3, where the last graph is a composite of the data. Although the RRR of the most electrically pure aluminum ever produced is comparable to that for copper (50,000), aluminum with RRR values in the range of 10,000 to 20,000 is more readily obtained.

Equation 1.1.3 was fitted to the primary data set over the entire temperature range. The values of the parameters, $P_i$, i = 1,2 ... 7 obtained by nonlinear least squares fit are:

$P_1 = 4.716 \times 10^{-8}$ $\quad$ $P_5 = 130.9$

$P_2 = 2.446$ $\quad$ $P_6 = 2.5$

$P_3 = 623.6$ $\quad$ $P_7 = 0.8168$

$P_4 = -0.16$

with all units in SI.

The data at high RRR were then examined for systematic residual deviations as a function of temperature. These residuals were represented by the $W_c$ term in Eq. 1.1.5. The resulting equation for $W_c$ is:

$$W_c = -0.0005\ \ell n(T/330)\ \exp(-(\ell n(T/380)/0.6)^2)$$

$$-0.0013\ \ell n(T/110)\ \exp(-(\ell n(T/94)/0.5)^2),$$

where $W_c$ and T are in SI units.

3.2 Deviations from Recommended Equation

Equation 1.1.3 represented the overall primary aluminum data to yield random deviations. Again some of the individual data sets exhibit systematic trends. The deviations of these data from Eq. 1.1.3 are shown in Figs. 3.2.1, 3.2.2, and 3.2.3. Although temperature dependent deviations exist for individual data sets, the overall pattern is random in nature. No systematic trends with RRR were noted.

The primary data were selected from the literature data on relatively large, well annealed specimens. Therefore, the deviations exhibited in Figs. 3.2.1 through 3.2.3 are indicative of the combined effect of a) experimental measurement errors and b) the inability of Eq. 1.1.3 to account for the effects of chemical impurity variations. The effects of physical defect variations, small specimen size variations, and magnetic fields are exhibited, in part, by the deviations of the secondary data. The thermal conductivity variations caused by other than chemical impurity variations are not expected to be represented as well by Eq. 1.1.3. However, the RRR (or $\rho_0$) correlating parameter does account for an appreciable part of these variations. Some users may find this to be an adequate representation and, therefore, discussions of these comparisons are included for completeness.

The deviations of the secondary data sets are illustrated in Figs. 3.2.4 through 3.2.10. Figures 3.2.7 and 3.2.10 are composite deviation plots.

Eq. 1.1.3 is compared to the most commonly used sources of reference data by Ho and Touloukian, references 14A,32A, respectively, in Fig. 3.2.11. The agreement

is within the combined uncertainties except in the region around 60 K. In this region data by Cook, reference 5, were published after both data sets and is the reason for the large differences.

### 3.2.1 Physical Defect Effects

Investigations of physical defects in aluminum have produced only a few references 21,25. Each of these references will be discussed below.

Changes in thermal conductivity due to elongation are studied in reference 21. The conclusion is that increasing deformation lowers the thermal conductivity maximum and shifts it to a higher temperature. Unfortunately, it appears that the figure captions do not correspond to the proper figures; caption 3 belongs to Fig. 2 and caption 4 to Fig. 1. Note that in Fig. 2, the nondeformed specimen has the wrong temperature dependence above the temperature of the maximum thermal conductivity. The deviations from Eq. 1.1.3 for this specimen were within $\pm$60%. The deviations from Eq. 1.1.3 for the specimens in Fig. 1 were within $\pm$10% for the undeformed specimen. The deformed specimens were not compared.

Reference 25 showed the effects on the thermal conductivity of an "as fabricated" specimen and an annealed specimen of the same stock. Also included was a high purity specimen. The peak value of the thermal conductivity for this specimen was about 1580 $W \cdot m^{-1} \cdot K^{-1}$, for the "as fabricated" specimen, 389 $W \cdot m^{-1} \cdot K^{-1}$, and for the annealed specimen, the peak value was 332 $W \cdot m^{-1} \cdot K^{-1}$. The authors comment on the effect of the anneal, indicating that the decrease in peak value of the annealed specimen it is due to the large amount of impurities present in the original stock. The deviations from Eq. 1.1.3 for the high purity specimen were within $\pm$7% as were those for the annealed specimen. The deviations for the "as fabricated" specimen were within $\pm$8%.

Although the temperature dependence of physical defect scattering mechanisms is different from that due to impurity scattering, Eq. 1.1.3 represents the unannealed specimen data to within ±10%. This indicates that the residual electrical resistivity characterizes both types of scattering for the range of RRR included here.

### 3.2.2 Size Effects

Amundsen and Olsen[1] studied the size effects of several aluminum specimens. As the specimen size decreases, the peak value of the resistivity increases. Notice that magnetic fields were used to find the thermal resistivity of each specimen. The ratio of the thermal and electrical resistivities was shown to be constant, except at the highest fields, where the thermal resistivity increased faster than the electrical resistivity.

Although not specifically studied, we can make some general comments regarding the thermal conductivity of several specimens at low temperatures as a function of specimen size. The peak thermal conductivity is shifted toward lower temperatures for the larger specimens. The justification of this effect resides in its observation in other metals.

### 3.2.3 Magnetic Field Effects

Although magnetic field effects on thermal conductivity were not studied explicitly, reference 14 showed that the peak conductivity value in a 0.5 T magnetic field was 5400 $W \cdot m^{-1} \cdot K^{-1}$, while in a zero field, the value was 10500 $W \cdot m^{-1} \cdot K^{-1}$. It is interesting to notice that this peak disappears completely for a field somewhere between 0.5 and 1 T.

---

[1] Amundsen, T. and Olsen, T., Size Dependent Thermal conductivity in Aluminum Films, Phil. Mag., 11, 564-74 (1965).

Reference 31 reported that the peak conductivity value in a 1 T field was 3800 $W \cdot m^{-1} \cdot K^{-1}$, while in a zero field the value was 5800 $W \cdot m^{-1} \cdot K^{-1}$. This study supports the statement that the peak in thermal conductivity disappears between 0.5 and 1 T.

Reference 32 reported low temperature thermal conductivity data for fields up to 5 T. At zero field and a temperature of 20 K, the specimen had a conductivity value of 6500 $W \cdot m^{-1} \cdot K^{-1}$. At a field of 5 T, the conductivity of the same specimen dropped to about 1800 $W \cdot m^{-1} \cdot K^{-1}$. This report indicates that the peak in thermal conductivity disappears for a field between 1 and 2 T. Amundsen and Souik[2] reported measurements on two single crystal specimens of pure aluminum in fields up to 1.3 T and temperatures below 4 K. The increase in thermal resistivity was linear in both specimens above 0.3 T, falling sharply off below this field. A maximum increase in resistivity of 1.5 times was induced by the magnetic field, but the ratio of thermal resistivity to electrical resistivity was essentially independent of the field (less than 10% variation).

Sparks[3] reported measurements on two specimens with similar thermal histories from 5 to 20 K. There were large differences in RRR and in thermal conductivity values due to different impurity concentrations. At 6 K, and zero field, a factor of two difference is found in the thermal conductivities. For a field of 8 T, he found a decrease of 29% at 5 K, and a 50% decrease at 20 K.

### 3.3 Electrical Resistivity and Lorenz Ratio

It was desirable to examine the Lorenz ratio of aluminum during the course of this investigation. Therefore, an approximation of electrical resistivity was

[2]Amundsen, T and Souik, R. P., Measurements of the Thermal Magnetoresistance of Aluminum, J. Low Temp. Phys., 2(1), 121-9 (1970).
[3]Sparks, L. L., Magnetic Field Effect on Thermal Conductivity of Selected Metals, Advances in Cryogenic Engineering, 24, 224-31, Plenum Press (1977).

needed. To do this, we selected those sources from this thermal conductivity compilation that also contained electrical resistivity data and fitted Eq. 1.2.3 to the data. The electrical resistivity data used is shown in Figs. 3.3.1 and 3.3.2 with a composite of the data in Fig. 3.3.3. The parameters for Eq. 1.2.3 are

$P_1 = 0.09052 \times 10^{-16}$ $\quad$ $P_5 = 40.$

$P_2 = 4.551$ $\quad$ $P_6 = 13.64$

$P_3 = 5.173 \times 10^{10}$ $\quad$ $P_7 = 0.7416$

$P_4 = 1.26$

All units are SI.

The deviations of the experimental data from this equation are illustrated in Figs. 3.3.4 through 3.3.6. Again, as for copper, there is considerable spread in the deviations in the range 10-80 K. It is recognized that this is partly due to the large range of $\rho$ values represented (several orders of magnitude) as well as the inadequacy of the simple equation used for representation. Nevertheless, it is felt that for this purpose the approximation is useful.

Smooth values of $\rho$ and T at selected RRR values are plotted in Fig. 3.3.7. From the $\rho$(T,RRR) and $\lambda$(T,RRR) equations smooth values of L(T,RRR) are plotted in Fig. 3.3.8. As for copper, the irregularities in the shape of these curves from that expected are within the combined uncertainties of the two equations used.

In Section 1.5, we discuss the procedure for selecting values of $\rho_0$ and calculating RRR for each thermal conductivity data set. These values of $\rho_0$ along with the Sommerfeld value of Lorenz ratio were used to best fit each low temperature data set. The resulting values of RRR obtained by this procedure are compared to the values reported in the references in Fig. 3.3.9 and are listed in Table 3.3.1. Figure 3.3.9 shows values of RRR (calc), those values from the

above procedure, versus RRR (obs), those values reported in the references listed in the annotated bibliography. Also shown in this figure is the line that represents RRR (calc) = RRR (obs). Systematic deviations from this line indicate ranges in which the derived Eq. 1.1.3 is invalid. With the exception of four points from the secondary data sets, all of the points lie near the line. Equation 1.1.3 is thus valid for the low temperatures from RRR of 10 to 10,000. Inspection of Table 3.3.1 indicates that the calculated values of RRR are generally smaller than the observed values. This suggests that the Lorenz ratio of aluminum at low temperatures may be slightly smaller than the Sommerfeld value.

## 3.4 Summary for Aluminum

Equation 1.1.3 represents the thermal conductivity of an annealed specimen of aluminum over the whole temperature range. The deviations from the primary set are shown in Figs. 3.2.1-3.2.3. Deviations for specimens in which physical defects are important (unannealed specimens) are within $\pm$20%.

Based on the deviations illustrated in Figs. 3.2.1 through 3.2.10 and the large range that occurs in low temperature thermal conductivity of aluminum (nearly three orders of magnitude) due to the introduction of chemical impurities and physical defects, it is clear that a large proportion of these effects is reflected by the residual electrical resistivity. The incorporation of RRR (or $\rho_0$) in Eq. 1.1.3 produces an equation that represents the data for a wide range of aluminum specimens.

Equation 1.1.3 with the parameters listed here was used to generate thermal conductivity values for selected temperatures and values of RRR. These values are listed in Table 3.4.1 and plotted in Fig. 3.4.1.

List of Tables and Figures for Aluminum

## Tables


| | | Page |
|---|---|---|
| Table 3.3.1 | Comparison of Calculated and Observed RRR Values for Aluminum . . . . . | 96 |
| Table 3.4.1 | Thermal Conductivity Values for Aluminum Calculated from Eq. 1.1.3 at Selected Temperatures and RRR Values . . . . . | 97 |


## Figures


| | | Page |
|---|---|---|
| Figure 3.1.1 | Experimental thermal conductivity data selected from the following primary references in the aluminum annotated bibliography: (1,5,9,11) . . . . . | 98 |
| Figure 3.1.2 | Experimental thermal conductivity data selected from the following primary references in the aluminum annotated bibliography: (12,17,25,26,29,33) . . . . . | 99 |
| Figure 3.1.3 | Composite of the data in figures 3.1.1 and 3.1.2 . . . . . | 100 |
| Figure 3.2.1 | Thermal conductivity deviations of the aluminum data from the following primary references compared to Eq. 1.1.3: (1,5,9,11) . . . . . | 101 |
| Figure 3.2.2 | Thermal conductivity deviations of the aluminum data from the following primary references compared to Eq. 1.1.3: (12,17,25,26,29,33) . . . . . | 102 |
| Figure 3.2.3 | Composite of the deviations in figures 3.2.1 and 3.2.2 . . . . . | 103 |
| Figure 3.2.4 | Thermal conductivity deviations of the aluminum data from the following secondary references compared to Eq. 1.1.3: (2,3,6,7,10,14) . . . . . | 104 |
| Figure 3.2.5 | Thermal conductivity deviations of the aluminum data from the following secondary references compared to Eq. 1.1.3: (15,16,19,20,21,23) . . . . . | 105 |
| Figure 3.2.6 | Thermal conductivity deviations of the aluminum data from the following secondary references compared to Eq. 1.1.3: (23,25,26,27,28) . . . . . | 106 |
| Figure 3.2.7 | Composite of the deviations in figures 3.2.4 through 3.2.6 . . . . . | 107 |

Page

Figure 3.2.8 Thermal conductivity deviations of the aluminum data from the following secondary references compared to Eq. 1.1.3: (3,13,18,21,22,24,30) . . . . . 108

Figure 3.2.9 Thermal conductivity deviations of the aluminum data from the following secondary references compared to Eq. 1.1.3: (30,31,32) . . . . . 109

Figure 3.2.10 Composite of the deviations in figures 3.2.8 and 3.2.9 . . . . . 110

Figure 3.2.11 Comparison of Eq. 1.1.3 to the values recommended for aluminum in the following references: (14A,32A) . . . . . 111

Figure 3.3.1 Experimental electrical resistivity data for aluminum selected from the following references in the aluminum annotated bibliography: (4,9,11,25,26) . . . . . 112

Figure 3.3.2 Experimental electrical resistivity data for aluminum selected from the following reference in the aluminum annotated bibliography: (33) . . . . . 113

Figure 3.3.3 Composite of the electrical resistivity data in figures 3.3.1 and 3.3.2 . . . . . 114

Figure 3.3.4 Electrical resistivity deviations of the aluminum data from the following references compared to Eq. 1.2.3: (4,9,11,25,26) . . . . . 115

Figure 3.3.5 Electrical resistivity deviations of the aluminum data from the following reference compared to Eq. 1.1.3: (33) . . . . . 116

Figure 3.3.6 Composite of the electrical resistivity deviations shown in figures 3.3.4 and 3.3.5 . . . . . 117

Figure 3.3.7 Electrical resistivity for aluminum as a function of temperature calculated from Eq. 1.2.3 at selected values of RRR . . . . . 118

Figure 3.3.8 Lorenz ratio for aluminum as a function of temperature calculated from Eq. 1.2.3 and Eq. 1.1.3 at selected values of RRR . . . . . 119

Figure 3.3.9 RRR values calculated as per Section 1.5, RRR(CALC), versus reported RRR values, RRR(OBS), for aluminum . . . . 120

Figure 3.4.1 Thermal conductivity for aluminum as a function of temperature calculated from Eq. 1.1.3 at selected values of RRR . . . . . 121

Table 3.3.1. Comparison of Calculated and Observed RRR Values for Aluminum.

| Reference | RRR (obs.) | RRR (calc.) |
|---|---|---|
| | Primary Data | |
| 1 | 467.0 | 420.0 |
| 1 | 676.0 | 605.0 |
| 1 | 840.0 | 720.0 |
| 5 | 11600.0 | 11600.0 |
| 11 | 2750.0 | 2700.0 |
| 11 | 4370.0 | 4100.0 |
| 25 | 12.8 | 12.8 |
| 25 | 97.0 | 91 |
| | Secondary Data | |
| 14 | 2800.0 | 1550.0 |
| 14 | 4500.0 | 1720.0 |
| 22 | 520.0 | 520.0 |
| 23 | 147.0 | 147.0 |
| 23 | 86.0 | 86.0 |
| 23 | 36.0 | 36.0 |
| 23 | 17.0 | 17.0 |
| 30 | 15000.0 | 11900.0 |
| 30 | 24000.0 | 18000.0 |

Table 3.4.1. Thermal Conductivity Values for Aluminum Calculated from Eq. 1.1.3 at Selected Temperatures and RRR Values.

| T (K) | $\lambda(W \cdot m^{-1} \cdot K^{-1})$ | | | | | |
|---|---|---|---|---|---|---|
| | RRR = 30 | RRR = 100 | RRR = 300 | RRR = 1000 | RRR = 3000 | RRR = 10000 |
| 1 | 29 | 98 | 295 | 984 | 2954 | 9842 |
| 2 | 57 | 195 | 589 | 1966 | 5892 | 19521 |
| 3 | 86 | 292 | 883 | 2941 | 8765 | 28499 |
| 4 | 114 | 390 | 1175 | 3897 | 11475 | 35887 |
| 5 | 143 | 487 | 1463 | 4817 | 13885 | 40840 |
| 6 | 171 | 583 | 1746 | 5677 | 15853 | 43072 |
| 7 | 200 | 678 | 2020 | 6452 | 17272 | 42980 |
| 8 | 228 | 772 | 2282 | 7116 | 18109 | 41300 |
| 9 | 256 | 864 | 2528 | 7651 | 18406 | 38717 |
| 10 | 284 | 953 | 2755 | 8044 | 18260 | 35708 |
| 12 | 338 | 1122 | 3133 | 8420 | 17095 | 29474 |
| 14 | 391 | 1272 | 3398 | 8340 | 15360 | 23801 |
| 16 | 442 | 1400 | 3544 | 7960 | 13478 | 19074 |
| 18 | 489 | 1500 | 3582 | 7418 | 11658 | 15308 |
| 20 | 532 | 1572 | 3534 | 6801 | 9997 | 12366 |
| 25 | 617 | 1628 | 3178 | 5227 | 6706 | 7527 |
| 30 | 662 | 1542 | 2666 | 3843 | 4492 | 4791 |
| 35 | 664 | 1373 | 2130 | 2756 | 3036 | 3151 |
| 40 | 631 | 1172 | 1652 | 1972 | 2096 | 2143 |
| 45 | 581 | 980 | 1274 | 1440 | 1497 | 1519 |
| 50 | 526 | 817 | 997 | 1087 | 1117 | 1128 |
| 60 | 430 | 588 | 664 | 696 | 706 | 710 |
| 70 | 361 | 454 | 492 | 507 | 512 | 513 |
| 80 | 312 | 372 | 394 | 403 | 405 | 406 |
| 90 | 278 | 320 | 334 | 340 | 341 | 342 |
| 100 | 255 | 286 | 297 | 300 | 301 | 302 |
| 150 | 223 | 239 | 244 | 245 | 246 | 246 |
| 200 | 222 | 234 | 237 | 238 | 239 | 239 |
| 250 | 224 | 233 | 235 | 236 | 237 | 237 |
| 300 | 226 | 234 | 236 | 237 | 237 | 237 |
| 400 | 231 | 237 | 239 | 239 | 239 | 239 |
| 500 | 230 | 235 | 237 | 237 | 237 | 237 |
| 600 | 226 | 230 | 231 | 231 | 231 | 231 |
| 700 | 220 | 229 | 224 | 224 | 224 | 224 |
| 800 | 214 | 217 | 217 | 218 | 218 | 218 |
| 900 | 209 | 212 | 212 | 212 | 212 | 212 |

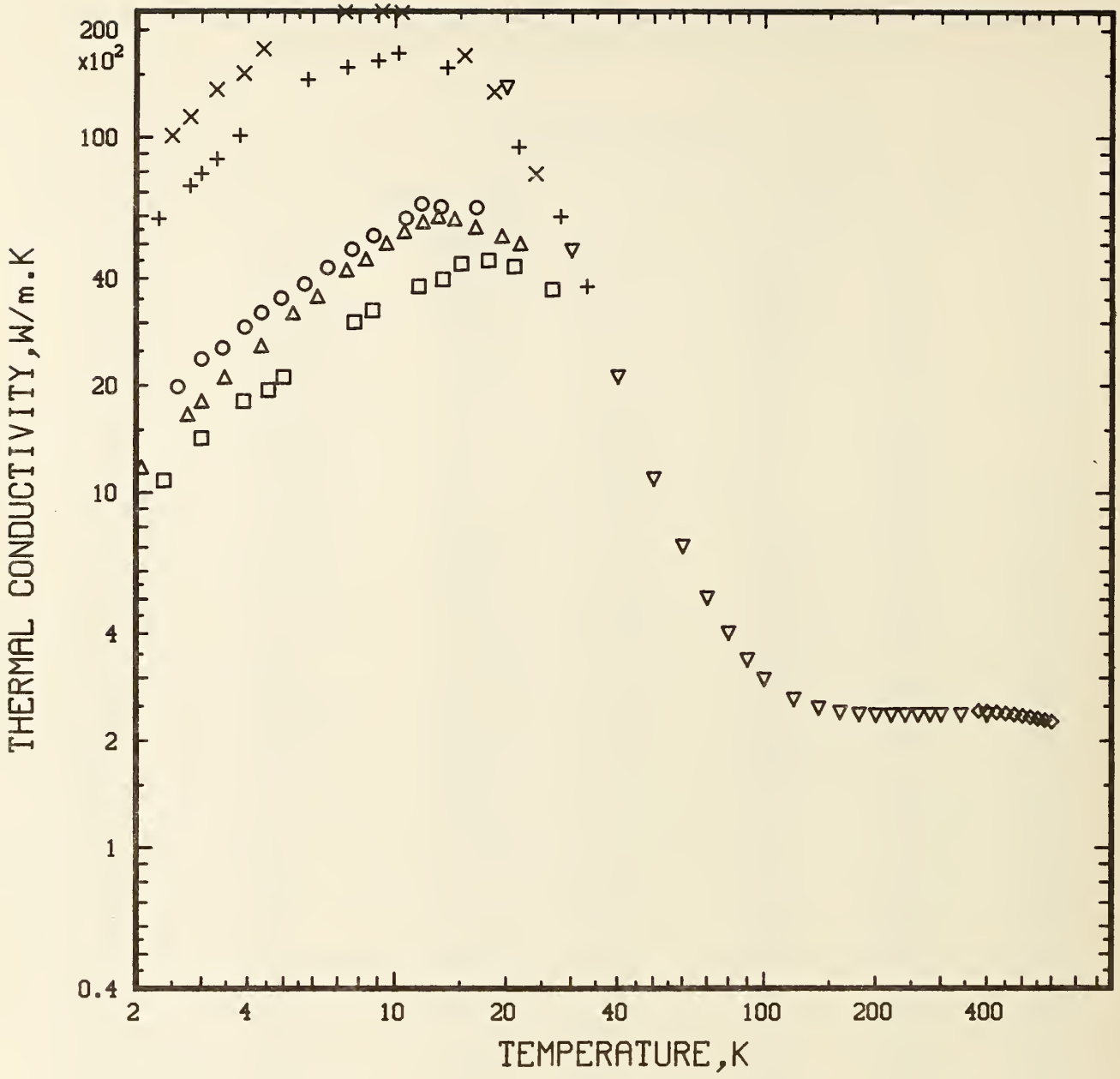


Figure 3.1.1 Experimental thermal conductivity data selected from the following primary references in the aluminum annotated bibliography:(1,5,9,11)

○ - (1), △ - (1), □ - (1), ▽ - (5),
◇ - (9), + - (11), × - (11)

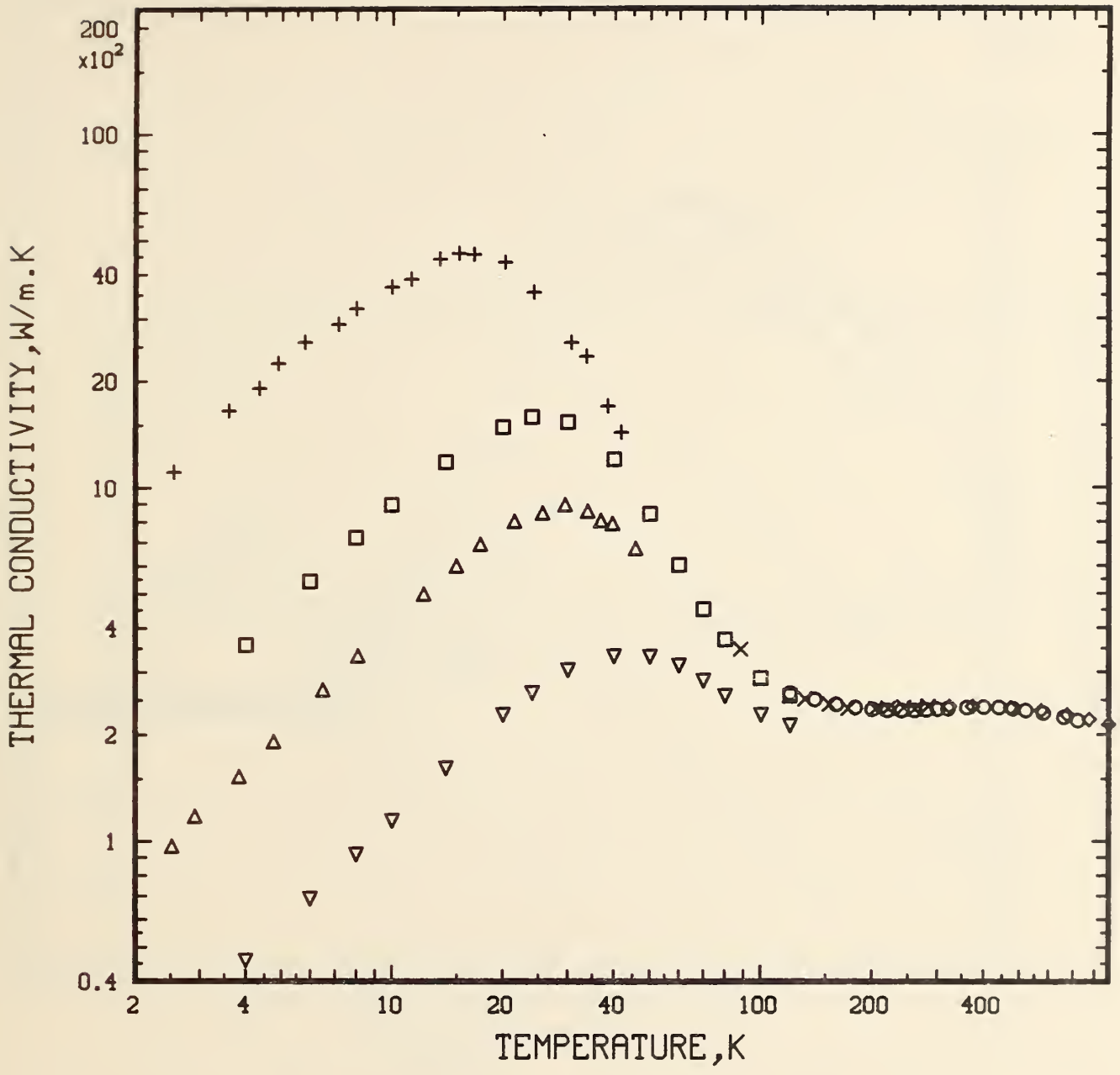


Figure 3.1.2 Experimental thermal conductivity data selected from the following primary references in the aluminum annotated bibliography:(12,17,25,26,29,33)

○ - (12), △ - (17), □ - (25), ▽ - (25),
◇ - (26), + - (29), × - (33)

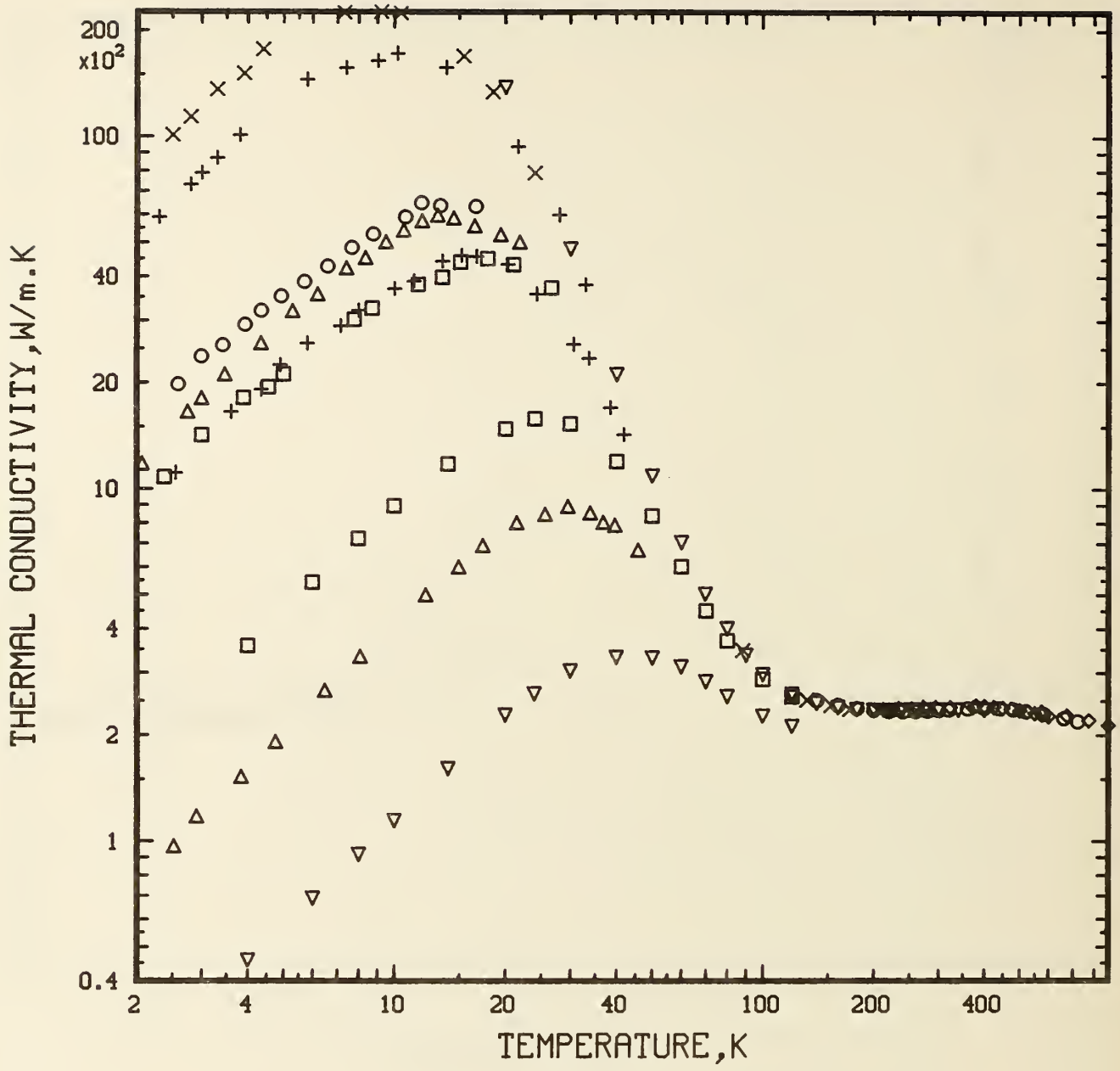


Figure 3.1.3 Composite of the data in figs. 3.1.1 and 3.1.2

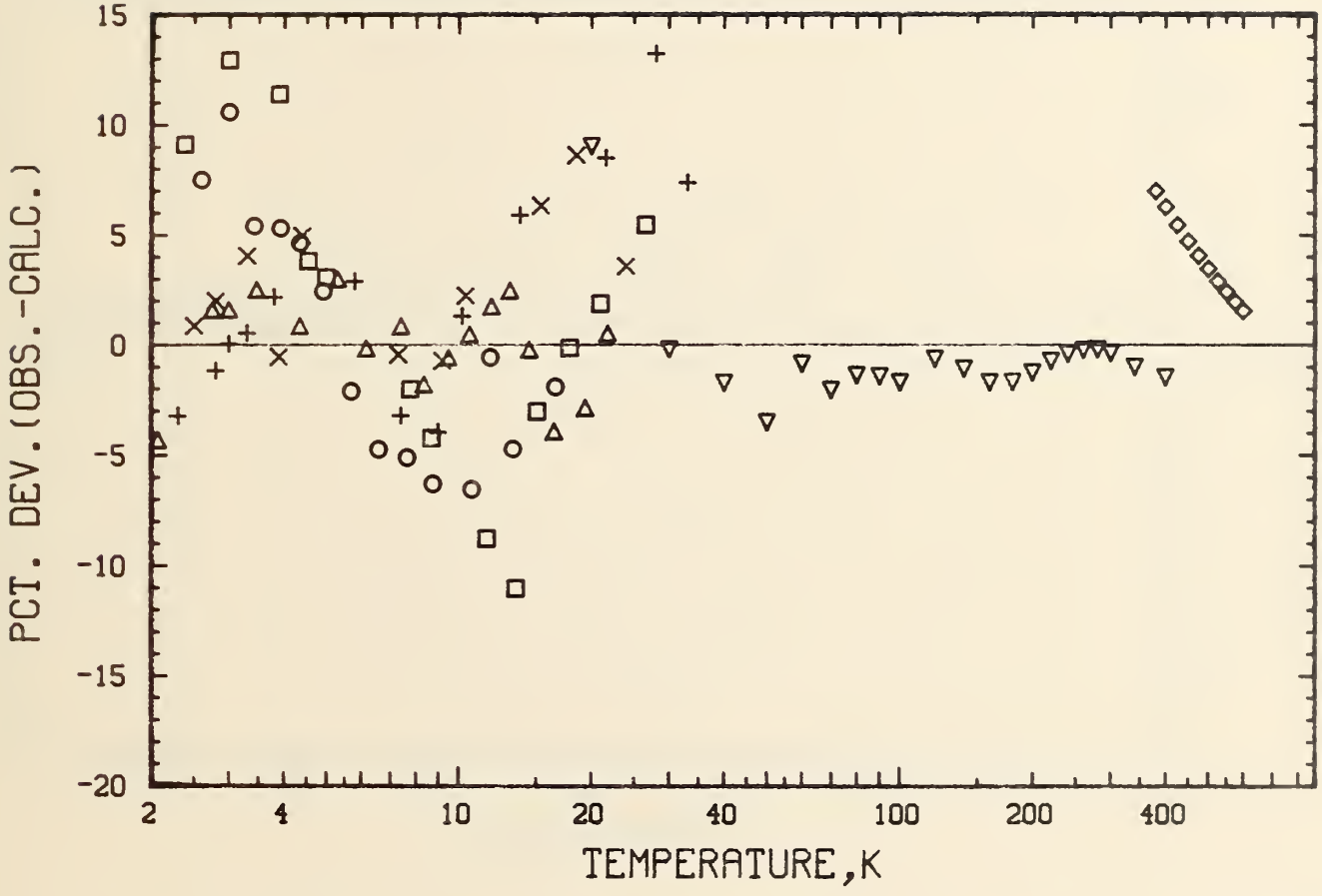


Figure 3.2.1 Thermal conductivity deviations of the aluminum data from the following primary references compared to eq. (1.1.3): (1,5,9,11)

○ - (1), △ - (1), □ - (1), ▽ - (5),
◇ - (9), + - (11), × - (11)

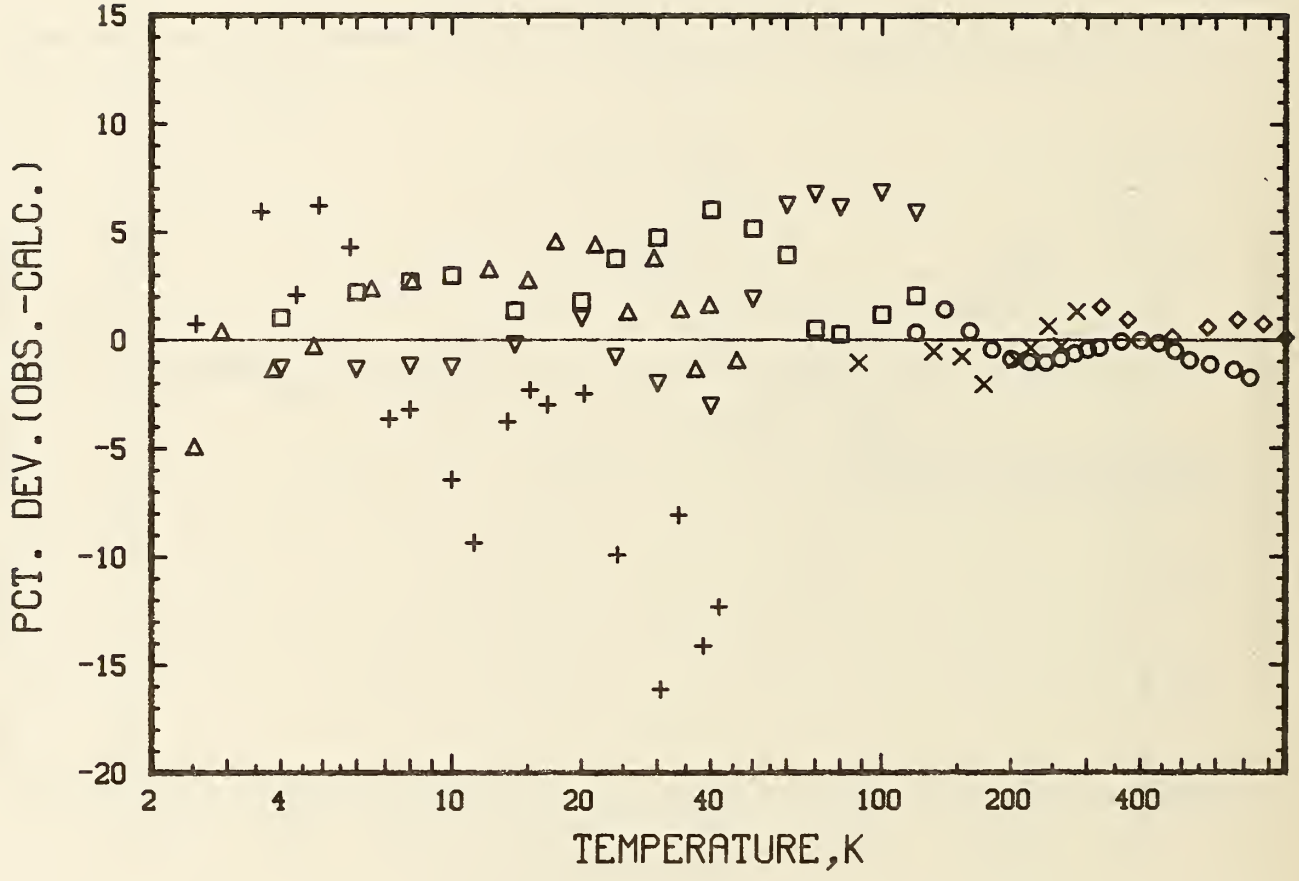


Figure 3.2.2 Thermal conductivity deviations of the aluminum data from the following primary references compared to eq. (1.1.3): (12,17,25,26,29,33)

○ - (12), △ - (17), □ - (25), ▽ - (25),
◇ - (26), + - (29), × - (33)

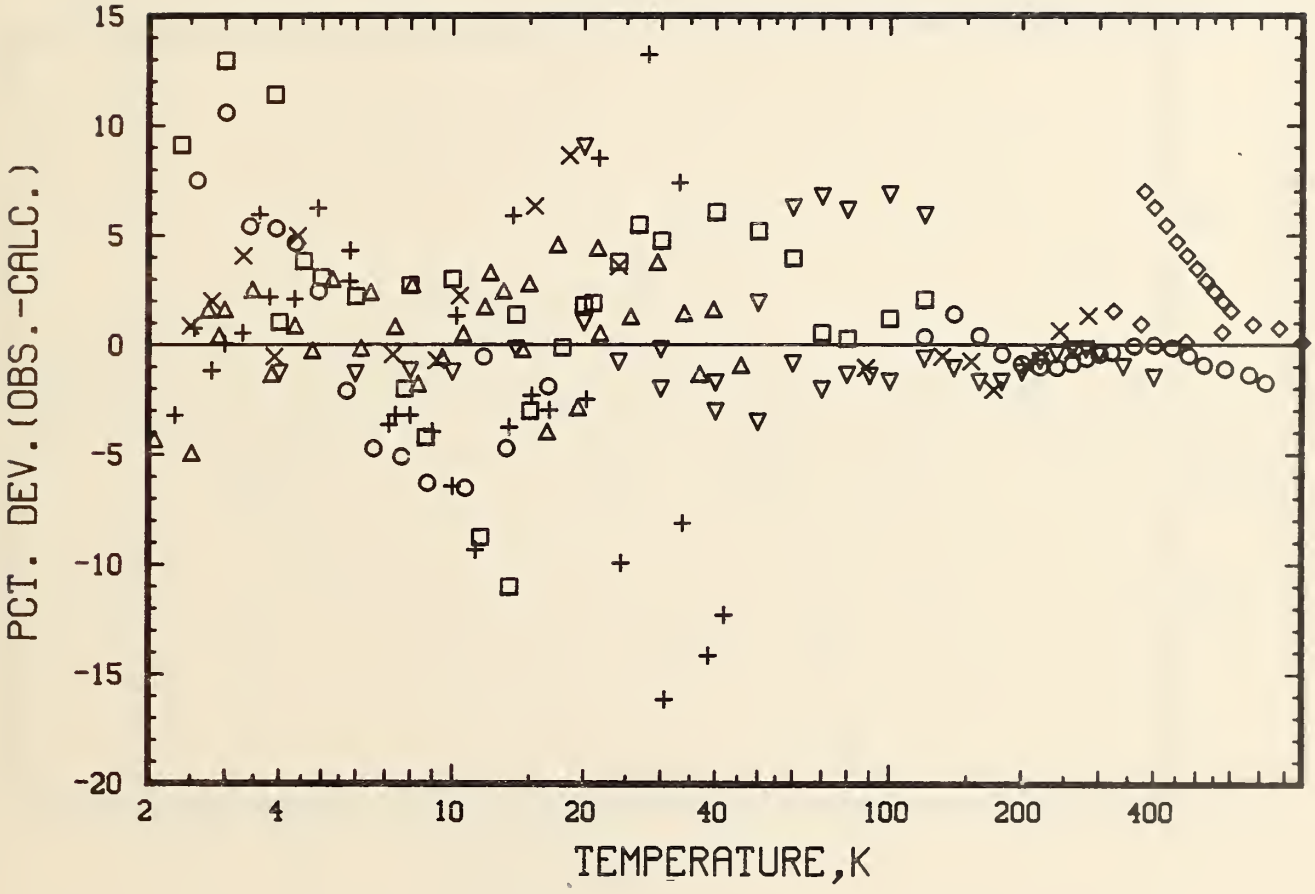


Figure 3.2.3 Composite of the deviations in figs. 3.2.1 and 3.2.2

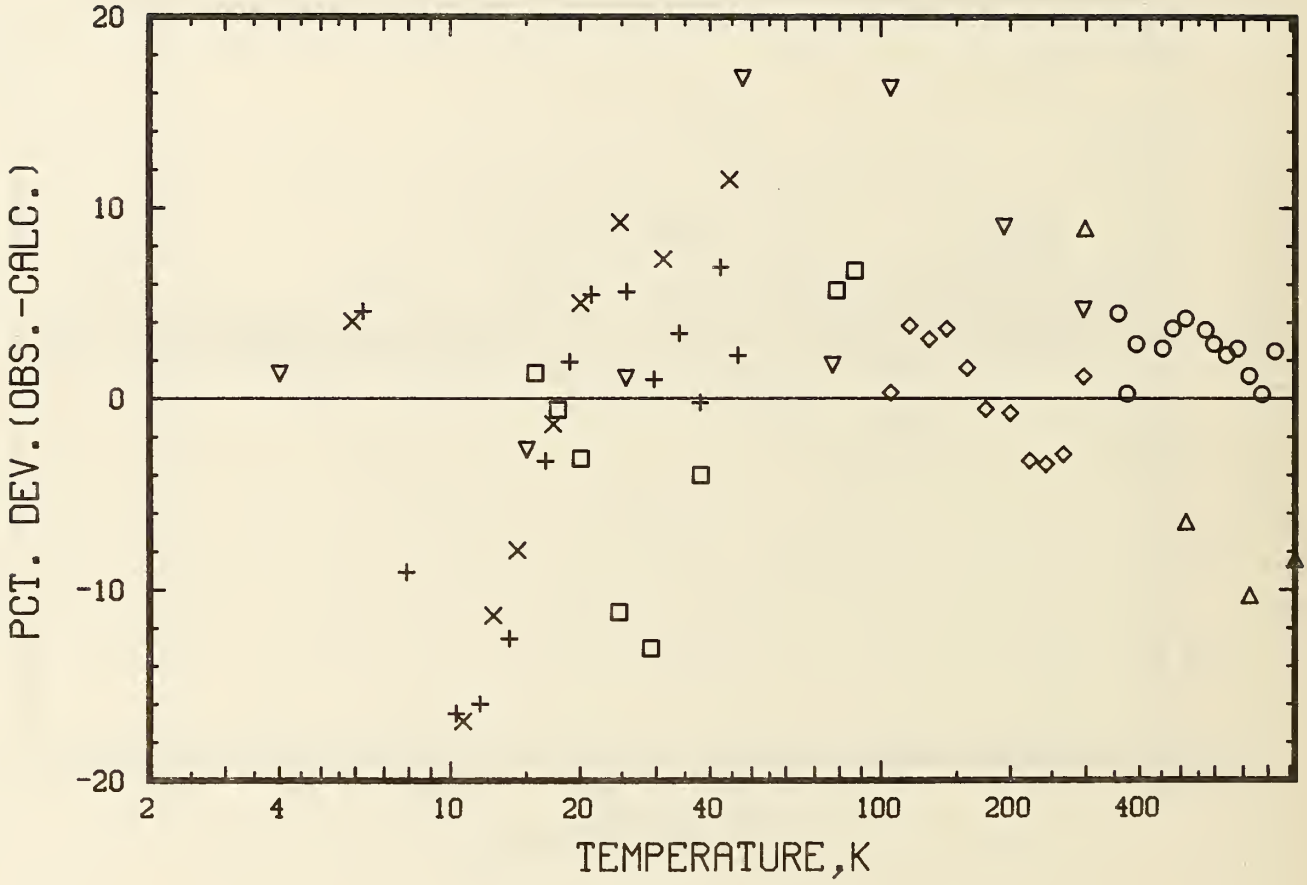


Figure 3.2.4 Thermal conductivity deviations of the aluminum data from the following secondary references compared to eq. (1.1.3):(2,3,6,7,10,14)

○ - (2), △ - (3), □ - (6), ▽ - (7),
◇ - (10), + - (14), × - (14)

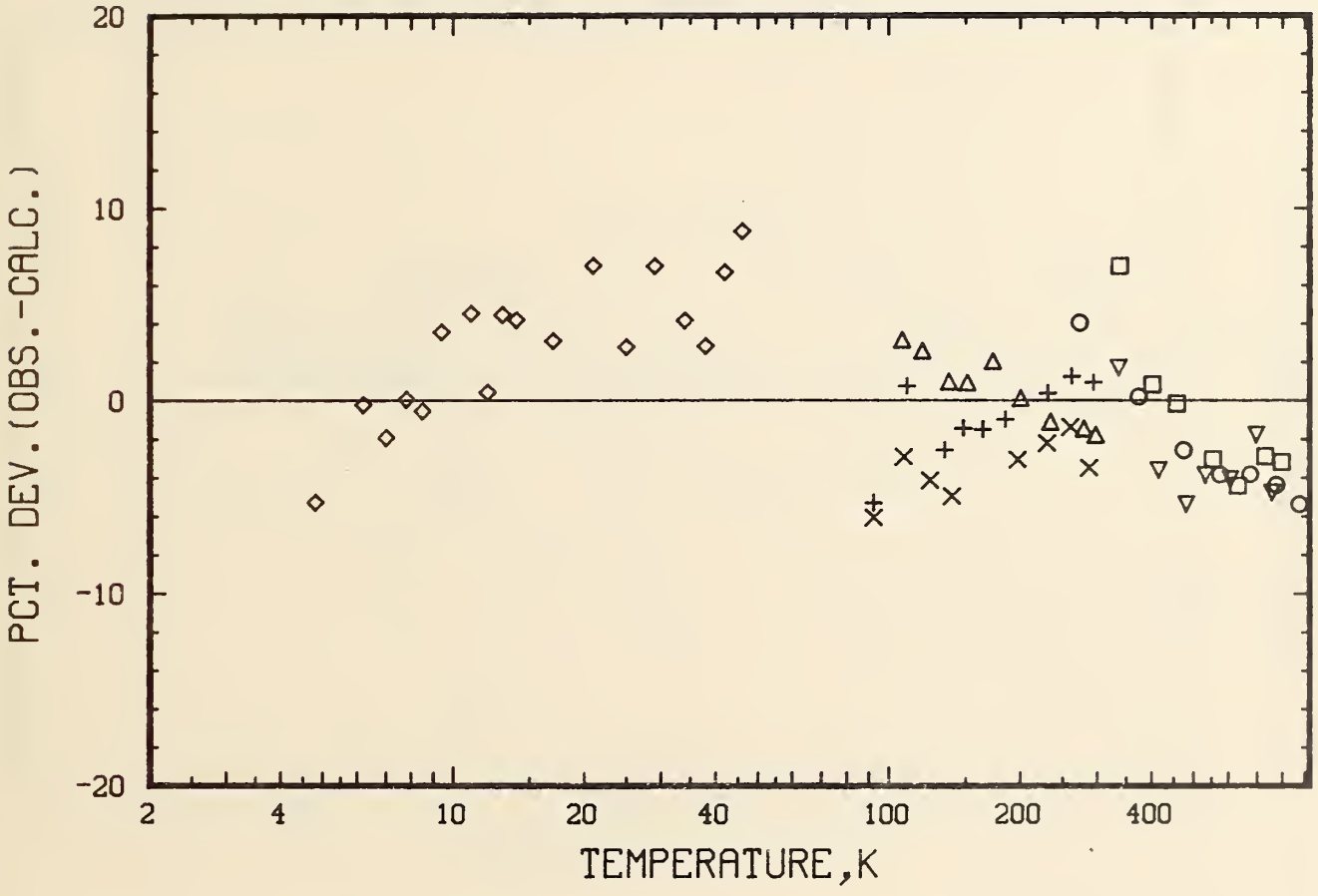


Figure 3.2.5 Thermal conductivity deviations of the aluminum data from the following secondary references compared to eq. (1.1.3):(15,16,19,20,21,23)

○ - (15), △ - (16), □ - (19), ▽ - (20),
◇ - (21), + - (23), × - (23)

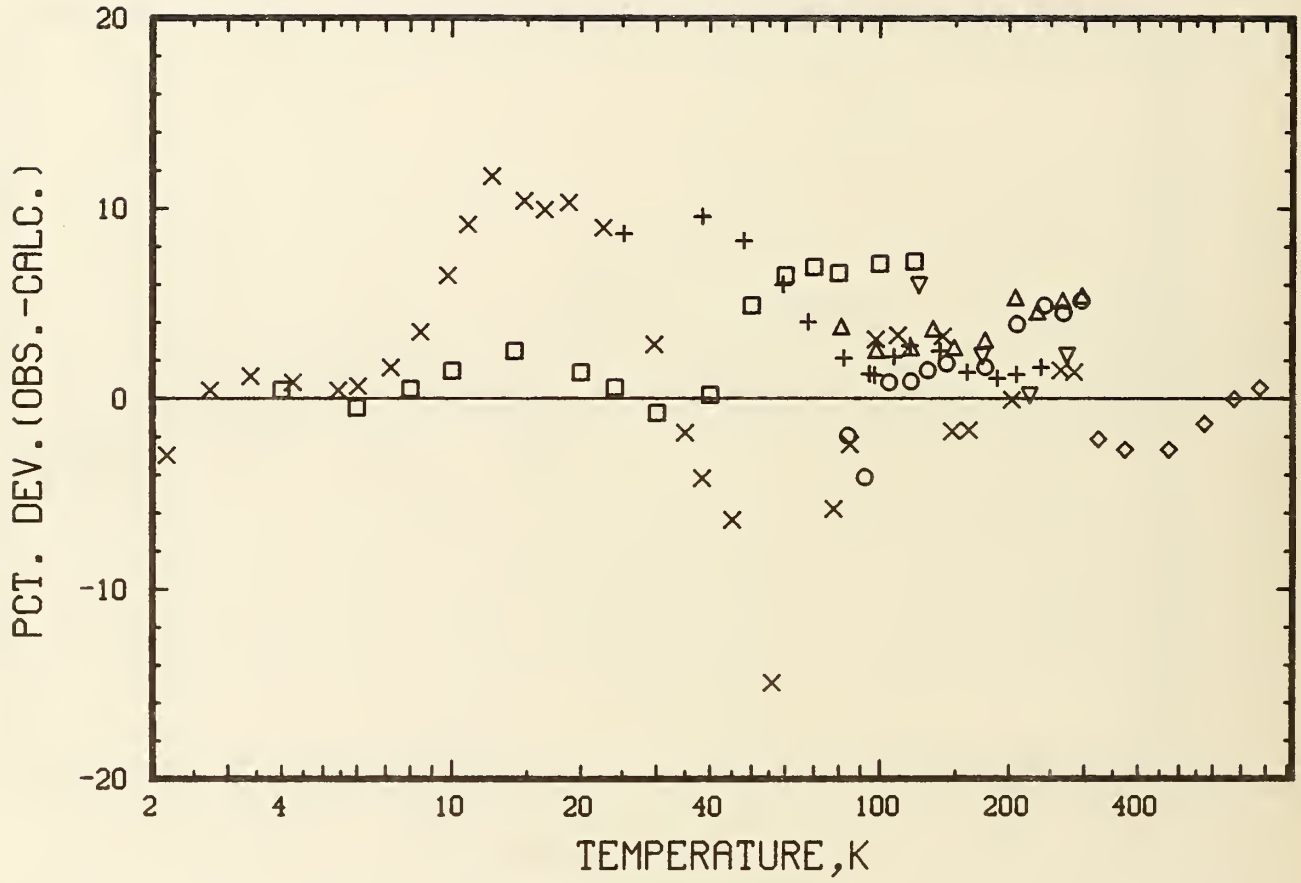


Figure 3.2.6 Thermal conductivity deviations of the aluminum data from the following secondary references compared to eq. (1.1.3):(23,25,26,27,28)

○ - (23), △ - (23), □ - (25), ▽ - (26),
◇ - (26), + - (27), × - (28)

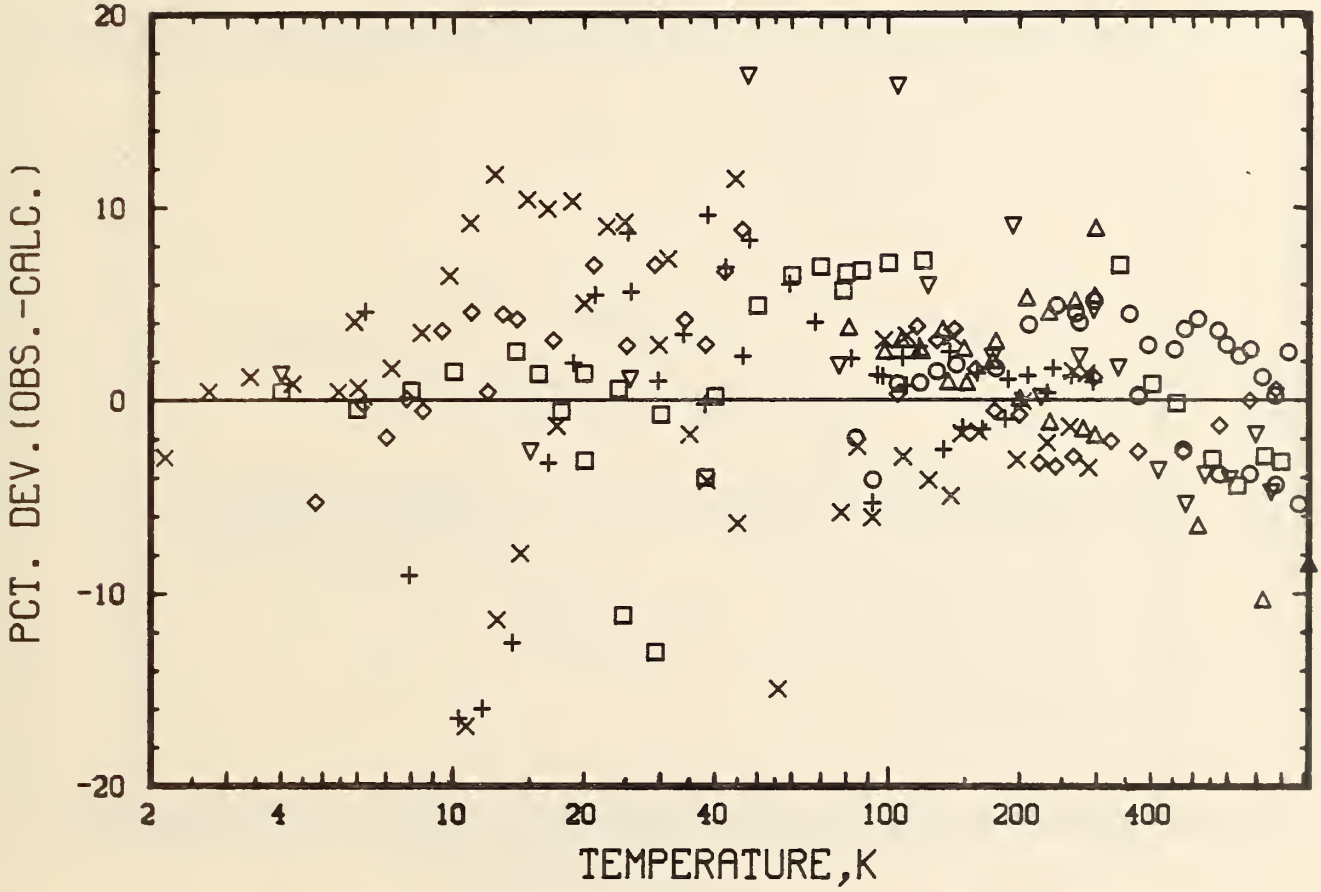


Figure 3.2.7 Composite of the deviations in figs.3.2.4 through 3.2.6

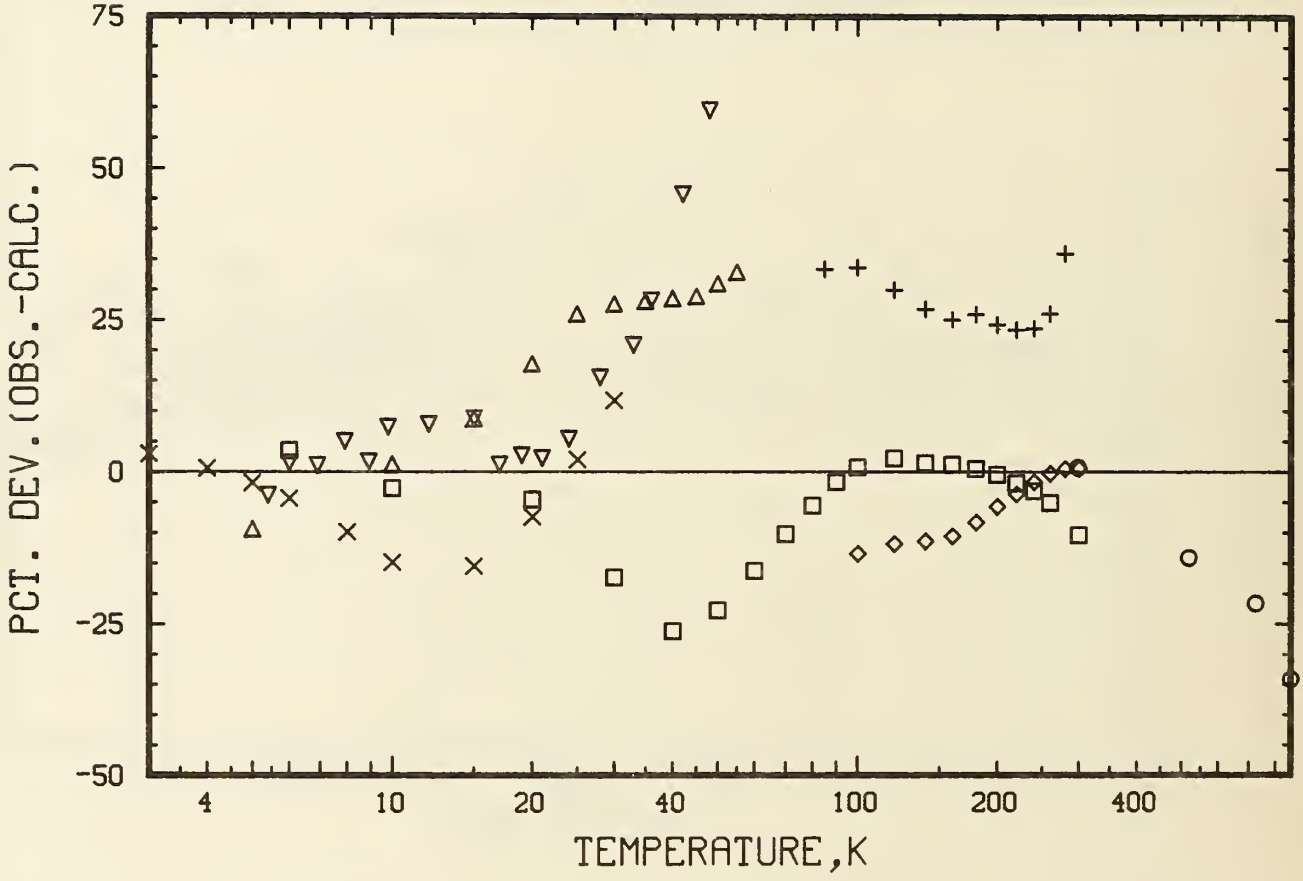


Figure 3.2.8 Thermal conductivity deviations of the aluminum data from the following secondary references compared to eq. (1.1.3):(3,13,18,21,22,24,30)

○ - (3), △ - (13), □ - (18), ▽ - (21),
◇ - (22), + - (24), × - (30)

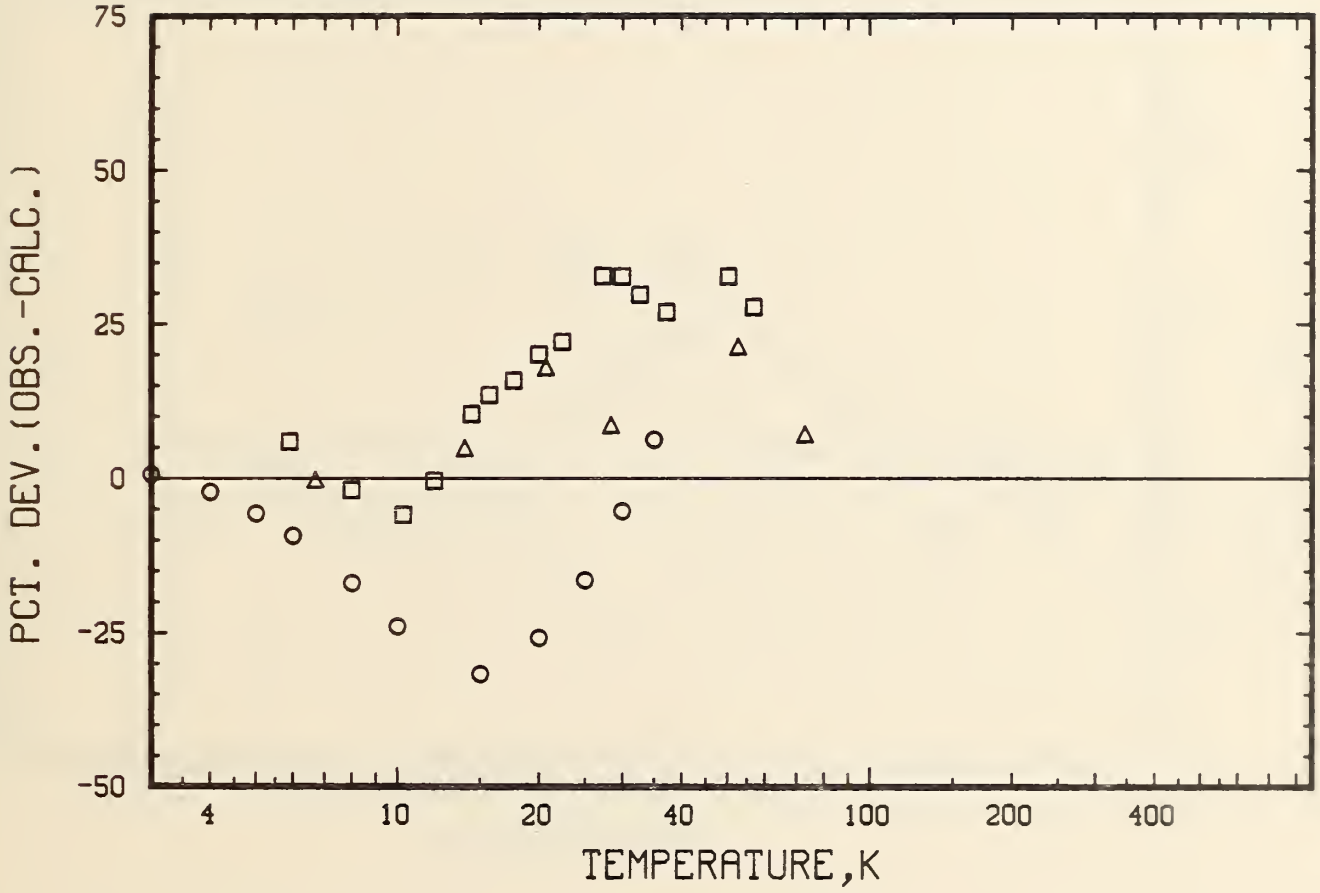


Figure 3.2.9 Thermal conductivity deviations of the aluminum data from the following secondary references compared to eq. (1.1.3):(30,31,32)

○ - (30), △ - (31), □ - (32)

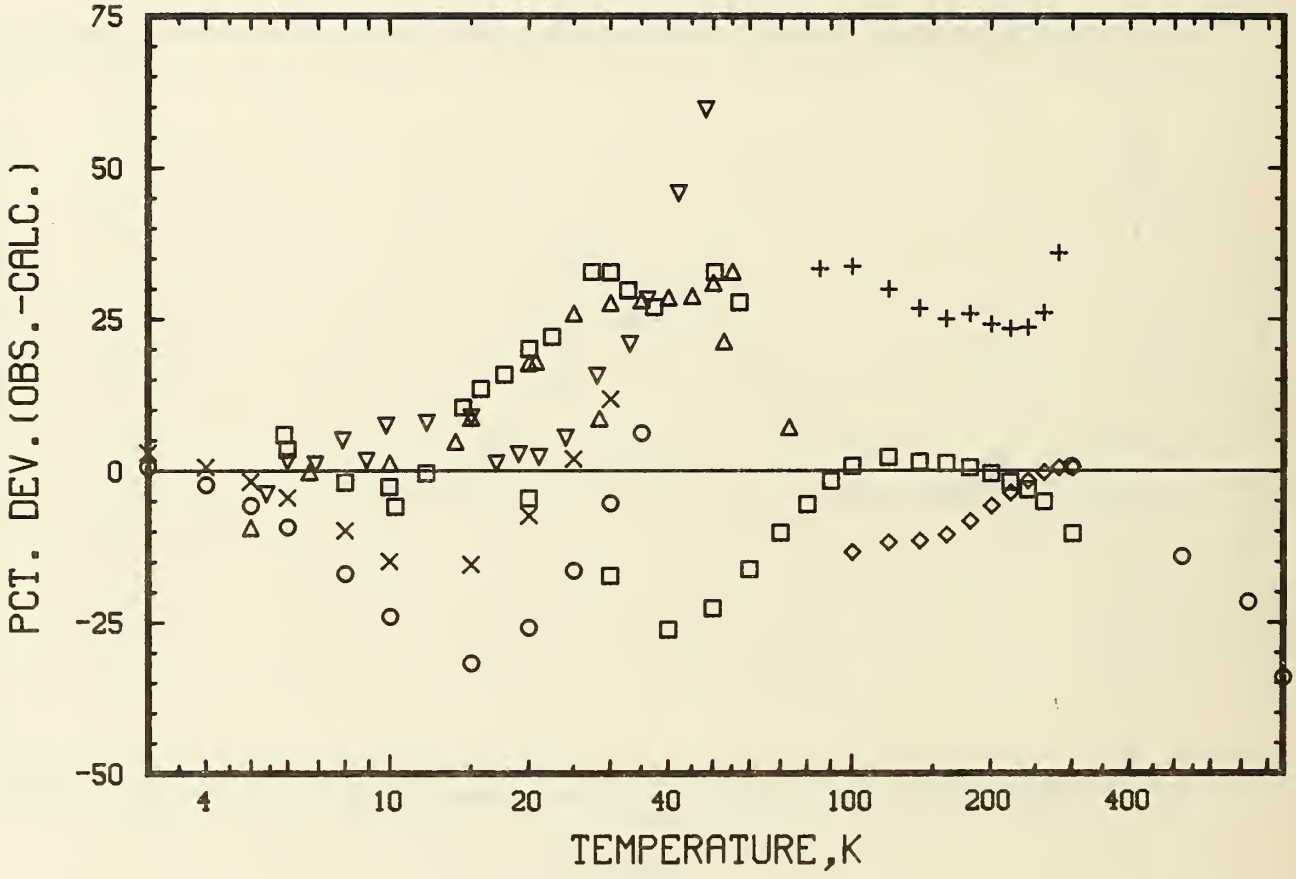


Figure 3.2.10 Composite of the deviations in figs. 3.2.8 and 3.2.9

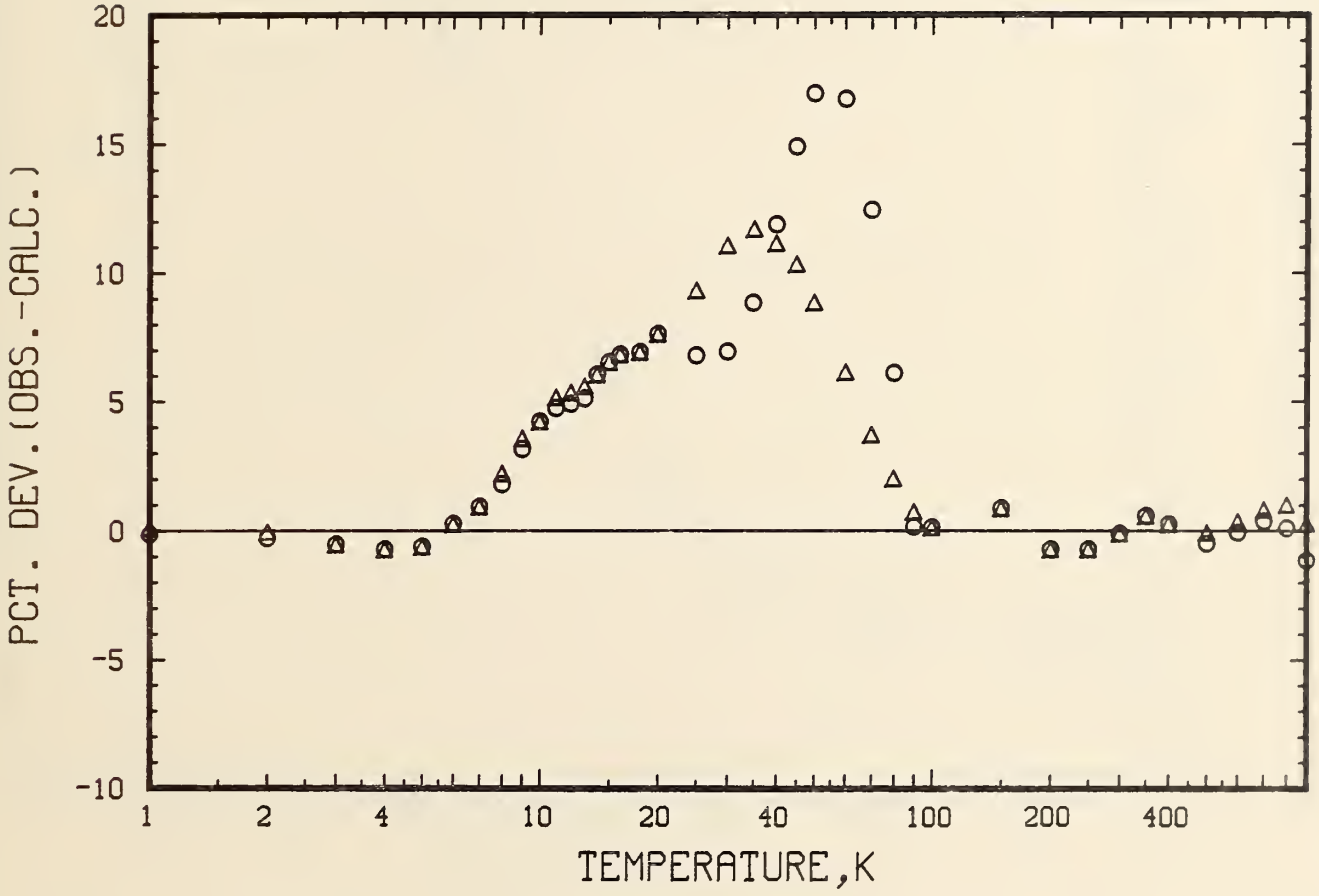


Figure 3.2.11 Comparison of eq.(1.1.3) to the values recommended for aluminum in the following references:(14A,32A)

○ = (14A), △ = (32A)

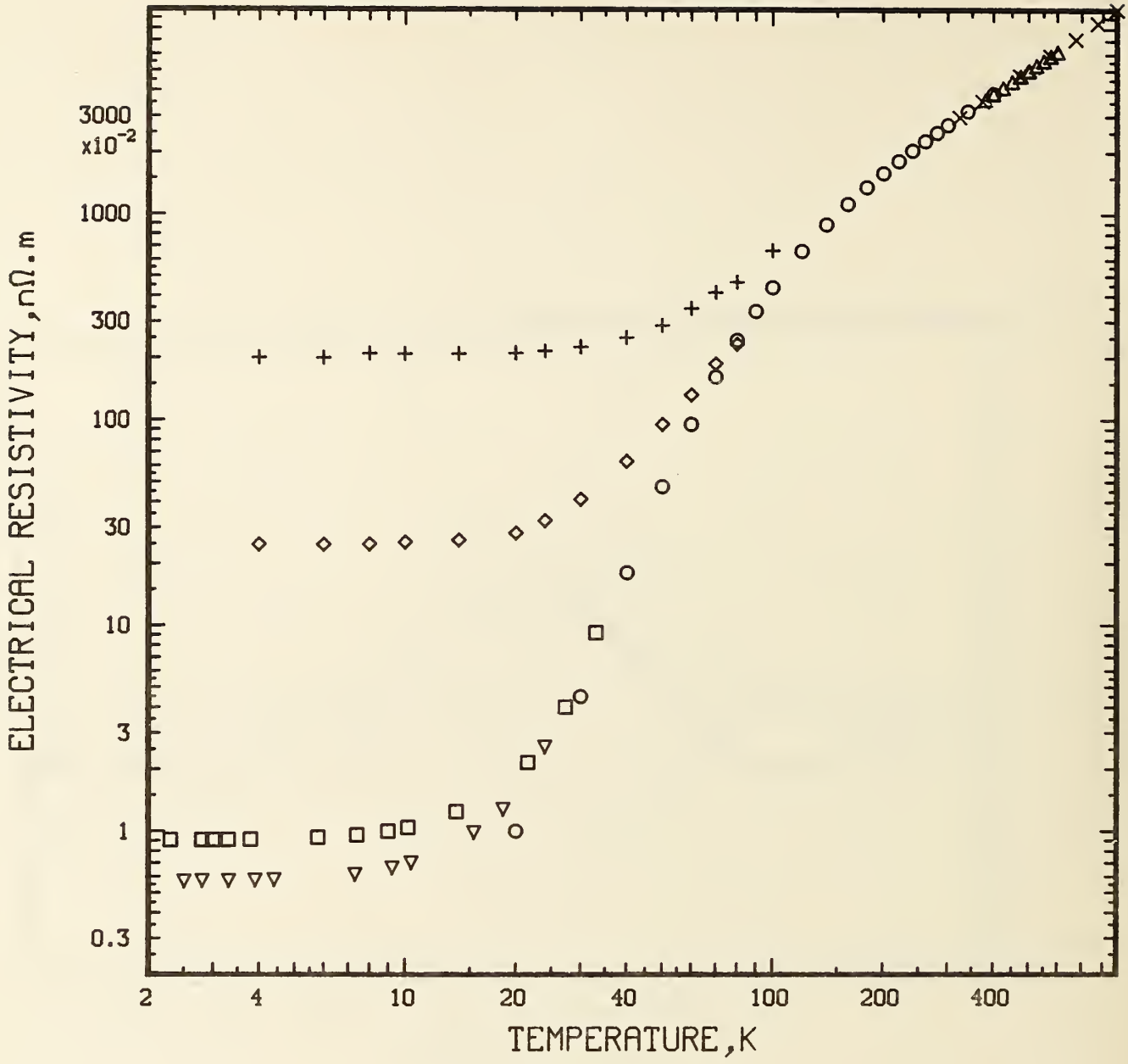


Figure 3.3.1 Experimental electrical resistivity data for aluminum selected from the following references in the aluminum annotated bibliography: (4,9,11,25,26)

○ - (4), △ - (9), □ - (11), ▽ - (11),
◇ - (25), + - (25), × - (26)

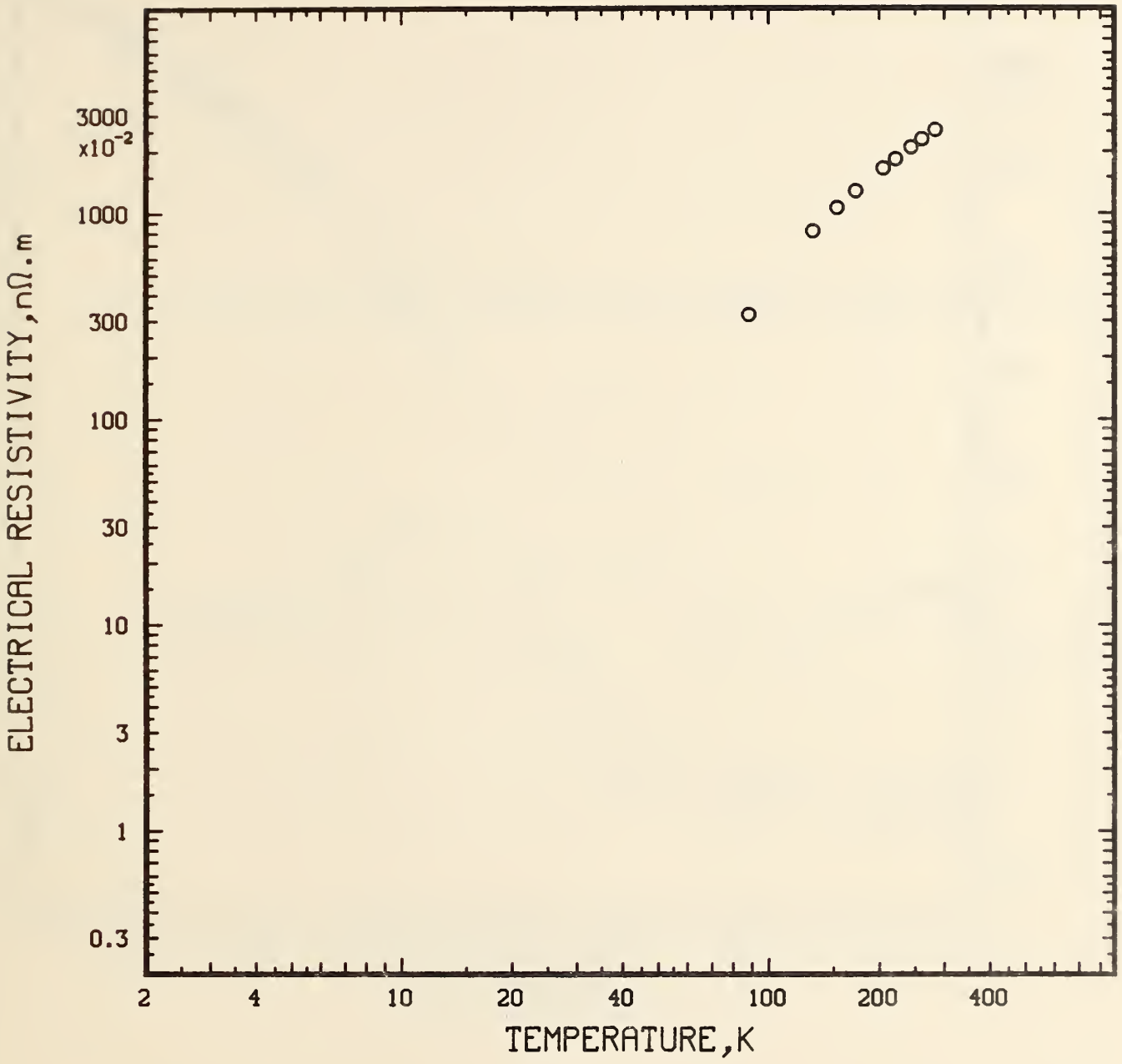


Figure 3.3.2 Experimental electrical resistivity data for aluminum selected from the following reference in the aluminum annotated bibliography: (33)

O - (33)

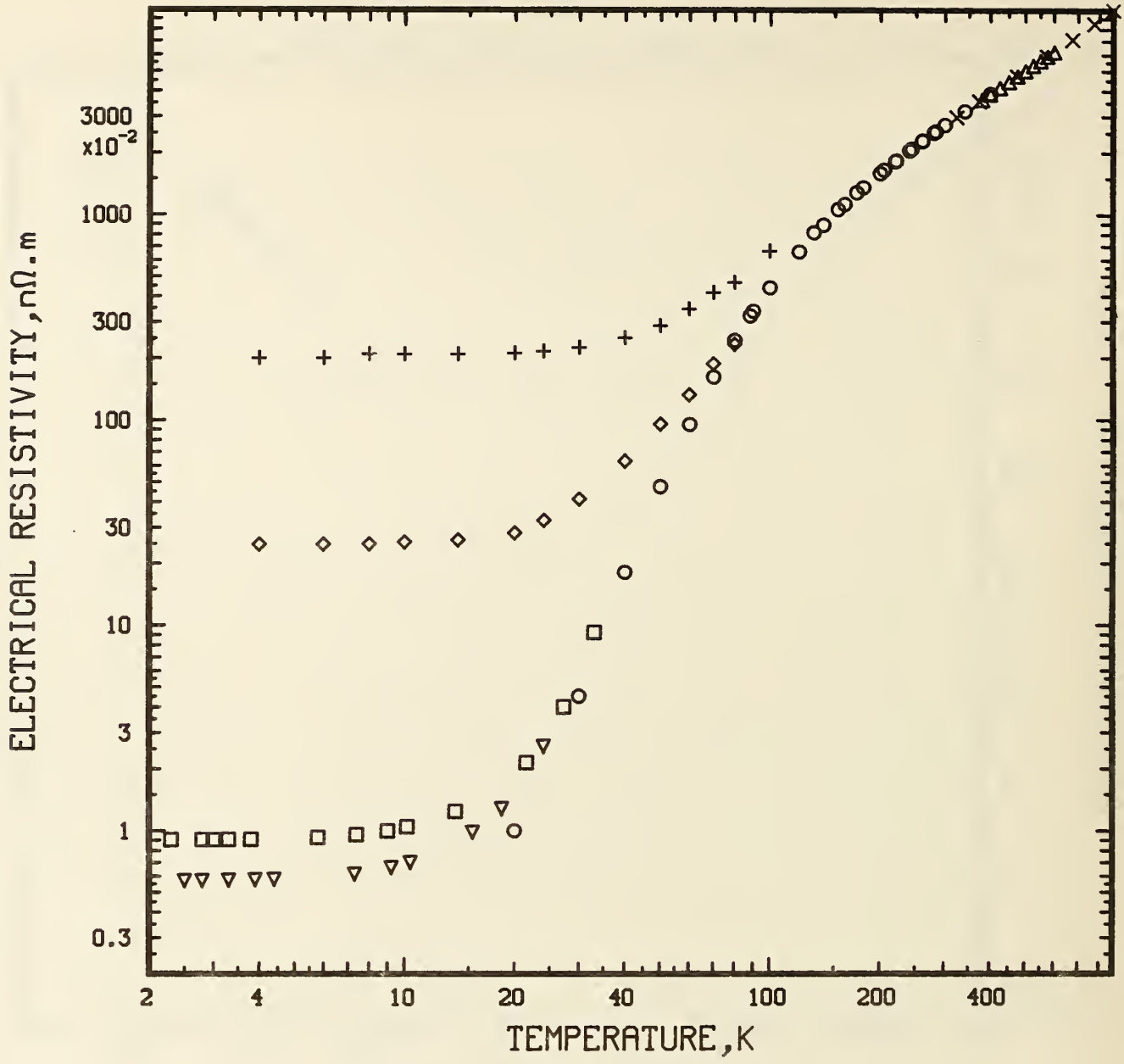


Figure 3.3.3 Composite of the electrical resistivity data in figs. 3.3.1 and 3.3.2

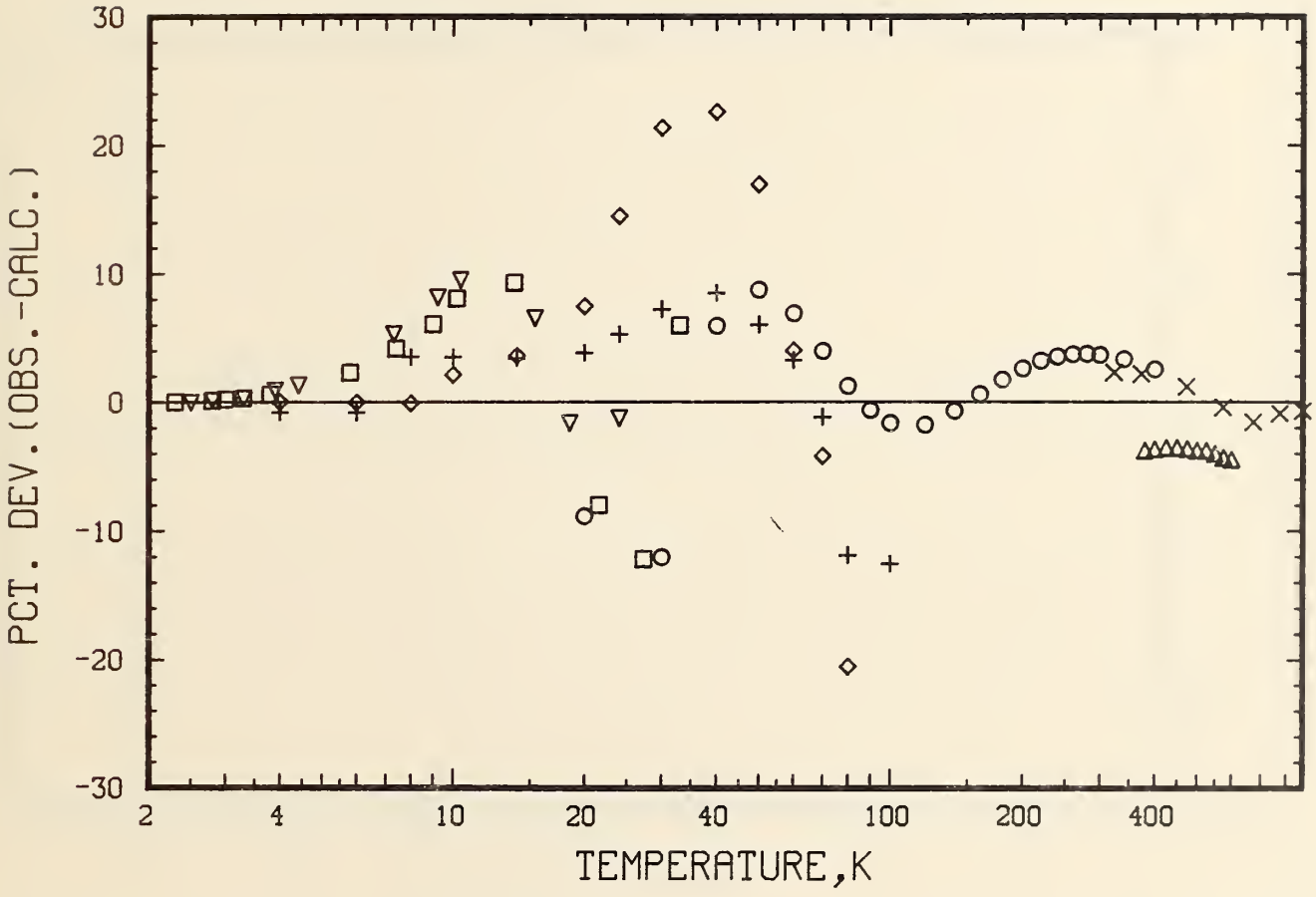


Figure 3.3.4 Electrical resistivity deviations of the aluminum data from the following references compared to eq. (1.2.3):(4,9,11,25,26)

○ - (4), △ - (9), □ - (11), ▽ - (11),
◇ - (25), + - (25), × - (26)

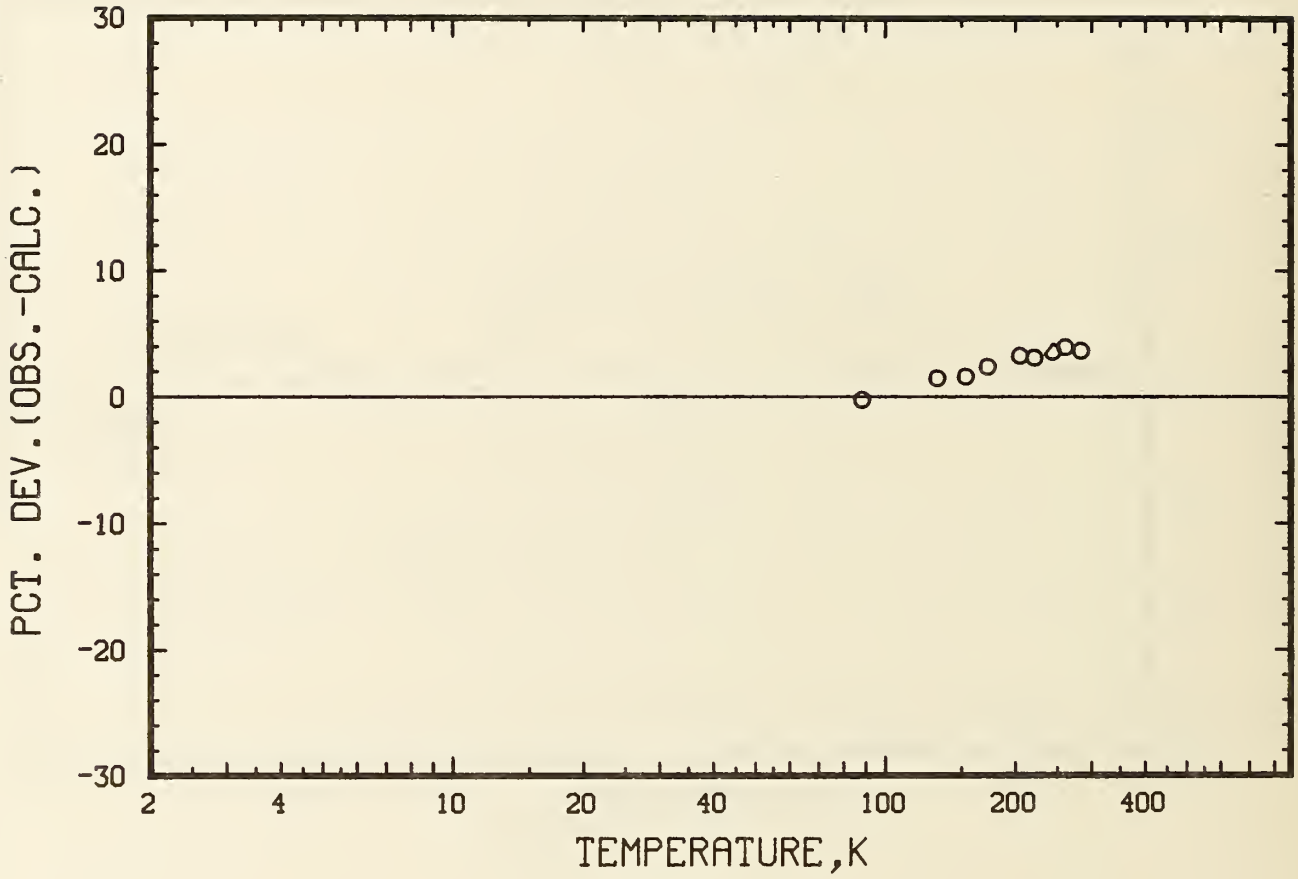


Figure 3.3.5 Electrical resistivity deviations of the aluminum data from the following reference compared to eq. (1.2.3):(33)

O - (33)

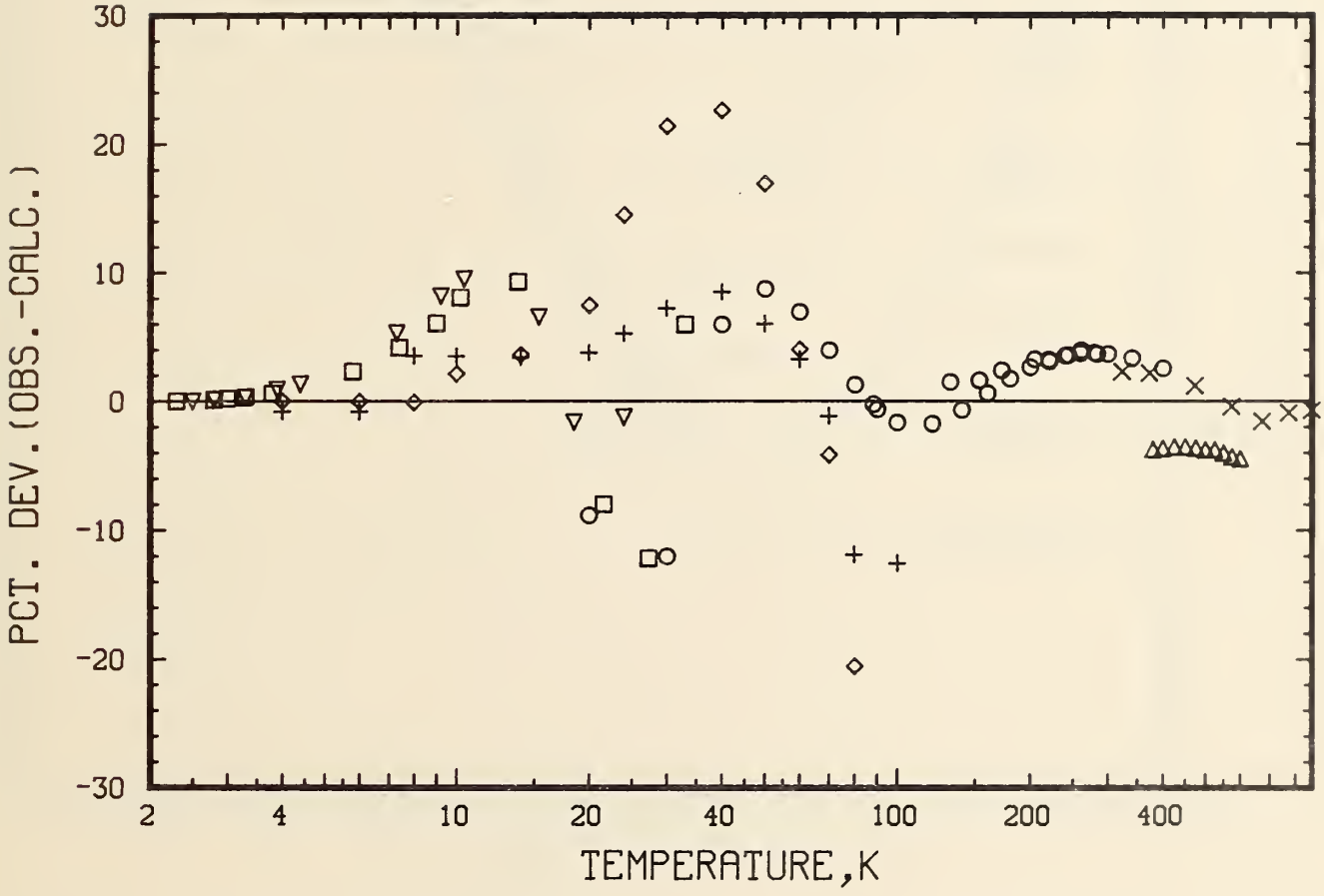


Figure 3.3.6 Composite of the electrical resistivity deviations shown in figs. 3.3.4 and 3.3.5

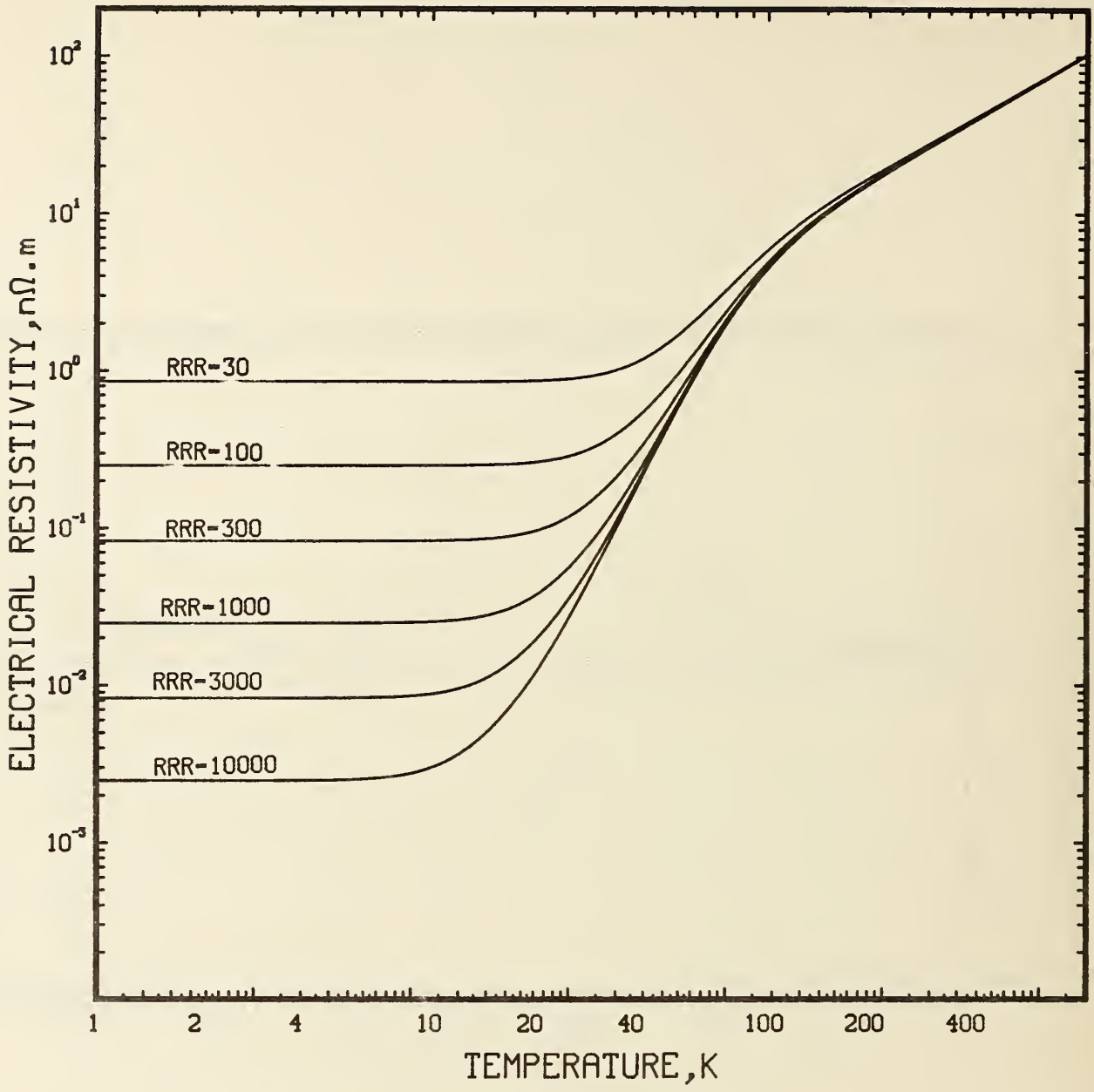


Figure 3.3.7 Electrical resistivity for aluminum as a function of temperature calculated from eq.(1.2.3) at selected values of RRR.

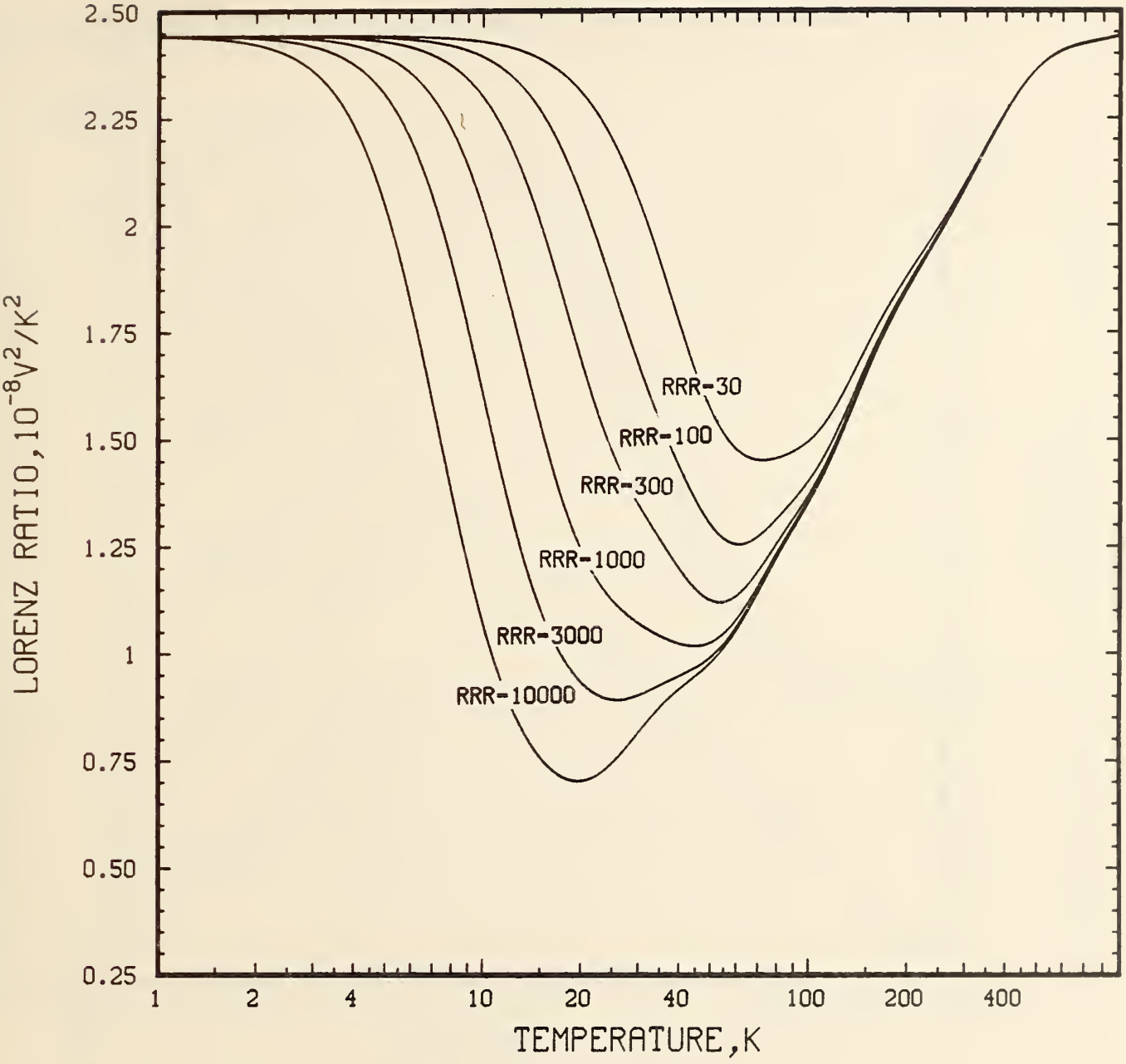


Figure 3.3.8 Lorenz ratio for aluminum as a function of temperature calculated from eq.(1.2.3) and eq.(1.1.3) at selected values of RRR.

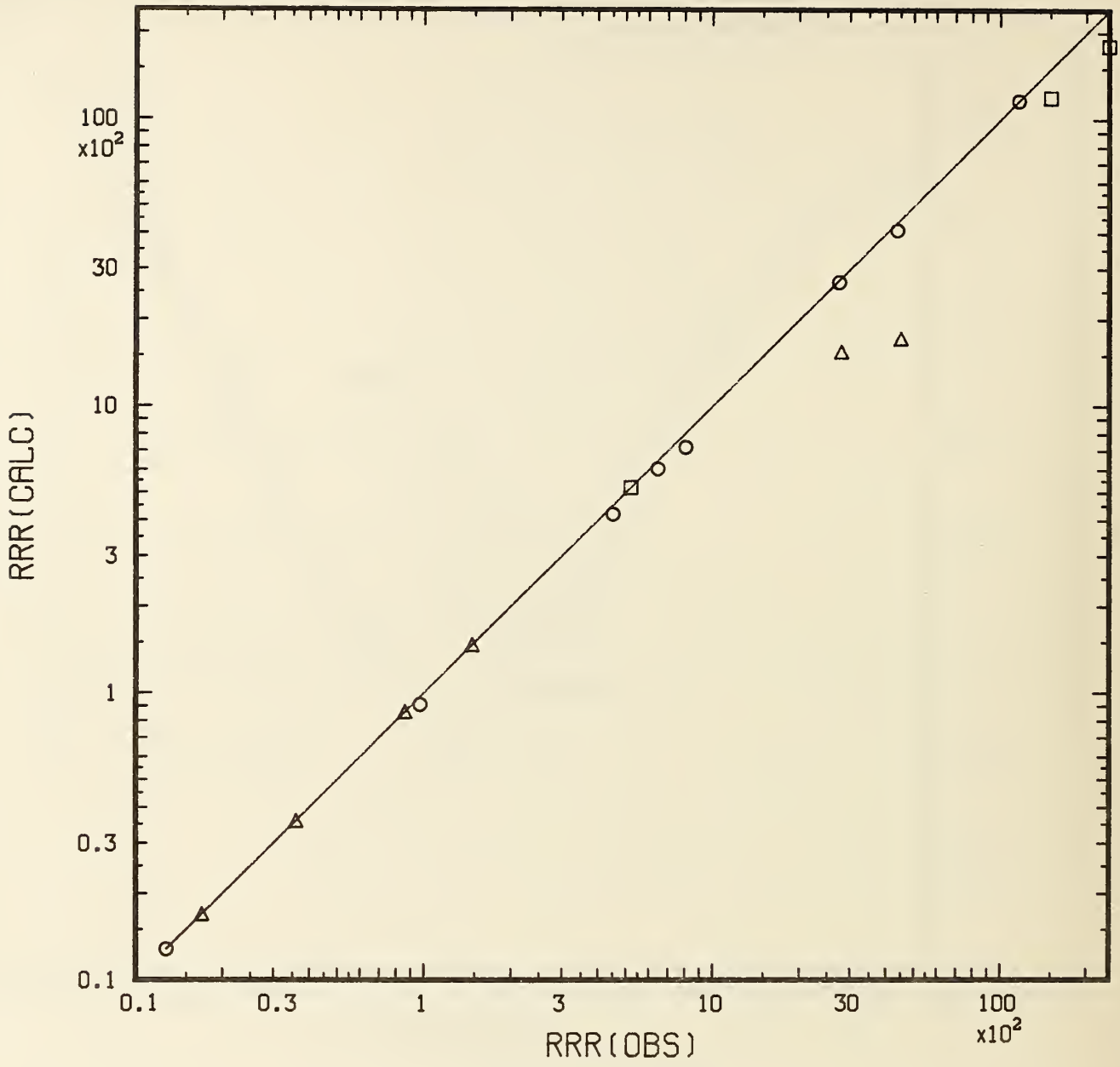


Figure 3.3.9 RRR values calculated as per Section 1.5, RRR(CALC), versus reported RRR values, RRR(OBS), for aluminum.

○ - Primary, △ - Secondary,
□ - Secondary

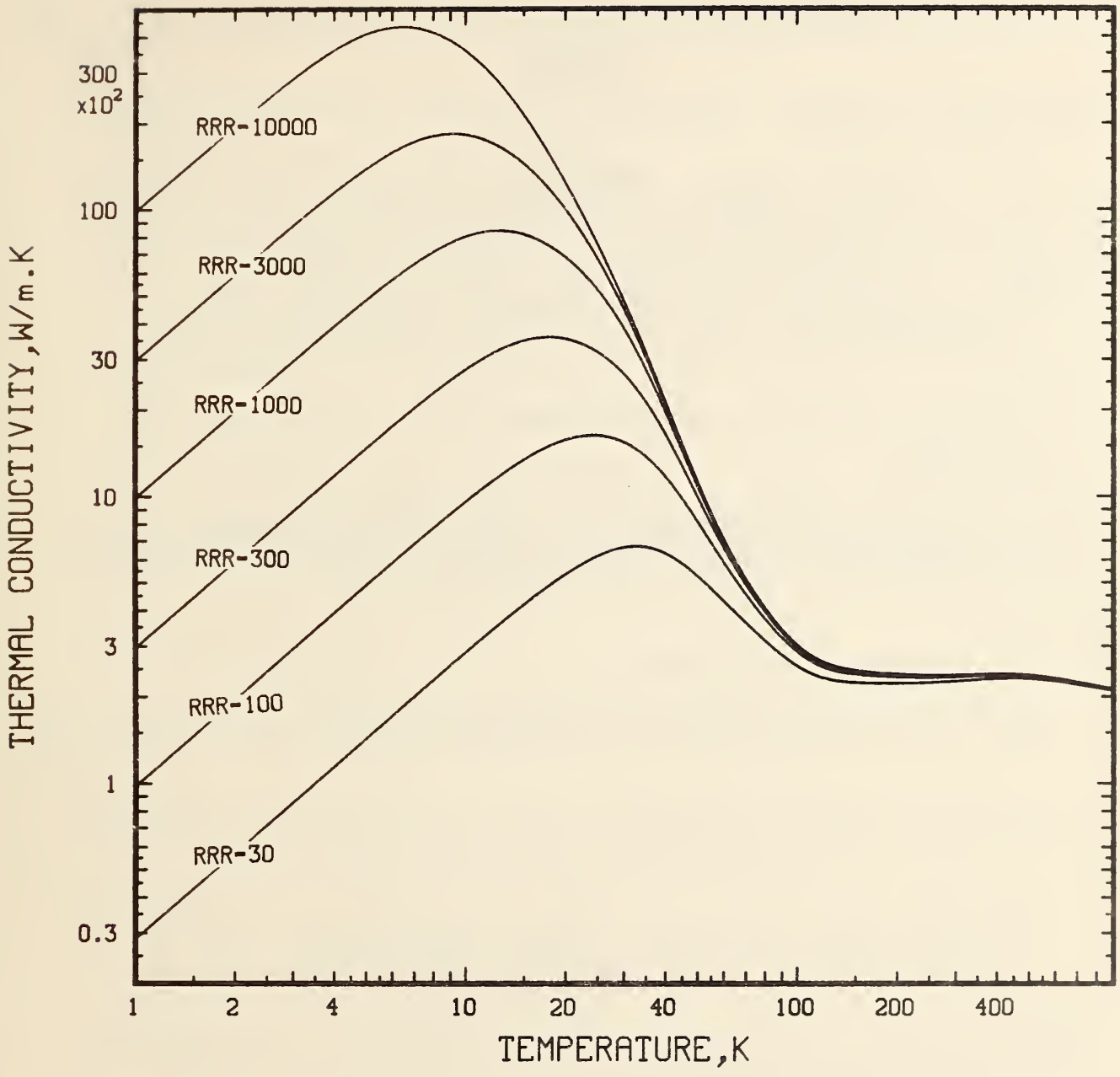


Figure 3.4.1 Thermal conductivity for aluminum as a function of temperature calculated from eq.(1.1.3) at selected values of RRR.

## 3.5 FORMAT FOR ANNOTATED BIBLIOGRAPHY OF ALUMINUM

### REFERENCE

AUTHOR, TITLE, CITATION

### ANNOTATION

PURPOSE

SPECIMEN
a) Dimensions/Shape; b) Crystal Status; c) Thermal/Mech. History; d) Purity Specification; e) RRR; f) $\rho_o$; g) Other Characterization Data

APPARATUS
a) Type; b) Thermometry/Calibration/Anchoring; c) Thermal Isolation; d) Other (Q meas.)

DATA
a) Temperature Range/Difference; b) Content of Tables, Figures and Equations/Data Extraction; c) Uncertainty/Imprecision; d) Disputable Corrections to Measurements by Authors; e) Errata (by Author or Reviewer)

ANALYSIS
a) Comparisons; b) Conclusions

[1] Andrews, F. A., Webber, R. T. and Spohr, D. A., Thermal Conductivities of Pure Metals at Low Temperatures. I. Aluminum, Phys. Rev., 84(5), 994-6, (1951)

PURPOSE
To measure $\lambda$ for three high purity Al specimens.

SPECIMEN
a) 4 in. (10 cm) long, 0.15 in. (0.38 cm) dia./rod; b) Al 1,2: single crystals, Al 3: polycrystalline; c) Al 3: annealed; d) Al 1,2: 0.001% Mg, 0.001% Si, 0.0006% Fe, 0.0004% Cu, 0.0004% Na. Al 3: 0.002% Mg, < 0.001% Si, < 0.0005% Fe, < 0.0005% Cu, faint trace of Na; e) Al 1 (RRR = 840), Al 2 (RRR = 676), Al 3 (RRR = 467); f) Al 1 ($\rho_o$ = 3.04 n$\Omega$·cm), Al 2 (3.85 n$\Omega$·cm), Al 3 ($\rho_o$ = 5.51 n$\Omega$·cm).

APPARATUS
a) Longitudinal; b) gas thermometers; c) 0.05 $\mu$m of Hg (6.7 x $10^{-3}$ Pa) vacuum.

DATA
a) 2 to 27 K/0.03 K at 2 K, 0.15 K at 20 K; b) figure 1 - $\lambda$/data points are listed in TPRC data series; c) uncertainty: from 2 to 4.2 and 14.5 to 20.5 K: ±4%; from 4.2 to 14.5 K: ±10%; d) corrections due to departures of the thermometer system from ideal behavior at liquid helium temperatures were taken from Hulm, J. K., Proc. Roy. Soc. London, Ser. A, 204, 98 (1950).

ANALYSIS
b) $\lambda^{-1} = (AT)^{-1} + BT^2$.

[2] Bailey, L. C., The Thermal Conductivities of Certain Approximately Pure Metals and Alloys at High Temperatures, Proc. Roy. Soc. London, Ser. A, 134, 57-76 (1932)

PURPOSE
To continue the work of C. H. Lees on the effect of temperatures between -160 °C and 15 °C, on $\lambda$ of nine metals and six alloys.

SPECIMEN
a) 7 to 8 cm long, 0.585 cm dia./rods; c) turned down from larger rods; d) 99% Al; g) specimens same as Lees, C. H., Philos. Trans. Roy. Soc. London, Ser. A, 208, 381-443 (1908)/density = 2.7 g/cm$^3$ at 293 K.

APPARATUS
a) Longitudinal; b) thermocouples (chromel-alumel)/hot junction calibrated at: melting ice, steam, aniline vapor, benzophenone vapor, sulphur vapor. Cold junction: 293 K. Main current balanced against standard cell; c) powdered magnesia between guard tube and specimen, asbestos wool between guard tube and vessel.

DATA
a) 85 to 554 °C; b) Table 1 - $\lambda$.

ANALYSIS
a) Schofield, F. H., Proc. Roy. Soc. London, Ser. A, 107, 206 (1925); Griffiths, E., Proc. Roy. Soc. London, Ser. A, 115, 236 (1927); $\lambda$ reaches a maximum at 225 °C.

[3] Bidwell, C. C. and Hogan, C. L., Thermal Conductivity of Aluminum; Solid and Liquid States, J. Appl. Phys., 18, 776, (Aug 1947)

PURPOSE
To investigate $\lambda$ for Al up to the melting point and beyond, with a modified Forbes bar method.

SPECIMEN
a) 25 cm long, 2.5 cm dia./rod; d) specimen 1 = 99.2% Al, 0.10% Si, 0.67% Fe, 0.01% Cu; Mn, Mg < 0.01%, specimen 2 = 99.95% Al; g) source: Aluminum Company of America.

APPARATUS
a) modified Forbes bar method; b) thermocouples; c) finely screened Sil-o-cel insulation.

DATA
a) specimen 1, 25 to 590 °C, specimen 2, 25 to 900 °C; b) data points taken from text p. 779; d) correction for temperature drift.

ANALYSIS
a) data on specimen 1 is in agreement with Konno, S., Philos. Mag., 40, 542 (1920); b) the data are consistent with $k/\rho C = K/t + K'$.

[4] Cook, J. G., Moore, J. P., Matsumura, T., and Van der Meer, M. P., The Thermal and Electrical Conductivity of Aluminum, Proceedings of the Fourteenth Thermal Conductivity Conf. (Storrs, Conn., June 2-4, 1975) P. G. Klemens and T. K. Chu, eds., Plenum Press, New York (1976) pp. 65-71

PURPOSE
To measure $\lambda$, $\rho$, and the absolute Seebeck coefficient of pure Al from 80 to 400 K.

SPECIMEN
e) specimen A (RRR = 8500), specimen B (RRR = 11000), specimen C (RRR = 950), specimen D (RRR = 17); f) specimen A ($\rho_0 = 2.8 \times 10^{-4}$ $\mu\Omega\cdot$cm), specimen B ($\rho_0 = 2.1 \times 10^{-4}$ $\mu\Omega\cdot$cm), specimen C ($\rho_0 = 2.5 \times 10^{-4}$ $\mu\Omega\cdot$cm), specimen D ($\rho_0 = 0.14$ $\mu\Omega\cdot$cm).

DATA
a) 20 to 400 K; b) Table 1 - specimen characterization, Table 2 - $\lambda$; c) uncertainty: ±1.2%; d) correction for impurities and thermal expansion.

ANALYSIS
a) data does not agree with Seeberg, P. and Olsen, T., Phys. Norv., 2, 197 (1967); b) $\lambda = A + BT^{-4} + CT^2 + DT^{-1}$; $\lambda_g^{-1} = T/17 + 5000\ T^{-2}$.

[5] Cook, J. G., Moore, J. P., Matsumura, T., and Van der Meer, M. P., The Thermal and Electrical Conductivity of Aluminum, ORNL-5079, (Sep 1975)

PURPOSE
To measure $\lambda$, $\rho$, and the absolute Seebeck coefficient of pure Al from 80 to 400 K.

SPECIMEN
e) specimen A (RRR = 8500), specimen B (RRR = 11000), specimen C (RRR = 950), specimen D (RRR = 17); f) specimen A ($\rho_0$ = 2.8 x $10^{-4}$ $\mu\Omega\cdot$cm), specimen B ($\rho_0$ = 2.1 x $10^{-4}$ $\mu\Omega\cdot$cm), specimen C ($\rho_0$ = 2.5 x $10^{-4}$ $\mu\Omega\cdot$cm), specimen D ($\rho_0$ = 0.14 $\mu\Omega\cdot$cm).

DATA
a) 20 to 400 K; b) Table 1 - specimen characterization, Table 2 - $\lambda$; c) uncertainty: ±1.2%; d) correction for impurities and thermal expansion.

ANALYSIS
a) data does not agree with Seeberg, P., Olsen, T., Phys. Norv., 2, 197 (1967); b) $\lambda = A + BT^{-4} + CT^2 + DT^{-1}$; $\lambda_g^{-1} = T/G + HT^{-2}$.

COMMENT
The data set contained in Reference 22 was not used because of comments made in this paper.

[6] De Nobel, J., Heat Conductivity of Steels and a Few Other Metals at Low Temperatures, Physica (Utrecht), 17(5), 551-62 (May 1951)

PURPOSE
To measure $\lambda$ for Al, Fe, Monel metal, Ni-Cr steel and Mn-Cr steel by two methods and compare the results.

SPECIMEN
a) /rod; c) /rolled; g) Brinell hardness 17.

APPARATUS
a) longitudinal; b) I gas thermometers, II resistance thermometers; c) vacuum insulation.

DATA
a) 16 to 87 K; b) Table II - $\lambda$.

ANALYSIS
b) for pure metals (> 99.93%), $\lambda$ is proportional to T at very low temperatures and a maximum occurs between 3 and 20 K.

[7] Der Nigohossian, G., Optimization of Electrical Leads for Cryogenic Apparatus, Commissariat a L'Energie Atomique, Saclay, France, Centre d'Etudes Nucleaires de Saclay, Rep. No. CEA-R-3167 (Feb 1967) 120 pp

PURPOSE
To optimize the geometry of electrical leads to cryogenic containers so that heat leakage is minimized.

SPECIMEN
a) 30 mm; b) single crystal.

APPARATUS
a) longitudinal; b) Au-Co vs. Cu thermocouples for 70 to 300 K, carbon resistance thermometers for lower temperatures; c) vacuum insulation, gas cooled shield.

DATA
a) 4 to 295 K; b) figure p. 75 - $\rho$, figure p. 76 - $\lambda$; c) uncertainty: ±10% (measurements with carbon resistance thermometers).

ANALYSIS
a) $\lambda$ data agrees with Roder, Powell, and Hall, Conference of Low Temperature Physics and Chemistry, Madison, Wisc., 364-367 (1958).

[8] Donth, E. and Gladun, C., Measurement of Thermal Conductivity at Low Temperatures by a Non-Stationary Method, Cryogenics, 2, 223-5 (Jun 1962)

PURPOSE
To present a method of non-stationary $\lambda$ measurement at low temperatures.

SPECIMEN
a) /rod; d) 99.5% Al.

APPARATUS
a) longitudinal; b) lead resistance thermometers; c) vacuum insulation, radiation shield.

DATA
a) 22 to 90 K; b) figure 3 - $\lambda$.

ANALYSIS
b) the method allows the determination, continuously and quickly (15-120 minutes), of $\lambda$ over a wide temperature range.

[9] Duggin, M. J., The Thermal Conductivities of Aluminum and Platinum, J. Phys. D: Appl. Phys., 3, L21-23 (1970)

PURPOSE
To measure $\lambda$ of Al, Pt.

SPECIMEN
a) /slab; d) 99.99%.

APPARATUS
a) guarded axial heat flow.

DATA
a) 380 to 600 K; b) Table 2 - $\lambda$, $\rho$, L; c) uncertainty: $\pm$2.5%.

ANALYSIS

a) results agree with recommended values from TPRC (Powell, et al., 1966).

[10] Erdman, C. A., A Dynamic Technique for Measuring Thermal Conductivity in Cylindrical Geometry, Designed for Use in Radiation Damage Studies, Ph.D. Thesis in nuclear engineering, Univ. of Illinois, Urbana-Champaign (1971)

PURPOSE
To develop a valid technique for measuring $\lambda$ which involves a small amount of equipment at the sample location.

SPECIMEN
a) 6 in. long (15 cm), 0.625 in. (1.59 cm) dia./rod; b) single crystal; c) /machined from 1.25 in. (3.18 cm) dia./rod; d) 99.995% Al.

APPARATUS
a) radial; b) thermocouples anchored to brass holder; c) vacuum insulation and shield.

DATA
a) 100 to 300 K; b) Table 9 - $\lambda$; c) uncertainty: ±6.6% at 296 K, ±8.9% at 105 K; d) corrections for radiation and conduction.

ANALYSIS
a) data agree with recommended values for high purity polycrystalline Al from the Seventh Thermal Conductivity Conference (Gaithersburg, MD, 1967).

[11] Fenton, E. W., Rogers, J. S., and Woods, S. B., Lorenz Numbers of Pure Aluminum, Silver and Gold at Low Temperatures, Can. J. Phys., 41, 2026-33 (Jul 1963)

PURPOSE
To attain accurate values of L for Al, Au, Ag and compare with the Sommerfeld value.

SPECIMEN
a) length/area ($cm^{-1}$): specimen 1 - 3500, specimen 2 - 1500, specimens 1,2: 6 cm long; c) specimens 1,2 acid etched and annealed at 550 °C in air for 10 min./specimens cut from 0.010 in. (0.025 cm) sheet, rod specimens rolled square and drawn once; d) 99.9999% Al; f) specimen 1 ($\rho_0$ = 9.03 x $10^{-10}$ Ω·cm), specimen 2 ($\rho_0$ = 5.68 x $10^{-10}$ Ω·cm); g) source: Consolidated Mining and Smelting Co. of Canada.

APPARATUS
a) longitudinal; b) gas thermometers//all leads to specimen are anchored to Cu pillars; c) temperature controlled radiation shield.

DATA
a) 2 to 50 K; b) figure 4 - L, Table 2 - $\rho_0$, $\rho_i/\lambda$ data points listed in TPRC data series; c) uncertainty: ±1.5%.

ANALYSIS
b) results agree with theoretical Sommerfeld value to about 1 1/2%.

[12] Flynn, D. R., private communication (1965)

DATA
a) 120 to 720 K; b) /data points listed in TPRC data series.

[13] Gladun, C. and Holzhauser, W., Studies of Heat Conductivity at Low Temperatures, Monatsber. Dtsch. Akad. Wiss. Berlin, 6(4), 310-3 (1964)

PURPOSE
To report development of an improved non-equilibrium apparatus and data for Cu, Al, and Ti.

SPECIMEN
d) 99.99% Al.

APPARATUS
a) longitudinal.

DATA
a) 4 to 55 K; b) figure 4 - λ.

ANALYSIS
b) $\lambda \sim T^2$, $\rho \sim T^5$ for $T < 30$ K.

[14] Gostishcher, V. I. and Drozd, A. A., Heat Conductivity of Aluminum in Strong Transverse Magnetic Fields, Phys. Met. Metallogr. (USSR) (Engl. Transl.), 39(6), 168-70 (1975), Transl. of Fiz. Met. Metalloved., 39(6), 1307 (1975)

PURPOSE
To investigate the effect of strong transverse magnetic fields on $\lambda$ for high-purity aluminum, in view of its use as a sheath for superconductors.

SPECIMEN
a) 3.5 cm long, 0.15 cm dia., 0.3 cm dia. at thermocouple, thermometer and heater locations/rod; b) polycrystalline; c) /extruded through a round die; e) run 1 (RRR = 2800), run 2 (RRR = 4500); f) run 1, ($\rho_o$ = 8.55 x $10^{-10}$ $\Omega$·cm), run 2 ($\rho_o$ = 5.32 x $10^{-10}$ $\Omega$·cm); g) run 1, 15 days after extrusion, run 2, 3.5 months after extrusion.

APPARATUS
a) longitudinal; b) carbon resistance thermometers and Cu-Ag thermocouples; c) radiation shield with maintained thermal gradient similar to specimen.

DATA
a) 6 to 48 K; b) figure 1 - $\lambda$.

ANALYSIS
b) $\lambda$ in strong fields is independent of density of imperfections but determined by topology of the Fermi surface.

[14A] Ho, C. Y., Powell, R. W., Liley, P. E., Thermal Conductivity of the Elements: A Comprehensive Review, J. Phys. Chem. Ref. Data, 3, Supplement No. 1, 242-257 (1974)

PURPOSE
To provide a comprehensive listing of data on $\lambda$ of the elements.

SPECIMEN

d) high purity; f) $\rho_o$ = 5.94 x $10^{-10}$ $\Omega$·cm for T below 150 K.

APPARATUS
a) not given.

DATA
a) 0 to 8500 K; b) Table 2 - $\lambda$, recommended values; c) uncertainty: ±5% below room temperature, ±3% above room temperature, and ±8% for the molten phase up to 1273 K. The values above 1273 K are provisional.

[15] Hogan, C. L., The Thermal Conductivity of Metals at High Temperature, Lehigh Univ., Bethlehem, PA., Ph.D. Thesis, (1950) 42 pp.

PURPOSE
To measure $\lambda$ for metals and alloys in the temperature range 0 to 1000 °C.

SPECIMEN
a) 12 in. (30.5 cm) long, 0.25 in. (0.64 cm) bore/tube; d) 99.996% Al; g) source: Norton RA 98 material.

APPARATUS
a) Forbes bar method; b) Chromel-Alumel thermocouples glued with Alundum; c) Sil-o-cel insulation.

DATA
a) 0 to 790 °C; b) /data points listed in TPRC data series; c) uncertainty: ±5%.

ANALYSIS
b) the basic theory of Wilson and Makinson is found to be valid.

[16] Lees, C. H., The Effects of Temperature and Pressure on the Thermal Conductivities of Solids. Part II, Philos. Trans. Roy. Soc. London, Ser. A, 208, 381-443 (1908)

PURPOSE
To measure $\lambda$ and $\rho$ for certain metals and alloys, and compare the results with electronic theories.

SPECIMEN
a) 7 to 8 cm long, 0.585 cm dia./rod; c) /specimen turned down from larger rod; d) 99% Al; g) density at 20 °C = 2.70 g/cm$^3$, source: Johnson, Matthey and Co.

APPARATUS
a) longitudinal; b) Pt resistance thermometer - oil contact/calibrated at boiling point of $O_2$, icepoint and boiling point of $H_2O$.

DATA
a) -166 to 24 °C; b) Table on p. 413 - $\lambda$, Graph on p. 432 - $\rho$; d) radiative heat loss, resistance of thermometer leads, offset of Pt resistor temperature from bar temperature.

ANALYSIS
a) Jager and Diesselhorst measurements, (Abh. Phys. Tech. Reichsanstalt, 3, p. 269 (1900), compared at 18 °C; b) found little variation in $\lambda$ in temperature range investigated.

[17] Mendelssohn, K. and Rosenberg, H. M., The Thermal Conductivity of Metals at Low Temperatures. I. The Elements of Groups 1, 2, 3, Proc. Phys. Soc., London, 65(6), 385-8, (Jun 1952)

PURPOSE
To measure $\lambda$ for metals at low temperatures.

SPECIMEN
a) 15 cm long; 1 to 2 mm dia./rod; b) polycrystalline; c) annealed; d) 99.994% Al; g) source: Johnson, Matthey and Co.

APPARATUS
a) longitudinal; b) gas thermometers.

DATA
a) 4 to 50 K; b) figure 4 - $\lambda$/data points listed in TPRC data series; c) uncertainty: ±3% (maximum).

ANALYSIS
a) results disagree with those of Webber, R. T., Andrews, F. A., and Spohr, D. A., Phys. Rev., 84, 994 (1951); b) $\lambda^{-1} = \alpha T^2 + \beta/T$.

[18] Merisov, B. A., Khotkevich, V. I., Zlobintsev, G. M., and Kozinets, V. V., Thermal Conductivity of Some Metals and Alloys at 4.2 to 273 K, J. Eng. Phys. (USSR) (Engl. Transl.), 12(5), 364-6 (1967)

PURPOSE
To report a thermal potentiometer method of measuring $\lambda$ in which the radiation correction is experimentally determined.

SPECIMEN
d) 0.05% Cu, 0.03% Fe, 0.35% Si, 0.10% others.

APPARATUS
a) thermal potentiometer method; b) Ge resistance thermometer from 4.2 to 20 K, Cu-constantan thermocouple from 20 to 273 K.

DATA
a) 6 to 273 K; b) figure 2 - $\lambda$/data points taken from Table in Merisov, et al., Thermophysical Properties of Substances at Low Temperatures, First All-Union Meeting, Feb. 16-19, 1971, 85-88 (1972); c) uncertainty: ±5%; d) experimentally determined correction for radiation heat loss.

[19] Mikryukov, V. E., Thermal and Electrical Properties of Cu, Ag, Al, and the Alloy System Cu-Be, J. Moscow Univ. 12(6), 57-67 (1957), Vestn. Mosk. Univ., Ser. Mat., Mekh., Astron., Fiz., Khim., 12(6), 57-67 (1957)

PURPOSE
To present data on $\lambda$ and $\rho$ for some metals.

SPECIMEN
d) 99.99% Al.

APPARATUS
a) not given.

DATA
a) 65 to 523 °C; b) Table 4 - $\lambda$ and $\rho$.

ANALYSIS
b) the Wiedemann-Franz law is not valid in this temperature range.

[20] Mikryukov, V. E. and Karagezyan, A. G., Thermal and Electrical Properties of Alloys of the Systems Al-Mg and Al-Cu, Inzh. Fiz. Zh., 4(12), 90-3 (1961)

PURPOSE
To investigate the temperature dependence of $\lambda$ and $\rho$, using the Wiedemann-Franz law for the systems Al-Cu and Al-Mg from room temperature to melting point.

SPECIMEN
a) 300 mm long, 3 mm dia.; c) annealed in vacuum at 430 to 520 °C; d) 99.9% Al.

DATA
a) 60 to 480 °C; b) /data points listed in TPRC data series.

ANALYSIS
a) Wiedeman-Franz ratio in agreement with theoretical values; b) in the investigated alloys, thermal transport is basically by electrons.

[21] Misiorek, H., Zarrzewski, T., and Rafalowicz, J., Influence of Plastic Deformation on the Thermal Conductivity Maximum of Copper and Aluminum in the Temperature Range 4.2 to 70 K, Phys. Status Solidi A, 47, K137-40 (1978)

PURPOSE
To determine the effect of increasing plastic deformation on λ maximum of Cu and Al in the range of 4.2 to 70 K.

SPECIMEN
c) both specimens annealed at 540 °C for 4 h in He atmosphere/deformed by extension at 77 K; d) 99.999% and 99.99% Al.

APPARATUS
a) longitudinal steady state.

DATA
a) 5 to 50 K; b) figures 3, 4 - λ (undeformed); e) captions for all figures switched: figure 1 should be labelled as 4, figure 2 as 3, figure 3 as 1, figure 4 as 2.

ANALYSIS
b) with increasing deformation, maximum λ decreases in value and is shifted toward higher temperatures.

[22] Moore, J. P., McElroy, D. L., and Barisoni, M., Thermal Conductivity Measurements Between 78 and 340 on Aluminum, Iron, Platinum, and Tungsten, Proceedings of the Sixth Thermal Conductivity Conf. (1966)

PURPOSE
To measure λ, ρ and the Seebeck coefficient for Al, Fe, Pt, and W between 78 and 340 K.

SPECIMEN
c) /machined from stock; d) 99.999% Al; e) RRR = 520; g) $\rho_{273.15}$ = 2.440 μΩ·cm, source: Reynolds Aluminum Co.

APPARATUS
a) longitudinal; b) Chromel-P and constantan thermocouples/calibrated against Pt resistance thermometers/thermocouple wires thermally grounded on guard cylinder; c) guard cylinder.

DATA
a) 100 to 380 K; b) Table 3 - λ.

ANALYSIS
a) λ values reported by Powell, et al. (1965) agreed to within 1/4%; c) the experimental λ curve has a minimum which disagrees with the theoretical curve in magnitude and temperature.

COMMENT
This data set not used because of reported error in technique. See Cook, J. G., Moore, J. P., Matsumura, T, and Van der Meer, M. P., The Thermal and Electrical Conductivity of Aluminum, ORNL-5079 (1975).

[23] Mucha, J. and Rafalowicz, J., Thermal Conductivity Minimum of Aluminum, Phys. Status Solidi A, 48, 221-4 (1978)

PURPOSE
To measure λ minima for six different pure aluminum specimens, and to test Wilson's equation.

SPECIMEN
a) 10.0 to 20.0 cm long, 0.8 cm dia./rod; b) polycrystalline; c) annealed at 500 °C, 48 h cooldown; d) specimen H1: 99.861%, H2: 99.526%, RO: 99.9931%, R6: 99.97%; e) specimen H1 (RRR = 36), H2 (RRR = 17), RO (RRR = 147), R6 (RRR = 86).

APPARATUS
a) longitudinal; b) constantan-manganin thermocouples; c) $10^{-7}$ mm ($10^{-5}$ Pa) insulation, screen at specimen temperature.

DATA
a) 80 to 380 K; b) figure 1 - λ.

ANALYSIS
b) deviation of 6 to 7% of experimental data for least squares fit of $W = e_o/L_oT + AT^2 - BT^4$. The Wilson equation fails to describe the λ curve in the minimum range.

[24] Mucha, J., Wlosowicz, D., and Rafalowicz, J., Thermal Conductivity of Constructional Aluminum at Temperatures Ranging from 77 to 300 K, Chlodnictwo, 4(11), 7-8 (1974)

PURPOSE
To report λ for 99.8% and 98.5% Aluminum (constructional) from 77 to 300 K.

SPECIMEN
d) 99.8% Al, 0.07% Fe, 0.057% Si, 0.006% Cu, 0.001% Ti, 0.008% V, 0.004% Mn, 0.001% Zn, 0.007% Cr, 0.006% Mg.

APPARATUS
a) longitudinal; b) room to $N_2$ temperatures: Cu-constantan thermocouples; He temperatures: carbon resistors/thermocouples scaled separately for room and $N_2$ temperatures with a Hg thermometer, carbon resistors.

DATA
a) 77 to 300 K; b) Graph p. 7 - λ; c) uncertainty: ±5% (maximum).

[25] Powell, R. L., Hall, W. J., and Roder, H. M., Low Temperature Transport Properties of Commercial Metals and Alloys. II. Aluminums, J. Appl. Phys., 31(3), 496-503 (1960)

PURPOSE
To present data for $\lambda$, $\rho$, L, thermoelectric force and thermoelectric power from 4 to 120 K.

SPECIMEN
a) specimen A, B, C: 3.66 mm dia./rods; b) specimen A: single crystal; specimen B, C: polycrystalline; c) specimen A: ground from 3.68 to 3.66 mm, annealed in vacuum at 400 °C for 2 h; specimen B: turned and drawn from 0.5 in. (1.25 cm) sheet to 3.66 mm rod; specimen C: turned and drawn from 0.5 in. (1.25 cm) sheet to 3.66 mm rod, annealed in vacuum at 350 °C for 1 h; d) specimen A: 99.995% Al; specimen B: 99.308%; specimen C: 98.917%; g) other characteristics found in Table 1.

APPARATUS
a) longitudinal; b) Au-Co vs. Cu thermocouples.

DATA
a) 4 to 120 K; b) Table II - $\lambda$, figure 1 - $\rho$, figure 6 - L.

ANALYSIS
b) L for high $\lambda$ samples were considerably below the Sommerfeld value while those for the low $\lambda$ samples were somewhat above it.

[26] Powell, R. W., Tye, R. P., and Woodman, M. J., The Thermal Conductivity of Pure and Alloyed Aluminum. I. Solid Aluminum as a Reference Material, Advances in Thermophysical Properties at Extreme Temperatures and Pressures, Third Symposium on Thermophysical Properties, ASME, 227-88 (1965)

PURPOSE
To investigate the suitability of high purity and other aluminums as a $\lambda$ reference standard.

SPECIMEN
Low temperature:
a) specimen S.P. (super pure): 8 cm x 0.44 cm x 0.44 cm/bar; d) specimen S.P.: 99.993% Al.

High temperature:
a) specimen S.P.: 28.0 cm x 2.81 cm dia.; specimen C51: 27.4 cm x 3.17 cm dia./rods; d) specimen S.P.: 99.993% Al; specimen C51: 99.6% Al.

APPARATUS
a) longitudinal; b) Ni-Cr, constantan, 90% Pt, 10% Rh thermocouples.

DATA
Low temperature:
a) specimen S.P.: 123 to 323 K; b) Table III - $\lambda$, $\rho$, and L; d) radiative heat loss correction.

High temperature:
a) specimen S.P., C51: 323 to 873 K; b) Table III - $\lambda$, $\rho$, and L; d) radiative heat loss correction.

ANALYSIS
b) $\lambda = AT\rho + B$.

[27] Powers, R. W., Schwartz, D., and Johnston, H. L., The Thermal Conductivity of Metals and Alloys at Low Temperatures, Ohio State Univ., Columbus, Rep. No. TR 264-5 (Apr 1951) Contract No. W33-038-AC-14794 (16243) 23 pp.

PURPOSE
To describe an apparatus for $\lambda$ measurements and discuss the results for pure Al, Cu, and Ni from 25 to 300 K.

SPECIMEN
a) 20 in. (51 cm) long, 0.5 in. (1.3 cm) dia.; c) cold-drawn, 55% reduction; d) 99.99+% purity; g) source: Aluminum Company of America.

APPARATUS
a) longitudinal; b) Cu-constantan thermocouples/thermocouples calibrated with a gas thermometer; c) 3 gold plated temperature controlled shields and $10^{-5}$ mm of Hg ($10^{-3}$ Pa) insulation.

DATA
a) 25 to 238 K; b) Table II and Table III - $\lambda$; c) uncertainty: ±0.6% at 250 K, ±0.7% at 100 K, ±1.8% at 30 K; d) corrections for radiation and conduction.

[28] Roberts, R. B. and Crisp, R. S., Thermoelectric Power and Thermal Conductivity an Integral Method - Aluminum, Philos. Mag., 36(1), 81-9 (1977)

PURPOSE
To develop and evaluate an apparatus for the simultaneous measurement of $\lambda$ and thermoelectric power of metal wire using an integral method from 2 to 300 K.

SPECIMEN
a) 18 cm long, 0.25 and 0.50 mm dia., for $T < 70$ K and $T > 70$ K respectively/wire; c) annealed at 600 °C at $10^{-6}$ mm of Hg ($10^{-4}$ Pa) 24 h, slow cooled/1 mm wire drawn to 0.5 mm and 0.25 mm dia. for two specimens; d) 99.9999% Al.

APPARATUS
a) integral method; b) carbon resistance thermometer, thermocouple/thermocouple calibrated against Pt thermometer calibrated by CSIRO Sydney to the IPTS 68, carbon resistor was calibrated against He $\lambda$ and boiling point and against Pt thermometer at 15 K; c) thin-walled stainless steel tube heat shield and Al Mylar surrounded complete assembly.

DATA
a) 2 to 300 K; b) /data points supplied by author; c) uncertainty: less than ±1.0%.

ANALYSIS
a) data agrees with TPRC recommended values for 100 to 300 K; b) the integral method was shown to be capable of yielding accurate measurements of $\lambda$.

[29] Rosenberg, H. M., The Thermal Conductivity of Metals at Low Temperatures, Philos. Trans. Roy. Soc. London, Ser. A, 247(933), 441-97 (1955)

PURPOSE
To investigate and report on $\lambda$ for 32 metallic elements in the 2 to 40 or 90 K range, to give a general picture of $\lambda$ at low temperatures. Also to measure $\rho$ so the Wiedemann-Franz relation could be studied.

SPECIMEN
a) 2.97 cm long, 0.394 cm dia./rod; b) polycrystalline; c) annealed in vacuum at 600 °C, several h; d) 99.994% Al; e) $\rho_{293}/\rho_{20}$ = 279; g) source: Johnson, Matthey and Co.

APPARATUS
a) longitudinal; b) gas thermometers//thermally anchored to liquefier and vacuum jacket; c) $10^{-5}$ mm of Hg ($10^{-3}$ Pa) insulation.

DATA
a) 2 to 42 K; b) figure 12 - $\lambda$/data points listed in TPRC data series; c) uncertainty: ±3%; d) corrections for external volume of gas thermometer.

ANALYSIS
a) compared to Andrews, Webber, and Spohr (1951); b) $\lambda^{-1} = \alpha T^2 + \beta T^{-1}$; $W_0$ seems to vary as $T^{2.2}$ over large temperature range.

[30] Seeberg, P. and Olsen, T., The Thermal Conductivity of Pure Aluminum at Low Temperatures, Phys. Norv., 2(3), 197-201 (1967)

PURPOSE
To measure $\lambda$ for super pure aluminum and determine how the phonon scattering term ($W_i$) varies with purity.

SPECIMEN
a) specimens 1,2 - 102, 65 cm long, 2.98, 2.03 mm dia. respectively/rods; c) air annealed at 480 °C, 24 h/cold rolled, drawn, wound into helix; d) zone refined high purity Al; e) specimen 1 (RRR = 24,000), specimen 2 (RRR = 15,000); f) specimen 1 ($\rho_0$ = 1.3 x $10^{-10}$ Ω·cm), specimen 2 ($\rho_0$ = 1.9 x $10^{-10}$ Ω·cm); g) electron mean free path, specimen 1 (0.75 mm), specimen 2 (0.4 mm).

APPARATUS
a) longitudinal; b) < 4 K: carbon resistors, > 4 K: Ge resistance thermometers/< 4 K: calibrated against He vapor pressure.

DATA
a) 2.5 to 33.5 K; b) figure 1 - $\lambda$; c) uncertainty: ±2% (maximum), T < 4; ±5% (maximum), 5 < T < 30.

ANALYSIS
b) $\lambda^{-1} = \alpha T^2 + \beta T^{-1}$; Matthiessen's rule fails to provide a satisfactory description of the electronic $\lambda$ in metals, and the deviation of Al follows a pattern similar to tin and indium.

[31] Sirota, N. N., Drozd, A. A., and Gostishcher, V. I., Measurement of Electrical and Thermal Conductivity of Metals in Strong Magnetic Fields, Thermophysical Properties of Substances at Low Temperatures (Proceedings of the First All-Union Meeting, Feb. 16-19, 1971) M. P. Orlova, ed., All-Union Scientific Research Institute of Physico-Technical and Radiotechnical Studies (Moscow, 1972) pp. 149-58

PURPOSE
To measure $\lambda$ for aluminum in strong, perpendicular magnetic fields.

SPECIMEN
d) 99.999% Al.

APPARATUS
a) longitudinal-stationary heat flow; b) carbon resistance thermometers/ calibrated in strong magnetic fields (both perpendicular and parallel); c) temperature controlled shield.

DATA
a) 7 to 73 K; b) figure 6 - $\lambda$, figures 5 and 7 $\rho$ and L.

[32] Sirota, N. N., Gostishcher, V. I., and Drozd, A. A., Thermal Conductivity of Aluminum in Strong Magnetic Fields at Low Temperatures, JETP Lett., 16(4), 170-2 (Aug 1972)

PURPOSE
To study $\lambda$ for metals in strong magnetic fields at low temperatures to separate electronic and lattice components.

SPECIMEN
a) 60 x 3 x 3 mm/bar; b) single crystal; c) /cut from ingot; e) RRR = 6000; f) $\rho_0 = 1.2 \times 10^{-10}$ $\Omega \cdot$cm.

APPARATUS
a) longitudinal; b) resistance thermometers; c) radiation shield with temperature gradient similar to specimen.

DATA
a) 6 to 57 K; b) figure 1 - $\lambda(H=0)$; c) uncertainty: ±2%; e) RRR = 6000 is inconsistent with data, closer to 600.

ANALYSIS
b) temperature dependence of the lattice component of $\lambda$ in region of maximum: $\lambda_g = AT^3e^{-\beta T}$. A transverse magnetic field exerts a strong influence on $\lambda$ for high purity Al.

[32A] Touloukian, Y. S., Powell, R. W., Ho, C. Y., and Klemens, P. G., Thermophysical Properties of Matter, Volume 1: Thermal Conductivity, Metallic Elements and Alloys, 68-81 (1970)

PURPOSE
To provide an extensive list of data for $\lambda$ of the metallic elements and alloys.

SPECIMEN
d) 99.9999%; f) $\rho_0 = 5.93 \times 10^{-10}$ $\Omega \cdot cm$.

APPARATUS
a) not given.

DATA
a) 0 to 8000 K; b) Figure and Table 1R - $\lambda$, recommended values; c) uncertainty: ±3% near room temperature, ±3 to 5% at other temperatures; e) the values below 1.5 Tm are calculated to fit the experimental data by using n = 2.00, a = 0.61, m = 2.61, $\alpha'' = 4.87 \times 10^{-6}$, and $\beta = 0.0245$.

[33] Wilkes, K. E., Thermal Conductivity Measurements Between 77 K and 373 K on Iron, Cobalt, Aluminum, and Zinc, M.S. Thesis, Purdue University, (1968) 93 pp.

PURPOSE
To resolve discrepancies and fill gaps in the literature for $\lambda$ for Co, Al, and Zn.

SPECIMEN
a) 10.16 cm long, 1.225 cm dia./rod; b) polycrystalline; c) unannealed; d) 0.5 ppm Cu, 0.5 ppm Si, and 0.1 ppm Mg; f) $\rho_{273} = 0.02425$ $\mu\Omega.m$, $\rho_{77} = 0.0021$ $\mu\Omega \cdot m$; g) density = 2698 $Kg/m^{-3}$ at 23 °C.

APPARATUS
a) longitudinal; b) Chromel-constantan thermocouples/T < 273 K: calibrated with a resistance thermometer and tables from Powell, R. L., and Sparks, L. L., NBS Report 9249, T > 273 K: calibrated against a platinum-rhodium thermocouple/all thermocouple leads from specimen tied to support rods; c) $5 \times 10^{-5}$ mm of Hg ($7 \times 10^{-3}$ Pa) insulation.

DATA

a) 88 to 283 K; b) Table 4 - $\lambda$, figure 13 - $\rho/\rho$ data points generated from equation of line on figure 13; d) corrections for radiation and conduction.

ANALYSIS
a) $\rho$ curve is very close to Flynn; Powell, Tye, Woodman; and Moore, McElroy, Barisoni but $\lambda$ curves differ; b) L is well below theoretical but appears to approach theoretical value well above room temperature.

# 4. Iron

## 4.1 General

A total of 41 references on iron are included in the annotated bibliography of Section 4.5. The following references represent the primary data sets: 3A, 8, 9, 11, 13, 15, 16, 18, 23, 25, 28, 29, 31, 33, and 34.

The primary data cover a range of temperatures from 1.5 to 1000 K, and a range of RRR from 4 to 200. These data are illustrated in Figs. 4.1.1 through 4.1.3 with a composite of the data given in Fig. 4.1.4. Iron produced in bulk form is generally of much lower electrical purity than either copper or aluminum. RRR values above 550 are not reported.

Equation 1.1.3 was used to represent the iron data over the entire temperature range. The values for the parameters, $P_i$, i = 1, 2 ... 7, obtained by nonlinear least squares fit are:

$P_1 = 166.9 \times 10^{-8}$ $\quad$ $P_5 = 238.6$

$P_2 = 1.868$ $\quad$ $P_6 = 1.392$

$P_3 = 1.503 \times 10^{5}$ $\quad$ $P_7 = 0.0$

$P_4 = -1.22$

with all units in SI.

The data at high RRR were examined for systematic residual deviations as a function of temperature. The residuals were represented by the $W_c$ term in Eq. 1.1.5 with the following equation:

$$W_c = -0.004\ \ell n(T/440)\ \exp(-(\ell n(T/650/0.8)^2)$$

$$-0.002\ \ell n(T/90)\ \exp(-(\ell n(t/90)/0.45)^2)$$

where $W_c$ and T are in SI units.

4.2 Deviations From Recommended Equation

The deviations of the primary data from Eq. 1.1.3 are illustrated in Figs. 4.2.1 through 4.2.3 with a composite shown in Fig. 4.2.4. Only three data sets exhibit differences of greater than $\pm$10%. Although deviations, systematic with temperature, exist for individual data sets, the overall pattern is random in nature. No systematic trends varying with RRR were identified.

The primary data were selected from the literature data on relatively large, well annealed specimens. Therefore, the deviations exhibited in Figs. 4.2.1 through 4.2.4 are indicative of the combined effect of a) experimental measurement errors and b) the inability of Eq. 1.1.3 to account for the effects of chemical impurity variations. The effects of physical defect variations, small specimen size variations, and magnetic fields are exhibited, in part, by the deviations of the secondary data. The thermal conductivity variations caused by other than chemical impurity variations are not expected to be represented as well by Eq. 1.1.3. However, the RRR (or $\rho_0$) correlating parameter does account for an appreciable part of these variations. Some users may find this to be an adequate representation and, therefore, discussions of these comparisons are included for completeness.

The deviations of the secondary data sets are divided into two groups according to the magnitude of the deviations. They are illustrated in Figs. 4.2.5 through 4.2.10.

The equation developed here is also compared to the reference data in the following references 9A, 12, 20, and 32A in Fig. 4.2.11. The differences are within the combined uncertainties of the sources. It is noted that we did not include data within our primary set for RRR above 200. Therefore the comparison to the data in references 9A, 32A are an extrapolation of our equation.

### 4.2.1 Physical Defect Effects

Investigations of physical defects in iron have produced only a few references 20, 29, 33. Each of these references will be discussed below.

Reference 33 reports the effects of annealing on thermal conductivity. The peak value of the thermal conductivity of the unannealed specimen was 99 $W \cdot m^{-1} \cdot K^{-1}$, while for the annealed specimen of the same Armco iron stock, it was 112 $W \cdot m^{-1} \cdot K^{-1}$. The deviations from Eq. 1.1.3 for the unannealed specimen were within $\pm$9%, while those for the annealed specimen were within $\pm$8%.

Although not directly related to physical defects, references 20 and 29 report on the effects of impurities. Reference 20 states that as much as 7% variation in thermal conductivity is possible at 298 K for a specimen of Armco iron. This difference is caused by variations of impurity concentrations in the Armco stock. Reference 29 reports that the peak conductivity of pure (99.99%) iron is 287 $W \cdot m^{-1} \cdot K^{-1}$ at 32 K, while for SAE 1020 steel 99.48% Fe, peak value is 65 $W \cdot m^{-1} \cdot K^{-1}$ at 160 K. The deviations from Eq. 1.1.3 the pure iron were within $\pm$4%, while those for the steel were within $\pm$5%.

Reference 20 also reports on the effect of ice-water quenching on thermal conductivity. A 1% increase was reported for specimens of thickness greater than 8 mm. For a specimen of less than this thickness, ice-water quenching should produce a greater effect on the thermal conductivity. No thermal strain effect was produced.

Although the temperature dependence of the physical defect scattering mechanism is different from that due to impurity scattering, Eq. 1.1.3 represents the unannealed specimen data quite well (within $\pm$10%). This indicates that the residual electrical resistivity characterizes both types of scattering for the range of RRR included here.

4.2.2 Size Effects

No size effect studies were found in our literature on iron.

4.2.3 Magnetic Field Effects

Although magnetic field effects on thermal conductivity were not studied explicitly, some interesting changes occur for iron (and ferromagnetic metals in general). We will discuss these effects below.

Reference 3 shows that the thermal resistivity of a single crystal, oriented in the [111] direction, decreases as the magnetic field increases from 0 to 12 KOe. Fickett[1] reports that ferromagnetic metals can show a decrease in resistivity with increasing fields. This decrease in a pure ferromagnetic metal is rather large. Note that the opposite behavior is seen in nonferromagnetic metals.

Takaki amd Igaki[2] report that the electrical resistivity decreases rapidly when a magnetic field of less than 0.8 kA/m is applied. The resistivity reaches a minimum at 32 and 40 kA/m in single crystal specimens whose orientations are [111] and [011], respectively. This effect also occurs for polycrystalline specimens in longitudinal fields of 56 to 64 kA/m.

One of the conclusions drawn in this paper indicates that a modified residual resistivity ratio, $RRR_H$, should be used to characterize the purity of iron ($RRR_H = \rho^{(298)}/\rho_{MIN}^{(4.2\ K)}$, where $\rho_{MIN}$ is the minimum value of $\rho$ for a specimen in a longitudinal magnetic field of 56-64 kA/m).

---

[1]Fickett, F. R., Electrical Properties of Materials and Their Measurement at Low Temperatures, NBS Technical Note 1053, National Bureau of Standards, Boulder, Colorado, p. 41 (1982).

[2]Takaki, S. and Igaki, K, Electrical Resistivity of High Purity Iron at 4.2 K, Trans. Jpn. Inst. Met. 17, 353-9 (1976).

Equation 1.1.3 is expected to represent the thermal conductivity of specimens in a magnetic field reasonably well for temperatures above 30 K. Below this temperature, the deviations are expected to increase dramatically.

4.3 Electrical Resistivity and Lorenz Ratio

It was desirable to examine the Lorenz ratio of iron during the course of this investigation. Therefore an approximation of electrical resistivity as a function of temperature and RRR was required. To obtain an approximate equation we selected those sources from the primary set that also reported electrical resistivity data and fitted Eqs. 1.2.3 to those data. The electrical resistivity data used here are shown in Figs. 4.3.1 to 4.3.3. The parameters obtained for this equation are:

$P_1 = 41.47 \times 10^{-16}$ $\quad$ $P_5 = 180.3$

$P_2 = 3.241$ $\quad$ $P_6 = 1.947$

$P_3 = 7.638 \times 10^{11}$ $\quad$ $P_7 = 0.1367$

$P_4 = 1.95$

The systematic residuals, $\rho_c$, obtained from this fit were then represented by

$$\rho_c = -3 \times 10^{-3} \ln(T/370) \exp(-(\ln(T/600)/0.6)^2)$$

$$-3 \times 10^{-9} \ln(T/105) \exp(-(\ln(T/120)/0.45)^2)$$

All units are SI.

The deviations of the data from this fit are shown in Figs. 4.3.4 to 4.3.6. Again the spread in the mid-range (40 to 100 K) is relatively large with a correspondingly large uncertainty. However, for the purpose at hand this is considered adequate.

Smooth values of $\rho$ vs. T at selected RRR values are plotted in Fig. 4.3.7. From Eqs. 1.1.3 and 1.2.3 smooth values of L(T,RRR) are plotted in Fig. 4.3.8. No unexpected irregularities appear in Fig. 4.3.8.

In Section 1.5 we discuss the procedure for selecting values of $\rho_0$ and calculating RRR for each thermal conductivity data set. These values of $\rho_0$ along with the Sommerfeld value of Lorenz ratio were used to best fit each low temperature data set. The resulting values of RRR obtained by this procedure are compared to the values reported in the references in Fig. 4.3.9 and are listed in Table 4.3.1. Figure 4.3.9 shows values of RRR (calc), those values from the above procedure, versus RRR (obs), those values reported in the references listed in the annotated bibliography. Also shown in this figure is the line that represents RRR (calc) = RRR (obs). Systematic deviations from this line indicate ranges in which the derived Eq. 1.1.3 is invalid. For iron, the calculated values of RRR are within 10% of the observed values for the range 13 to 200. Also, Table 4.3.1 indicates that the Sommerfeld value of the Lorenz ratio is valid for iron.

## 4.4 Summary for Iron

Equation 1.1.3 represents the primary iron data to within $\pm$10% of the experimental value at a given temperature. Deviations for unannealed specimens (i.e., those containing physical defects) are within $\pm$10%.

Based on the deviations illustrated in Figs. 4.2.1 through 4.2.3 it is clear that the use of RRR in Eq. 1.1.3 accounts for a large proportion of the impurity effect in iron. Equation 1.1.3 with the parameters listed here was used to generate smoothed values of thermal conductivity as a function of temperature and selected values of RRR. These are listed in Table 4.4.1 and Fig. 4.4.1.

List of Tables and Figures for Iron

Tables


| | | Page |
|---|---|---|
| Table 4.3.1 | Comparison of Calculated and Observed RRR Values for Iron | 149 |
| Table 4.4.1 | Thermal Conductivity Values for Iron Calculated From Eq. 1.1.3 at Selected Temperatures and RRR Values | 150 |


Figures


| | | Page |
|---|---|---|
| Figure 4.1.1 | Experimental thermal conductivity data selected from the following primary references in the iron annotated bibliography: (8,9,11,13,15,16) | 151 |
| Figure 4.1.2 | Experimental thermal conductivity data selected from the following primary references in the iron annotated bibliography: (3A,18,23,25,28) | 152 |
| Figure 4.1.3 | Experimental thermal conductivity data selected from the following primary references in the iron annotated bibliography: (29,31,33,34) | 153 |
| Figure 4.1.4 | Composite of the data in figures 4.1.1 through 4.1.3 | 154 |
| Figure 4.2.1 | Thermal conductivity deviations of the iron data from the following primary references compared to Eq. 1.1.3: (8,9,11,13,15,16) | 155 |
| Figure 4.2.2 | Thermal conductivity deviations of the iron data from the following primary references compared to Eq. 1.1.3: (3A,18,23,25,28) | 156 |
| Figure 4.2.3 | Thermal conductivity deviations of the iron data from the following primary references compared to Eq. 1.1.3: (29,31,33,34) | 157 |
| Figure 4.2.4 | Composite of the deviations in figures 4.2.1 through 4.2.3 | 158 |
| Figure 4.2.5 | Thermal conductivity deviations of the iron data from the following secondary references compared to Eq. 1.1.3: (1,3,4,5,6,10) | 159 |
| Figure 4.2.6 | Thermal conductivity deviations of the iron data from the following secondary references compared to Eq. 1.1.3: (11,12,14,17,19,22) | 160 |

Page

Figure 4.2.7 Thermal conductivity deviations of the iron data from the following secondary references compared to Eq. 1.1.3: (21,22A,24,26,27,30,32) . . . . . 161

Figure 4.2.8 Thermal conductivity deviations of the iron data from the following secondary refeences compared to Eq. 1.1.3: (33,34,35,36) . . . . . 162

Figure 4.2.9 Composite of the deviations in figures 4.2.6 through 4.2.8 . . . . . 163

Figure 4.2.10 Thermal conductivity deviations of the iron data from the following secondary references compared to Eq. 1.1.3: (2,7,22B) . . . . . 164

Figure 4.2.11 Comparison of Eq. 1.1.3 to the values recommended for iron in the following references: (9A,12,20,32A) . . . . 165

Figure 4.3.1 Experimental electrical resistivity data for iron selected from the following references in the iron annotated bibliography: (3A,8,11,15,16,25) . . . . . 166

Figure 4.3.2 Experimental electrical resistivity data for iron selected from the following references in the iron annotated bibliography: (31,34) . . . . . 167

Figure 4.3.3 Composite of the electrical resistivity data in figures 4.3.1 and 4.3.2 . . . . . 168

Figure 4.3.4 Electrical resistivity deviations of the iron data from the following references compared to Eq. 1.2.3: (3A,8,11,15,16,25) . . . . . 169

Figure 4.3.5 Electrical resistivity deviations of the iron data from the following references compared to Eq. 1.2.3: (31,34) . . . . . 170

Figure 4.3.6 Composite of the electrical resistivity deviations shown in figures 4.3.4 and 4.3.5 . . . . . 171

Figure 4.3.7 Electrical resistivity for iron as a function of temperature calculated from Eq. 1.2.3 at selected values of RRR . . . . . 172

Figure 4.3.8 Lorenz ratio for iron as a function of temperature calculated from Eq. 1.2.3 and Eq. 1.1.3 at selected values of RRR . . . . . 173

Figure 4.3.9 RRR values calculated as per Section 1.5, RRR(CALC), versus reported RRR values, RRR(OBS), for iron . . . . . 174

Figure 4.4.1 Thermal conductivity for iron as a function of temperature calculated from Eq. 1.1.3 at selected values of RRR . . . . . 175

Table 4.3.1. Comparison of Calculated and Observed RRR Values for Iron.

| Reference | RRR (obs.) | RRR (calc.) |
|---|---|---|
| | Primary Data | |
| 3A | 20.89 | 20.89 |
| 3A | 21.24 | 21.24 |
| 3A | 21.55 | 21.55 |
| 8 | 23.0 | 23.0 |
| 11 | 13.0 | 12.7 |
| 13 | 23.33 | 24.1 |
| 15 | 98.0 | 90.0 |
| 15 | 95.0 | 103.0 |
| 16 | 40.3 | 40.3 |
| | Secondary Data | |
| 10 | 189.0 | 189.0 |
| 11 | 13.0 | 13.9 |
| 11 | 13.0 | 12.8 |
| 12 | 23.0 | 23.4 |
| 14 | 29.4 | 29.4 |
| 36 | 36.4 | 36.4 |

Table 4.4.1. Thermal Conductivity Values for Iron Calculated from Eq. 1.1.3 at Selected Temperatures and RRR Values.

| T (K) | $\lambda(W \cdot m^{-1} \cdot K^{-1})$ | | | |
|---|---|---|---|---|
| | RRR = 10 | RRR = 30 | RRR = 100 | RRR = 300 |
| 1 | 2.5 | 8.1 | 28 | 84 |
| 2 | 5.1 | 16.3 | 56 | 168 |
| 3 | 7.6 | 24 | 83 | 251 |
| 4 | 10.1 | 32 | 111 | 333 |
| 5 | 12.6 | 41 | 138 | 414 |
| 6 | 15.2 | 49 | 166 | 492 |
| 7 | 17.7 | 57 | 192 | 567 |
| 8 | 20 | 65 | 218 | 637 |
| 9 | 23 | 73 | 244 | 702 |
| 10 | 25 | 81 | 269 | 761 |
| 12 | 30 | 96 | 315 | 858 |
| 14 | 35 | 111 | 357 | 925 |
| 16 | 40 | 125 | 393 | 961 |
| 18 | 45 | 139 | 422 | 970 |
| 20 | 49 | 152 | 445 | 957 |
| 25 | 61 | 179 | 471 | 863 |
| 30 | 71 | 198 | 462 | 735 |
| 35 | 79 | 208 | 429 | 609 |
| 40 | 86 | 210 | 384 | 500 |
| 45 | 91 | 204 | 336 | 410 |
| 50 | 94 | 194 | 292 | 340 |
| 60 | 96 | 170 | 225 | 247 |
| 70 | 94 | 150 | 183 | 195 |
| 80 | 92 | 133 | 156 | 164 |
| 90 | 89 | 122 | 138 | 144 |
| 100 | 87 | 114 | 126 | 130 |
| 150 | 81 | 94 | 100 | 102 |
| 200 | 78 | 88 | 91 | 92 |
| 250 | 76 | 82 | 85 | 85 |
| 300 | 72 | 77 | 79 | 79 |
| 400 | 64 | 67 | 68 | 69 |
| 500 | 58 | 60 | 60 | 61 |
| 600 | 52 | 53 | 54 | 54 |
| 700 | 46 | 47 | 47 | 47 |
| 800 | 41 | 41 | 42 | 42 |
| 900 | 36 | 37 | 37 | 37 |
| 1000 | 32 | 32 | 33 | 33 |

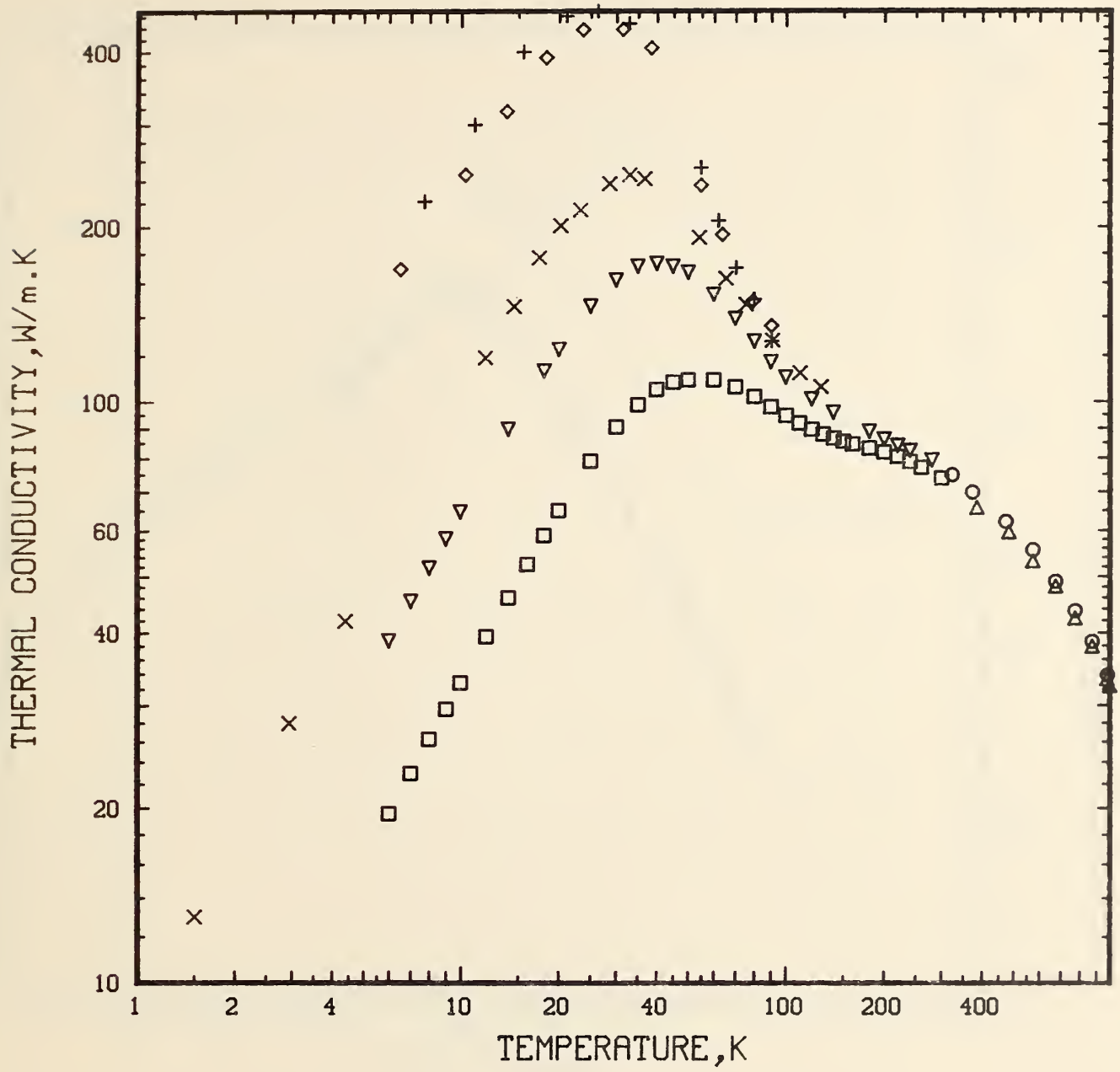


Figure 4.1.1 Experimental thermal conductivity data selected from the following primary references in the iron annotated bibliography:(8,9,11,13,15,16)

○ = (8), △ = (9), □ = (11), ▽ = (13),
◇ = (15), + = (15), × = (16)

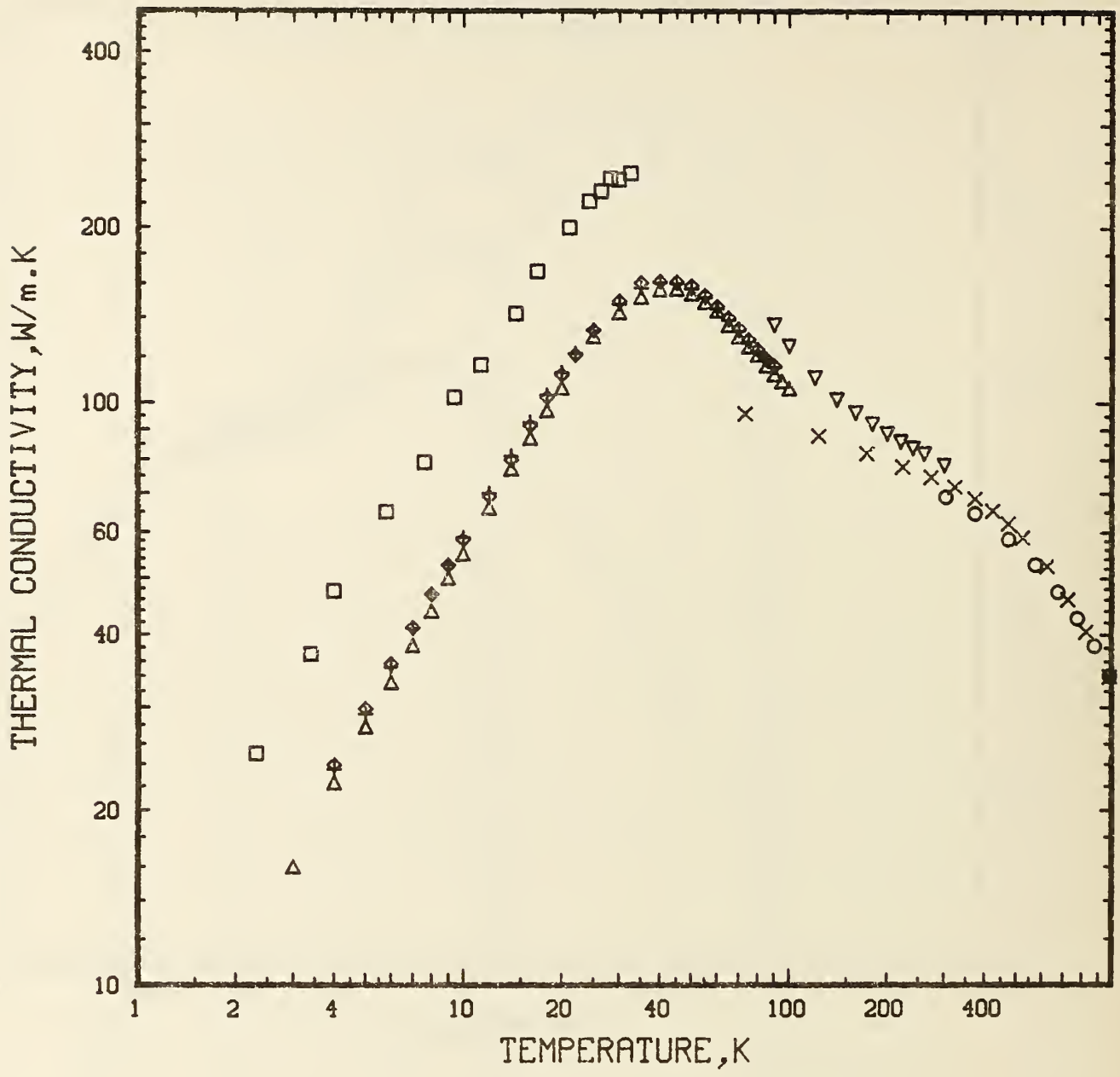


Figure 4.1.2 Experimental thermal conductivity data selected from the following primary references in the iron annotated bibliography:(3A,18,23,25,28)

○ = (18), △ = (3A), □ = (23), ▽ = (25),
◇ = (3A), + = (3A), × = (28)

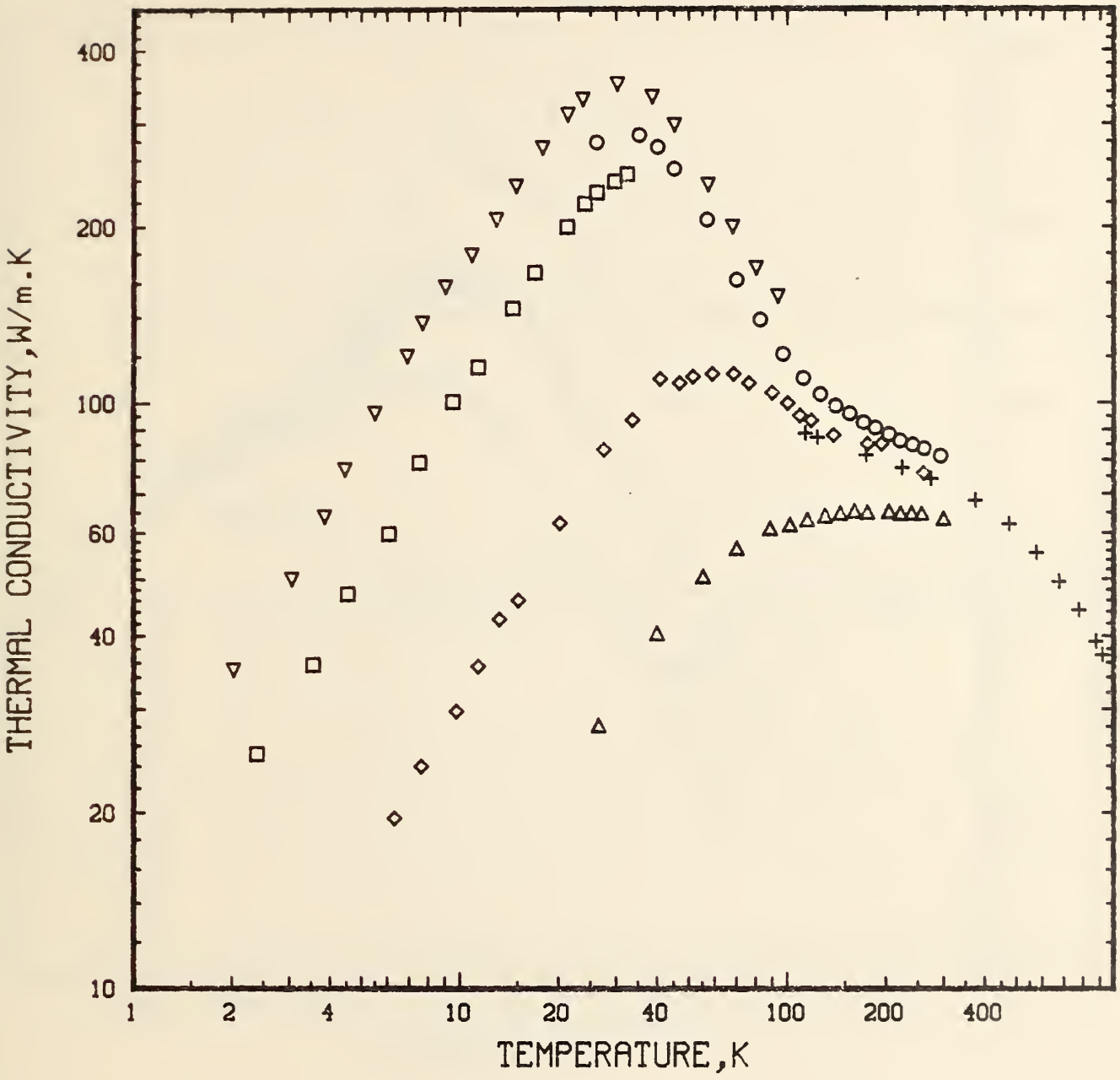


Figure 4.1.3 Experimental thermal conductivity data selected from the following primary references in the iron annotated bibliography:(29,31,33,34)

○ = (29), △ = (29), □ = (31), ▽ = (31),
◇ = (33), + = (34)

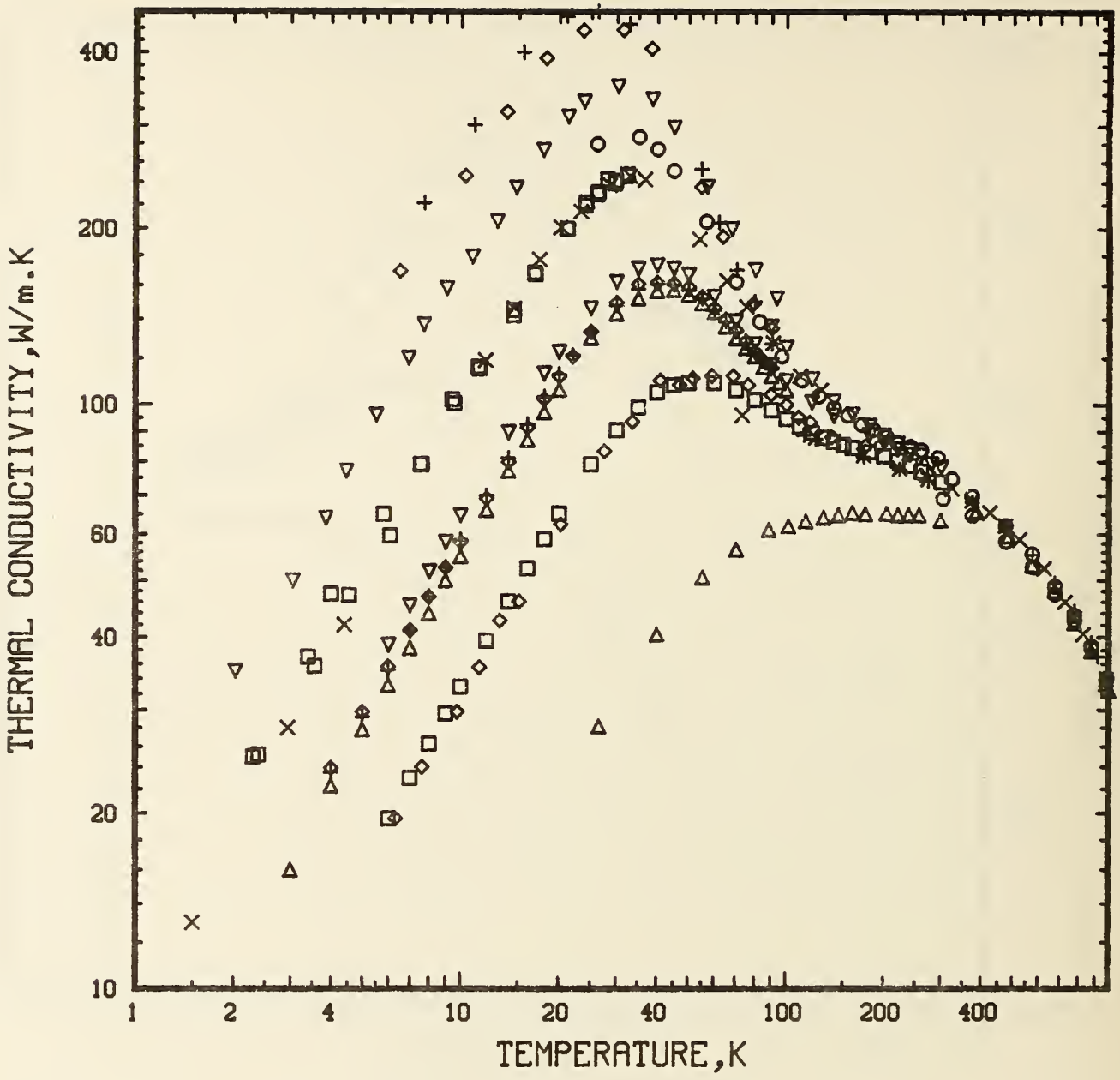


Figure 4.1.4 Composite of the data in figs. 4.1.1 through 4.1.3

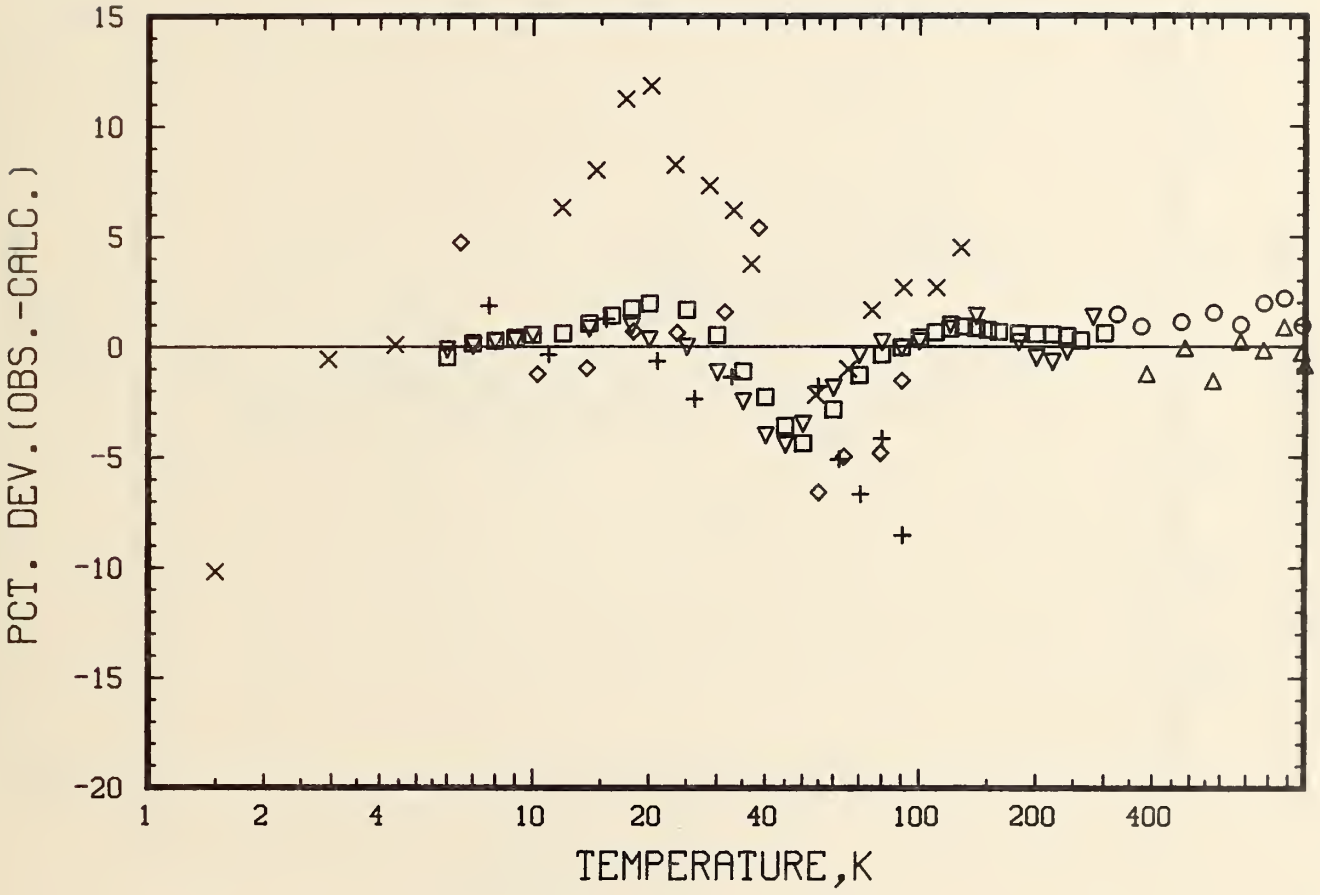


Figure 4.2.1 Thermal conductivity deviations of the iron data from the following primary references compared to eq. (1.1.3): (8,9,11,13,15,16)

○ - (8), △ - (9), □ - (11), ▽ - (13),
◇ - (15), + - (15), × - (16)

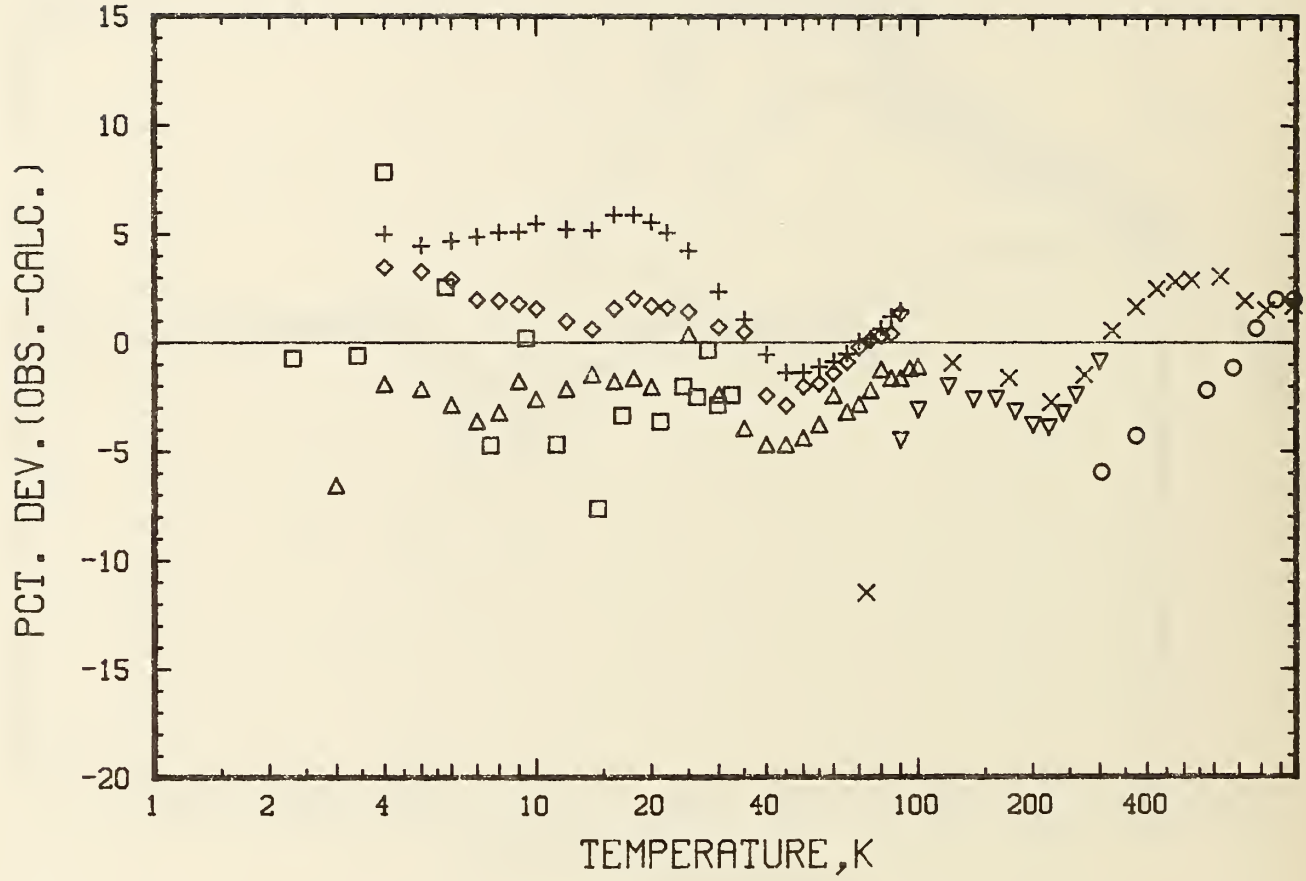


Figure 4.2.2 Thermal conductivity deviations of the iron data from the following primary references compared to eq. (1.1.3): (3A,18,23,25,28)

○ = (18), △ = (3A), □ = (23), ▽ = (25),
◇ = (3A), + = (3A), × = (28)

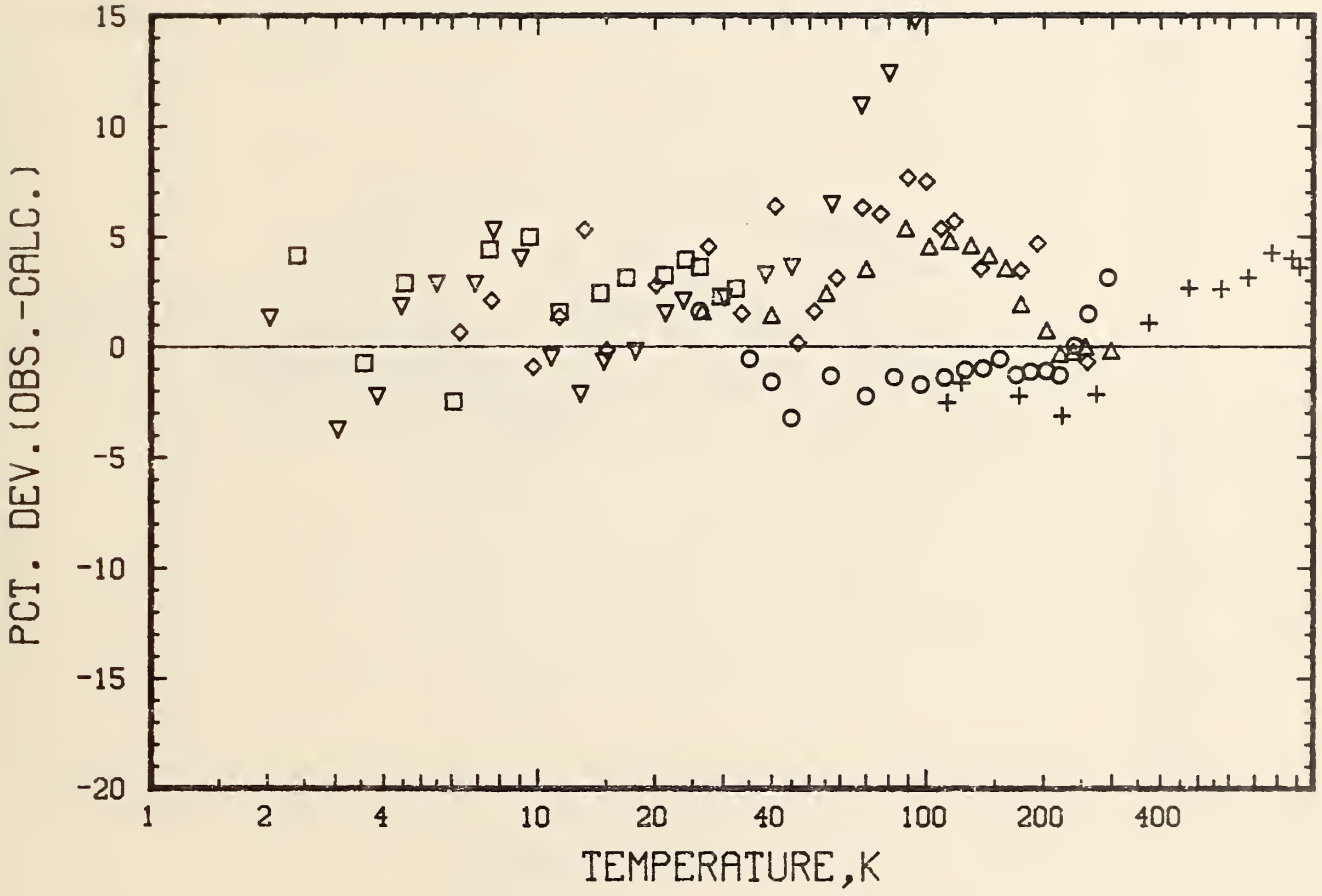


Figure 4.2.3 Thermal conductivity deviations of the iron data from the following primary references compared to eq. (1.1.3): (29,31,33,34)

○ - (29), △ - (29), □ - (31), ▽ - (31),
◇ - (33), + - (34)

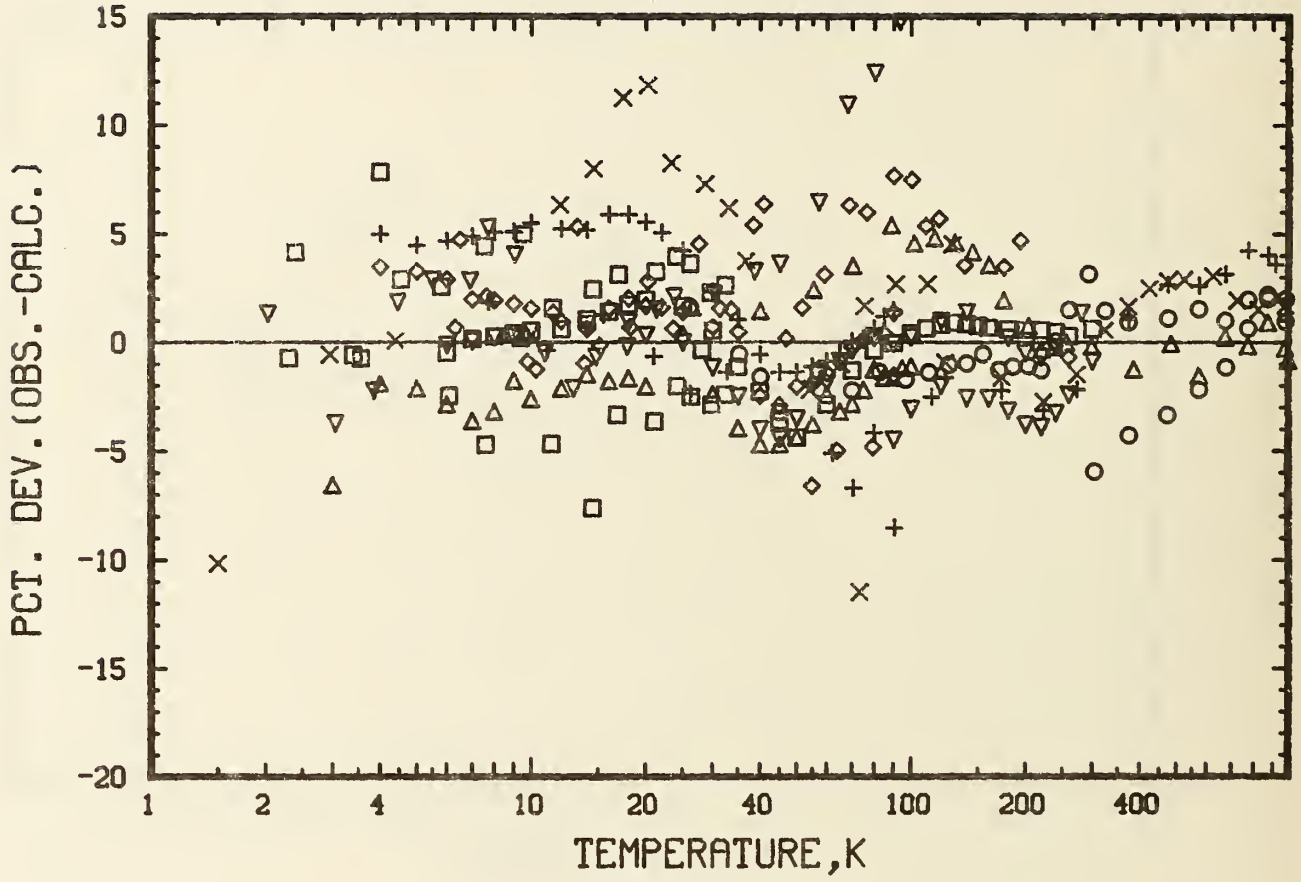


Figure 4.2.4 Composite of the deviations in figs. 4.2.1 through 4.2.3

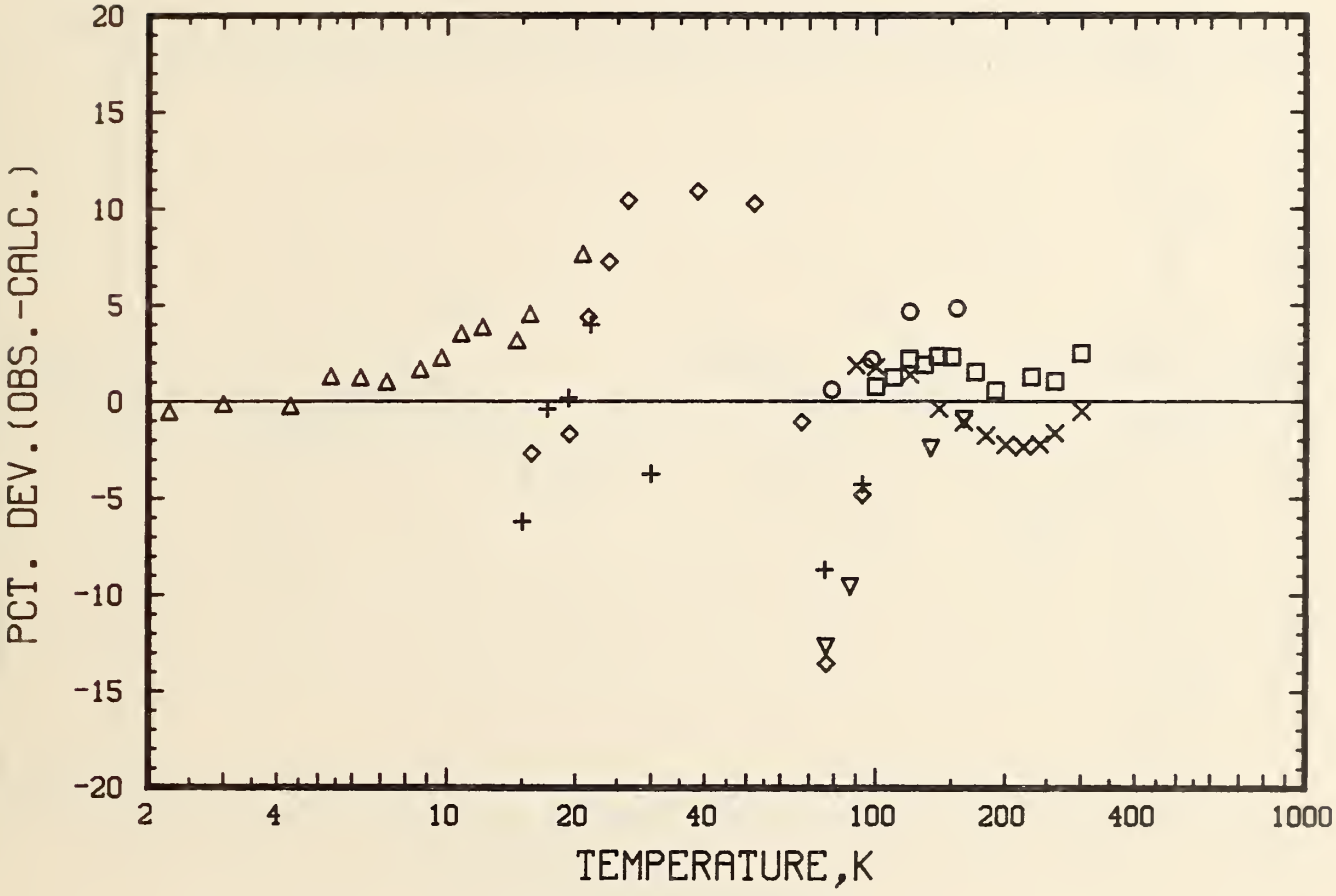


Figure 4.2.5 Thermal conductivity deviations of the iron data from the following secondary references compared to eq. (1.1.3):(1,3,4,5,6,10)

○ - (1), △ - (3), □ - (4), ▽ - (5),
◇ - (6), + - (6), × - (10)

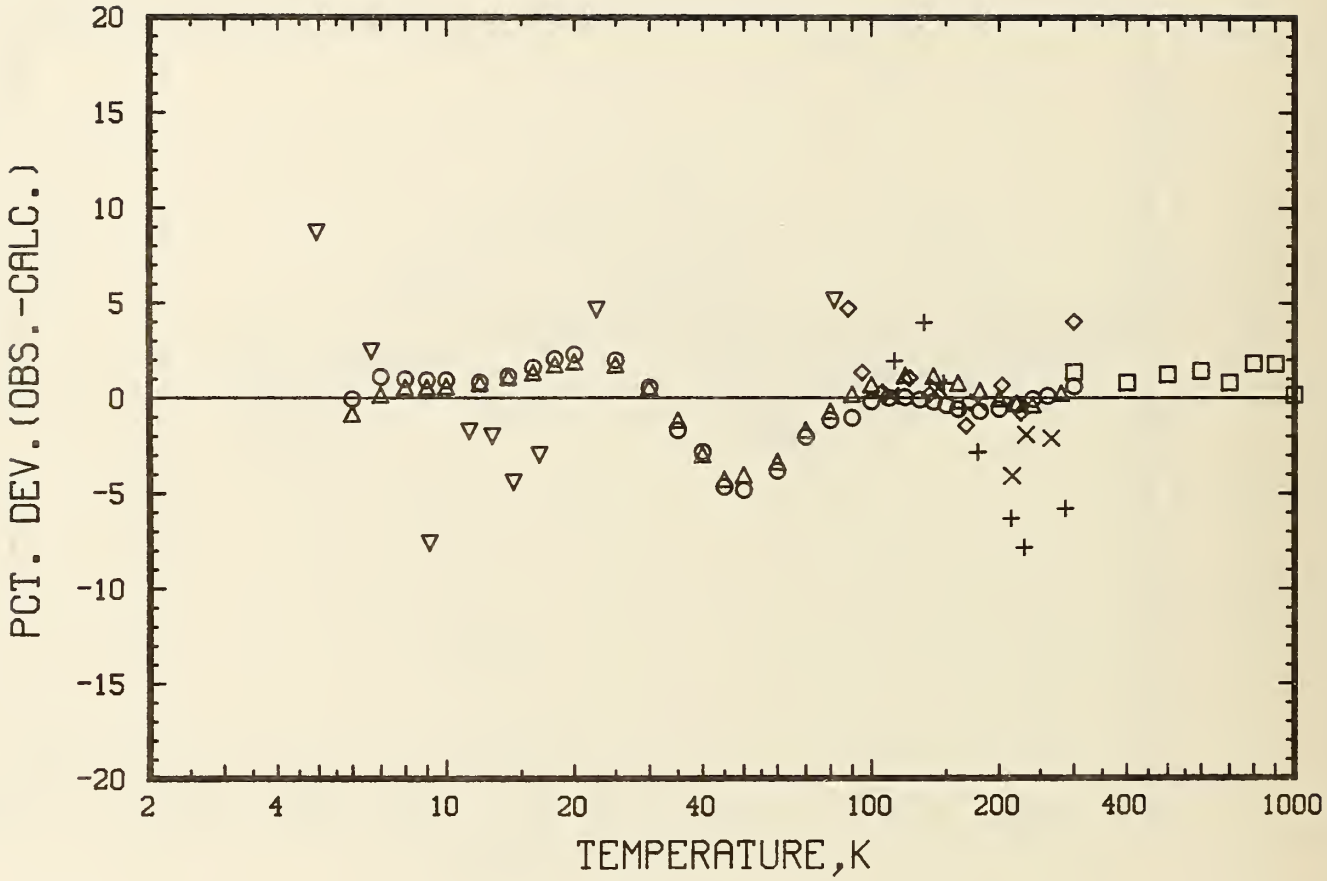


Figure 4.2.6 Thermal conductivity deviations of the iron data from the following secondary references compared to eq. (1.1.3):(11,12,14,17,19,22)

○ = (11), △ = (11), □ = (12), ▽ = (14),
◇ = (17), + = (19), × = (22)

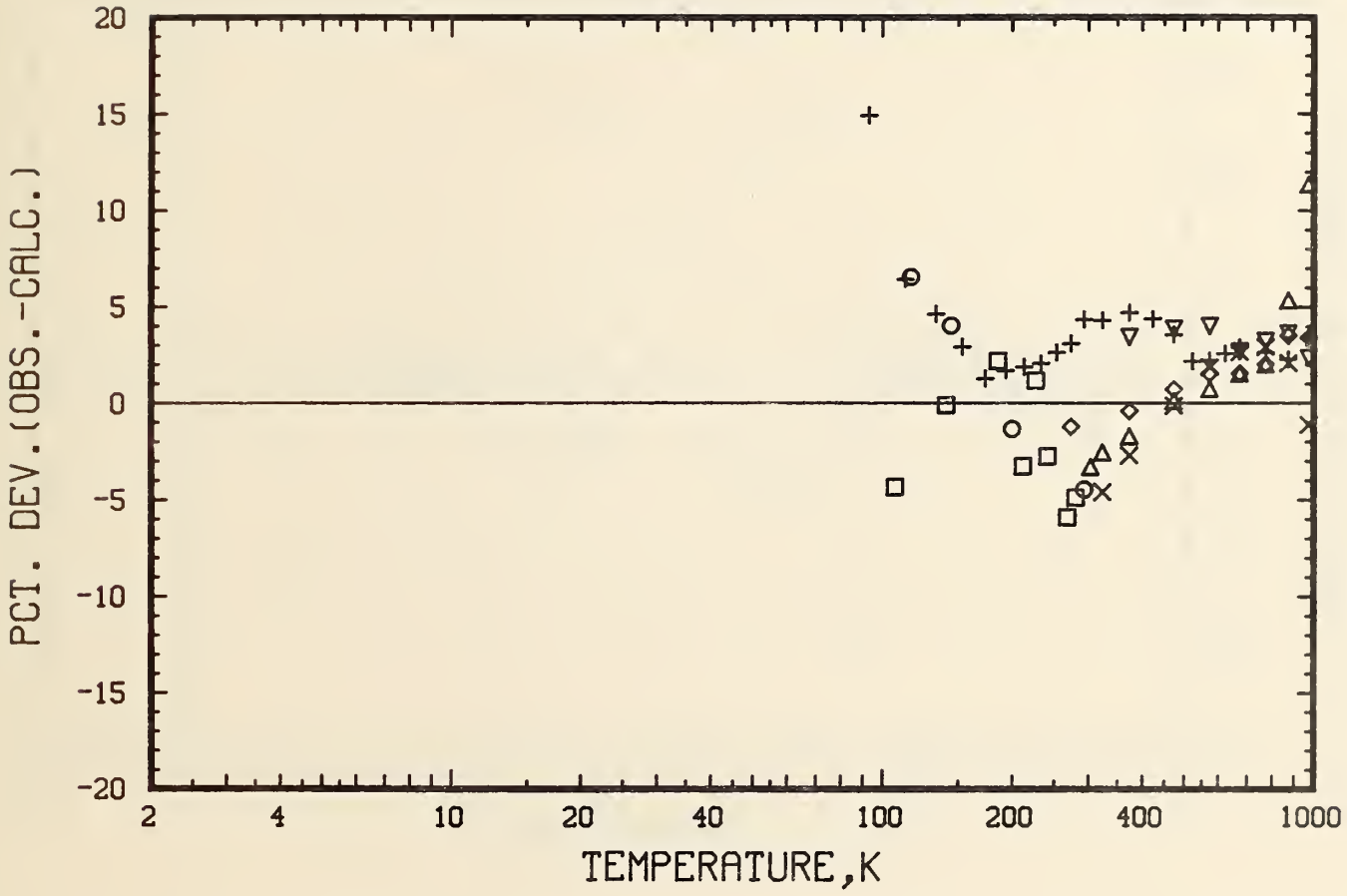


Figure 4.2.7 Thermal conductivity deviations of the iron data from the following secondary references compared to eq. (1.1.3):(21,22A,24,26,27,30,32)

○ - (21), △ - (22A), □ - (24), ▽ - (26),
◇ - (27), + - (30), × - (32)

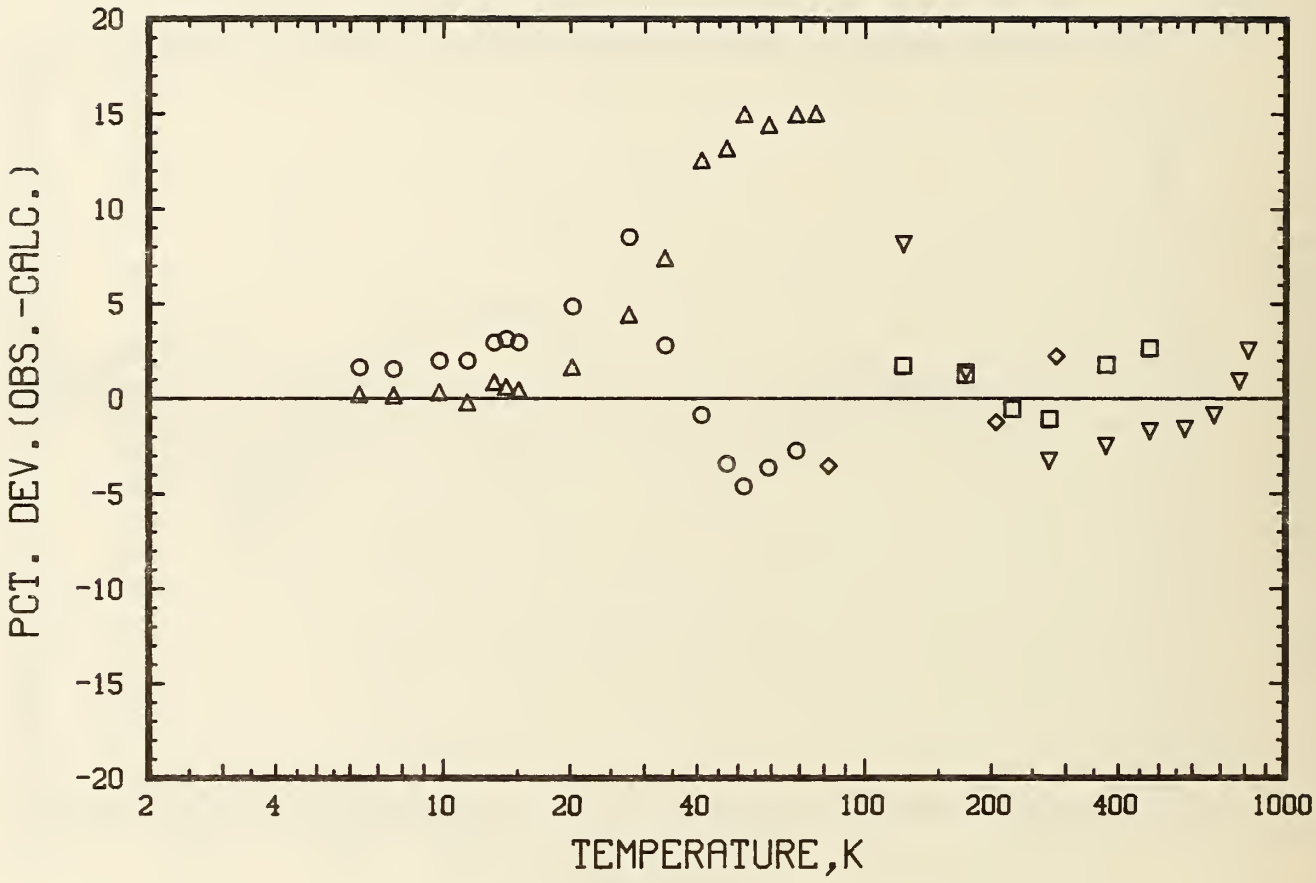


Figure 4.2.8 Thermal conductivity deviations of the iron data from the following secondary references compared to eq. (1.1.3):(33,34,35,36)

○ - (33), △ - (33), □ - (34), ▽ - (35), ◇ - (36)

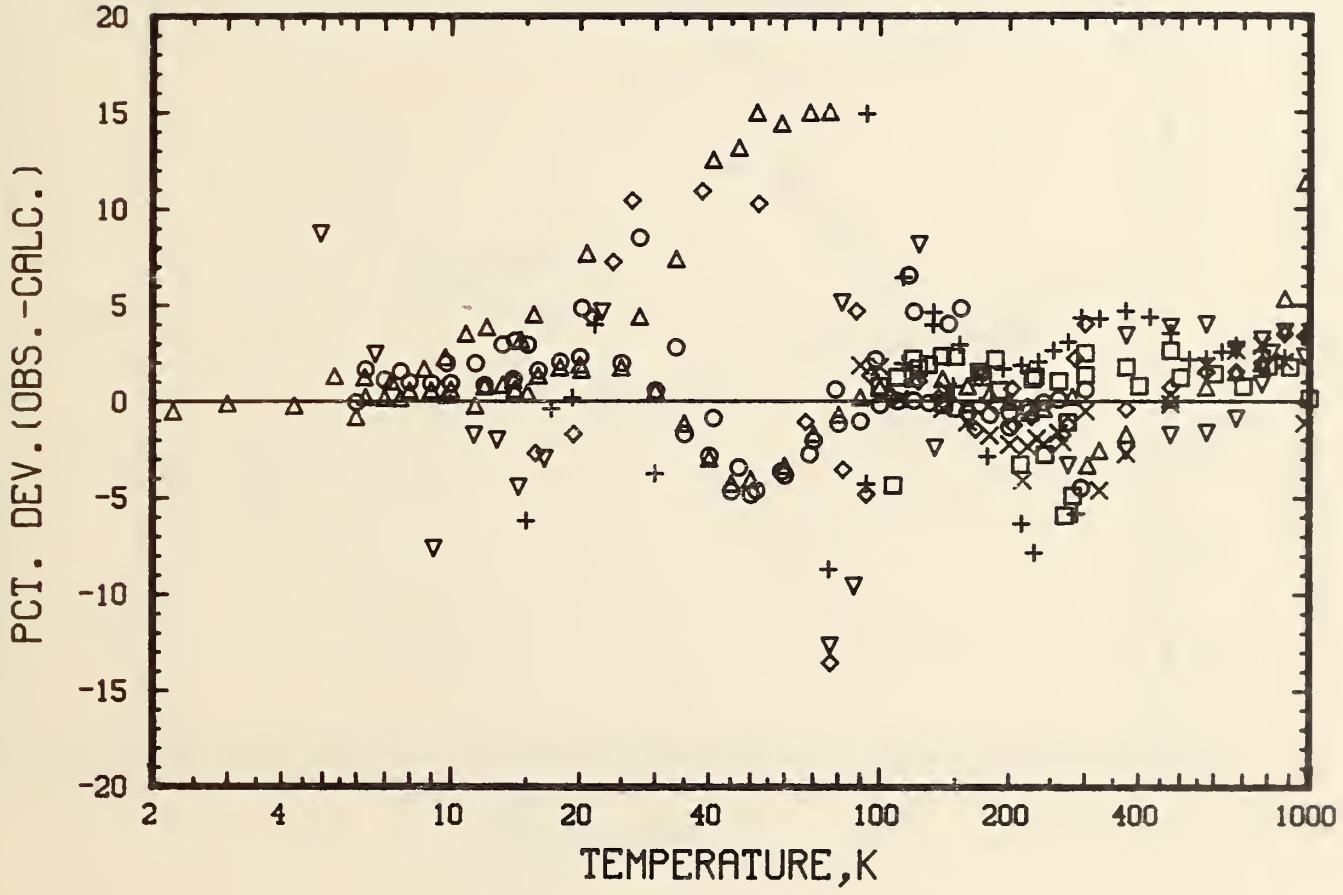


Figure 4.2.9 Composite of the deviations in figs.4.2.6 through 4.2.8

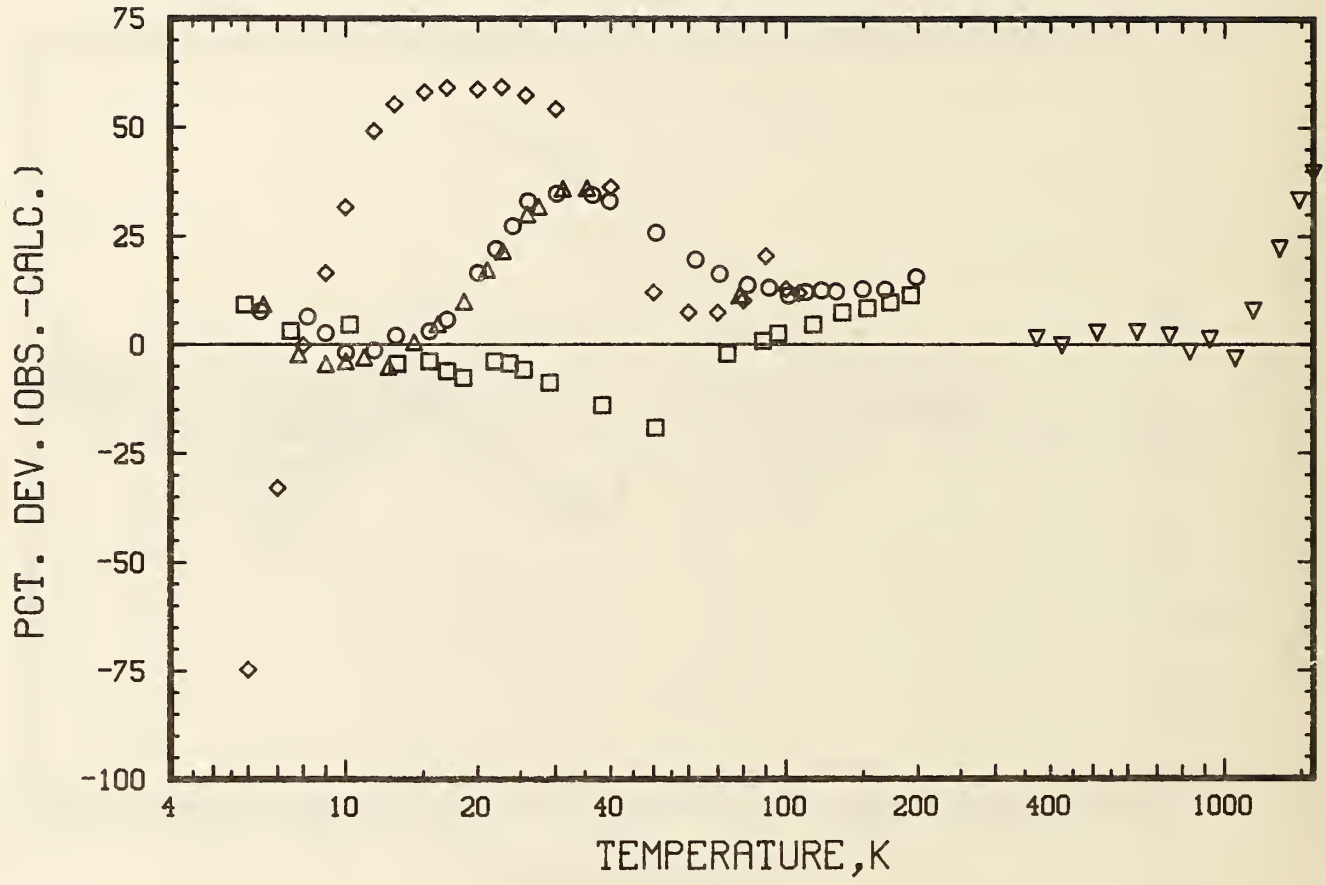


Figure 4.2.10 Thermal conductivity deviations of the iron data from the following secondary references compared to eq. (1.1.3):(2,7,22B)

○ - (2), △ - (2), □ - (2), ▽ - (7),
◇ - (22B)

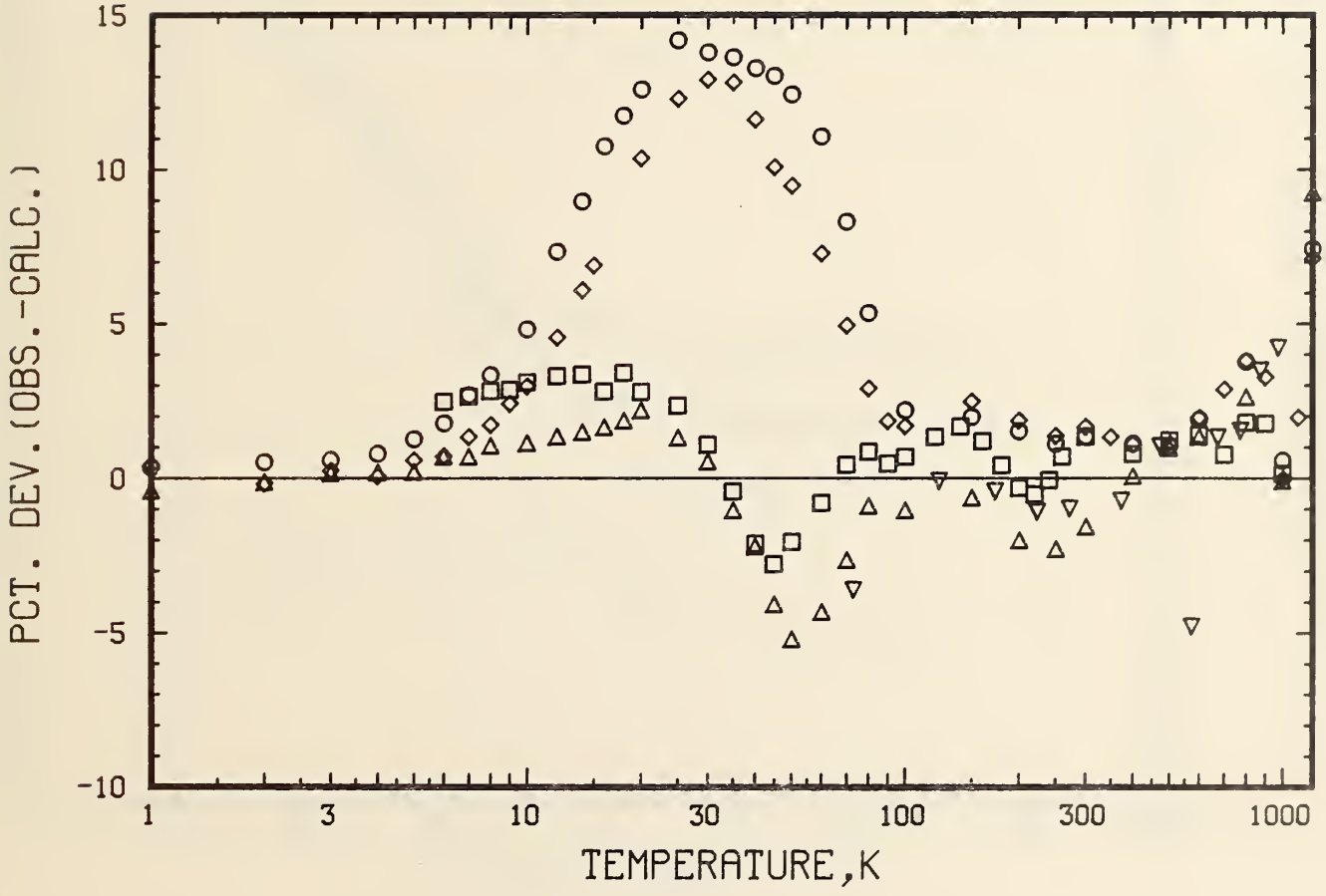


Figure 4.2.11 Comparison of eq.(1.1.3) to the values recommended for iron in the following references:(9A,12,20,32A)

○ - (9A), △ - (9A), □ - (12), ▽ - (20),
◇ - (32A)

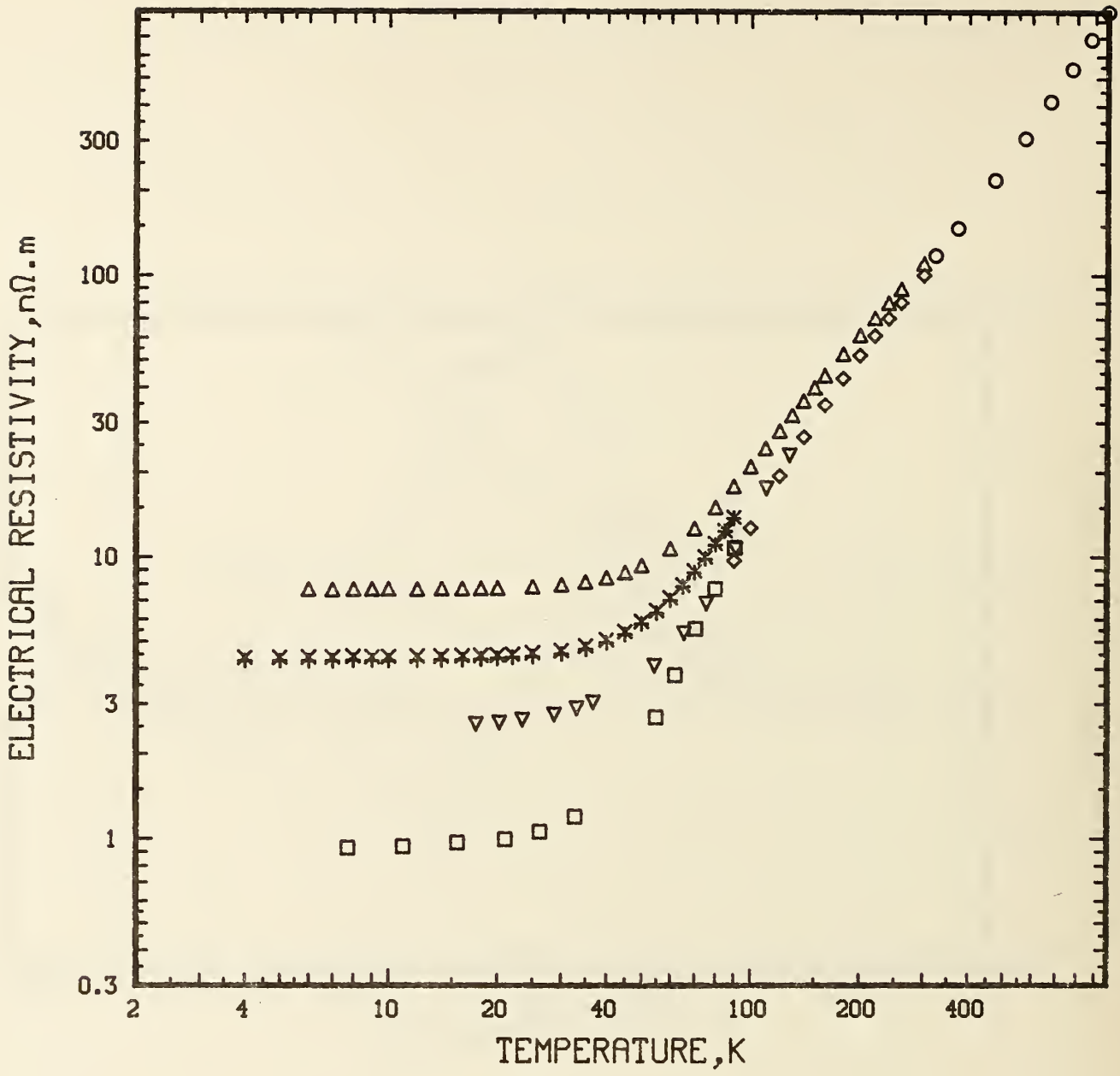


Figure 4.3.1 Experimental electrical resistivity data for iron selected from the following references in the iron annotated bibliography: (3A,8,11,15,16,25)

○ - (8), △ - (11), □ - (15), ▽ - (16),
◇ - (25), + - (3A), × - (3A)

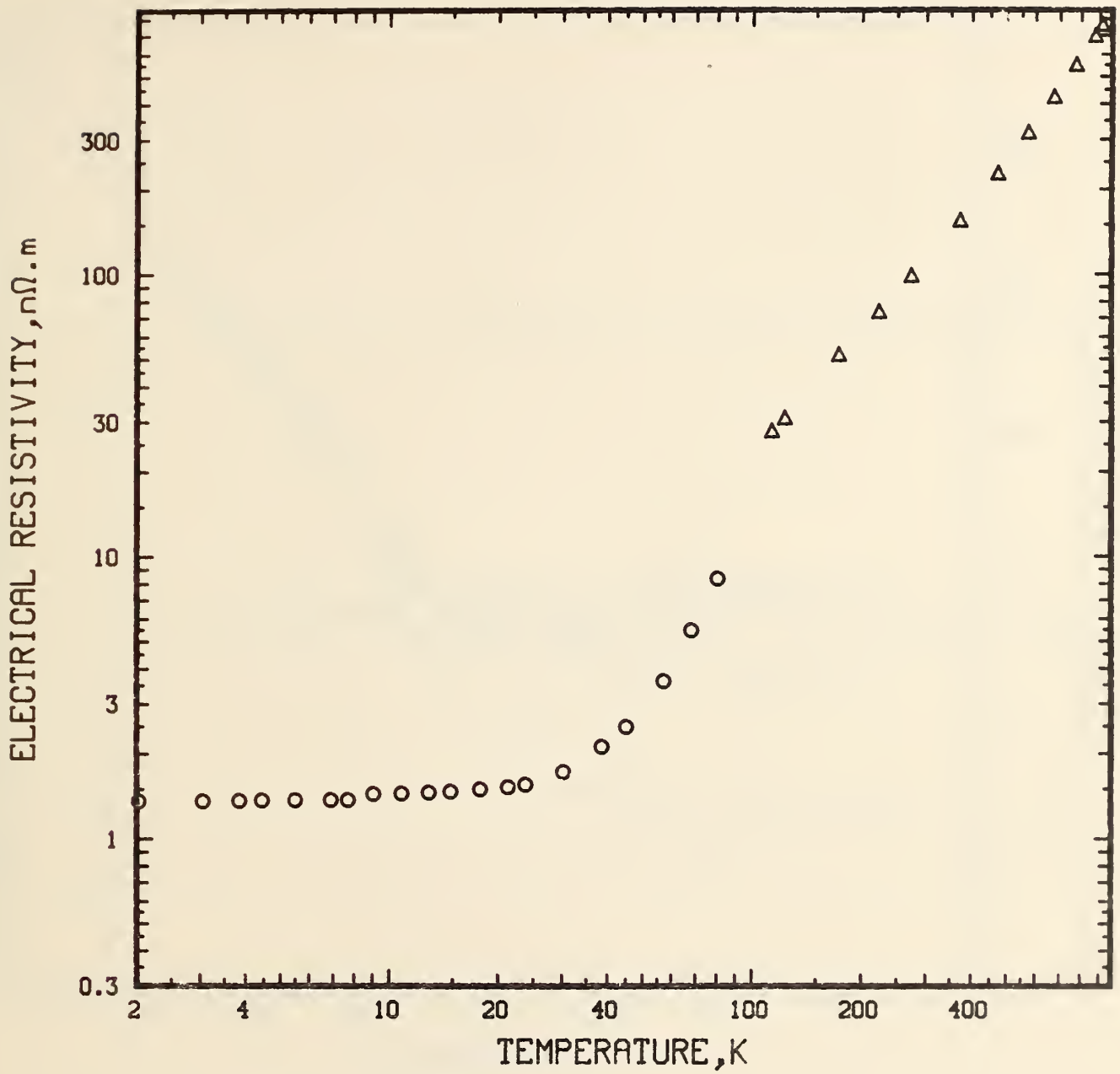


Figure 4.3.2 Experimental electrical resistivity data for iron selected from the following references in the iron annotated bibliography: (31,34)

○ - (31), △ - (34)

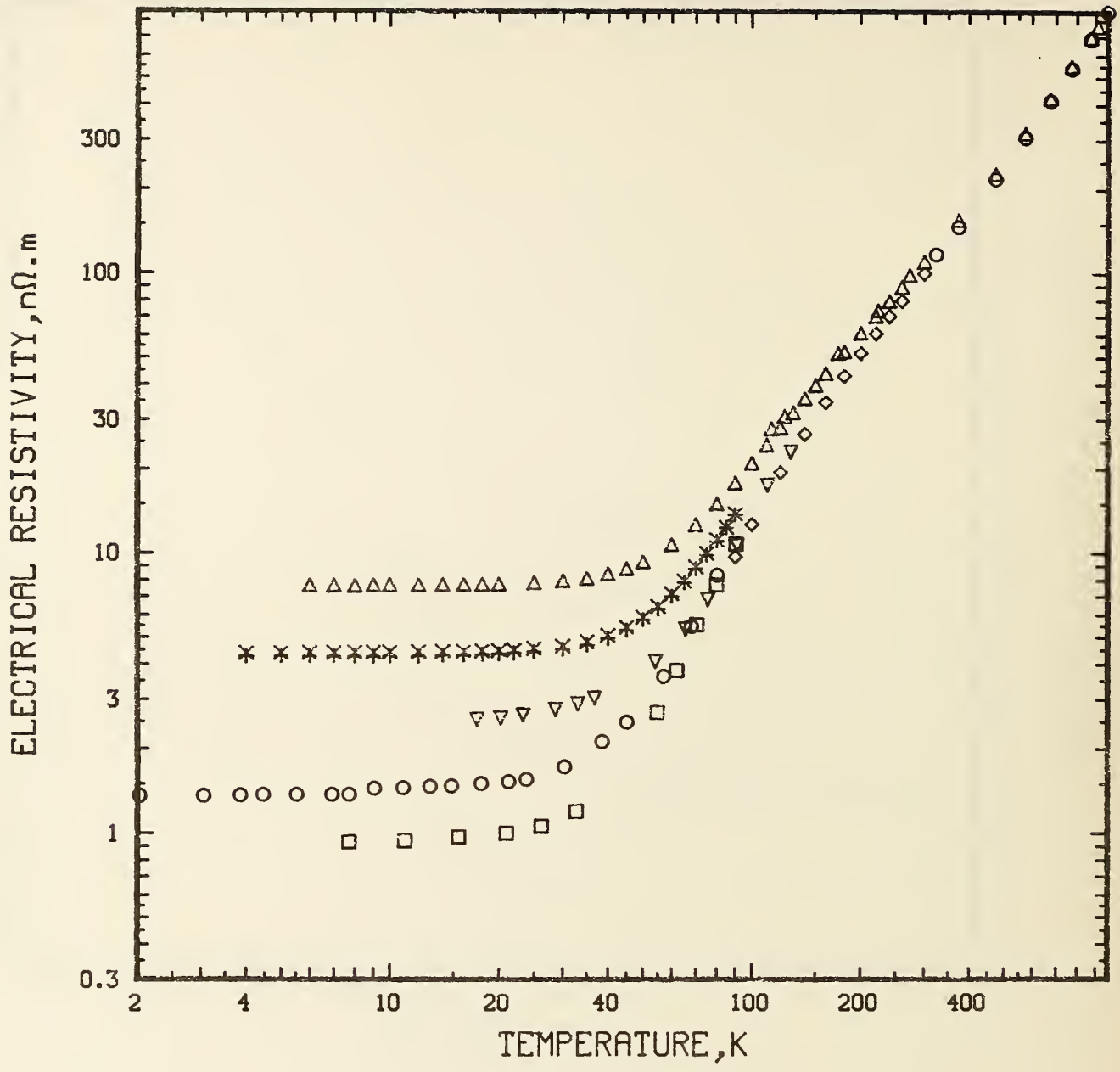


Figure 4.3.3 Composite of the electrical resistivity data in figs. 4.3.1 and 4.3.2

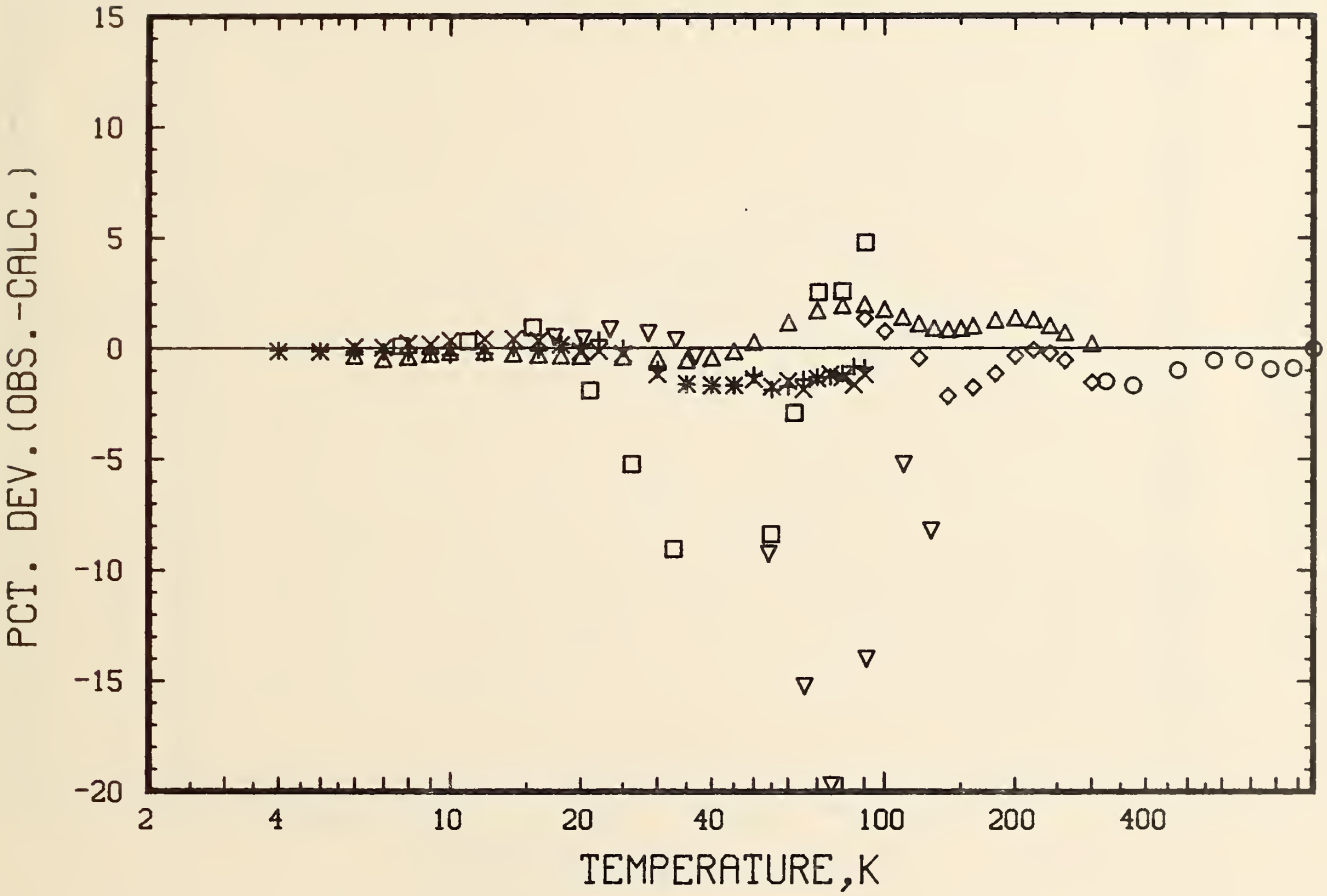


Figure 4.3.4 Electrical resistivity deviations of the iron data from the following references compared to eq. (1.2.3):(3A,8,11,15,16,25)

○ - (8), △ - (11), □ - (15), ▽ - (16),
◇ - (25), + - (3A), × - (3A)

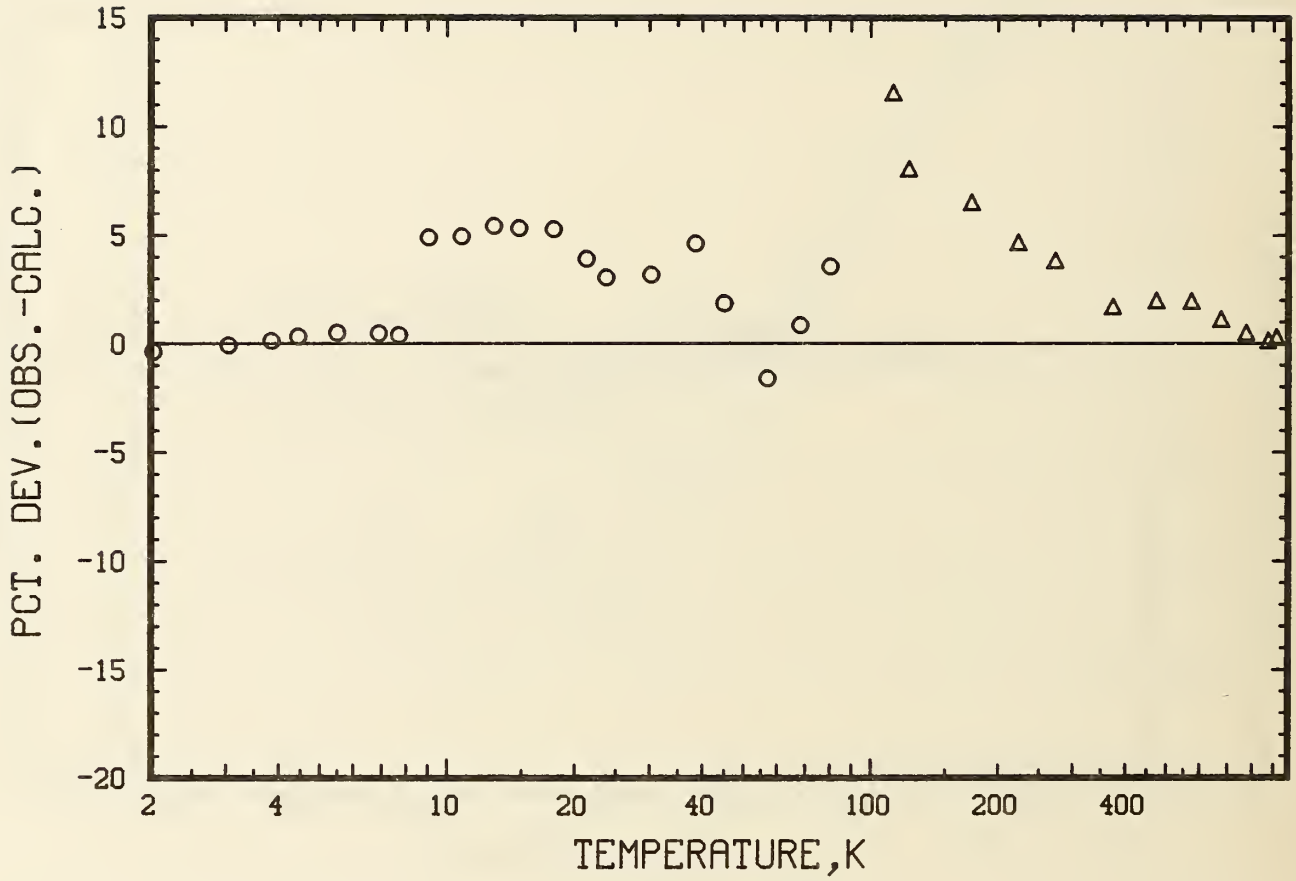


Figure 4.3.5 Electrical resistivity deviations of the iron data from the following references compared to eq. (1.2.3):(31,34)

○ = (31), △ = (34)

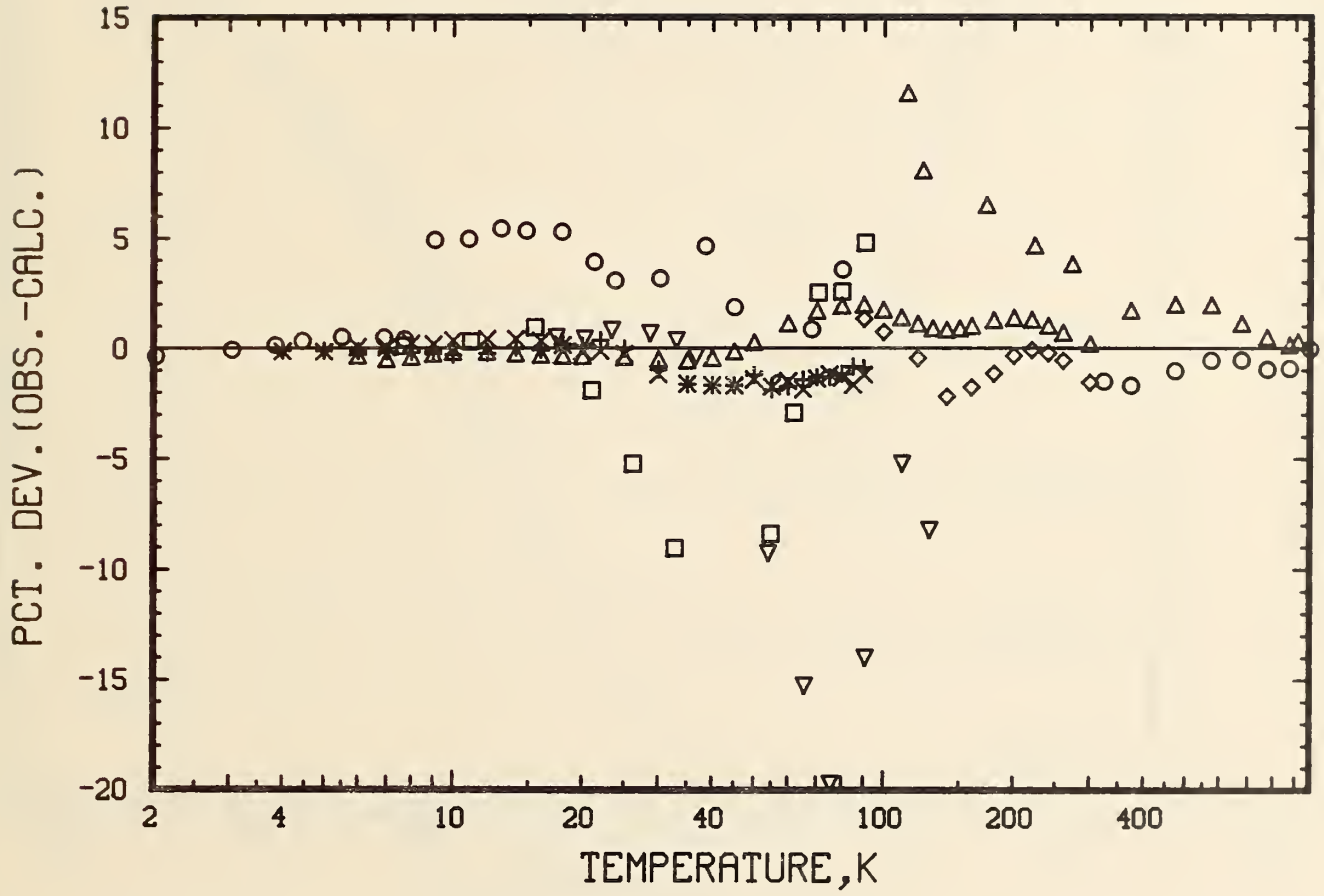


Figure 4.3.6 Composite of the electrical resistivity deviations shown in figs. 4.3.4 and 4.3.5

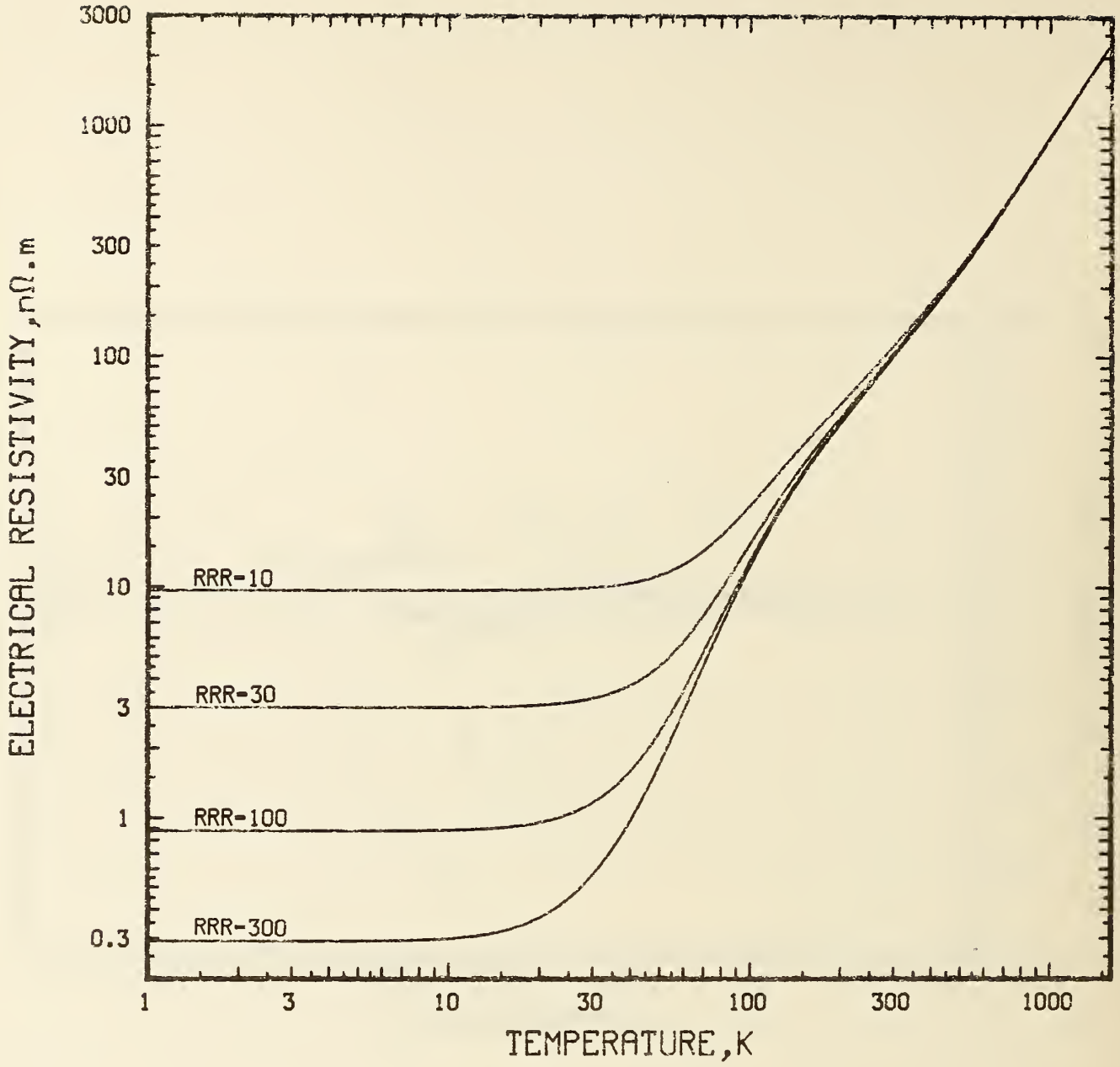


Figure 4.3.7 Electrical resistivity for iron as a function of temperature calculated from eq.(1.2.3) at selected values of RRR.

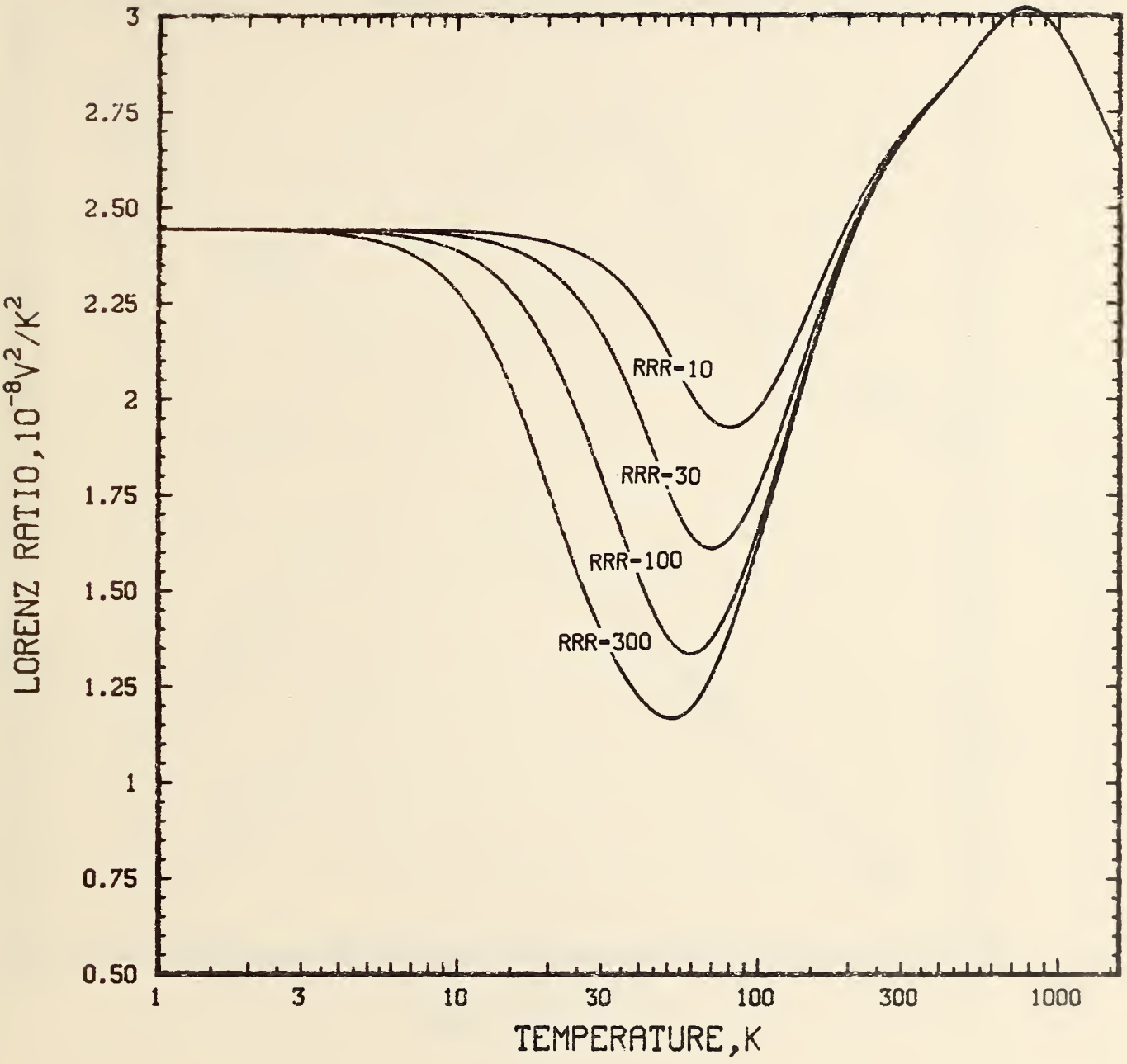


Figure 4.3.8 Lorenz ratio for iron as a function of temperature calculated from eq.(1.2.3) and eq.(1.1.3) at selected values of RRR.

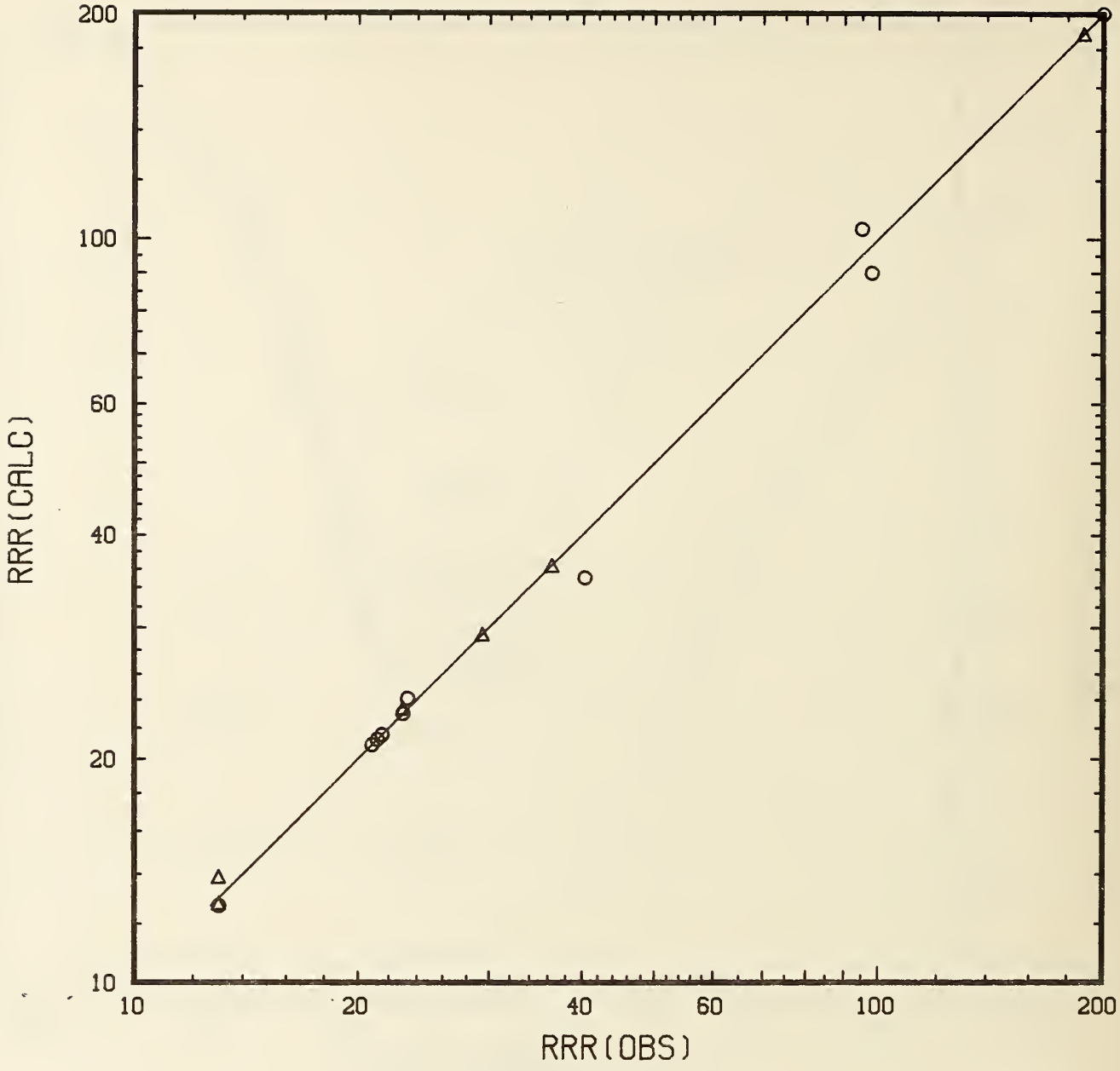


Figure 4.3.9 RRR values calculated as per Section 1.5, RRR(CALC), versus reported RRR values, RRR(OBS),for iron.

○ = Primary, △ = Secondary,
□ = Secondary

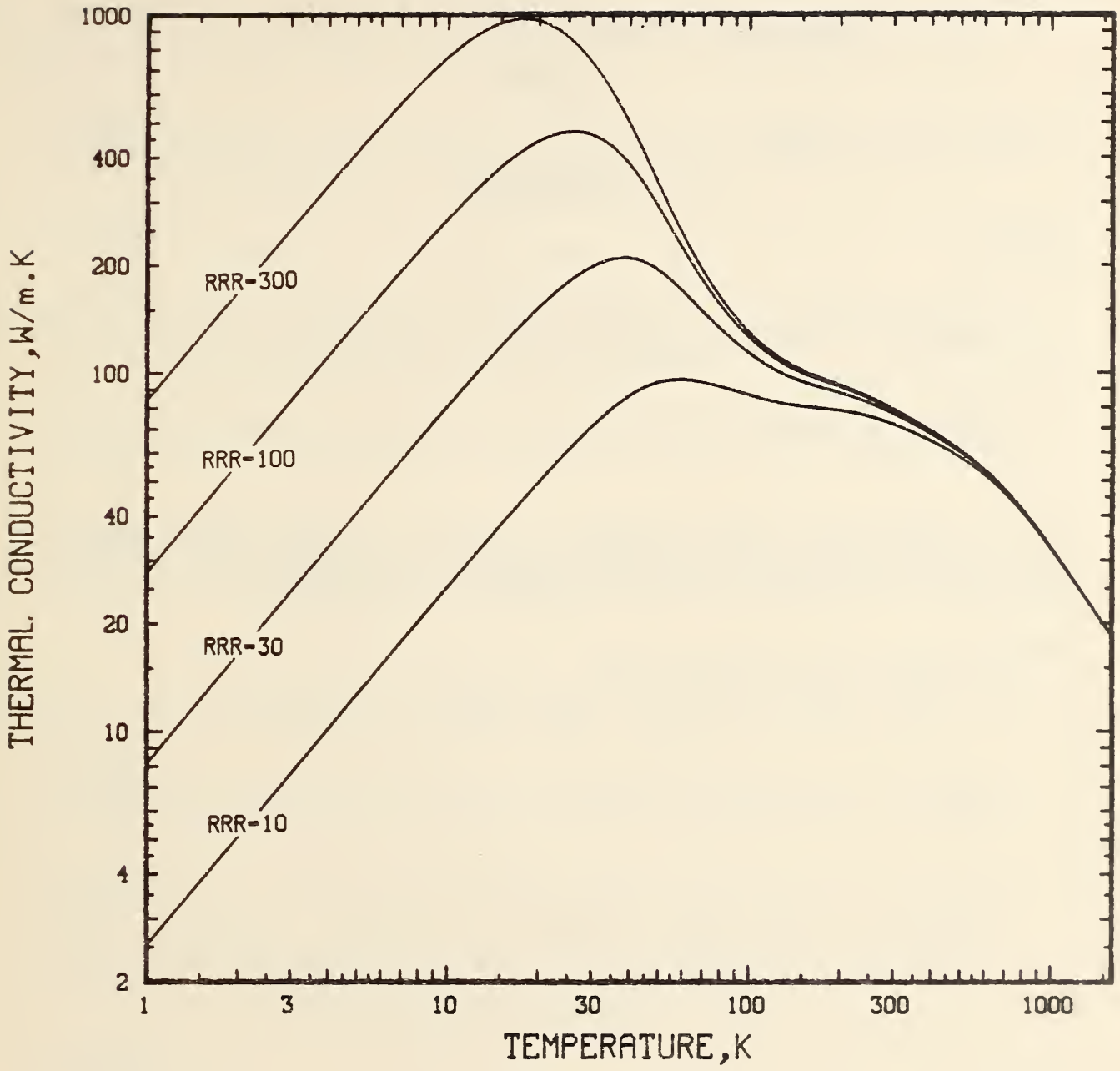


Figure 4.4.1 Thermal conductivity for iron as a function of temperature calculated from eq.(1.1.3) at selected values of RRR.

## 4.5 FORMAT FOR ANNOTATED BIBLIOGRAPHY OF IRON

### REFERENCE

AUTHOR, TITLE, CITATION

### ANNOTATION

PURPOSE

SPECIMEN
a) Dimensions/Shape; b) Crystal Status; c) Thermal/Mech. History; d) Purity Specification; e) RRR; f) $\rho_o$; g) Other Characterization Data

APPARATUS
a) Type; b) Thermometry/Calibration/Anchoring; c) Thermal Isolation; d) Other (Q meas.)

DATA
a) Temperature Range/Difference; b) Content of Tables, Figures and Equations/Data Extraction; c) Uncertainty/Imprecision; d) Disputable Corrections to Measurements by Authors; e) Errata (by Author or Reviewer)

ANALYSIS
a) Comparisons; b) Conclusions

[1] Androulakis, J. G. and Kosson, R. L., Experimental Determination of the Thermal Conductivity of Solids Between 90 and 200 K, 7th Conference on Thermal Conductivity, Nat. Bur. Stand. (U.S.), Spec. Publ. No. 302, 337-348 (1968)

PURPOSE
To describe details of an apparatus for measuring $\lambda$ which can be used for good and poor conductors by varying sample geometry.

SPECIMEN
c) /machined from bar; g) SAE 1020 steel.

APPARATUS
a) longitudinal; b) Cu-constantan thermocouples; c) feedback controlled guard, radiation shields; $10^{-5}$ - $10^{-6}$ Pa vacuum.

DATA
a) 78.8 to 154 K; b) figure 7 - $\lambda$; c) uncertainty: ±8% at 89 K, ±5% at 200 K.

ANALYSIS
a) results agree with Powell, R. L. and Blanpied, W. A., NBS, Circular 556, and Scott, R. B., Cryogenic Engineering, D. Van Nostrand Co., New York (1959).

[2] Arajs, S., Oliver, B. F., and Dunmyre, G. R., Thermal Conductivity of High-Purity Iron at Low Temperatures, J. Appl. Phys., 36, No. 7, 2210-2 (1965)

PURPOSE
To study $\lambda$ of a high purity iron as a function of temperature and compare the results with theory.

SPECIMEN
a) specimen A: 15 cm long, 1.75 cm dia./rod; b) specimen B: polycrystalline; c) specimen A: distilled and reduced to metal with $H_2$, electron beam zone refined, annealed in Pd purified $H_2$, specimen B: annealed/ specimen A: swaged and cleaned with chemical polish before anneal; d) specimen A: 99.997%, specimen B: 99.926%.

APPARATUS
a) longitudinal.

DATA
a) specimen A (run 1): 6 to 198 K, specimen A (run 2): 6 to 78.4 K, specimen B: 5 to 193 K; b) figure 1 - $\lambda$.

ANALYSIS
a) $\lambda$ maximum higher than those of Rosenberg, H. M., Phil. Trans. R. Soc. (London), A247, 441 (1955) and Kemp, W. R. G., Klemens, P. G., and Tainsh, R. J., Ann. Phys. (Leipzig), 5, 35 (1959).

[3] Beitchman, J. G., Trussel, C. W., and Coleman, R. V., Electron Transport and Lorenz Number in Iron, Phys. Rev. Lett., 25(18), 1291-94 (Nov 1970)

PURPOSE
To measure $\rho$ and W of Fe single crystals from 2 to 77 K with and without magnetic fields and investigate theoretical predictions for L and electron transport theory.

SPECIMEN
b) single crystal, <111> axial orientation; e) 700 < RRR < 2000.

DATA
a) 2.2 to 20 K; b) figure 1 - W(H = 0, 95 A/m).

ANALYSIS
b) intrinsic temperature dependence of $\rho$ is $\alpha T^2$, and behavior of single domain state (with $H \neq 0$) is not too different from non-transition metals.

[3A] Berman, R., Hardy, N. D., Sahota, M., Hust, J. G., and Tainsh, R. J., Standard Reference Materials for Thermal Conductivity Below 100 K, Proceedings of the Seventeenth Conference on Thermal Conductivity, Gaithersburg, MD, 105-16 (1983)

PURPOSE
To report results of a CODATA round-robin investigation involving standard reference materials of stainless steel, tungsten, and electrolytic iron.

SPECIMEN from Leeds University
a) SRM 734; b) approximately 1/4 in. (dia.) x 2 in. (6 x 50 mm); c) RRR = 21.24.

SPECIMEN from National Measurement Laboratory
a) SRM 734; b) approximately 1/4 in. (dia.) x 2 in. (6 x 50 mm); c) RRR = 21.55.

APPARATUS
a) not described.

DATA from Leeds University
a) 3 to 100 K; b) Table - $\lambda$/data made available by private communication.

DATA from CSIRO
a) 4 to 90 K; b) Table - $\lambda$, $\rho$, L/data made available by private communication.

[4] Bideau, D., Troadec, J. P., Meury, J. L., Rosse, G., and Dang Tran Quan, Simultaneous Measurements of Thermoelectric Power and Thermal Conductivity of Small Samples from 100 to 300 K, Rev. Phys. Appl., 13(8), 415-8 (Aug 1978)

PURPOSE
To simultaneously measure thermoelectric power and $\lambda$ on small samples from 100 to 300 K, and present evaluation of apparatus.

SPECIMEN
a) 6 mm long, 6.4 mm diam./rod; c) /faces polished; d) SRM 734 electrolytic Fe.

APPARATUS
a) longitudinal; b) Cu-constantan thermocouples//In foil for thermal contact, tempered specimen leads; c) radiation shield, $10^{-6}$ mm of Hg ($10^{-4}$ Pa), insulation.

DATA
a) 100 to 300 K; b) figure 6 - $\lambda$; c) uncertainty: <±3%.

ANALYSIS
a) results deviate <3% from Hust, J. G., Giarratano, P. J., Nat. Bur. Stand. (U.S.), Spec. Publ. No. 260 (1975).

[5] Cason, J. L., Jr., Thermal Conductivity Measurements of Eu O across the Curie Point, S.D. School of Mines and Technol., Rapid City, Dept. of Physics, Rept. No. TR-22 (Oct 1967), Contract No. NONR-2964 (01), 85 pp., M.S. Thesis

PURPOSE
To measure $\lambda$ of Fe as a standard for other measurements.

SPECIMEN
a) 19 mm long, 3 mm dia./rod; g) source: Battelle Memorial Institute; Armco.

APPARATUS
a) absolute longitudinal; b) Cu-constantan thermocouples on specimen, GRT on heat sink, PRT in bath; c) radiation shield, heater temperature monitor, vacuum insulation.

DATA
a) 76.6 to 160 K; b) figure 13 - $\lambda$; c) total uncertainty: ±20% at 68 K, ±14% at 297 K.

ANALYSIS
b) results agree within 6% of Powell, R. W., Progress in International Research on Thermodynamic and Transport Properties, Academic Press, New York (1962).

[6] deNobel, J., Heat Conductivity of Steels and a Few Other Metals at Low Temperatures, Physica (Utrecht), 17, 551-62 (1951)

PURPOSE
To measure λ for some metals and alloys used in cryostat construction.

SPECIMEN
c) specimen 6936: forged, specimen 1166A/4: annealed at 800 °C, furnace cooled; d) specimen 6936: 99.93% Fe, specimen 1166A/4: 0.14% C, 0.08% Si, 0.07% Mn; g) source: Sir R. A. Hadfield, specimen 1166A/4: mild steel, 104 hardness B., specimen 6936: 103 hardness B.

APPARATUS
a) longitudinal; b) gas thermometers/calibrated against Pt thermometer in bath; c) $10^{-6}$ mm of Hg ($10^{-4}$ Pa) vacuum.

DATA
a) 16 to 93 K; b) Table 2 - λ; d) correction for thermometry heat leak.

ANALYSIS
b) λ is proportional to T at low temperatures.

[7] Fieldhouse, I. B., Hedge, J. C., and Lang, J. I., Measurements of Thermal Properties, WADC Tech. Rep. 58-274, 20 pp; ASTIA 206892 (1958)

PURPOSE
To calibrate a λ apparatus.

SPECIMEN
a) 0.625 in. (1.59 cm) I.D. x 3.0 in. (7.6 cm) O.D. x 1.0 in. (2.5 cm) thick/disks; g) source: Armco.

APPARATUS
a) radial; b) Pt vs. Pt + 10% Rh thermocouples; c) bubble alumina, end guard heaters, water-cooled steel housing.

DATA
a) 208 to 2410 K; b) Table 1 - λ; c) uncertainty: ±5%.

ANALYSIS
a) results agree with Powell, R. W., Proc. Phys. Soc., London, 46, pp. 659-74 (1934).

[8] Fulkerson, W., Moore, J. P., and McElroy, D. L., Comparison of the Thermal Conductivity, Electrical Resistivity and Seebeck Coefficient of a High-Purity Iron and an Armco Iron to 1000 °C, J. Appl. Phys., 37(7), 2639-53 (1966)

PURPOSE
To make a comparative investigation of ingot and high purity Fe for $\lambda$, $\rho$, and S up to 1000 °C

SPECIMEN
a) 3 in. (7.6 cm) dia., 1.13 to 1.45 in. (2.87-3.68 cm) thick, 9 in. (23 cm) tall stack/disks; e) RRR = 9.6, 23.0; g) source: Armco.

APPARATUS
a) radial; b) Pt - 10% Rh vs. Pt annealed reference grade thermocouple; c) guard disks.

DATA
a) 323 to 1273 K; b) Table III - $\lambda$, Table IV - $\rho$; c) uncertainty in $\lambda$: ±1.5%; uncertainty in $\rho$: ±0.3%.

ANALYSIS
a) results agree with previous measurements.

[9] Godfrey, T. G., Fulkerson, W., Kollie, T. G., Moore, J. P., and McElroy, D. L., Thermal Conductivity of Uranium Dioxide and Armco Iron by an Improved Radial Heat Flow Technique, U.S.A.E.C. Rep. ORNL-3556, 1-67 (1964)

PURPOSE
To describe an improved apparatus (radial heat flow) for making measurements on solids from -57 to 1100 °C and report results and analysis on $UO_2$ and ingot Fe.

SPECIMEN
a) 1.375 in. (3.493 cm) outer radius, 5/8 in. (1.59 cm) inner radius, 1 in. (2.54 cm) thick; d) < 99.4%.

APPARATUS
a) radial; b) Pt vs. Pt-10% Rh reference grade thermocouple; c) He atm, end guard heaters, granular alumina, insulation.

DATA
a) 385 to 990 K; b) Table E1 - $\lambda$/data points listed in TPRC data series; c) uncertainty: ±1.5%.

ANALYSIS
a) over the temperature range 100 to 1000 °C, results agree to ±3% with Powell, R. W., ASME, N.Y. (1962), Laubitz, M. J., Can. J. Phys. 38(7), 887 (1960), and Cody, G. D., Abeles, B., and Beers, D. S., Trans. Metall. Soc. AIME, 221(2), 25 (1961).

[9A] Ho, C. Y., Powell, R. W., and Liley, P. E., Thermal Conductivity of the Elements: A Comprehensive Review, J. Phys. Chem. Ref. Data, 3, Supplement No. 1, 242-257 (1974)

PURPOSE
To provide a comprehensive listing of data on $\lambda$ of the elements.

SPECIMEN

d) high purity; f) $\rho_0 = 1.43 \times 10^{-8}$ $\Omega \cdot$cm for T below 200 K.

APPARATUS
a) not given.

DATA
a) 0 to 6500 K; b) Table 78 - $\lambda$, recommended values; c) uncertainty: ±5% below 100 K, ±3% from 100 K to room temperature, ±2% from room temperature to about 1000 K, increasing to ±8% at 1600 K, and ±15% at the melting point.

[10] Holder, T. K., Thermal Conductivity, Electrical Resistivity and Seebeck Coefficient of High Purity Iron and Selected Iron Alloys from 90 to 400 K, O.R.N.L., Tenn., Metals and Ceramics Div., Rep. No. ORNL/TM-5539, Contract No. W-7405-Eng-26. Also M.S. Thesis, 110 pp. (Jun 1977)

PURPOSE
To report $\lambda$, $\rho$, and S of pure Fe and some Fe alloys from 90 to 400 K, calculate $\lambda_e$ and $\lambda_g$ and compare to theory.

SPECIMEN
a) 7.6 cm long, 0.65 cm dia./rod; d) 99.994%; e) RRR = 189; g) zone refined.

APPARATUS
a) longitudinal; b) chromel-P: constantan thermocouples//all specimen leads tempered; c) temperature controlled guard, vacuum insulation.

DATA
a) 90 to 300 K; b) Table 2 - $\lambda$, $\rho$, Table 12 - L; c) uncertainty: ±1.2%; d) isothermal corrections due to small thermocouple differences.

ANALYSIS
b) alloys deviated from Matthiessen's rule.

[11] Hust, J. G., Thermal Conductivity Standard Reference Materials from 4 to 300 K. I. Armco Iron, National Bureau of Standards, Boulder, Colo., Report No. 9740 (Aug 1969) 97 pp.

PURPOSE
To measure $\lambda$, $\rho$, L and thermopower of several specimens of Armco Fe from 4 to 300 K to check usefulness as an SRM.

SPECIMEN
a) 23 cm long, 3.6 mm dia./rod; c) annealed at 870 °C in gas-heated air muffle for 1/2 h then in $10^{-6}$ mm for 1.5 h at 875 °C, held at 150 °C for 24 h and repeated/machined between anneals; d) 0.015% C, 0.028% Mn, 0.005% P, 0.025% S, 0.003% Si, 0.04 Cu; e) RRR (mean) = 13; g) source: Battelle Memorial Institute, hardness B: 37.1, grain size: 0.064 mm.

APPARATUS
a) longitudinal; b) 8 thermocouples; c) glass fiber around specimen, temperature controlled shield.

DATA
a) specimens 2, 2a, 4: 6 to 300 K; b) Tables 20, 21, 22 - $\lambda$, $\rho$, L; c) uncertainty: ±2.5% at 300 K, decreases as $T^4$ to 200 K, 0.7% at 200 to 50 K increasing as 1/T to 1.5% at 4 K.

ANALYSIS
a) RRR mean values are 5.5% below values of Lucks, C. F., rms deviation is 3.6% compared to Luck's 6.5%.

[12] Hust, J. G. and Giarratano, P. J., Thermal Conductivity and Electrical Resistivity Standard Reference Materials: Electrolytic Iron SRM's 734 and 797 from 4 to 1000 K, Nat. Bur. Stand. (U.S.), Spec. Publ. No. 260-50, 32 pp. (Jun 1975)

PURPOSE
To review development of SRM's, give selection criteria and compile and compare data on $\lambda$ and $\rho$ for electrolytic Fe and other similar specimens.

SPECIMEN
a) 23 cm long, 3.6 mm dia./rod; c) annealed at 1000 °C for 2 h, held at 800 °C for 2 h; d) 99.90%; e) mean RRR = 23; g) density = 7.867 g/cm$^3$, Rockwell hardness and grain size: B24, 0.05 mm respectively.

APPARATUS
a) longitudinal; b) thermocouples; c) glass fiber, temperature controlled shield, insulation.

DATA
a) 6 to 1000 K; b) Table 1 - $\lambda$, $\rho$, L; c) uncertainty: 2.5% below 280 K, 3% above 280 K.

[13] Hust, J. G. and Sparks, L. L., Thermal Conductivity Standard Reference Materials from 4 to 300 K. II. OSRM Iron-1265, National Bureau of Standards, Boulder, Colo., Report No. 9771 (Oct 1970) 35 pp.

PURPOSE
To measure $\lambda$, $\rho$, and L for OSRM Fe-1265 from 4 to 300 K and study the variability by RRR measurements.

SPECIMEN
a) 23 cm long, 3.6 mm dia./rod; c) annealed at 1000 °C in vacuum or He for 2 h; d) < 99.87%; e) RRR = 23.33 ±0.24; g) density: 7.867 g/cm$^3$, hardness B: 23.5 Rockwell, Grain size: 0.0507 mm, OSRM Fe-1265.

APPARATUS
a) longitudinal; b) 8 thermocouples; c) glass fiber around specimen, temperature controlled shield.

DATA
a) 6 to 280 K; b) Table 8 - $\lambda$, $\rho$, L; c) uncertainty: ±2.5% at 300 K, decreases as $T^4$ to ±0.7% at 200 K, ±0.7% from 200 to 50 K, increases inversely with T to ±1.5% at 4 K.

ANALYSIS
b) Mathiessen's rule application shows dependence of $\rho_i$ on $\rho_o$.

[14] Karweil, J. and Schafer, K., The Thermal Conductivity of Some Poorly Conducting Alloys between 3 and 20 K, Ann. Phys. (Leipzig), 36, 567-77 (1939)

PURPOSE
To determine $\lambda$, $\rho$, and L for some important alloys from 3 to 20 K.

SPECIMEN
a) 2.54 mm dia., 12 cm long/rod; c) /drawn; d) electrolytic Fe; f) RRR = 29.4.

APPARATUS
a) longitudinal; b) gas thermometers, thermocouples/thermocouples calibrated at $LO_2$/leads to specimen run through bath; c) radiation shield, insulation.

DATA
a) 4.9 to 82 K; b) graph p. 575 - $\lambda$.

ANALYSIS

b) Lorenz ratio is reasonably constant at low temperatures.

[15] Kemp, W. R. G., Klemens, P. G., and Tainsh, R. J., Thermal and Electrical Conductivities of Rhodium and Iron, Ann. Phys. (Leipzig), 5(7), 35-41 (1959)

PURPOSE
To measure $\sigma$ and $\lambda$ for pure Fe and Rh specimens from 2 to 90 K.

SPECIMEN
a) specimen 1: 28 x 2.5 x 2.5 mm, specimen 2: 2.4 x 1.7 x 30 mm/bars; c) specimens 1,2: annealed at 950 °C and reannealed/cut from a precipitated plate, compressed between anneals, specimen 2 face ground; e) specimen 1 ($\rho_0$ = 0.09 $\mu\Omega$·cm), specimen 2 ($\rho_0$ = 0.092 $\mu\Omega$·cm); g) similar material as used by Grüneisen, E., doubly refined electrolytic Fe.

APPARATUS
a) longitudinal; b) gas thermometers; c) vacuum, temperature controlled shield, insulation.

DATA
a) specimen 1: 6.5 to 90 K, specimen 2: 7.7 to 91 K; b) figure 3 - $\lambda$, Tables 1,2 - $\rho_0$, $\rho$, respectively.

ANALYSIS
a) results of $\rho_0/\rho_{273}$ higher than Grüneisen, E. and Goens, E., Z. Phys. 44, 615 (1927).

[16] Kemp, W. R. G., Klemens, P. G., and White, G. K., Thermal and Electrical Conductivities of Iron, Nickel, Titanium and Zirconium at Low Temperatures, Aust. J. Phys., 9(2), 180-8 (1956)

PURPOSE
To measure $\lambda$ for several metals down to 2 K and determine $\lambda_g$, $\lambda_e$ and L.

SPECIMEN
a) 2 mm dia./rod; c) annealed in vacuum at 750 °C for 4 h; d) 99.995%; e) RRR = 40.3; f) $\rho_0$ = 0.248 $\mu\Omega$·cm; g) source: Johnson Matthey.

APPARATUS
a) longitudinal; b) gas thermometers; c) temperature controlled shield, vacuum insulation.

DATA
a) 1.5 to 128 K; b) figures 1,2,4 - $\lambda$, L, $\rho$, respectively.

ANALYSIS
a) results agree with Rosenberg, R. M., Philos. Trans. Roy. Soc. London, Ser. A, 247, 441 (1955).

[17] Kohlhaas, R. and Kierspe, W., The Thermal Conductivity of Pure Iron and Some Ferritic and Austenitic Steels Between the Temperature of Liquid Air and Room Temperature, Arch. Eisenhuettenwes., 36(4), 301-9 (1965)

PURPOSE
To measure $\lambda$ and $\rho$ of pure Fe and steels between liquid air and room temperature, determine $\lambda_e$ and $\lambda_g$, estimate $\lambda$ from $\rho$ and examine effect of alloying elements on $\lambda$.
SPECIMEN
g) 0.5 cm dia, 15 cm long/rod; d) 99.93%.

APPARATUS
a) longitudinal; b) Fe-constantan thermocouples; c) vacuum.

DATA
a) 88 to 300 K; b) Tables 2, 3 - $\lambda$, $\rho$; c) uncertainty: ±3.5%.

ANALYSIS
b) $\lambda_e$, $\lambda_g$ are temperature dependent.

[18] Laubitz, M. J., Thermal and Electrical Properties of Armco Iron at High Temperatures, Can. J. Phys., 38(7), 887-907 (1960)

PURPOSE
To accurately determine $\lambda$, $\sigma$ and thermoelectric power of Armco Fe from 0 to 1000 °C in an effort to solve discrepancies in the literature.

SPECIMEN
a) 7.156 cm long, 2.324 cm dia./rod; c) annealed at 850 °C 1/2 h/specimen cut from 12 in. (30.5 cm) long sect.; g) source: Battelle Memorial Institute.

APPARATUS
a) longitudinal; b) 6 Pt/Pt - 10% Rh thermocouples//thermocouple leads anchored to guard; c) radiation shields, alumina guard and powder, vacuum insulation

DATA
a) 303 to 973 K; b) Table 2 - $\lambda$, Table 3 - $\rho$, L; c) uncertainty: ±2.5%: d) non-uniform power distribution of heater, deviations from thermal equilibrium, average correction: 0.06%.

ANALYSIS
a) results agree with Powell, R. W., Proc. Phys. Soc. 46, 659 (1934), but disagree with Hattori, D., Sci. Rep. Tohoku Univ. 26, 190 (1937), and Maurer, E., Arch. Eisenhuettenwes., 10, 1945 (1936).

[19] Lees, C. H., The Effects of Temperature and Pressure on the Thermal Conductivities of Solids - Part II. The Effects of Low Temperatures on the Thermal and Electrical Conductivities of Certain Approximately Pure Metals and Alloys, Philos. Trans. Roy. Soc. London, Ser. A, 208, 381-443 (1908)

PURPOSE
To make measurements of $\lambda$ for metals and alloys below 0 °C and to determine the variation with temperature.

SPECIMEN
a) 7-8 cm long, 0.585 cm dia./rod; c) /turned from bar; d) 99.99%, ("best scrap Fe"); g) density = 7.74 $gm/cm^{-3}$ at 21 °C.

APPARATUS
a) longitudinal; b) Pt resist thermometers/calibrated at boiling point of $O_2$, ice point and boilding point $H_2O$.

DATA
a) 113 to 286 K; b) Table p. 416 - $\lambda$, graph p. 425 - $\rho$; d) correction for radiation heat loss, conduction and offset of Pt temperature from rod temperature.

ANALYSIS
a) Jager and Diesselhorst compared at 18 °C; b) little variation in $\lambda$ over temperature range investigated; L doesn't agree with theory.

[20] Lucks, C. F., Armco Iron: New Concept and Broad-Data Base Justify Its Use as a Thermal Conductivity Reference Material, J. of Testing and Evaluation, 1, No. 5, 522-31 (1973)

PURPOSE
Evaluate published data on ingot iron to determine its continued use as a reference material.

DATA
a) 73 to 1273 K (no new data).

ANALYSIS
Recommends continued use of ingot iron as reference material.

[21] Lucks, C. F. and Deem, H. W., Thermal Properties of Thirteen Metals, ASTM Spec. Tech. Publ. No. 227 (1958)

PURPOSE
To measure λ of ingot Fe as a standard for other measurements.

SPECIMEN
a) 6 in. (15 cm) long, 3/4 in. (1.9 cm) dia./rod; c) /hot rolled; g) source: U. S. Steel Co.

APPARATUS
a) comparative longitudinal; b) No. 36 B and S gage: (Cu-constantan), (chromel-alumel), (Pt 6% Rh - Pt 30% Rh) or No. 30 B and S gage Pt-Pt 10% Rh thermocouples/ingot Fe as reference; c) double-walled guard tube, $5 \times 10^{-5}$ mm ($7 \times 10^{-3}$ Pa) vacuum.

DATA
a) specimen 1: 116 to 293 K; b) Table 12 - λ.

ANALYSIS
a) results agree with Am. Mach. 82, pp. 869-80 (1938).

[22] Lucks, C. F., Thompson, H. B., Smith, A. R., Curry, F. P., Deem, H. W., and Bing, G. F., The Experimental Measurement of Thermal Conductivities, Specific Heats and Densities of Metallic, Transparent and Protective Materials. Part I., USAF TR 6145-1, 1-127 (1951) [ATI 117 715]

PURPOSE
To survey literature and make experimental determinations of λ, specific heat and densities of metallic, transparent and protective materials used in missiles and supersonic aircraft.

SPECIMEN
a) 15 cm long, 2 cm dia./rod; c) /hot rolled; d) 99.44%; g) SAE 1020 steel from U.S. Steel Corp.

APPARATUS
a) comparative longitudinal; b) Cu-constantan thermocouples/calibrated to ingot Fe standard on hot end of specimen; c) double guard tube, vacuum insulation.

DATA
a) 111 to 265 K; b) Table 12 - λ (experimental), Table 19 - λ (interpolated).

ANALYSIS
a) results agree with Armstrong, L. D., and Dauphinee, T. M., Can. J. Res., Sect. A, 25, (Nov 1947) pp. 357-74, Shelton, S. M., J. Res. Nat. Bur. Stand., 12 (RP 669), (Apr 1934) pp. 441-50, Hattori, D., Sci. Rep. Tohoku Imp. Univ., 26, (1937) pp. 190-205, and Kannuluik, W. G., Proc. Roy. Soc. London, 141 (1933) pp. 159-68.

[22A] Maurer, E., Heat Conductivity of Chrome Steels at High Temperatures, Arch. Eisenhüttenw, 10(4), 145-54 (1936)

PURPOSE

SPECIMEN II
a) 98.7%

APPARATUS
a) longitudinal

DATA
a) 300 to 970 K/data points taken from TPRC.

[22B] McDonald, W. J., Jr., The thermal and Electrical Conductivities of High Purity Iron at Low Temperatures, M.S. Thesis, Univ. of Texas, Austin, Tex. (1962)

PURPOSE
To report low temperature $\lambda$ and $\sigma$ for a sample of polycrystalline Fe.

SPECIMEN
a) 0.062 x 0.062 x 1/5 in. (0.16 x 0.16 x 3.8 cm)/bar; b) polycrystalline; c) zone refined/machined from ingot; g) Rengstorff and Goodwin, J. Met. 7, 647 (1955).

APPARATUS
a) longitudinal; b) Au-Co vs. manganin thermocouples/calibrated in place/ specimen leads anchored to exchange gas chamber; c) radiation shield, vacuum insulation.

DATA
a) 6 to 107 K; b) figure 6 - $\lambda$, figure 7 - $\rho$, figure 10 - L.

ANALYSIS
b) $W_L = W - \alpha T^{-1}$; $\lambda \sim T^3$ for $T < 10$ K.

[23] Mendelssohn, K. and Rosenberg, H. M., The Thermal Conductivity of Metals at Low Temperatures. II. The Transition Elements, Proc. Phys. Soc., London, Sect. A, 65, 388-94 (1952)

PURPOSE
To measure $\lambda$ for the transition elements from 2 to 40 K and determine their temperature dependences.

SPECIMEN
a) 5 cm long, 1-2 mm dia./rod; c) annealed; d) 99.99% Fe; g) source: Johnson Matthey.

APPARATUS
a) longitudinal; b) gas thermometers.

DATA
a) 2.3 to 32 K; b) figure 2 - $\lambda$; c) uncertainty: ±3% maximum.

ANALYSIS
b) $1/\lambda = \alpha T^2 + \beta/T$.

[24] Moak, D. P., Thermal Energy Storage Supporting Research, Final Tech. Rep. NASA-CR-80058 N67-12043, 1-300 (1966)

PURPOSE
To measure $\lambda$ of ingot Fe for comparative measurements of some potential thermal energy storage materials for spacecraft.

SPECIMEN
a) 0.75 in. (1.9 cm) dia., 5.00 in. (12.7 cm) long/rod; d) 99.9% Fe; g) source: Armco.

APPARATUS
a) longitudinal; b) chromel-alumel thermocouples; c) vacuum, guard shield and bubbled alumina insulation.

DATA
a) 107 to 280 K; b) Table G-8 - $\lambda$; c) uncertainty: ±5%.

ANALYSIS
a) results agree with previous measurements and with Powell, R. W., et al., Armco Iron as a Thermal Conductivity Standard, Review of Published Data, p. 454, ASME and Academic Press, New York (1962).

[25] Moore, J. P., McElroy, D. L., and Barisoni, M., Thermal Conductivity Measurements Between 78 and 340 K on Aluminum, Iron, Platinum and Tungsten, Sixth Thermal Conductivity Conference, Dayton, Ohio, (Oct 1966), Air Force Materials Lab., Wright-Patterson AFB, Ohio, pp. 737-78

PURPOSE
To make $\lambda$, $\rho$, and S measurements from 78 to 340 K for Al, W, Pt, Fe, and compare to theory of Makinson for electronic component.

SPECIMEN
e) RRR = 201; g) electron beam zone refined (3 passes), density = 7.824 g/cm$^3$, source: Materials Research Corp.

APPARATUS
a) longitudinal; b) chromel-$\rho$ vs. constantan thermocouples/from calibrated spools/tempered to guard cylinder; c) temperature controlled guard cylinder, Au plated 5 x $10^{-7}$ mm of Hg (7 x $10^{-5}$ Pa) vacuum.

DATA
a) 90 to 300 K; b) Table 5 - $\lambda$, $\rho$; c) uncertainty: ±1.8%.

ANALYSIS
a) results agree with Richter, U. F. and Kohlhaas, R., Z. Naturforsch., Teil A, 19, (1964) p. 1632, and Powell, R. W., Hickman, M. J., Tye, R. P., and Woodman, M. J., ASME (1962), pp. 466-73.

[26] National Physical Laboratory, The Thermal Conductivity of Iron, NPL, England, Report for 1964, Basic Physics Division, 128-30 (1965)

PURPOSE
To show that the results of Lucks, Deem (1958) are inconsistant with present and previous values at high temperatures.

SPECIMEN
a) 10.45 cm dia. with 1.27 cm dia. axial hole/disks; d) 99.97% Fe; g) source: N.P.L. Metallurgy Division.

APPARATUS
a) radial; b) thermocouple; c) 2 x $10^{-5}$ mm (3 x $10^{-3}$ Pa) vacuum insulation, end guards

DATA
a) 373 to 973 K; b) Table 2 - $\lambda$/data points listed in TPRC data series.

ANALYSIS
a) Powell, R. W., Proc. Phys. Soc., London, 51, 407 (1939), Lucks, C. F., and Deem, H. W., Am. Soc. Test. Mater., Spec. Tech. Publ. No. 227 (1958), Powell, R. W., Hickman, M. J., Tye, R. P., and Woodman, M. J., Progress in International Research on Thermodynamic and Transport Properties, Academic Press, 466 (1962), Laubitz, M. J., Can. J. Phys., 41, 1663 (1963).

[27] Powell, R. W., Armco Iron as a Thermal Conductivity Standard, ASME 2nd Symposium of Thermophysical Properties, 454-65 (1962)

PURPOSE
To review published data on ingot iron to determine if it is useful as a thermal conductivity standard.

DATA
a) -180 to 1320 °C (no new data).

ANALYSIS
Conclude that ingot iron is a good standard up to 800 °C. Above 800 °C data spread is large.

[28] Powell, R. W., Hickman, M. J., Tye, R. P., and Woodman, M. J., Armco Iron as a Thermal Conductivity Standard, 43 New Determinations at N.P.L., Progress in International Research on Thermodynamic and Transport Properties, ASME 2nd Symposium on Thermophysical Properties, 466-73 (1962)

PURPOSE
To report new measurements on $\lambda$ and $\rho$ for ingot iron, recommended values to 1000 °C for use as a standard

SPECIMEN
a) 10 cm long, 0.63 cm dia./rod; c) machined to specifications; d) 99.84%; g) source: Battelle Memorial Institute.

APPARATUS
a) absolute longitudinal; b) 42 SWG Ni-Cr and constantan thermocouples; c) radiation shield, insulating powder, vacuum insulation.

DATA
a) 73 to 1273 K; b) Table 4 - $\lambda$, $\rho$, L; d) heat dissipation in heater wire not connected to rod, heat transfer to or from connecting leads, radiated heat.

ANALYSIS
a) agrees with Lucks, C. F. and Deem, H. W., Am. Soc. Test. Mater., Spec. Tech. Publ. No. 227 (1958); b) recommended for thermal conductivity standard.

[29] Powers, R. W., Ziegler, J. B., and Johnston, H. L., The Thermal Conductivity of Metals and Alloys at Low Temperatures: II Data on Iron and Several Steels Between 25 and 300 K. Influence of Alloying Constituents, USAF TR 264-6, 20 pp. (1951) [ATI 105923]

PURPOSE
To provide $\lambda$ data on pure Fe and commercially important steels from 25 to 300 K.

SPECIMEN
a) specimens 1, 2: 20 in. (51 cm) long, 0.5 in. (1.3 cm) dia./rods; d) specimen 1: 99.99%, specimen 2: 99.5%; g) specimen 1: pure Iron, source: Johnston-MacKay, Ltd., specimen 2: SAE 1020, source: Carnegie Illinois Steel Corp.

APPARATUS
a) longitudinal; b) Cu-constantan thermocouples; c) double radiation shield, vacuum insulation

DATA
a) 26 to 300 K; b) Table 2 - specimen 1 - $\lambda$, Table 3 - specimen 2 - $\lambda$; c) uncertainty: ±1.9% at 30 K, ±1.1% at 100 K, ±1.0% at room temperature.

ANALYSIS
a) agrees with Armstrong, L. D. and Dauphinee, T. M., Can. J. Res., Sect. A, 25, 356 (1947), Powell, R. W., J. Iron Steel Inst., London, CLIV, No. 2, 105 (1946).

[30] Richter, F. and Kohlhaas, R., Thermal Conductivity of Pure Iron Between -180 and 1000 °C with Special Regard to Phase Transformations, Arch. Eisenhuettenwes., 30(11), 827-833 (1965)

PURPOSE
To describe a process for calculating the absolute value of $\lambda$ for T > 300 °C, and report measurements for $\lambda$ and $\rho$ for pure Fe from -180 to 1000 °C.

SPECIMEN
a) 10-30 mm thick, 63 mm dia./disk; c) vacuum melted; d) 99.94%.

APPARATUS
a) longitudinal; b) Fe-constantan thermocouples.

DATA
a) 93 to 973 K; b) Equations 2,3, Table 2 - $\lambda$, $\rho$, L; c) uncertainty: ±8.7%.

ANALYSIS
b) $\lambda = \alpha + \beta T^{-1}$ T > 400 K.

[31] Rosenberg, H. M., The Thermal Conductivity of Metals at Low Temperatures, Philos. Trans. Roy. Soc. London, Ser. A, 247, 441-97 (1955)

PURPOSE
To investigate and report on $\lambda$ for 32 metals in the 2-40 or 90 K range, and to measure $\rho$ so that the Wiedemann-Franz Law could be studied.

SPECIMEN
a) 2.89 cm long, 0.202 cm dia./rod; b) polycrystalline; c) annealed in vacuum for several hours; d) 99.78%; e) RRR = 63; g) source: Johnson-Matthey, Co.

APPARATUS
a) longitudinal; b) gas thermometers; c) vacuum insulation

DATA
a) run 2: 2.0 to 93 K; b) figure 29/ taken from TPRC data series; c) uncertainty: ±3%; d) correction made for external volume of gas thermometer.

ANALYSIS
a) previous measurements not in agreement with present results; previous measurements discarded; b) $1/\lambda = \alpha T^2 + \beta/T$.

[32] Silverman, L., Thermal Conductivity Data Presented for Various Metals and Alloys up to 900 °C, J. Met., 5, 631-2 (1953)

PURPOSE
To present thermal conductivity data between room temperature and 900 °C for various metals and alloys used in the electron tube industry.

SPECIMEN
a) dimensions not given/rod; c) annealed at 900 °C; d) 99.89%; g) source: Svea Iron.

APPARATUS
a) comparative longitudinal; b) thermocouples/Pb was the primary standard with advance (55 Cu-45 Ni) as the working standard; c) guard tube.

DATA
a) 50 to 900 °C,; b) Table 2 - $\lambda$; c) uncertainty: ±2%.

ANALYSIS
b) $\lambda$ decreases with temperature.

[32A] Touloukian, Y. S., Powell, R. W., Ho, C. Y., and Klemens, P. G., Thermophysical Properties of Matter, Volume 1: Thermal Conductivity, Metallic Elements and Alloys, 68-81 (1970)

PURPOSE
To provide an extensive list of data for $\lambda$ of the metallic elements and alloys.

SPECIMEN
d) 99.998%; f) $\rho_0 = 3.27 \times 10^{-8}$ $\Omega \cdot$cm.

APPARATUS
a) not given.

DATA
a) 0 to 6500 K; b) Figure and Table 24R-1 - $\lambda$, recommended values; c) uncertainty: ±3% near room temperature, ±3 to 8% at other temperatures; e) the values below 1.5 Tm are calculated to fit the experimental data by using n = 2.10, a = 0.37, m = 2.47, $\alpha'' = 2.05 \times 10^{-5}$, and $\beta = 1.34$.

[33] Vuillermoz, P. L. and Pinard, P., Conductibilite Thermique du fer a basse temperature, C. R. Acad. Sci., Ser. B Paris, 277, 493-5 (1973)

PURPOSE
To test the accuracy of an apparatus designed to measure the thermal conductivity of small samples of semiconductors.

SPECIMEN
a) specimens 1, 2: 8.9 x 3.74 x 4.44 mm, specimen 3: 10.78 x 3.04 x 2.96 mm/bars; b) polycrystalline; c) specimen 1: annealed for 30 min at 870 °C, again for 90 min at 875 °C in vacuum, and 24 h at 150 °C in vacuum, specimens 2, 3: no anneal; d) specimen 3: 99.78%; g) specimens 1, 2: Armco.

APPARATUS
a) longitudinal.

DATA
a) 4 to 210 K; b) Fig. 1 - $\lambda$; c) uncertainty: ±6%.

ANALYSIS
a) Hust, J. G., Nat. Bur. Stand. Rep., private communication; b) conclude that the apparatus is sufficiently precise.

[34] Watson, T. W., Flynn, D. R., Robinson, H. E., Thermal Conductivity and Electrical Resistivity of Armco Iron, J. Res. Nat. Bur. Stand., Sect. C, 71(4), 285-91 (1967)

PURPOSE
To present $\lambda$ and $\rho$ data on samples of Armco Iron.

SPECIMEN
a) specimen 1: 37 cm long, 2.386 cm dia./rod; c) specimen 1: annealed for 1/2 h at 870 °C/specimen 2: cold worked; d) specimens 1 and 2: 99.67%; g) specimen 1 source: Battelle round-robin program, specimen 2 source: Redstone Arsenal.

APPARATUS
a) longitudinal; b) chromel P-alumel/calibrated at NBS; c) heat shield, diatomaceous earth insulation.

DATA
a) specimen 1: -160 to 640 °C, specimen 2: -150 to 200 °C; b) specimen 1: Table 2 - $\lambda$, $\rho$, L, specimen 2: Table 3 - $\lambda$, $\rho$, L; c) corrections for heat exchange with surroundings.

ANALYSIS
b) expected specimen 2 to have greater $\lambda$ values, lower $\rho$ values, but found the opposite to be true.

[35] Watson, T. W., Robinson, H. E., Thermal Conductivity of Some Commercial Iron-Nickel Alloys, J. Heat Transfer, 83, 403-8 (1961)

PURPOSE
To present $\lambda$ data for some Fe-Ni alloys from -150 to 540 °C.

SPECIMEN
a) 37 cm long, 2.54 cm dia./rod; d) 99.15%; g) AISI 1015 steel supplied by International Nickel Co.

APPARATUS
a) longitudinal; b) chromel-alumel thermocouples; c) radiation shield, diatomaceous earth insulation

DATA
a) -150 to 540 °C; b) Table 2 - $\lambda$.

ANALYSIS
a) agrees with Shelton, S. M., J. Res. Nat. Bur. Stand., 12(4), RP 669 (1934), Powell, R. W., Research, (London), 7(12) (1954), Powell, R. L. and Blanpied, W. A., Nat. Bur. Stand. (U.S.), Circ. No. 556 (1954).

[36] Wilkes, K. E., Thermal Conductivity Measurements between 77 K and 373 K on Iron, Cobalt, Aluminum, and Zinc, M.S. Thesis, Purdue Univ. (1968)

PURPOSE
To measure pure Fe as a check on the accuracy of apparatus.

SPECIMEN
a) 10.44 cm long, 1.247 cm dia./rod; d) 99.96%; e) RRR = 36.4; g) density: 7.879 g/cm.

APPARATUS
a) longitudinal; b) chromel-constantan thermocouples/calibrated against Pt resistance thermometer; c) vacuum insulation.

DATA
a) 82 to 372 K; b) Table 2 - $\lambda$, $\rho$; c) uncertainty: ±1.6%; d) radiation, gas conduction corrections.

ANALYSIS
a) agrees with Moore, J. P., McElroy, D. L., and Barisoni, K., Sixth Conf. on Thermal Conductivity, 737 (1966), Richter, Kohlhaas (1964).

# 5. Tungsten

## 5.1 General

The annotated bibliography for tungsten (Section 5.5) includes 39 references. The following data sets were selected as primary data: 4A, 26A, 11, 14, 20, 21, 22, 23, 25, 27, 29, 32, and 33.

The primary data ranges in temperature from 2 to 3000 K, and in RRR from 30 to 170. The primary data are shown in Figs. 5.1.1 through 5.1.4. As for the other metals, the data are divided into groups of seven and the last figure shows a composite of all data.

Because high purity, single crystal tungsten specimens exhibit unusual behavior at the lowest temperatures; these data are not included in the primary data set. As a consequence, the range of RRR included in the fit of the data is more restricted than the total range of data.

Equation 1.1.3 was fitted to the primary data over the entire range of temperatures. The values of the parameters, $P_i$, i = 1, 2, ... 7, obtained by nonlinear least squares fit are

$P_1 = 31.70 \times 10^{-8}$ $\quad$ $P_5 = 69.94$

$P_2 = 2.29$ $\quad$ $P_6 = 3.557$

$P_3 = 541.3$ $\quad$ $P_7 = 0.0$

$P_4 = -0.22$

with all units in SI.

The systematic residuals from this equation were then represented by the $W_c$ term in Eq. 1.1.5. The result is

$$W_c = -0.00085\ \ell n(T/130)\ \exp(-(\ell n(T/230)/0.7)^2)$$

$$+\ 0.00015\ \exp(-(\ell n(T/3500)/0.8)^2)$$

$$+\ 0.0006\ \ell n(T/90)\ \exp(-(\ell n(T/80)/0.4)^2)$$

$$+\ 0.0003\ \ell n(T/24)\ \exp(-(\ell n(T/33)/0.5)^2)$$

where $W_c$ and T are in SI units.

5.2 Deviations From Recommended Equation

The deviations of the primary data from Eq. 1.1.3 with these parameters are illustrated in Figs. 5.2.1 through 5.2.4. No deviations exhibit differences greater than $\pm$7%. Although there are systematic trends with respect to temperature, the overall pattern is random in nature. No systematic trends varying with RRR were identified.

The primary data were selected from the literature data on relatively large, well annealed specimens. Therefore, the deviations exhibited in Figs. 5.2.1 through 5.2.4 are indicative of the combined effect of a) experimental measurement errors and b) the inability of Eq. 1.1.3 to account for the effects of chemical impurity variations. The effects of physical defect variations, small specimen size variations, and magnetic fields are exhibited, in part, by the deviations of the secondary data. The thermal conductivity variations caused by other than chemical impurity variations are not expected to be represented as well by Eq. 1.1.3. However, the RRR (or $\rho_0$) correlating parameter does account for an appreciable part of these variations. Some users may find this to be an adequate representation and, therefore, discussions of these comparisons are included for completeness.

The deviations of the secondary data sets are illustrated in Figs. 5.2.5 through 5.2.10. These data are divided into two subgroups according to the magnitude of the deviations. The composite plots for each group are 5.2.7 and 5.2.10, respectively.

Again it was of interest to compare this equation to existing reference data. The deviations of these data are illustrated in Fig. 5.2.11. The data from reference 15 are for Standard Reference Material (designated as SRM 730) at values of RRR = 50, 75, and 100. The reference data from references 12A,27A are for an RRR of 2850 and therefore represent an extrapolation of the equation as given here. Note that the differences in deviations between references 12A and 27A are about 30% between 10 and 20 K. The differences otherwise are within the combined uncertainties of the reference data.

5.2.1 Physical Defect Effects

Investigations of physical defects in tungsten have produced some interesting references 3, 14, 22. Each of these references will be discussed below.

Reference 14 reports on the effects of annealing NBS sintered tungsten. The peak conductivity for the unannealed condition was 399 $W \cdot m^{-1} \cdot K^{-1}$, while annealing produced a peak value of 635 $W \cdot m^{-1} \cdot K^{-1}$. The deviations from Eq. 1.1.3 for both conditions were within $\pm$3%.

Reference 3 shows the effects of surface condition on thermal conductivity. A polished specimen was measured to have a conductivity of 23000 $W \cdot m^{-1} \cdot K^{-1}$ at 2 K and 33000 $W \cdot m^{-1} \cdot K^{-1}$ at 4 K. The specimen was then etched, and the resulting measurements were 25000 $W \cdot m^{-1} \cdot K^{-1}$ (at 2 K) and 35000 $W \cdot m^{-1} \cdot K^{-1}$ (at 4 K). The specimen was repolished and measured to have conductivities of 30000 $W \cdot m^{-1} \cdot K^{-1}$ at 2 K, 40000 $W \cdot m^{-1} \cdot K^{-1}$ at 4 K. The specimen was then sandblasted, and the conductivities were found to be 33000 $W \cdot m^{-1} \cdot K^{-1}$ at 2 K, 42000 $W \cdot m^{-1} \cdot K^{-1}$ at 4 K. Notice that the repolished specimen gave conductivities that were

comparable to the original condition, indicating that surface condition is approximately reversible.

Although not directly related to physical defects, reference 22 describes the effects of purity on thermal conductivity. Three specimens were involved: a high purity specimen, a "radial" specimen (99.8% W) and a W + 2% Ta specimen. The maximum decrease of 10% occurs at 90 K between the high purity and "radial" specimens. The W + 2 Ta specimen's conductivity was lowered by a factor of two at 90 K relative to the high purity specimen. The deviations from Eq. 1.1.3 for the high purity specimen were within $\pm$6%, while the "radial" specimen deviations were within $\pm$2%. The W + 2 Ta specimen was not compared to Eq. 1.1.3 because of our requirement that specimens must have less than 1% total impurities.

Although the temperature dependence of the physical defect scattering mechanism is different from that due to impurity scattering, Eq. 1.1.3 represents the unannealed specimen data quite well ($\pm$5%). This indicates that the residual electrical resistivity characterizes both types of scattering for the range of RRR included here.

### 5.2.2 Size Effects

In reference 31, the authors demonstrate that specimen size can cause a noticeable change in thermal conductivity values. For a specimen of 3.0 mm diameter (specimen W-7) the peak conductivity was 73000 $W \cdot m^{-1} \cdot K^{-1}$, while for one of 1.5 mm (W-5) the corresponding value was 36000 $W \cdot m^{-1} \cdot K^{-1}$. For a 1.0 mm diameter specimen (W-4) the value decreased to 15000 $W \cdot m^{-1} \cdot K^{-1}$. There is a definite correlation between thermal conductivity and specimen size. The deviations from Eq. 1.1.3 of the 3.0 mm specimen were within $\pm$28%, those for the 1.5 mm diameter specimen were within $\pm$4%. The deviations for the 1.0 mm diameter specimen were within $\pm$12%.

Reference 4 shows a similar effect. For a 3.2 mm diameter specimen, the peak conductivity was 86000 $W \cdot m^{-1} \cdot K^{-1}$, while for a 1.4 mm diameter specimen, the value was 58000 $W \cdot m^{-1} \cdot K^{-1}$. For a 0.8 mm diameter specimen, the peak value was 42000 $W \cdot m^{-1} \cdot K^{-1}$. The deviations from Eq. 1.1.3 of the 3.2 mm specimen were within $\pm$50%, while those for the 1.4 mm diameter specimen were within $\pm$48%. The deviations for the 0.8 mm diameter specimen were within $\pm$36%.

The maximum deviations indicated above have some common characteristics. They are all positive, which implies that the calculated value of Eq. 1.1.3 is much too small. The temperature range in which these deviations occur is between 5 and 25 K.

### 5.2.3 Magnetic Field Effects

Although magnetic field effects on thermal conductivity were not explicitly studied, reference 8 shows that an increase in the field decreases the specimen conductivity. For a zero field at 15 K, the conductivity was 8500 $W \cdot m^{-1} \cdot K^{-1}$, while for a field of 2.58 T, the value at 15 K was 61 $W \cdot m^{-1} \cdot K^{-1}$. The authors note that the field dependence increases towards lower temperatures. Reference 9 extends these measurements to higher magnetic fields. The conductivity of the specimen field at 15 K in a field of 3.64 T was 38 $W \cdot m^{-1} \cdot K^{-1}$.

Reference 30 also showed that there is a decrease in longitudinal magnetoresistance with increasing magnetic fields. The author states that for a field of 1.3 T, the resistance at 4 K had increased by five orders of magnitude relative to its value in a zero field. Thermal conductivity values were reported for specimens in the zero field. Reference 4 confirms that there are five orders of magnitude difference between a zero and a 2.3 T field.

## 5.3 Electrical Resistivity and Lorenz Ratio

During this investigation, it was frequently helpful to examine the Lorenz ratio as a function of RRR and temperature. For this reason it was necessary to obtain an approximation of the electrical resistivity as a function of temperature and RRR. For this approximation, we selected those data sources from the primary data that also contained electrical resistivity data. The data used is illustrated in Figs. 5.3.1 through 5.3.3. Figure 5.3.3 is a composite for all of the electrical resistivity data. These data were represented via a nonlinear least squares fit of Eq. 1.2.3. The resulting parameters are

$P_1 = 4.801 \times 10^{-16}$ $\qquad$ $P_5 = 55.63$

$P_2 = 3.839$ $\qquad$ $P_6 = 2.391$

$P_3 = 1.88 \times 10^{10}$ $\qquad$ $P = 0.0$

$P_4 = 1.22$

where all units are SI.

The systematic residuals from this equation were subsequently represented by the $\rho_c$ term in Eq. 1.2.4 as follows:

$$\rho_c = 0.7 \times 10^{-8} \, \ell n(T/560) \, \exp(-(\ell n(T/1000)/0.6)^2)$$

The deviations of the experimental data from this equation are illustrated in Figs. 5.3.4 through 5.3.6. Smooth curves are calculated and plotted in Fig. 5.3.7 at RRR values of 30, 100, and 300. From the $\lambda(T,RRR)$ and $\rho(T,RRR)$ equations, values of $L(T,RRR)$ were calculated at the same RRR values and are plotted in Fig. 5.3.8. No unusual behavior in this plot is observed.

In Section 1.5 we discuss the procedure for selecting values of $\rho_0$ and calculating RRR for each thermal conductivity data set. These values of $\rho_0$ along with the Sommerfeld value of Lorenz ratio were used to best fit each low

temperature data set. The resulting values of RRR obtained by this procedure are compared to the values reported in the references in Fig. 5.3.9 and are listed in Table 5.3.1. Figure 5.3.9 shows values of RRR (calc), those values from the above procedure, versus RRR (obs), those values reported in the references listed in the annotated bibliography. Also shown in the figure is the line that represents RRR (calc) = RRR (obs). Systematic deviations from this line indicate ranges in which the derived Eq. 1.1.3 is invalid. The primary data for tungsten extend only from 30 to 400 in RRR. These values agree to within 10%. The secondary data at RRR near 60,000 disagree from the line by as much as 30%. Equation 1.1.3 is considered valid only from 30 to 400. In this range it appears that the Sommerfeld value is valid for the Lorenz ratio of tungsten.

## 5.4 Summary for Tungsten

Equation 1.1.3 represents the primary tungsten data to within $\pm$10% of the experimental value at a given temperature. Deviations for unannealed specimens (i.e., those containing physical defects) are also in this range.

Based on the observed deviations of the primary data set, the uncertainty of the recommended values is as follows. The uncertainty of the low temperature $\lambda$ values is estimated to be $\pm$10% for RRR values from 30 to 300. At RRR values outside this range, the uncertainty is larger. At temperatures above 200 K, the uncertainty is smaller ($\pm$5%) and is expected to be valid for much larger RRR values.

Equation 1.1.3, with the parameters listed, was used to calculate thermal conductivity values for selected temperatures and RRR. These values are listed in Table 5.4.1 and plotted in Fig. 5.4.1.

List of Tables and Figures for Tungsten

Tables


| | | Page |
|---|---|---|
| Table 5.3.1 | Comparison of Calculated and Observed RRR Values for Tungsten . . . . . | 208 |
| Table 5.4.1 | Thermal Conductivity Values for Tungsten Calculated From Eq. 1.1.3 at Selected Temperatures and RRR Values . . . . . | 209 |


Figures


| | | Page |
|---|---|---|
| Figure 5.1.1 | Experimental thermal conductivity data selected from the following primary references in the tungsten annotated bibliography: (4A,11,14,20,22) . . . . . | 210 |
| Figure 5.1.2 | Experimental thermal conductivity data selected from the following primary references in the tungsten annotated bibliography: (4A,21,22,23,25,26A) . . . . . | 211 |
| Figure 5.1.3 | Experimental thermal conductivity data selected from the following primary references in the tungsten annotated bibliography: (27,29,32,33) . . . . . | 212 |
| Figure 5.1.4 | Composite of the data in figures 5.1.1 through 5.1.3 . . . | 213 |
| Figure 5.2.1 | Thermal conductivity deviations of the tungsten data from the following primary references compared to Eq. 1.1.3: (4A,11,14,20,22) . . . . . | 214 |
| Figure 5.2.2 | Thermal conductivity deviations of the tungsten data from the following primary references compared to Eq. 1.1.3: (4A,21,22,23,25,26A) . . . . . | 215 |
| Figure 5.2.3 | Thermal conductivity deviations of the tungsten data from the following primary references compared to Eq. 1.1.3: (27,29,32,33) . . . . . | 216 |
| Figure 5.2.4 | Composite of the deviations in figures 5.2.1 through 5.2.3 . . . . . | 217 |
| Figure 5.2.5 | Thermal conductivity deviations of the tungsten data from the following secondary references compared to Eq. 1.1.3: (1,2,5,7,8,10) . . . . . | 218 |
| Figure 5.2.6 | Thermal conductivity deviations of the tungsten data from the following secondary references compared to Eq. 1.1.3: (10,13,16,19,26) . . . . . | 219 |

| | | Page |
|---|---|---|
| Figure 5.2.7 | Composite of the deviations in figures 5.2.5 and 5.2.6 . . | 220 |
| Figure 5.2.8 | Thermal conductivity deviations of the tungsten data from the following secondary references compared to Eq. 1.1.3: (3,4,4B,11,28) . . . . . | 221 |
| Figure 5.2.9 | Thermal conductivity deviations of the tungsten data from the following secondary reference compared to Eq. 1.1.3: (31) . . . . . | 222 |
| Figure 5.2.10 | Composite of the deviations in figures 5.2.8 and 5.2.9 . . | 223 |
| Figure 5.2.11 | Comparison of Eq. 1.1.3 to the values recommended for tungsten in the following references: (12A,15,27A) . . . | 224 |
| Figure 5.3.1 | Experimental resistivity data for tungsten selected from the following references in the tungsten annotated bibliography: (5A,11,14,22) . . . . . | 225 |
| Figure 5.3.2 | Experimental electrical resistivity data for tungsten selected from the following references in the tungsten annotated bibliography: (4A,21,23,25,26A,33) . . . . . | 226 |
| Figure 5.3.3 | Composite of the electrical resistivity data in figures 5.3.1 and 5.3.2 . . . . . | 227 |
| Figure 5.3.4 | Electrical resistivity deviations of the tungsten data from the following references compared to Eq. 1.2.3: (5A,11,14,22) . . . . . | 228 |
| Figure 5.3.5 | Electrical resistivity deviations of the tungsten data from the following references compared to Eq. 1.2.3: (4A,21,23,25,26A,33) . . . . . | 229 |
| Figure 5.3.6 | Composite of the electrical resistivity deviations shown in figures 5.3.4 and 5.3.5 . . . . . | 230 |
| Figure 5.3.7 | Electrical resistivity for tungsten as a function of temperature calculated from Eq. 1.2.3 at selected values of RRR . . . . . | 231 |
| Figure 5.3.8 | Lorenz ratio for tungsten as a function of temperature calculated from Eq. 1.2.3 and Eq. 1.1.3 at selected values of RRR . . . . . | 232 |
| Figure 5.3.9 | RRR values calculated as per Section 1.5, RRR(CALC), versus reported RRR values, RRR(OBS), for tungsten . . . . | 233 |
| Figure 5.4.1 | Thermal conductivity for tungsten as a function of temperature calculated from Eq. 1.1.3 at selected values of RRR . . . . . | 234 |

Table 5.3.1. Comparison of Calculated and Observed RRR Values for Tungsten.

| Reference | RRR (obs.) | RRR (calc.) |
|---|---|---|
| | Primary Data | |
| 4A | 70.0 | 70.0 |
| 4A | 75.4 | 75.4 |
| 4A | 131.0 | 131.0 |
| 11 | 75.0 | 75.0 |
| 14 | 39.8 | 40.8 |
| 14 | 74.6 | 77.6 |
| 22 | 31.4 | 30.0 |
| 22 | 400.0 | 400.0 |
| 25 | 150.0 | 150.0 |
| 26A | 75.0 | 75.0 |
| 29 | 46.6 | 46.6 |
| 33 | 155.0 | 155.0 |
| | Secondary Data | |
| 3 | 40300.0 | 30000.0 |
| 4 | 96000.0 | 86000.0 |
| 7 | 2780.0 | 4850.0 |
| 11 | 75.0 | 75.0 |
| 28 | 16300.0 | 16300.0 |
| 31 | 8460.0 | 8400.0 |
| 31 | 27200.0 | 26000.0 |
| 31 | 39300.0 | 36500.0 |
| 31 | 69600.0 | 56500.0 |
| 31 | 85500.0 | 71000.0 |

Table 5.4.1. Thermal Conductivity Values for Tungsten Calculated from Eq. 1.1.3 at Selected Temperatures and RRR Values.

| T (K) | $\lambda$ (W·m$^{-1}$·K$^{-1}$) RRR = 30 | RRR = 100 | RRR = 300 |
|---|---|---|---|
| 1 | 14.6 | 50 | 151 |
| 2 | 29 | 100 | 302 |
| 3 | 44 | 150 | 452 |
| 4 | 59 | 200 | 602 |
| 5 | 73 | 249 | 749 |
| 6 | 88 | 299 | 894 |
| 7 | 102 | 347 | 1033 |
| 8 | 117 | 395 | 1166 |
| 9 | 131 | 442 | 1291 |
| 10 | 145 | 488 | 1404 |
| 12 | 173 | 574 | 1595 |
| 14 | 201 | 651 | 1730 |
| 16 | 227 | 718 | 1802 |
| 18 | 251 | 768 | 1803 |
| 20 | 273 | 799 | 1734 |
| 25 | 311 | 786 | 1378 |
| 30 | 325 | 692 | 1020 |
| 35 | 321 | 586 | 768 |
| 40 | 306 | 494 | 600 |
| 45 | 285 | 418 | 483 |
| 50 | 262 | 357 | 398 |
| 60 | 226 | 281 | 302 |
| 70 | 211 | 250 | 264 |
| 80 | 204 | 236 | 246 |
| 90 | 199 | 225 | 234 |
| 100 | 195 | 217 | 224 |
| 150 | 184 | 197 | 201 |
| 200 | 180 | 189 | 191 |
| 250 | 175 | 182 | 184 |
| 300 | 169 | 174 | 176 |
| 400 | 155 | 158 | 159 |
| 500 | 143 | 145 | 146 |
| 600 | 135 | 136 | 137 |
| 700 | 129 | 130 | 130 |
| 800 | 124 | 125 | 126 |
| 900 | 121 | 122 | 122 |
| 1000 | 118 | 119 | 119 |
| 1100 | 115 | 116 | 116 |
| 1200 | 113 | 114 | 114 |
| 1300 | 111 | 111 | 112 |
| 1400 | 109 | 110 | 110 |
| 1500 | 107 | 108 | 108 |
| 1600 | 106 | 106 | 106 |
| 1800 | 103 | 103 | 103 |
| 2000 | 100 | 101 | 101 |
| 2200 | 98 | 99 | 99 |
| 2400 | 96 | 97 | 97 |
| 2600 | 95 | 95 | 95 |
| 2800 | 93 | 93 | 93 |
| 3000 | 92 | 92 | 92 |

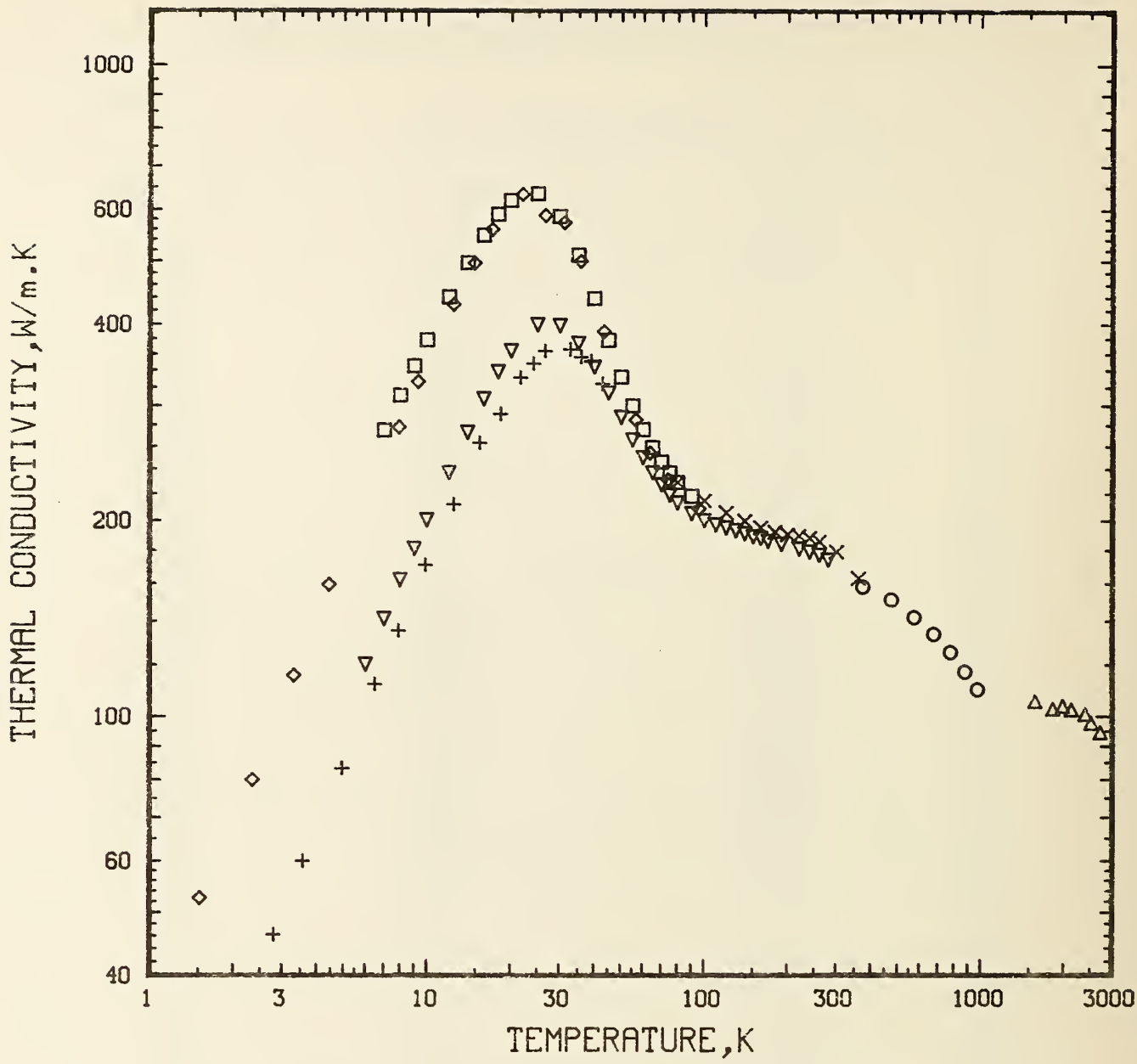


Figure 5.1.1 Experimental thermal conductivity data selected from the following primary references in the tungsten annotated bibliography:(4A,11,14,20,22)

○ - (11), △ - (11), □ - (14), ▽ - (14),
◇ - (4A), + - (20), × - (22)

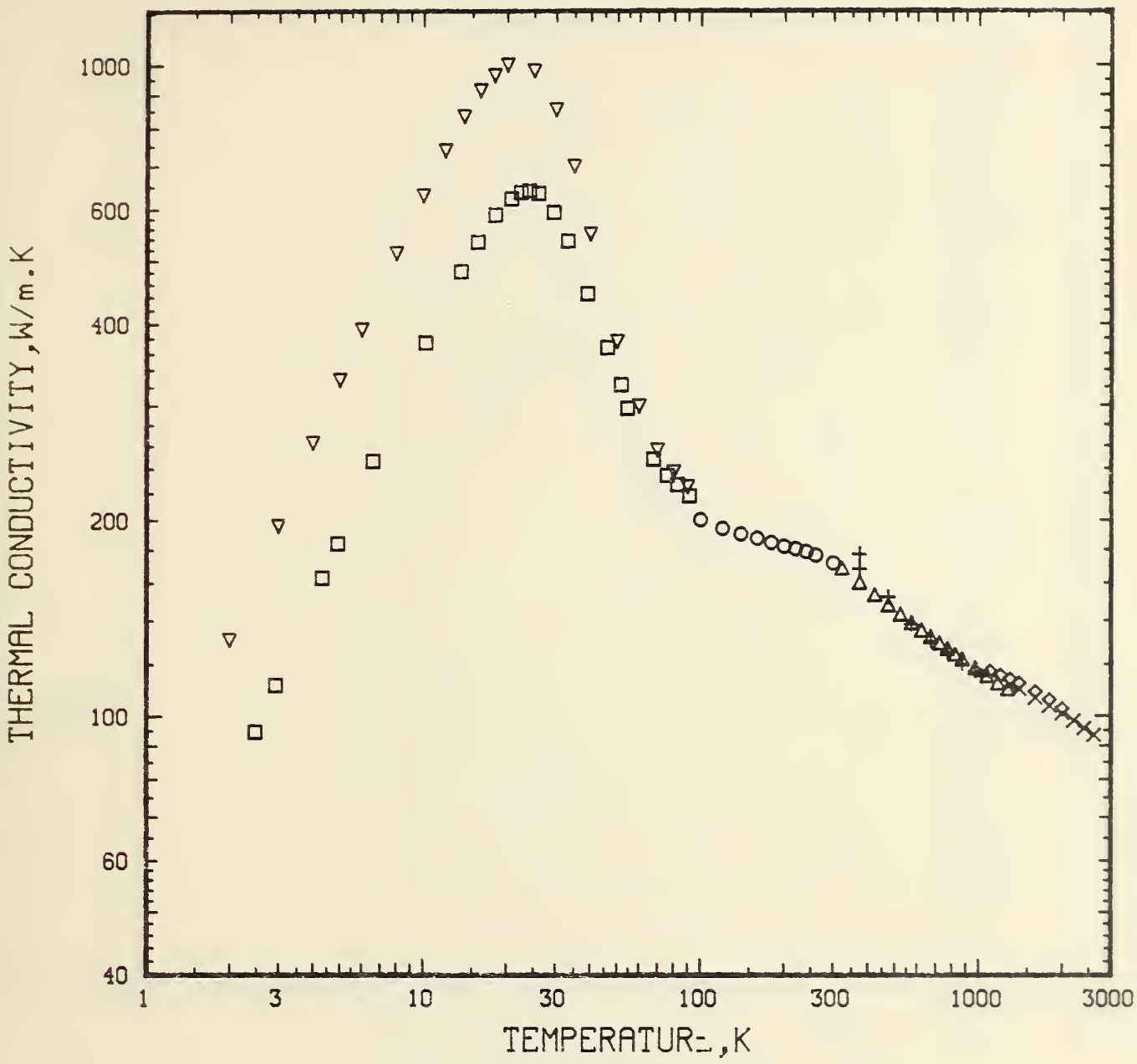


Figure 5.1.2 Experimental thermal conductivity data selected from the following primary references in the tungsten annotated bibliography:(4A,21,22,23,25,26A)

○ - (22), △ - (21), □ - (4A), ▽ - (4A),
◇ - (23), + - (25), × - (26A)

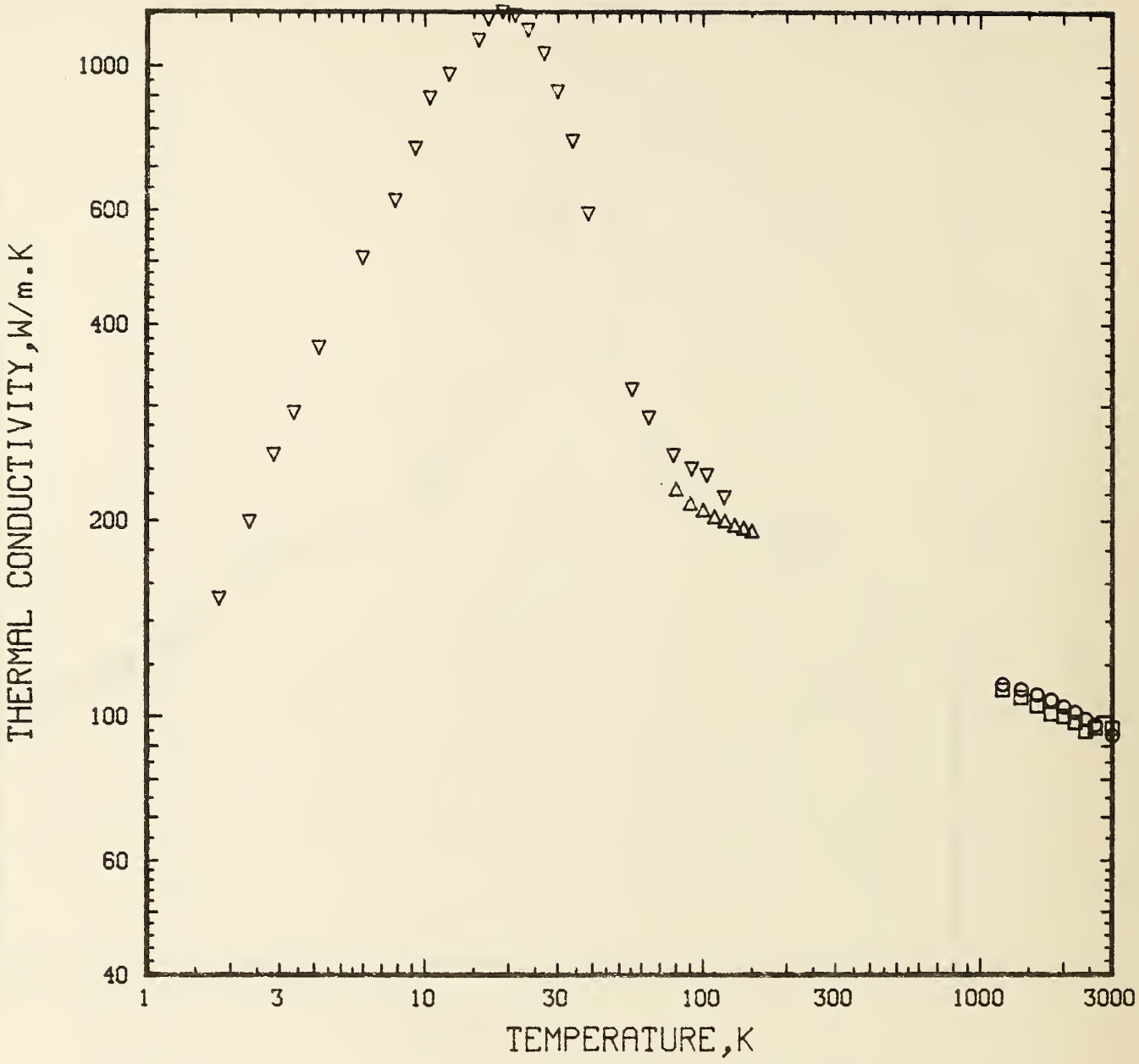


Figure 5.1.3 Experimental thermal conductivity data selected from the following primary references in the tungsten annotated bibliography:(27,29,32,33)

O - (27), Δ - (29), □ - (32), ∇ - (33)

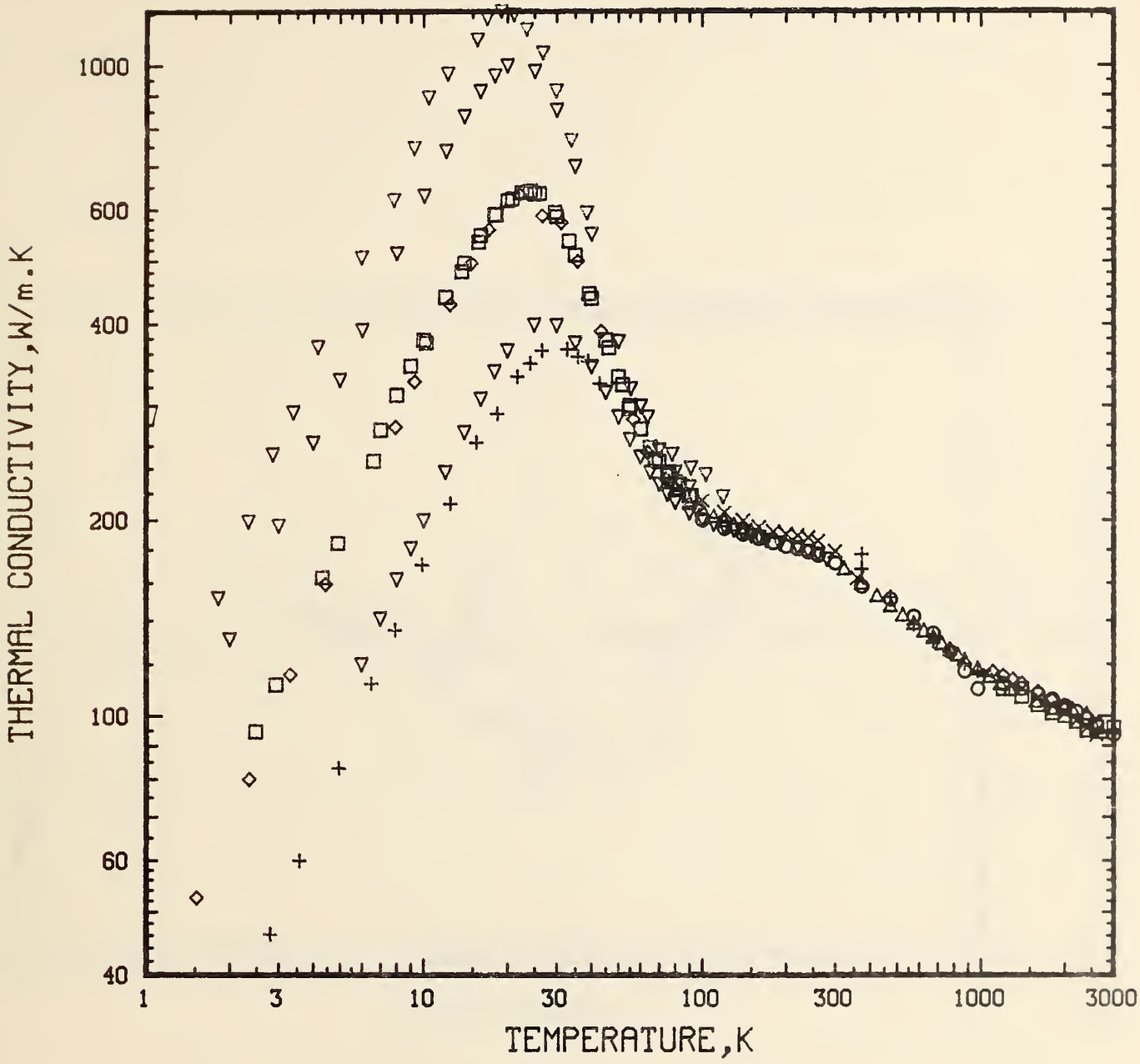


Figure 5.1.4 Composite of the data in figs. 5.1.1 through 5.1.3

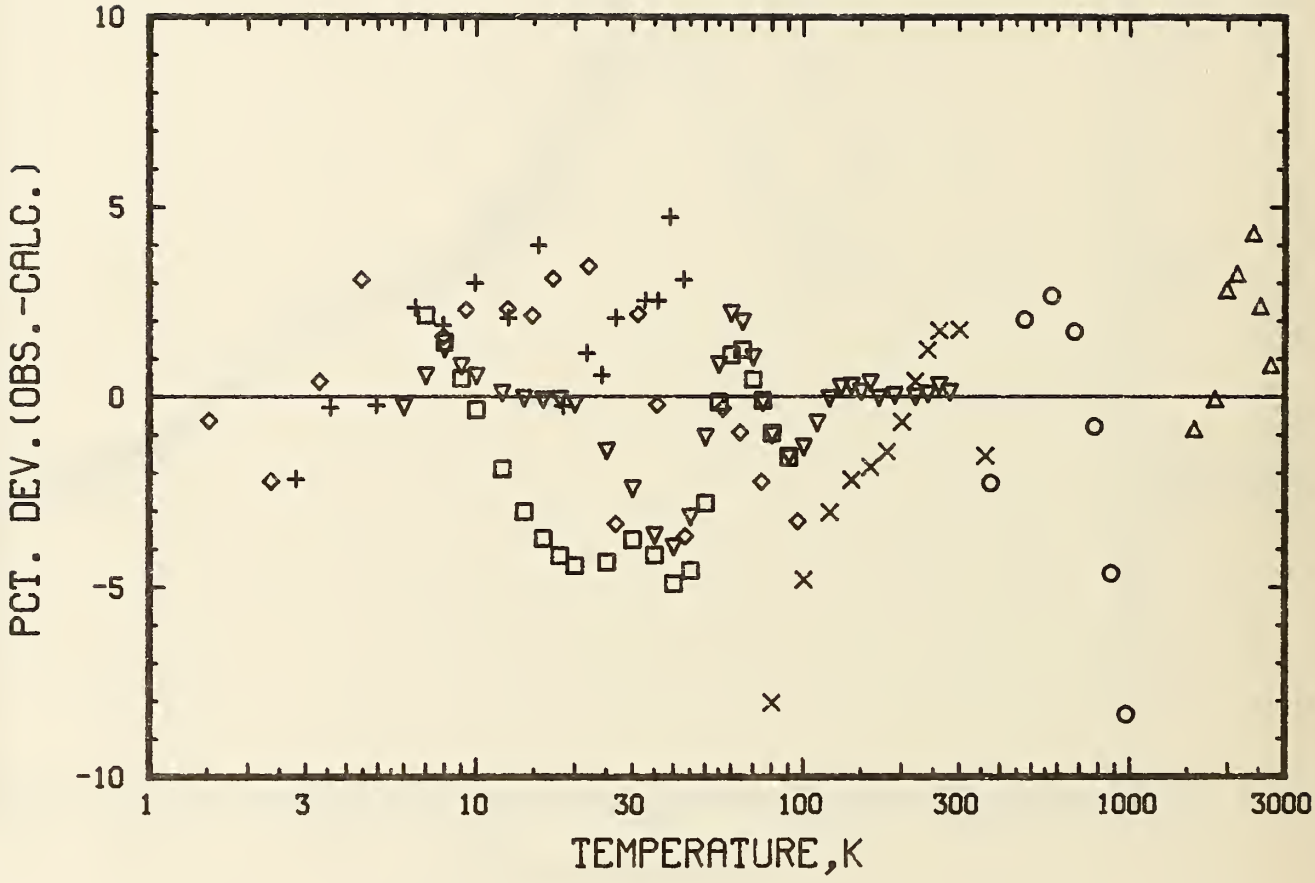


Figure 5.2.1 Thermal conductivity deviations of the tungsten data from the following primary references compared to eq. (1.1.3): (4A,11,14,20,22)

○ - (11), △ - (11), □ - (14), ▽ - (14),
◇ - (4A), + - (20), × - (22)

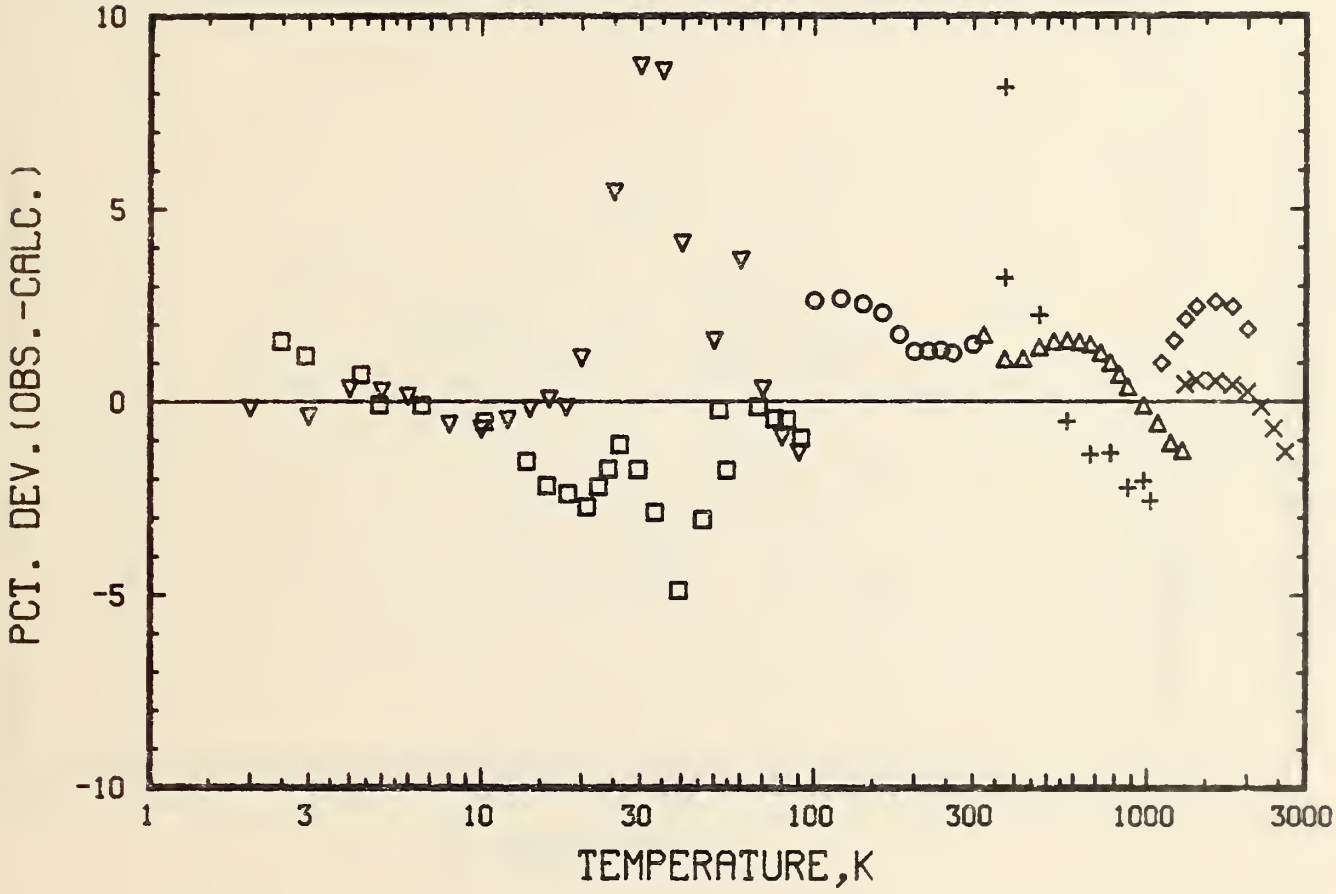


Figure 5.2.2 Thermal conductivity deviations of the tungsten data from the following primary references compared to eq. (1.1.3): (4A,21,22,23,25,26A)

○ - (22), △ - (21), □ - (4A), ▽ - (4A),
◇ - (23), + - (25), × - (26A)

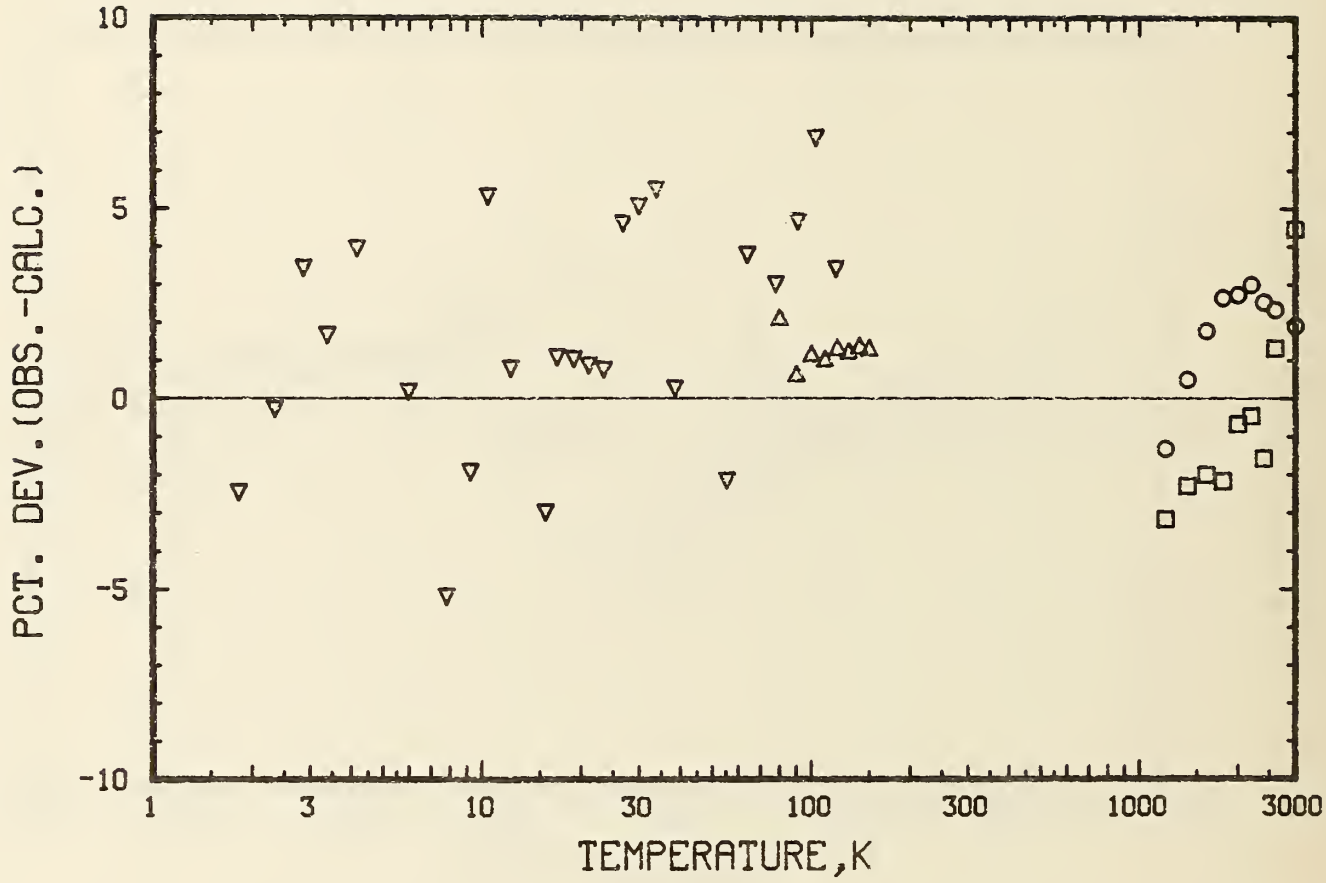


Figure 5.2.3 Thermal conductivity deviations of the tungsten data from the following primary references compared to eq. (1.1.3): (27,29,32,33)

○ - (27), △ - (29), □ - (32), ▽ - (33)

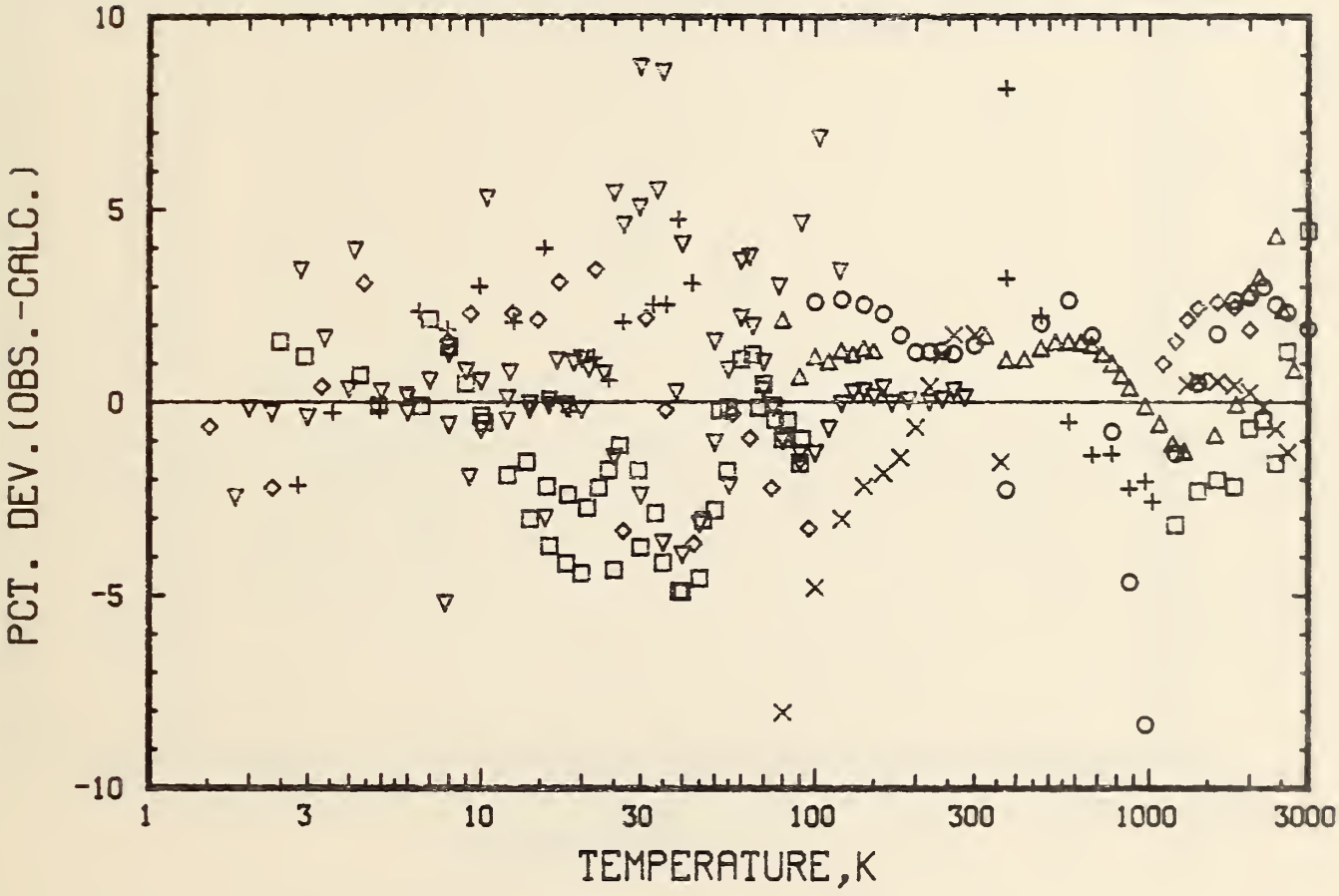


Figure 5.2.4 Composite of the deviations in figs. 5.2.1 through 5.2.3

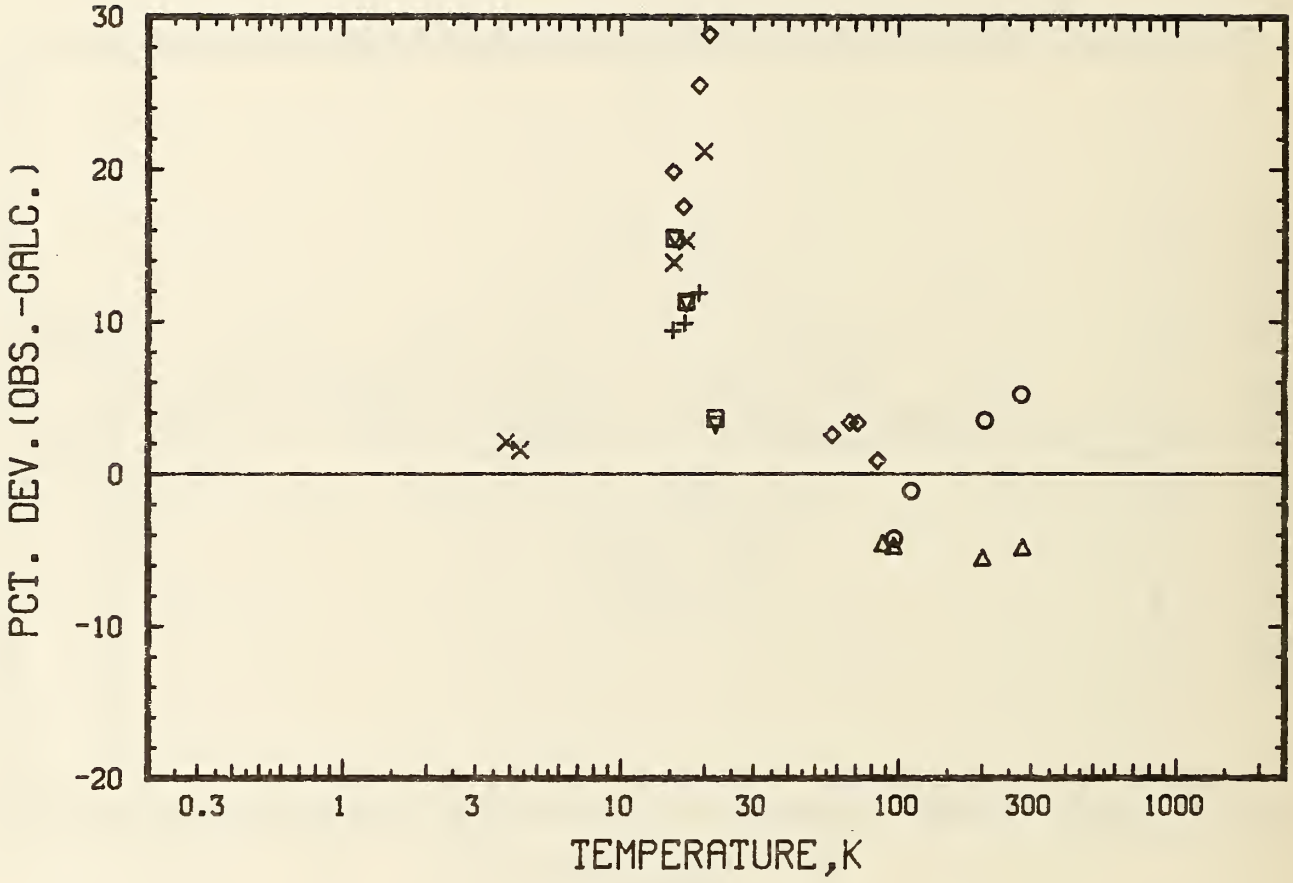


Figure 5.2.5 Thermal conductivity deviations of the tungsten data from the following secondary references compared to eq. (1.1.3):(1,2,5,7,8,10)

○ - (1), △ - (2), □ - (5), ▽ - (7),
◇ - (8), + - (10), × - (10)

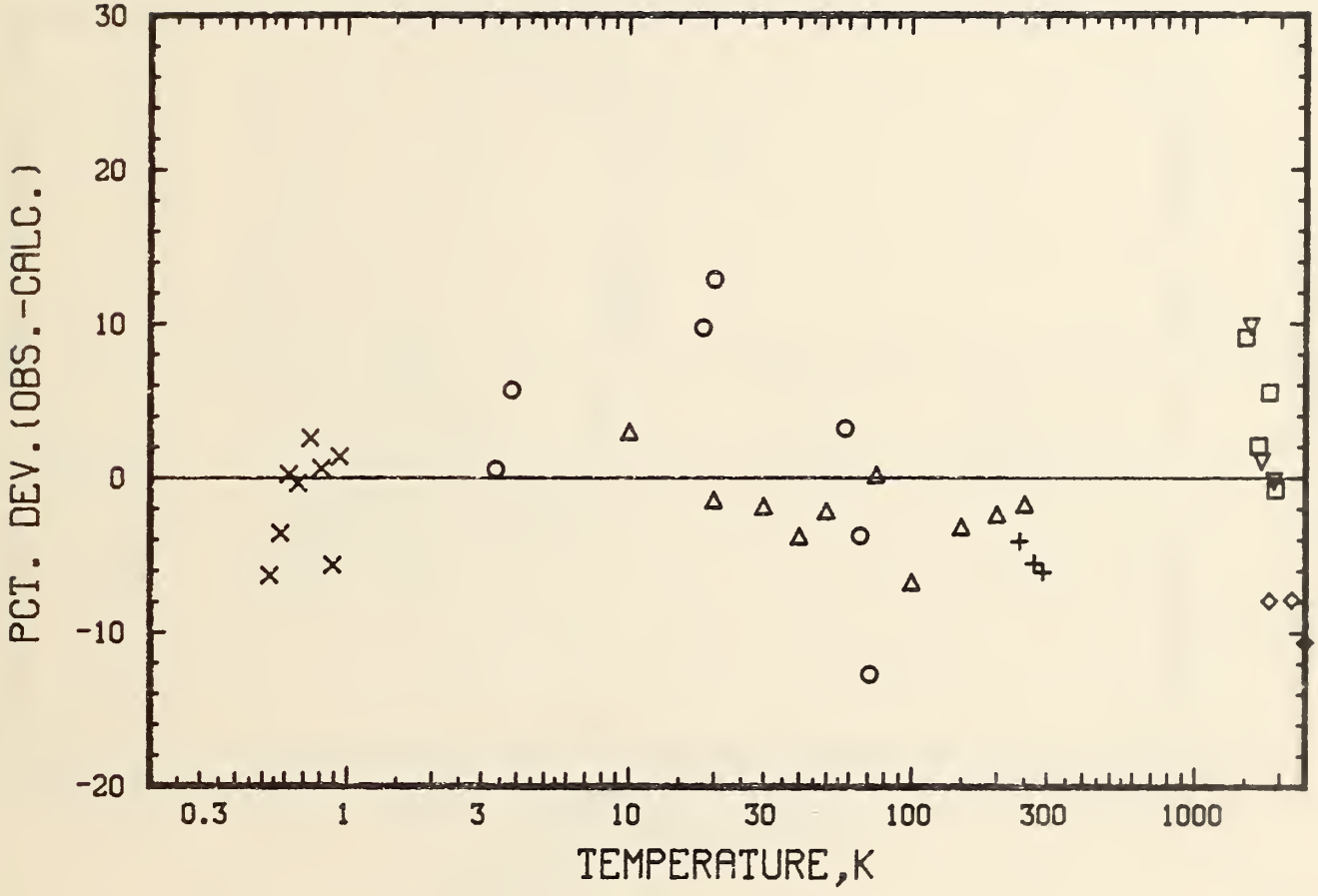


Figure 5.2.6 Thermal conductivity deviations of the tungsten data from the following secondary references compared to eq. (1.1.3):(10,13,16,19,26)

○ - (10), △ - (13), □ - (16), ▽ - (16),
◇ - (16), + - (19), × - (26)

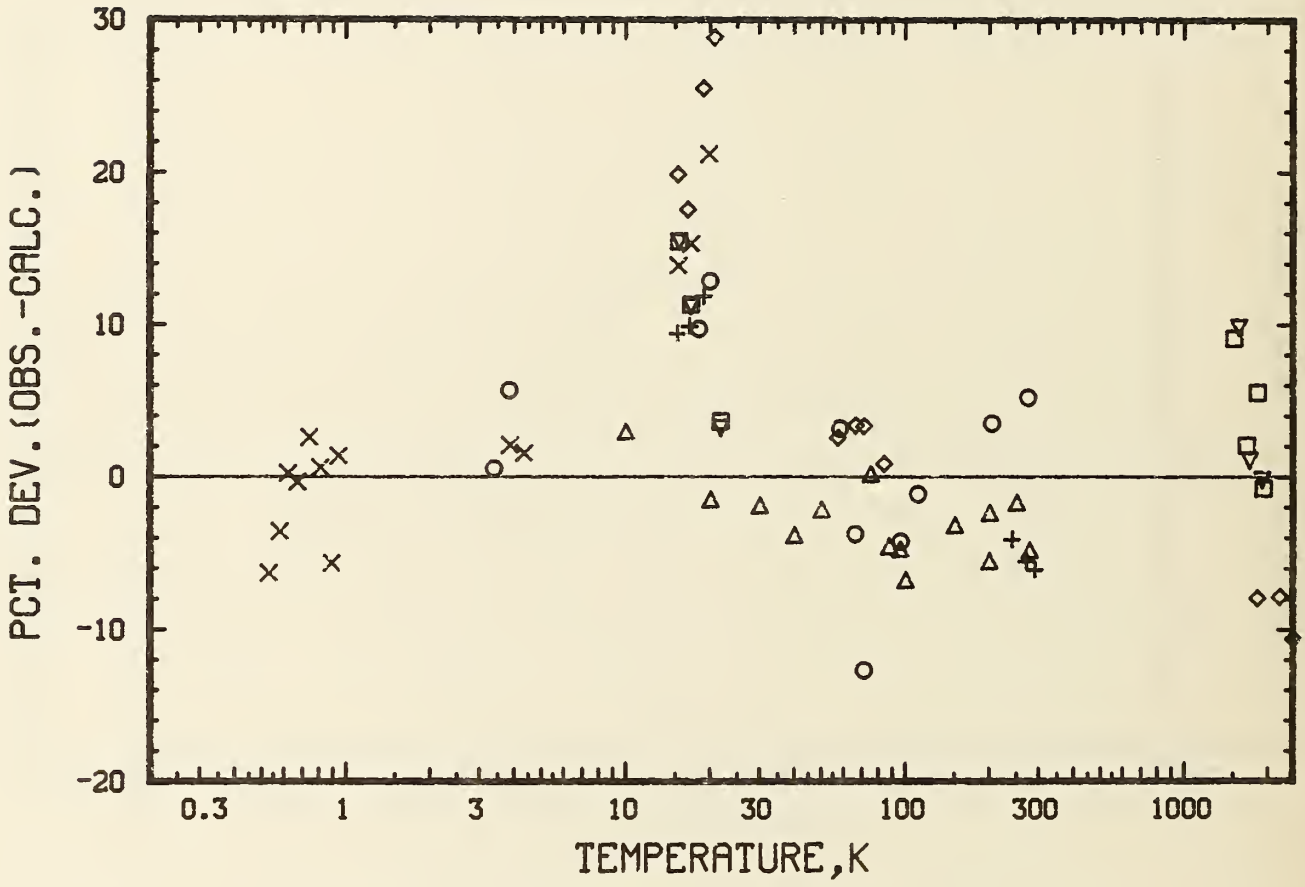


Figure 5.2.7 Composite of the deviations in figs.5.2.5 and 5.2.6

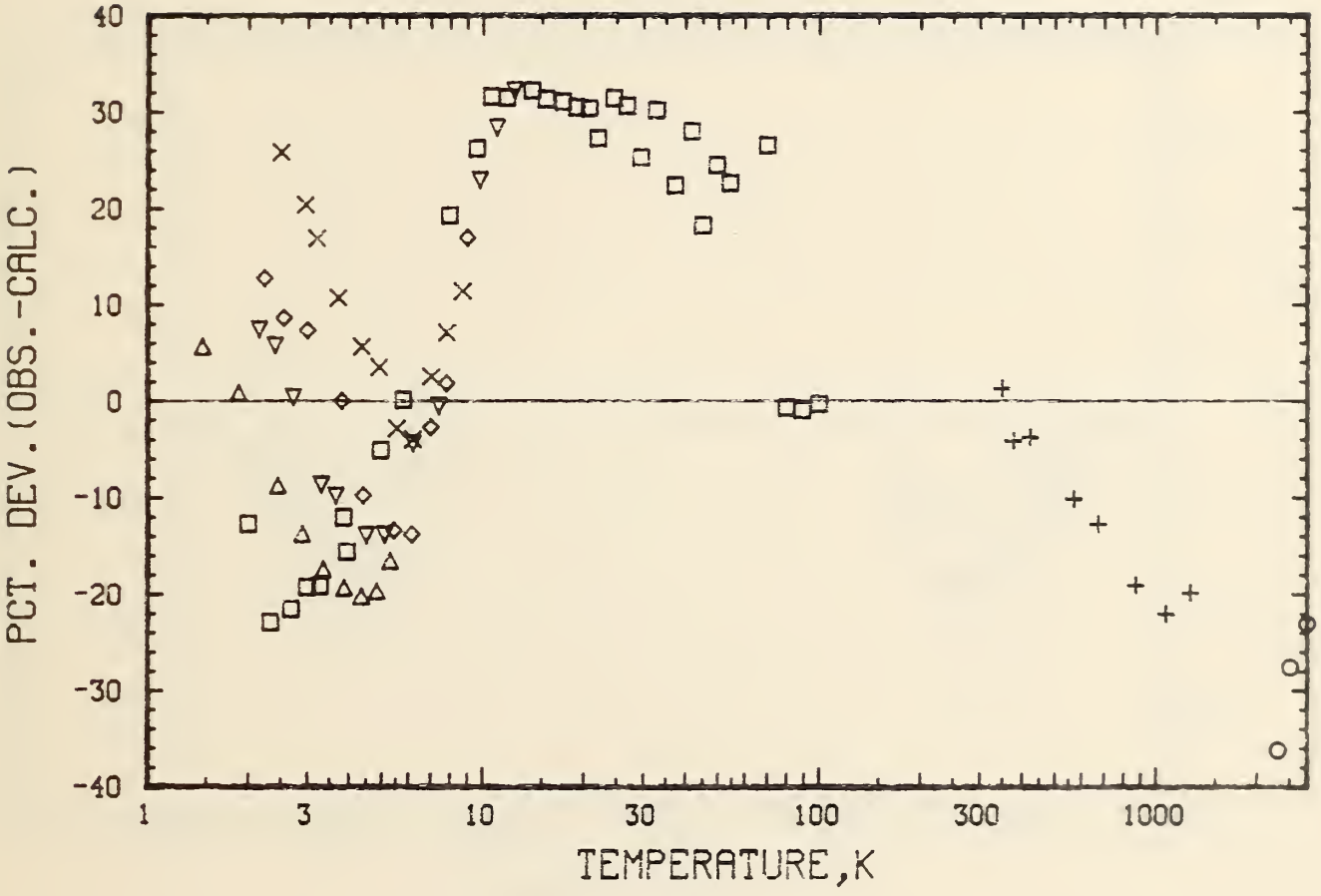


Figure 5.2.8 Thermal conductivity deviations of the tungsten data from the following secondary references compared to eq. (1.1.3):(3,4,4B,11,28)

○ - (11), △ - (3), □ - (4), ▽ - (4),
◇ - (4), + - (4B), × - (28)

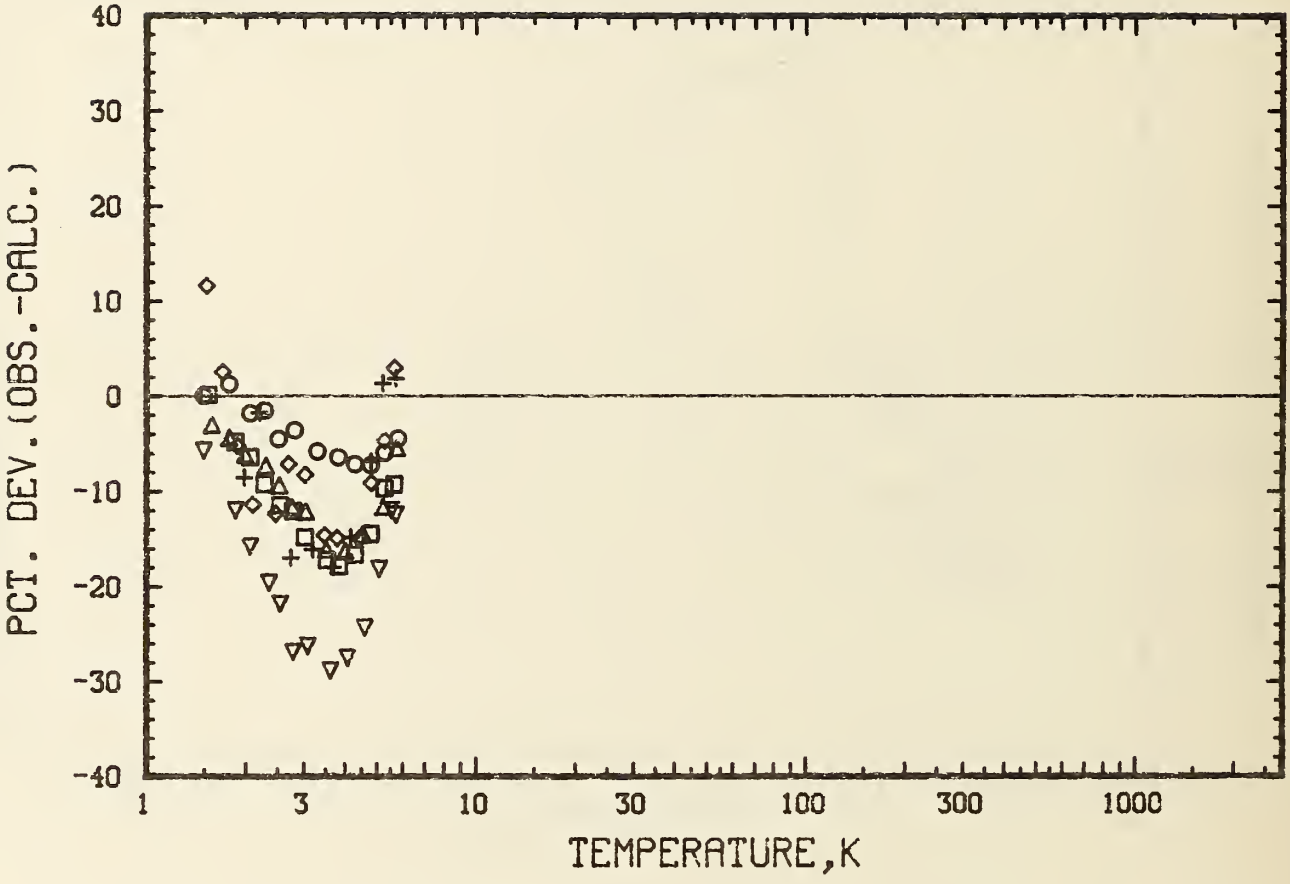


Figure 5.2.9 Thermal conductivity deviations of the tungsten data from the following secondary reference compared to eq. (1.1.3):(31)

○ - (31), △ - (31), □ - (31), ▽ - (31),
◇ - (31), + - (31)

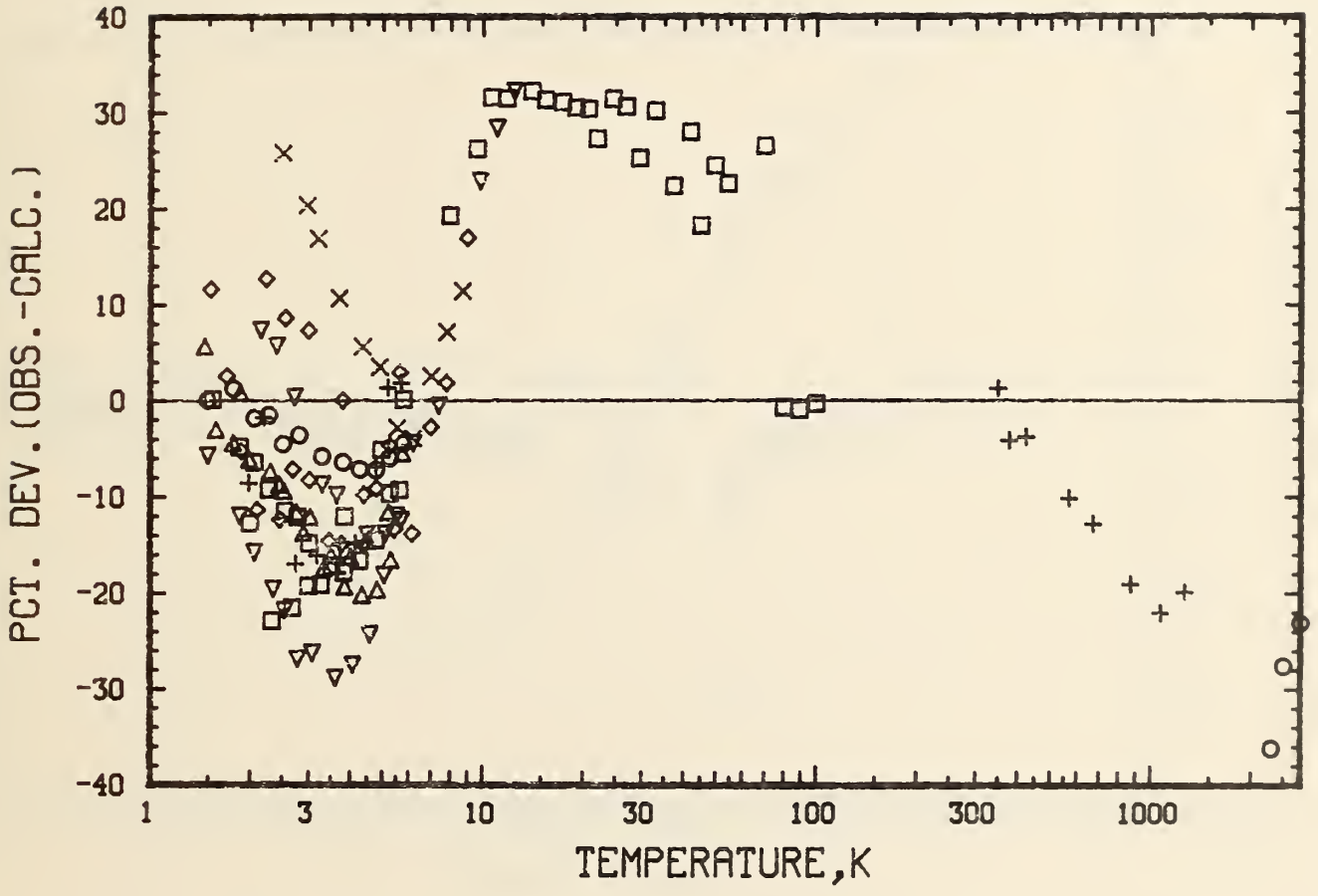


Figure 5.2.10 Composite of the deviations in figs. 5.2.8 and 5.2.9

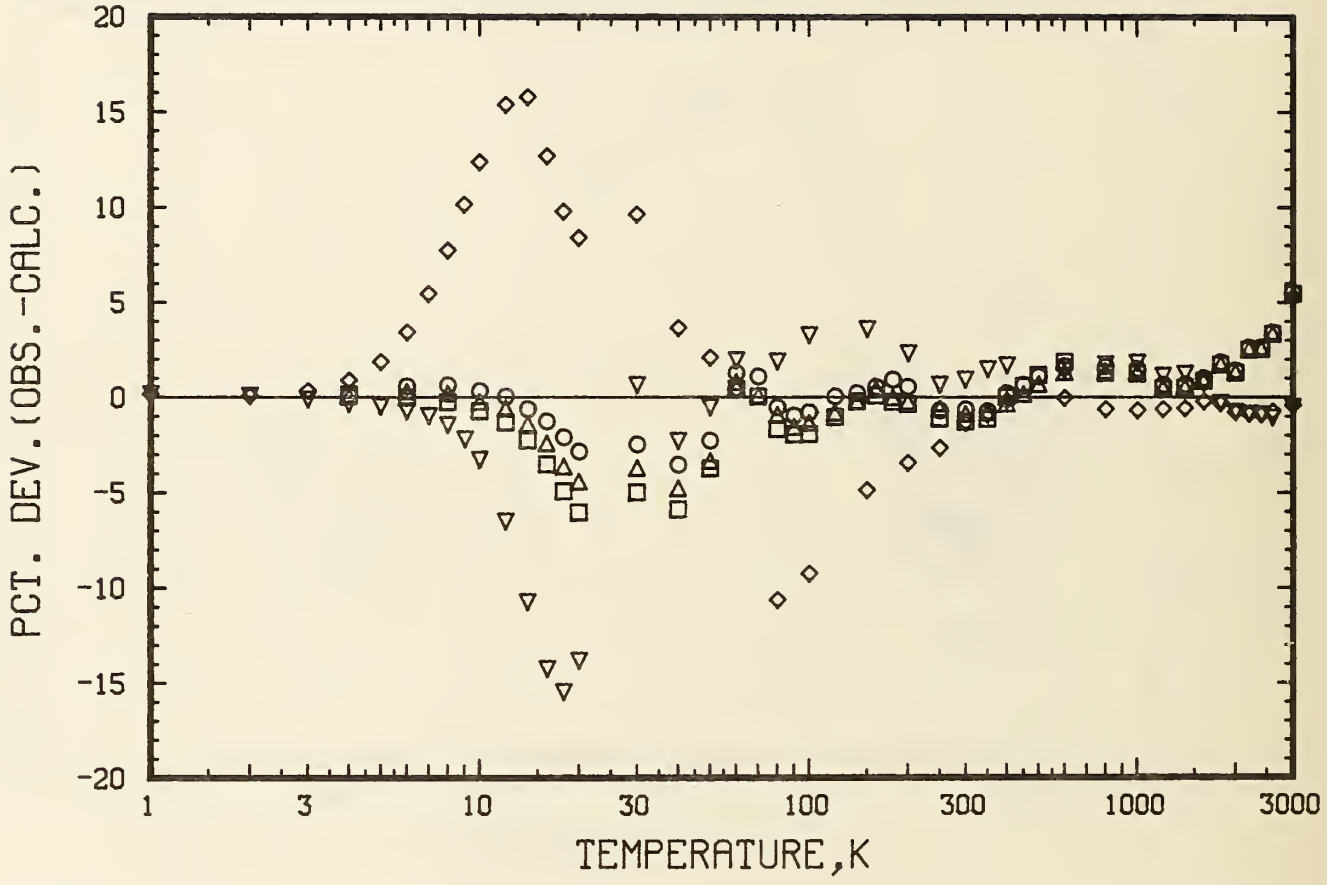


Figure 5.2.11 Comparison of eq.(1.1.3) to the values recommended for tungsten in the following references:(12A,15,27A)

○ - (15), △ - (15), □ - (15), ▽ - (27A),
◇ - (12A)

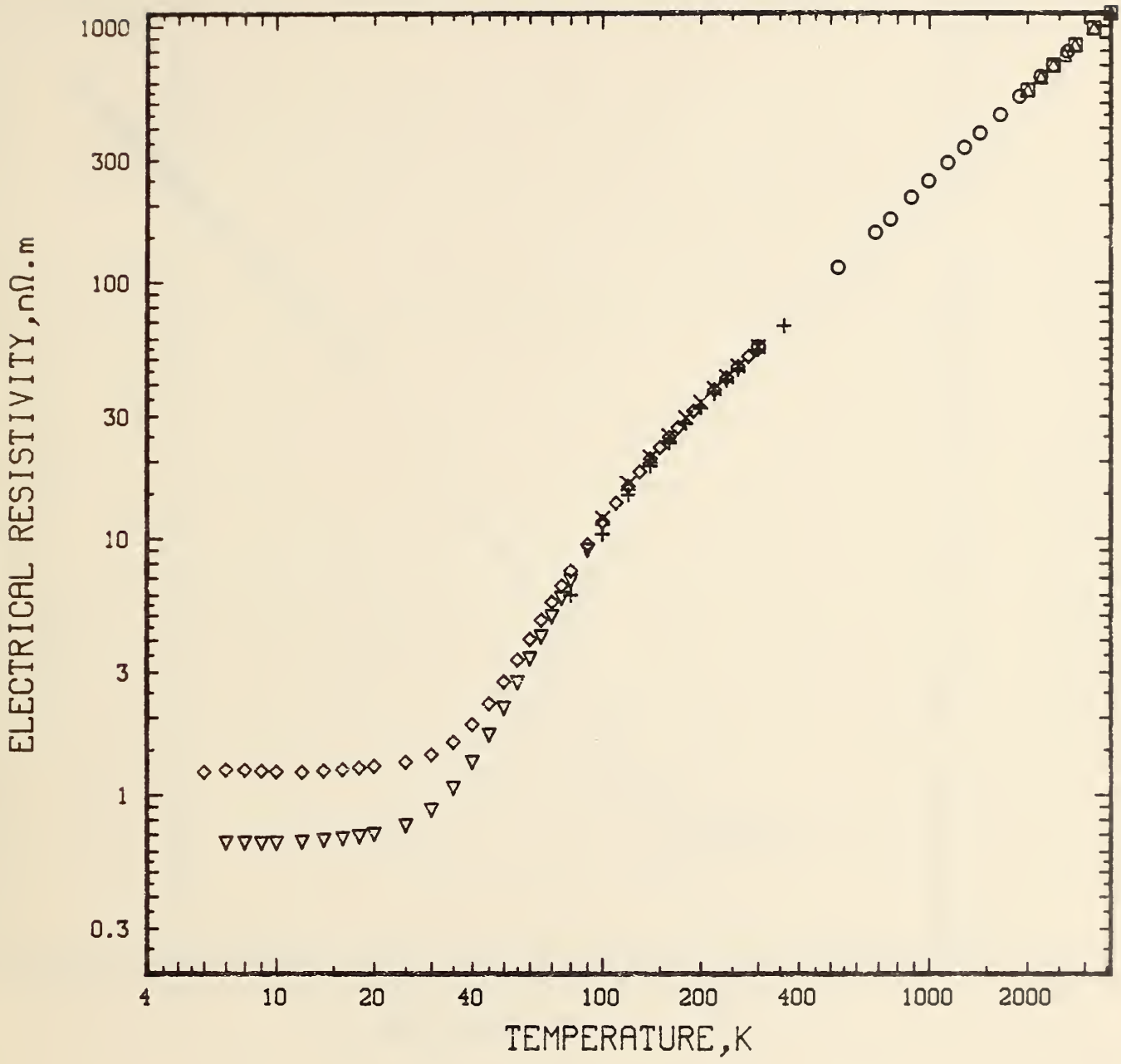


Figure 5.3.1 Experimental electrical resistivity data for tungsten selected from the following references in the tungsten annotated bibliography: (5A,11,14,22)

○ - (11), △ - (11), □ - (5A), ▽ - (14),
◇ - (14), + - (22), × - (22)

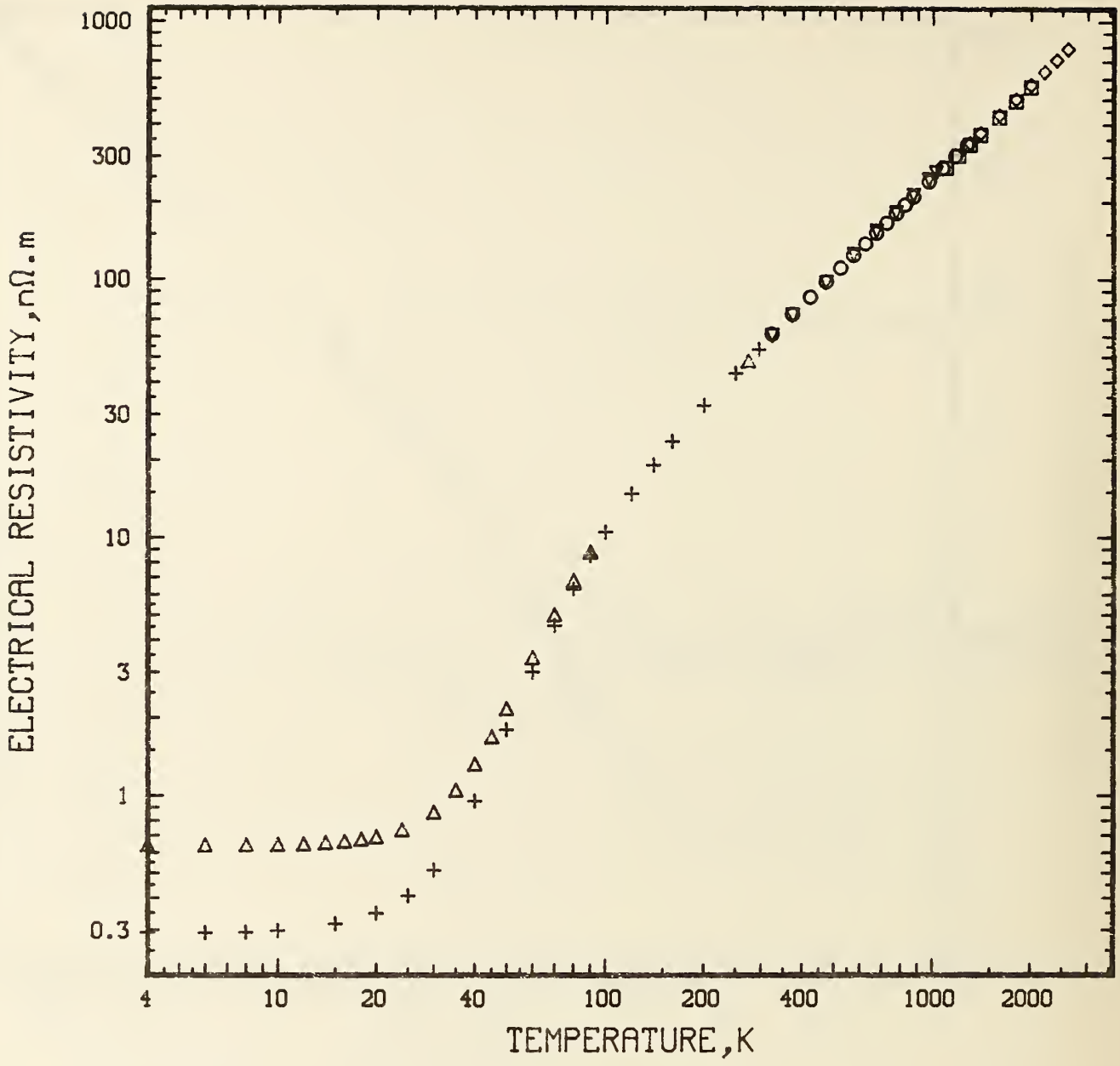


Figure 5.3.2 Experimental electrical resistivity data for tungsten selected from the following references in the tungsten annotated bibliography: (4A,21,23,25,26A,33)

○ - (21), △ - (4A), □ - (23), ▽ - (25),
◇ - (26A), + - (33)

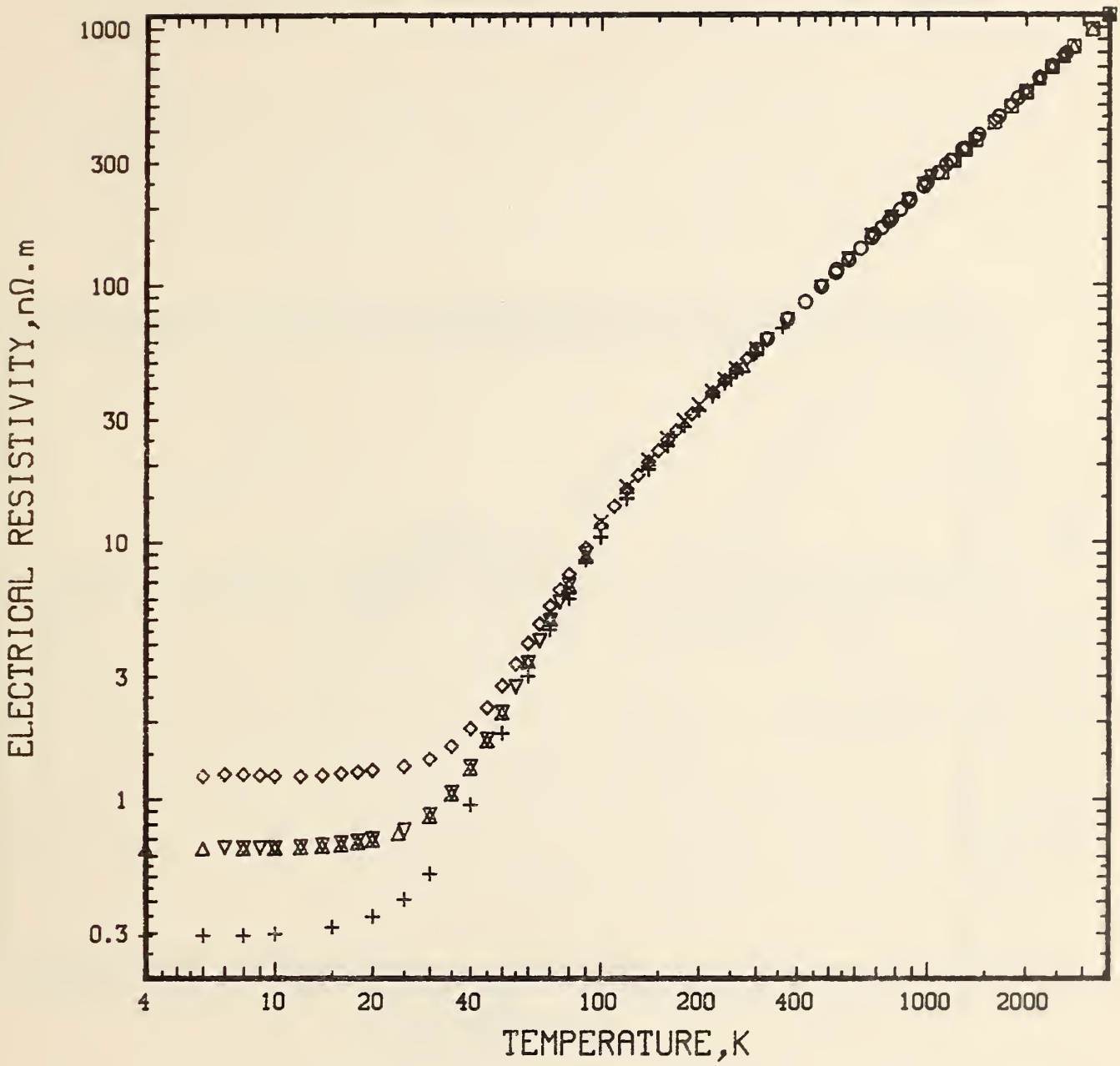


Figure 5.3.3 Composite of the electrical resistivity data in figs. 5.3.1 and 5.3.2

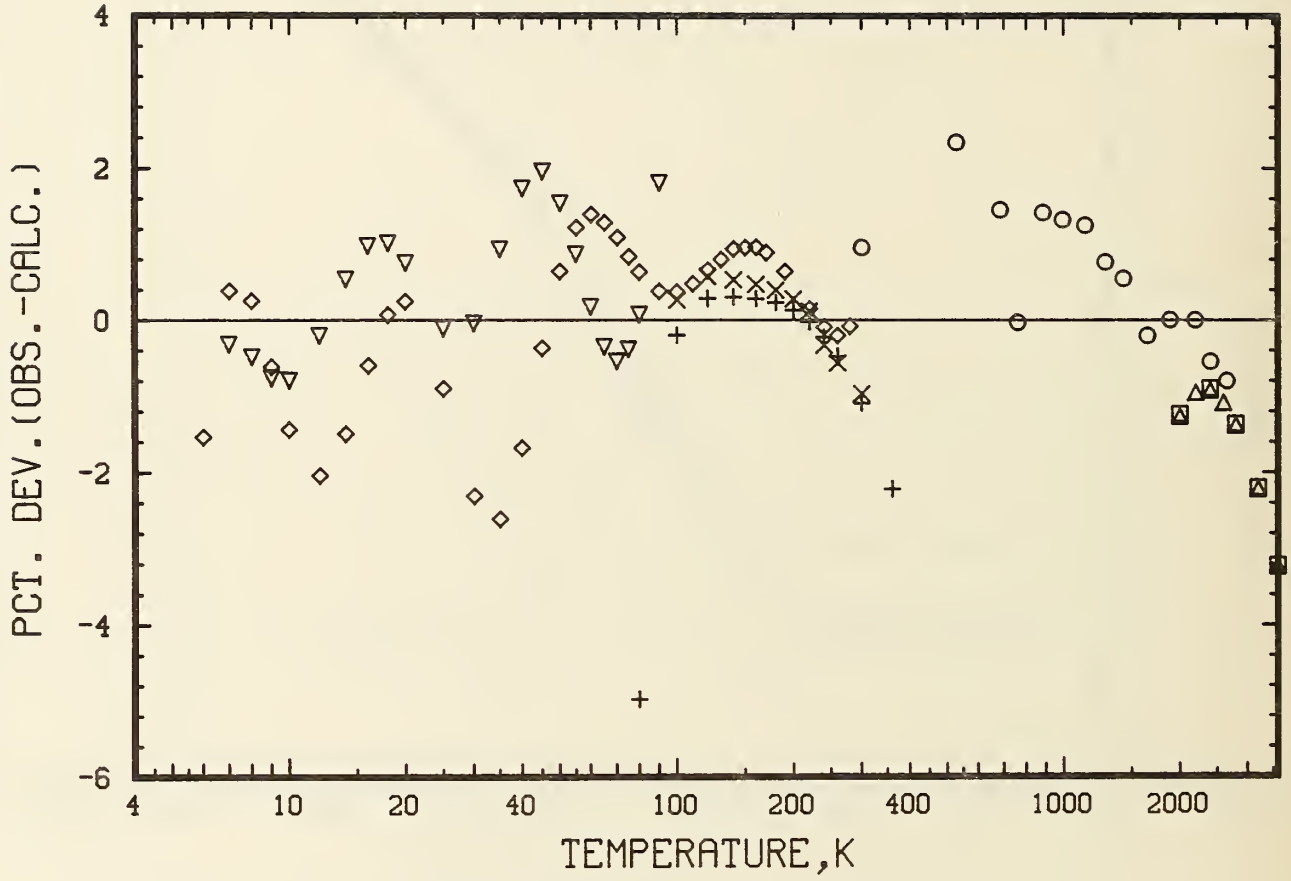


Figure 5.3.4 Electrical resistivity deviations of the tungsten data from the following references compared to eq. (1.2.3):(5A,11,14,22)

○ - (11), △ - (11), □ - (5A), ▽ - (14),
◇ - (14), + - (22), × - (22)

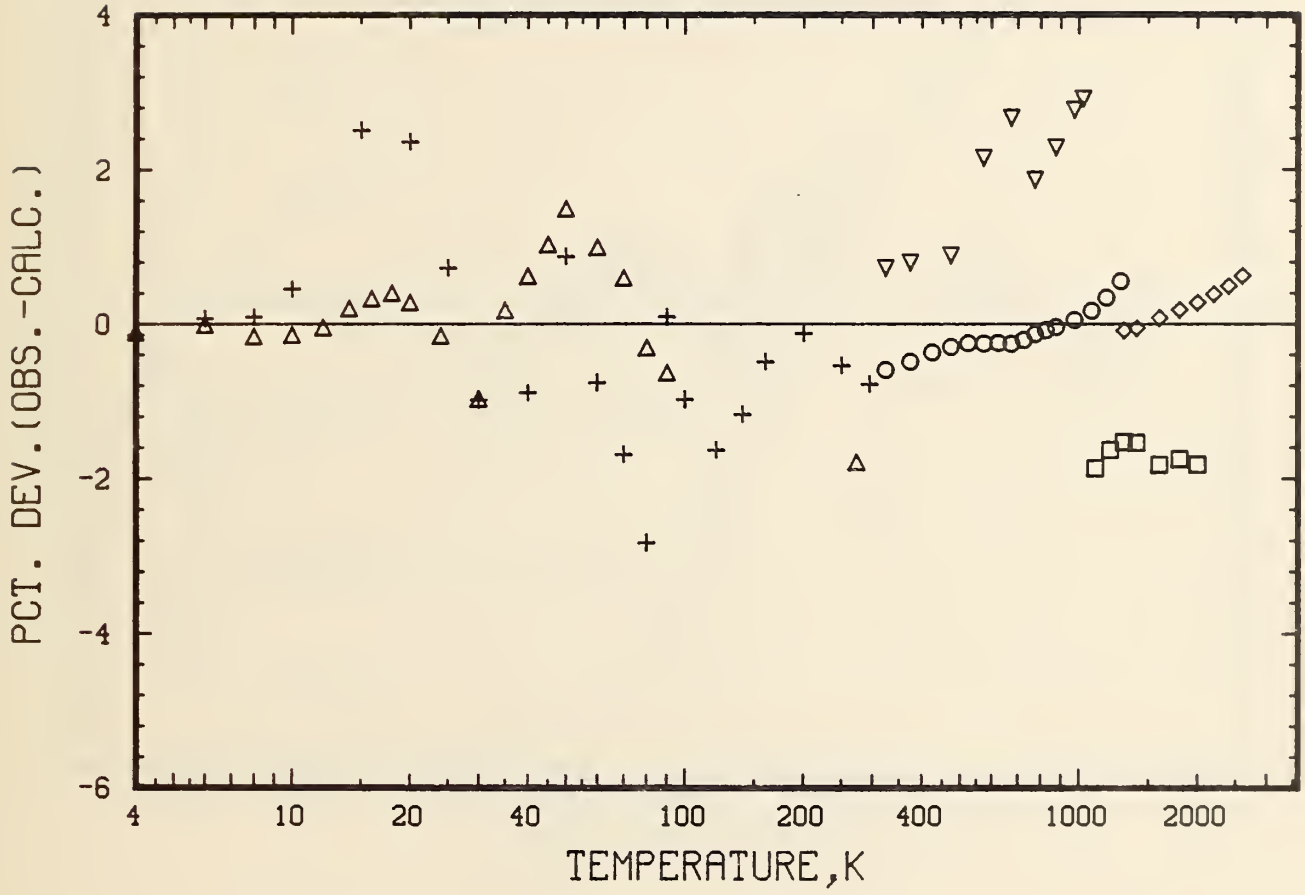


Figure 5.3.5 Electrical resistivity deviations of the tungsten data from the following references compared to eq. (1.2.3):(4A,21,23,25,26A,33)

○ - (21), △ - (4A), □ - (23), ▽ - (25),
◇ - (26A) + - (33)

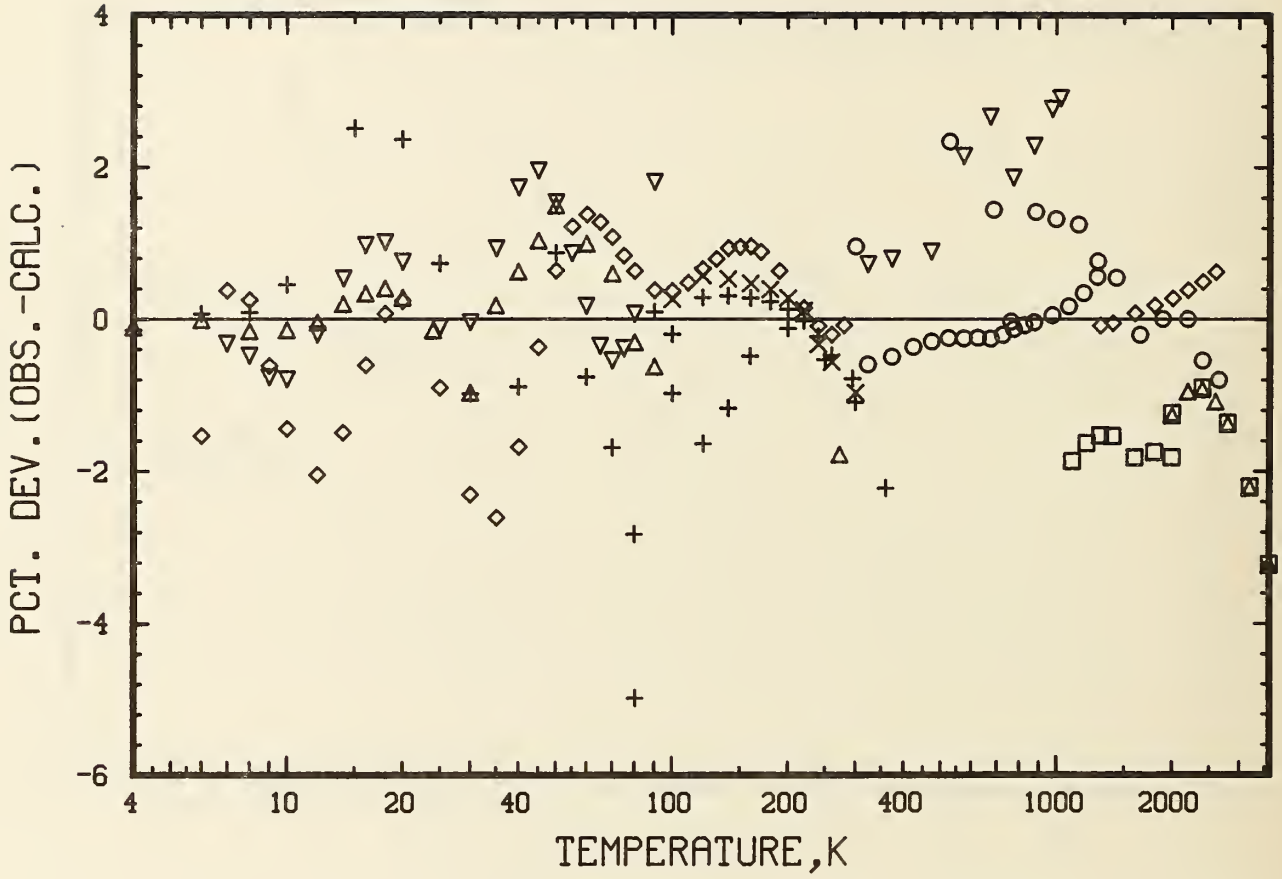


Figure 5.3.6 Composite of the electrical resistivity deviations shown in figs. 5.3.4 and 5.3.5

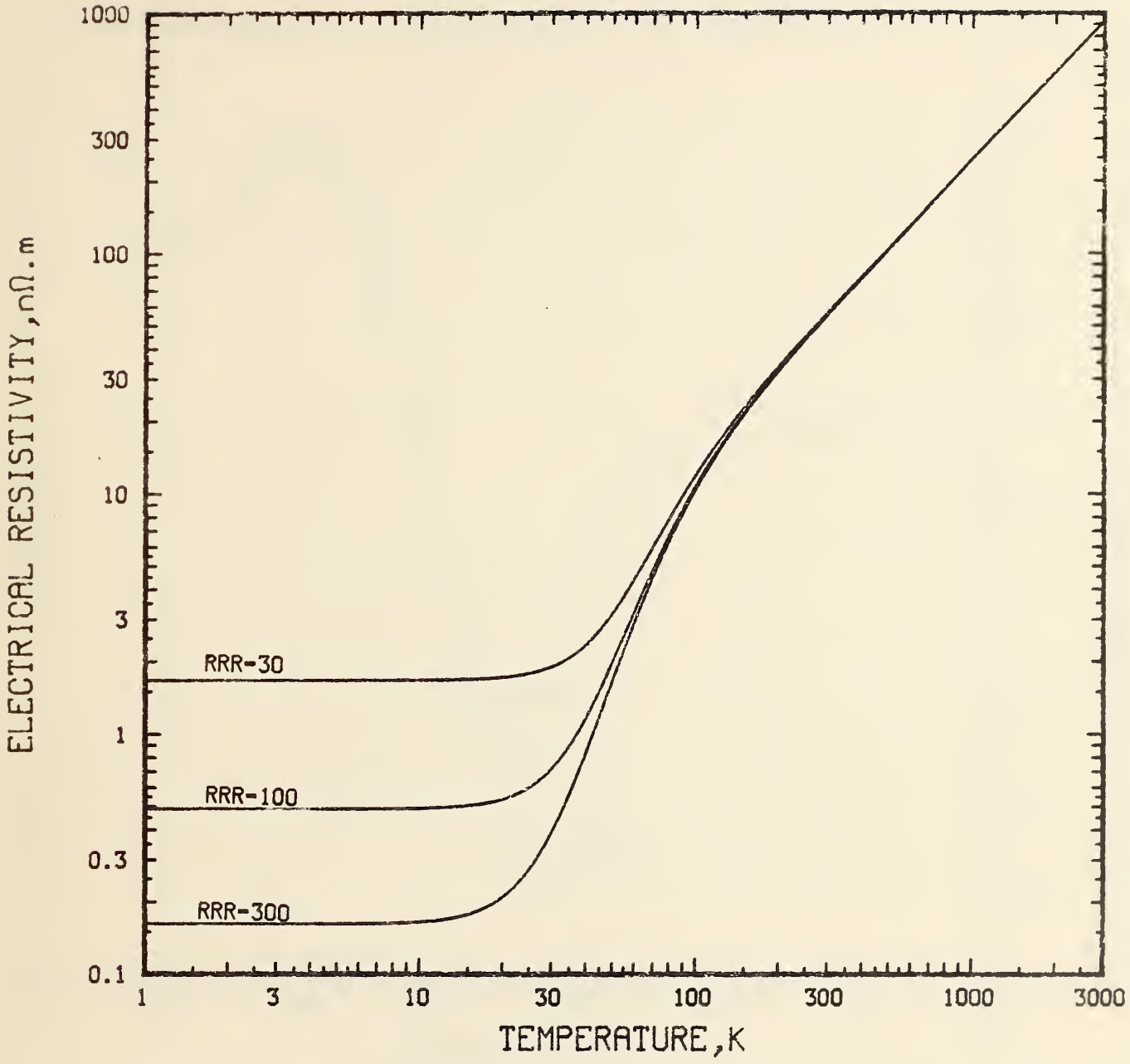


Figure 5.3.7 Electrical resistivity for tungsten as a function of temperature calculated from eq.(1.2.3) at selected values of RRR.

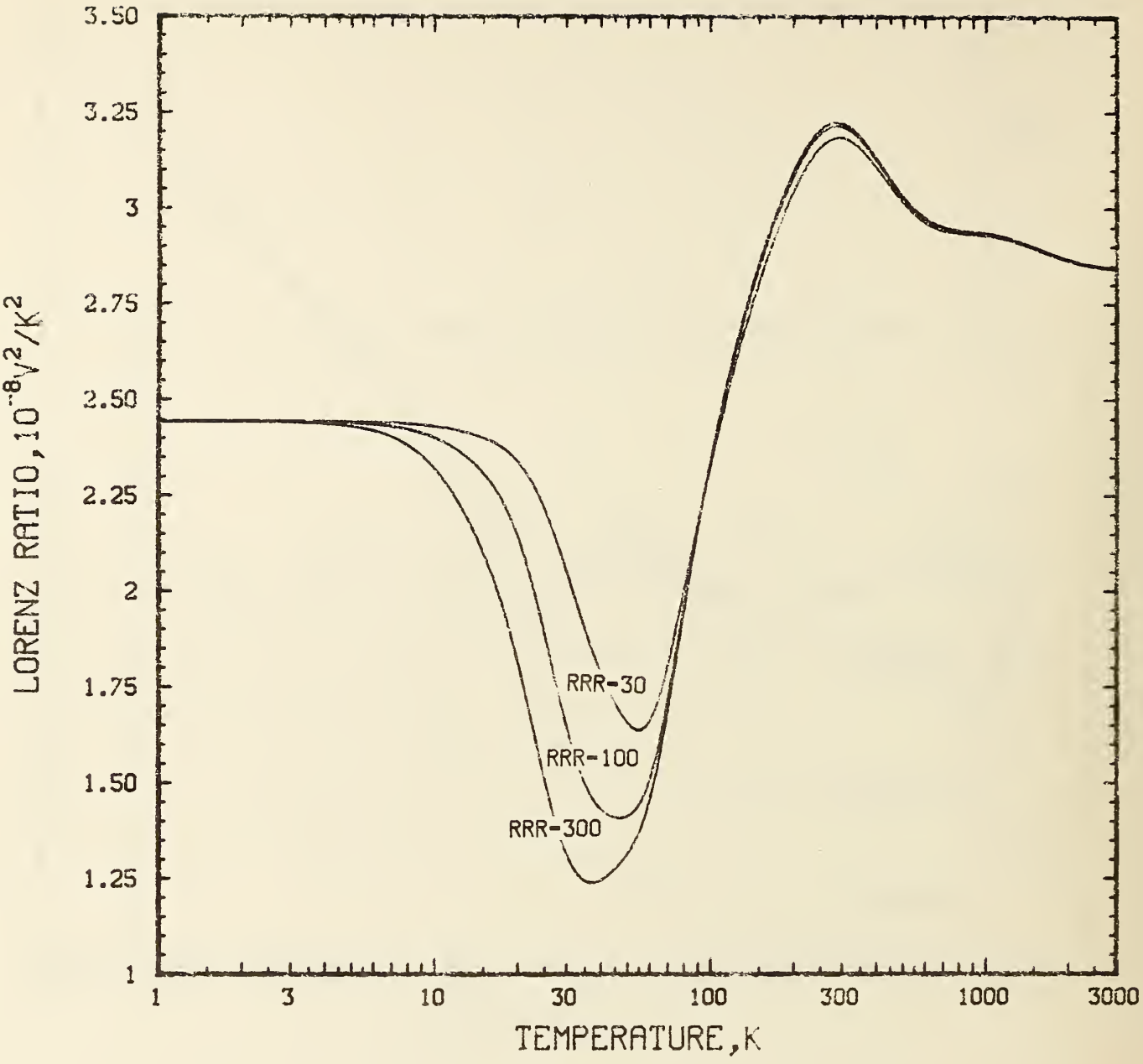


Figure 5.3.8 Lorenz ratio for tungsten as a function of temperature calculated from eq.(1.2.3) and eq.(1.1.3) at selected values of RRR.

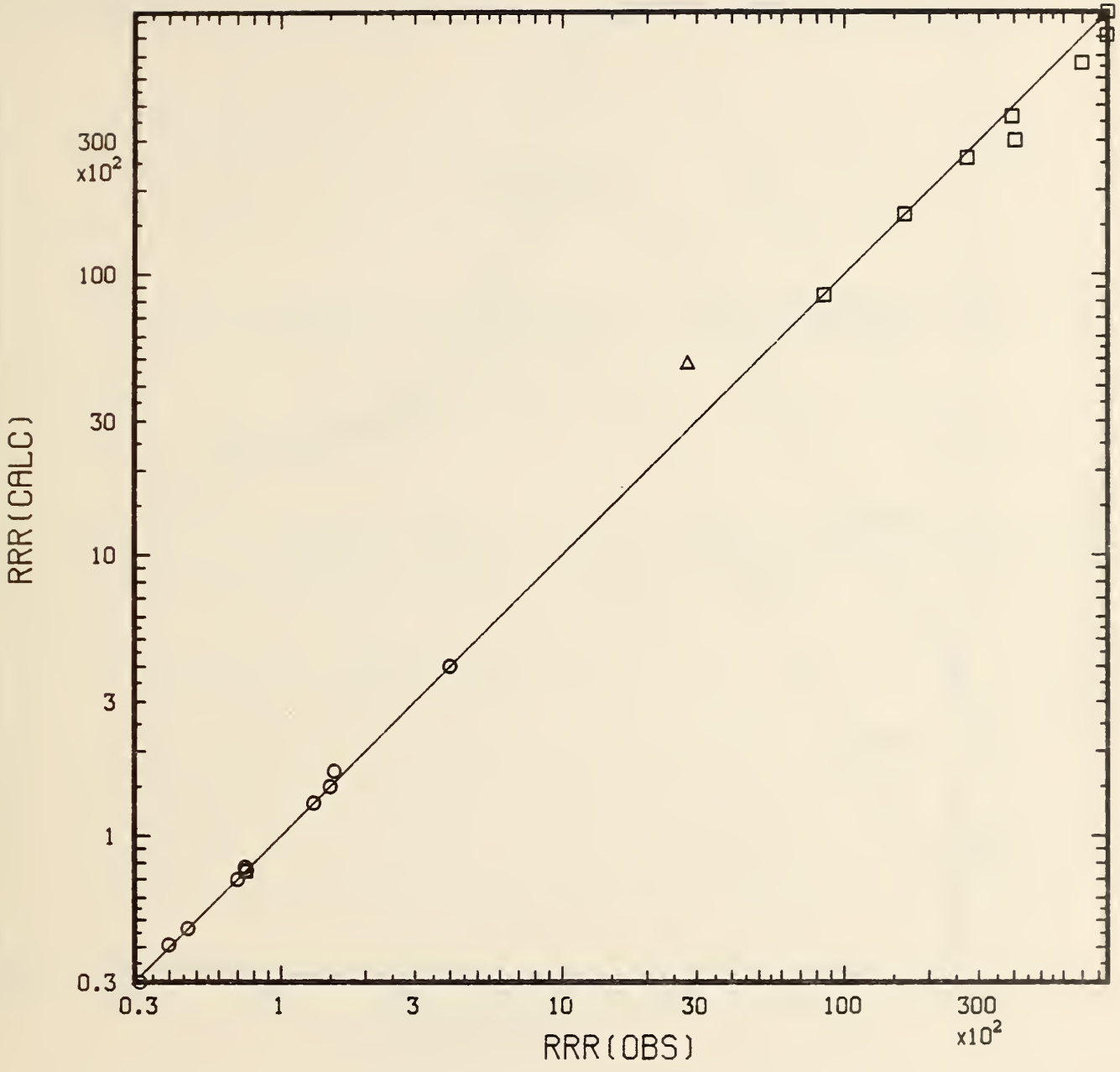


Figure 5.3.9 RRR values calculated as per Section 1.5, RRR(CALC), versus reported RRR values, RRR(OBS), for tungsten.

○ - Primary, △ - Secondary,
□ - Secondary

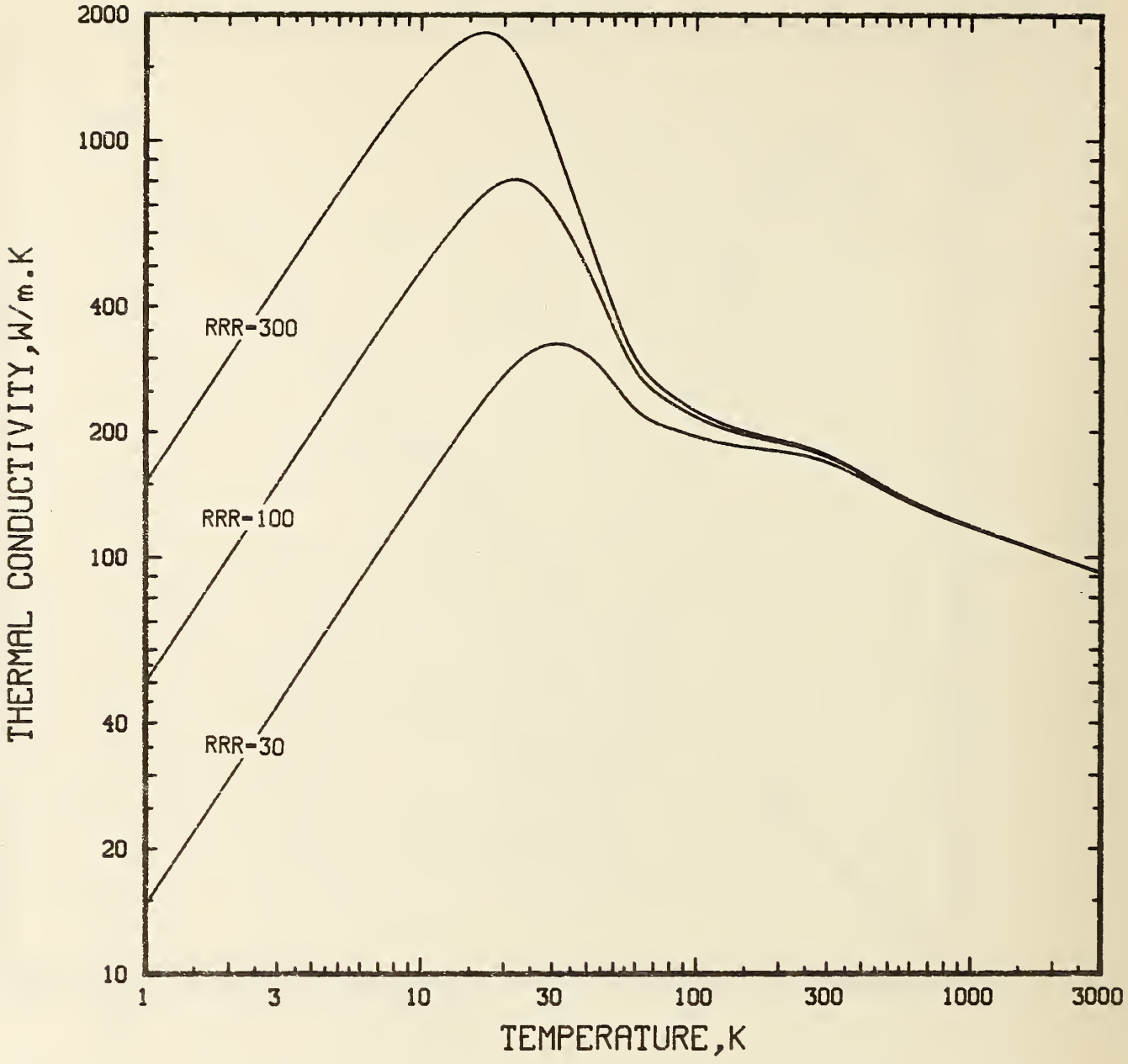


Figure 5.4.1 Thermal conductivity for tungsten as a function of temperature calculated from eq.(1.1.3) at selected values of RRR.

## 5.5 FORMAT FOR ANNOTATED BIBLIOGRAPHY OF TUNGSTEN

### REFERENCE

AUTHOR, TITLE, CITATION

### ANNOTATION

PURPOSE

SPECIMEN
a) Dimensions/Shape; b) Crystal Status; c) Thermal/Mech. History; d) Purity Specification; e) RRR; f) $\rho_o$; g) Other Characterization Data

APPARATUS
a) Type; b) Thermometry/Calibration/Anchoring; c) Thermal Isolation; d) Other (Q meas.)

DATA
a) Temperature Range/Difference; b) Content of Tables, Figures and Equations/Data Extraction; c) Uncertainty/Imprecision; d) Disputable Corrections to Measurements by Authors; e) Errata (by Author or Reviewer)

ANALYSIS
a) Comparisons; b) Conclusions

[1] Bäcklund, N. G., Measurement and Analysis of the Thermal Conductivity of Tungsten and Molybdenum at 100 to 400 K, Thermal Conductivity Conference, National Physical Laboratory, Teddington, England, 15-17 July (1964)

PURPOSE
To measure $\lambda$ for W and Mo from 100 to 400 K.

SPECIMEN
a) 4 mm dia., 10 cm long/rod; g) source: Johnson, Matthey Co.

APPARATUS
a) longitudinal; b) Fe-constantan thermocouples soldered to specimen/calibrated with earlier measurements (Bäcklund, J. Phys. Chem. Solids 20 (1961)); c) German silver shielding, isolating bricks between can and base plate, vacuum insulation.

DATA
a) 95.9 to 280 K; b) figures 3, 5 - $\rho$, $\lambda$ respectively; c) uncertainty: ±2%.

ANALYSIS
b) $\lambda_g$ is proportional to T.

[2] Bäcklund, N. G., Measurement and Analysis of the Thermal Conductivity of Tungsten and Molybdenum at 100 to 400 K, J. Phys. Chem. Solids, 28, 2219-23 (1967)

PURPOSE
To obtain information regarding the scattering processes of phonons and electrons in W and Mo.

SPECIMEN
a) 10 cm long, 4 mm dia./rod; f) $\rho_0$ = 1.24 $\mu\Omega\cdot$cm; g) source: Johnson, Matthey and Co.

APPARATUS
a) longitudinal; b) Fe-constantan thermocouples soldered to specimen; c) German silver shielding, isolating bricks between can and base plate; vacuum insulation.

DATA
a) 87.3 to 282 K; b) figure 5 - $\lambda$/data points listed in TPRC data series; c) uncertainty: ±1.5%.

ANALYSIS
b) scattering by electrons is expected to be constant, while Umklapp scattering is found only at higher temperatures.

[3] Baer, D. R. and Wagner, D. K., Effect of Surface Condition on the Transport Properties of Tungsten, J. Low Temp. Phys., 13(5/6), 445-69 (1973)

PURPOSE
To determine the effect of surface condition on $\rho$, W and L.

SPECIMEN W-12G
a) 0.74 mm dia./rod; b) single crystal; c) electropolished; f) $\rho_0$ = 1.26 x $10^{-10}$ $\Omega$·cm; g) crystal oriented to [110], $\rho_{299}/\rho_0$ = 43000.

APPARATUS
a) longitudinal; b) C resistance thermometers/calibrated against a standard Ge resistance thermometer; c) adsorbent in vacuum chamber to adsorb residual He.

DATA
a) 1.46 to 5.31 K; b) figure 12 - $1/\lambda$; c) uncertainty: ±1%.

ANALYSIS
b) surface scattering is specular for the electropolished surface, while diffuse for the electroetched and sandblasted surfaces.

[4] Batdalov, A. B., Tamarchenko, V. I., and Shalyt, S. S., Manifestation of Hydrodynamic Effect in the Thermal Conductivity of Tungsten, JETP Lett. (USSR), 20(6), 171-3 (Sep 1974)

PURPOSE
To determine $\lambda$ of a compensated metal.

SPECIMEN
a) specimens 1, 2, 3: 3.2, 1.4, 0.8 mm dia. respectively/rods; b) single crystals; c) /electrical etching reduced specimen 1 into 2 and 3; e) specimen 1 (RRR = 86000).

DATA
a) specimen 1: 2 to 102 K, specimen 2: 2.15 to 12.4 K, specimen 3: 2.23 to 9.0 K; b) figure 1 - $\lambda$.

ANALYSIS
b) the hydrodynamic contribution to the total thermal conductivity behaves like $T^{-3.4}$.

[4A] Berman, R., Hardy, N. D., Sahota, M. Hust, J. G., and Tainsh, R. J., Standards Reference Materials for Thermal Conductivity Below 100 K, Proceedings of the Seventeenth Conference on Thermal Conductivity, Gaithersburg, MD, 105-16 (1983)

PURPOSE
To report results of a CODATA round-robin investigation involving standard reference materials of stainless steel, tungsten, and electrolytic iron.

SPECIMEN from Leeds University
a) SRM 730; b) approximately 1/4 in. (dia) x 2 in. (6 x 50 mm); c) RRR = 70.

SPECIMEN from National Measurement Laboratory
a) SRM 730; b) approximately 1/4 in. (dia) x 2 in. (6 x 50 mm); c) RRR = 75.4, 131.

APPARATUS
a) not discussed

DATA from Leeds University
a) 1 to 95 K; b) Table - λ/data made available by private communication.

DATA from National Measurement Laboratory, CSIRO
a) 2 to 90 K; b) Table - λ/data made available by private communication.

[4B] Binkele, L., Zur Frage der Hochtemperatur-Lorenzzahl bei Wolfram-eine Analyse neuer Messwerte der thermischen und elektrischen Leitfahigkeif im Temperatubereich 300 bis 1300 K, submitted for publication in High Temperature-High Pressure (1982)

PURPOSE

SPECIMEN
a) SRM 730

APPARATUS
a) Details not given.

DATA
a) 300 to 1300 K

[5] Bremmer, H. and DeHaas, W. J., On the Conduction of Heat by Some Metals at Low Temperatures, Physica, 3, 672 (1936)

PURPOSE
To determine $\lambda$ for Pb, Cu and W.

SPECIMEN
a) RRR = 2174; g) source: N. V. Philips Lampworks Eindhoven.

APPARATUS
a) longitudinal; b) Pt resistance thermometers.

DATA
a) 1.55 to 21.8 K; b) Table 4 - W/data points listed in TPRC data series.

ANALYSIS
a) results disagree with Gruneisen, E. and Goens, E., Z. Phys., 44, 615 (1927).

[5A] Cezairliyan, A. and McClure, J. L., High Speed (Subsecond) Measurement of Heat Capacity, Electrical Resistivity, and Thermal Radiation Properties of Tungsten in the Range 2000 to 3600 K, J. Research NBS, 75A(4) (1971)

PURPOSE
To apply a high speed measurement technique on a tungsten specimen in the temperature range 2000 to 3600 K.

SPECIMEN
a) 4 in. length (101 mm), outside dia. 0.25 in. (6.3 mm), wall thickness 0.02 in. (0.5 mm)/tube; c) specimen produced from rod by electroerosion, annealed up to 3200 K; e) RRR = 41; g) polished outer surface, density at 293 K: $19.23 \times 10^3$ kg·m$^{-3}$.

APPARATUS
a) subsecond transient; b) photoelectric pyrometer/calibrated against W filament standard lamp; c) $10^{-4}$ mm of Hg ($10^{-3}$ Pa) vacuum.

DATA
a) 2000 to 3600 K; b) Table 2, Fig. 3 - $\rho$; c) uncertainty: ±1% between 2000 and 3600 K.

ANALYSIS
a) Results agree with Osborn (1941), Platunov (1964), Neimark (1968), Jones (1926); b) $\rho = 14.08 + 3.515 \times 10^{-2}\ T$ where $\rho$ is in units of $10^{-8}$ $\Omega$m and T in K.

[6] Cox M., Thermal and Electrical Conductivities of Tungsten and Tantalum, Phys. Rev., 64, 241 (Oct 1943)

PURPOSE
To measure λ and  of pure W and Ta.

SPECIMEN
a) specimens 2,8: 0.10 in. (0.025 cm) dia., 40 cm long/rods; c) specimen 2: aged 370 h at 2400, 2600 °C, specimen 8: aged 370 h at 2300 °C; g) source: General Electric Co.

APPARATUS
a) direct current heating; Hg thermometer and barometer for boiling point of $N_2$, $O_2$, $H_2O$ and ice bath.

DATA
a) 77.4 to 274 K; b) Table 3 - λ, ρ, L/λ data listed in TPRC data series.

ANALYSIS
a) ρ results agree with Holborn, L. (1919), Henning, F. (1921), Geiss, W. (1923), Forsythe, W. E. (1925), Meissner, W. (1930), Barratt, T. (1914), Weber, S. (1917), Grüneisen, E. (1927), Kannuluik, W. G. (1933), and DeHaas, W. J. (1938). λ results disagree with Grüneisen, E. (1927), Kannuluik, W. G. (1933), and DeHaas, W. J. (1938).

[7] DeHaas, W. J. and Biermasz, T. H., Sur la Conductibilité Thermique aux Basses Temperatures, Rapports et Communications, No. 24, 7e, Congres International du Froid, Supplement No. 82b, 204 (1936)

PURPOSE
To determine λ for several metals at low temperatures.

APPARATUS
a) longitudinal; b) Pt resistance thermometer.

DATA
a) 15.5 to 21.8 K; b) Table 8 - W, L/L data from Table 8, λ data points listed in TPRC data series.

[8] DeHaas, W. J. and deNobel, J., The Thermal and Electrical Resistance of a Tungsten Single Crystal at Low Temperatures and in Magnetic Fields, Physica, 5, 449 (1938)

PURPOSE
To separate $\lambda$ of W into $\lambda_e$ and $\lambda_g$ at low temperatures in strong magnetic fields.

SPECIMEN
a) 30 mm long/hexagonal rod; b) single crystal; e) RRR = 2780; g) source: Philips Works, axis is in [111] direction.

APPARATUS
a) longitudinal; b) Pb thermometers/calibrated against a Pt resistance thermometer in bath; c) $< 5 \times 10^{-6}$ mm of Hg ($7 \times 10^{-4}$ Pa) vacuum.

DATA
a) 15.3 to 88.4 K; b) Tables 1, 3 - $\lambda$, $\rho/\rho$ data from Table 3, $\lambda$ data points listed in TPRC data series.

ANALYSIS
b) W-F-L holds for $\rho$ and $\lambda_e$ in magnetic fields.

[9] deNobel, J., Thermal and Electrical Resistance of a Tungsten Single Crystal at Low Temperatures and in High Magnetic Fields, Physica, 15(5-6), 532-40 (Jul 1949)

PURPOSE
To investigate the relationship of the W-F-L law to $\rho$ and $\lambda$ due to electrons.

SPECIMEN
a) 30 mm long/hexagonal rod; b) single crystal; e) RRR = 2780; g) source: Philips Works, axis is in [111] direction, same specimen as used by DeHaas, W. J. (1938).

APPARATUS
a) longitudinal; b) Pb thermometers.

DATA
a) 15 to 20 K; b) Table 1 - $\lambda$/data points listed in TPRC data series, run 1-4: H = 0.82, 2.1, 2.6, 2.8 kA/m, perpendicular.

ANALYSIS
b) W-F-L is not valid in strong magnetic fields for $\sigma$ and $\lambda_e$, and it is not possible to separate $\lambda_g$ and $\lambda_e$.

[10] deNobel, J., Thermal and Electrical Resistivity of Some Tungsten Single Crystals at Low Temperatures and in Strong Magnetic Fields, Physica, 23, 261 (1957)

PURPOSE
To gain information about $\lambda_e$ and $\lambda_g$ from the change in anisotropy with increasing field strength.

SPECIMEN
b) single crystals, A oriented in [111] direction, I-38 and B oriented in [100] (±5°) direction; g) $\rho_{20}/\rho_{273} = 26 \times 10^{-4}$.

APPARATUS
a) longitudinal; b) phosphor bronze resistance thermometers.

DATA
a) specimen A: 15.3 to 20.3 K, specimen B: 3.86 to 20.2 K, specimen I-38: 3.38 to 75.9 K; b) Table 1 - λ/data points listed in TPRC data series.

ANALYSIS
b) A and B anisotropy ratio: 1.13, 1.23 respectively.

[11] Fitzer, E., Thermophysical Properties of Solid Materials. Project Section II. Cooperative Measurements on Heat Transport Phenomena of Solid Materials at High Temperature, AGARD Report No. 606, 1973

PURPOSE
To improve the data base used in the design and fabrication of high temperature equipment and systems under development by the NATO countries.

SPECIMEN Participant 5
a) /wire; c) sintered.

SPECIMEN Participant 31
a) /wire; c) sintered.

SPECIMEN Participant 41
a) /wire; c) arc cast; d) 99.55% W; g) $\rho(T)$.

APPARATUS Participant 5
a) comparative

APPARATUS Participant 31
a) direct electrical heating

APPARATUS Participant 41
a) direct electrical heating; b) pyrometer; d) argon environment.

DATA Participant 5
a) 300 to 900 K; b) Table 33 - $\lambda$.

DATA Partaicipant 31
a) 2100 to 2800 K; b) Table 33 - $\lambda$.

DATA Participant 41
a) 1500 to 2750 K; b) Table 35 - $\lambda$, Table 51 - $\rho$; c) uncertainty: ±2%.

ANALYSIS Participant 5
b) TPRC Recommended curves (1970, 1972).

ANALYSIS Participant 41
b) Jun, et al., High Temperature-High Pressure, 43 (1970); TPRC Recommended Curves (1970, 1972).

[12] Grüneisen, E. and Adenstedt, H., Anisotropie der Warmeleitung und Thermokraft Regularer Metalle (Wolfram) im Transversalen Magnetfeld bei 20 K, Ann. Phys. (Leipzig), 29, 597-604 (1937)

PURPOSE
To determine λ and thermopower of W in a transverse magnetic field.

SPECIMEN
a) 0.106 $cm^2$ x 7.0 cm; g) specimen axis 8° to the [110] direction.

APPARATUS
a) longitudinal; b) Constántan-manganin thermocouples; c) $10^{-4}$ to $10^{-5}$ mm of Hg ($10^{-2}$ to $10^{-3}$ Pa) vacuum.

DATA
a) 21.5 to 91.2 K; b) Tables 1, 2 - λ/data points listed in TPRC data series, H = 0.

ANALYSIS
a) agrees with Grüneisen, E. and Goens, E., Z. Phys., 44, 615 (1927).

[12A] Ho, C. Y., Powell, R. W., Liley, P. E., Thermal Conductivity of the Elements: A Comprehensive Review, J. Phys. Chem. Ref. Data, 3, Supplement No. 1, 242-257 (1974)

PURPOSE
To provide a comprehensive listing of data on λ of the elements.

SPECIMEN
d) high purity; f) $\rho_0 = 1.70 \times 10^{-9}$ Ω·cm for T below 200 K.

APPARATUS
a) not given.

DATA
a) 0 to 22273 K; b) Table 171 - λ, recommended values; c) uncertainty: ±2% near room temperature, ±3% from 300 to 1500 K, ±5% from 100 to 300 K and 1500 to 3000 K, and ±10% below 100 K and above 3000 K. The values above 3660 K are provisional.

[13] Hust, J. G., Thermal Conductivity Reference Materials, Progress Report, Proceedings of the Thirteenth Thermal Conductivity Conf., 22-4 (Nov 5-7, 1973)

PURPOSE
To present low temperature $\lambda$ measurements for sintered W.

SPECIMEN
c) sintered.

APPARATUS
a) longitudinal; b) vapor pressure of LHe for T < 20 K, Pt reference thermometer for T > 20 with differential thermocouples; b) controlled temperature glass fiber shield, vacuum insulation.

DATA
a) 10 to 250 K; b) Table 1 - $\lambda$, $\rho$, L.

ANALYSIS
b) SRM 734 can be extended to 800 °C and SRM 735 to 1000 °C.

[14] Hust, J. G., Thermal Conductivity Standard Reference Materials from 6 to 280 K: VI. N.B.S. Sintered Tungsten, NBSIR 73-351 (Jan 1974)

PURPOSE
To present measurements on the transport properties of NBS sintered W.

SPECIMEN
a) 23 cm long, 3.1 mm dia./rod; c) one specimen annealed at 2020 °C for 1 h, one unannealed; e) annealed (RRR = 74.6), unannealed (RRR = 39.8); f) annealed: $\rho_7$ = 0.6493 n$\Omega$·m, unannealed: $\rho_6$ = 1.229 n$\Omega$·m; g) density = (19.23 ± 0.05) g/cm$^3$, DPH hardness 1 kg = 405 and 514 for annealed and unannealed respectively.

APPARATUS
a) longitudinal; b) vapor pressure of LHe for T < 20 K, Pt reference thermometer for T > 20 with differential thermocouples; c) controlled temperature glass fiber shield, vacuum insulation.

DATA
a) annealed: 7 to 90 K, unannealed: 6 to 280 K; b) Table 12 - unannealed: $\lambda$, $\rho$, L, Table 13 - annealed: $\lambda$, $\rho$, L; c) uncertainty: $\lambda$ - 2.5% at 300 K, decreasing as $T^4$ to 0.70% at 200 K, 0.70% from 200 to 50 K, increasing inversely with temperature to 1.5% at 4 K, $\rho$ - 0.5%.

ANALYSIS
b) $\lambda = \sum_{i=1}^{n} a_i [\ell nT]^{i+1}$.

[15] Hust, J. G. and Giarratano, P. J., Thermal Conductivity and Electrical Resistivity Standard Reference Materials: Tungsten SRM's 730 and 799, from 4 to 3000 K, Nat. Bur. Stand. Spec. Publ. No. 260-52, 37 pp. (Sep 1975)

PURPOSE
To compile, correlate, and analyze $\lambda$ and $\rho$ data for arc cast and sintered W.

SPECIMEN
a) 0.51 to 1.27 cm dia./rods; c) W powder vacuum arc melted into billet, annealed at 1700 K for 1/2 h/billet machined into rod, acid etched and final swage before anneal; d) < 99.956%; e) specimens 1-3 (RRR = 50, 75, 100 respectively); f) specimens 1-3 ($\rho_0$ = 0.97, 0.65, 0.49 n$\Omega$·m respectively); g) AFML arc cast density: (19.20 ± 0.05) g/cm$^3$.

APPARATUS
a) longitudinal.

DATA
a) 4 to 3000 K; b) Tables 4, 5 - recommended values of $\rho$, $\lambda$ for AFML arc cast and NBS sintered W, respectively; c) uncertainty: in $\lambda$ is 2.5% at 300 K, decreasing to 0.7% at 200 K, 0.7% from 200 to 50 K increasing inversely with temperature to 1.5% at 4 K; in $\rho$ is 0.5%.

ANALYSIS
b) $\lambda = 1/(\alpha T^n + \beta^1 \rho_0/T) + AT/\rho\ [e^{-(\theta_1/T)^2} + Be^{-(\theta_2/T)^2}]$.

[16] Jun, C. K. and Hoch, M., Thermal Conductivity of Tantalum, Tungsten, Rhenium, Ta-10W, $T_{111}$, $T_{222}$, W-25 Re in the Temperature Range 1500 to 2800 K, Proceedings of the Sixth Thermal Conductivity Conference, 933-49 (Oct 19-21, 1966), Air Force Materials Lab., Wright-Patterson AFB, Ohio

PURPOSE
To report measurements on $\lambda$ for Ta, W, Re and Ta-10W, $T_{111}$, $T_{222}$ and W-25 Re alloys.

SPECIMEN
a) specimens 1,2,3: 2.5339, 2.4785, 2.0801 cm dia., 0.2999, 0.2714, 0.2700 cm thick, respectively/disks; c) /specimen 2 machined from specimen 1, specimen 3 machined from specimen 2; d) 99.998%; g) source: Fansteel Metallurgical Corp., density: specimens 1,2,3 = 18.89, 19.03, 19.23 g/cm$^3$, respectively.

APPARATUS
c) vacuum insulation.

DATA
a) specimen 1: 1513 to 1930 K, specimen 2: 1572 to 1905 K, specimen 3: 1836 to 2608 K; b) Table 7 - $\lambda$.

[17] Kannuluik, W. G., On the Thermal Conductivity of Some Metal Wires, Proc. R. Soc. London, Ser. A, 131, 320-35 (1931)

PURPOSE
To investigate λ for metals and alloys by an electrical steady state method.

SPECIMEN
a) 0.1022 cm dia./wire; c) annealing - specimen 1: 220 °C, specimen 2: 1300 °C; g) source: General Electric Co.

APPARATUS
a) direct electric heating; b) ice point, steambaths; c) $10^{-4}$ mm of Hg ($10^{-2}$ Pa) vacuum.

DATA
a) 273 to 286 K; b) Tables 4, 5 - λ, L/L data from Table 5, λ data points listed in TPRC data series; c) uncertainty: ±2%.

ANALYSIS
a) results disagree with Weber, S. (1917), Barratt, Winter (1914).

[18] Kannuluik, W. G., Eddy, C. E., and Oddie, T. H., The Thermal and Electrical Conductivities of Several Metals Between -18 °C and 100 °C, Proc. Roy. Soc. London, Ser. A, 141, 159-68 (1933)

PURPOSE
To extend observations of λ for metals from -18 °C to 100 °C.

SPECIMEN
a) specimen 1: 7.846 cm x 0.01053 $cm^2$, specimen 2: 7.940 cm x 0.01022 $cm^2$/rectangular, hexagonal bars respectively; b) single crystals; d) 0.001% Co, Cr, In and Os, each; g) specimen 1: axis in [100] direction, specimen 2: axis in [111] direction.

APPARATUS
a) direct electrical heating; b) ice point, steambaths; c) $10^{-4}$ mm of Hg ($10^{-2}$ Pa) vacuum.

DATA
a) 90.1 to 273 K; b) Table 2 - λ, ρ/ρ data points from Table 2, λ data points listed in TPRC data series; d) correction for radiative heat loss.

ANALYSIS
a) results agree with Grüneisen, E. and Goens, E., Z. Phys., 44, 615 (1927).

[19] Langmuir, I. and Taylor, J. B., The Heat Conductivity of Tungsten and the Cooling Effects of Leads Upon Filaments at Low Temperatures, Phys. Rev., 50, 68-87 (Jul 1, 1936)

PURPOSE
To obtain voltage and resistance measurements across a filament, thereby calculating $\lambda$ and the temperature distribution along the wire.

SPECIMEN
a) specimens 1, 2, 3: 25.82, 12.86, 5.87 cm long respectively, all specimens 0.00499 cm dia./wires; c) all tubes baked at 450 °C, filaments heated to 2000 K for 2 min., 2400 K for 4 h and 2800 K for 30 s; d) thoriated W filaments.

APPARATUS
a) direct electrical heating; b) $N_2$ bath; c) vacuum insulation.

DATA
a) 240 to 300 K; b) Table 8 - $\lambda$/data points listed in TPRC data series.

ANALYSIS
a) results agree with Barratt, T., Proc. Phys. Soc., London, 26, 347 (1914) and Kannuluik, W. G., Proc. Roy. Soc. London, Ser. A, 131, 320 (1931) 141, 159 (1933).

[20] Mendelssohn, K. and Rosenberg, H. M., The Thermal Conductivity of Metals at Low Temperatures. II. The Transition Elements, Proc. Phys. Soc., London, Sect. A, 65, 388-94 (1952)

PURPOSE
To measure $\lambda$ of transition elements at low temperatures.

SPECIMEN
a) 15 cm long; 1 to 2 mm dia./rod; b) polycrystalline; c) annealed; d) 99.99% W; g) source: Johnson, Matthey and Co.

APPARATUS
a) longitudinal; b) He gas thermometers.

DATA
a) 2 to 43 K; b) Fig. 2 - $\lambda$/data taken from TPRC data series; c) uncertainty: ±3%.

ANALYSIS
a) results agree with Hulm, J. K., Proc. Roy. Soc. London, Ser. A, 204, 98 (1950).

[21] Moore, J. P., Graves, R. S., Fulkerson, W., and McElroy, D. L., The Thermal Properties of Tungsten, Proceedings of the Fifth Thermal Conductivity Conference, Univ. of Denver, Vol. 2, V-G-1 - V-G-35 (1965)

PURPOSE
To present the temperature dependence of several physical properties of polycrystalline tungsten.

SPECIMEN
a) 3 in. (7.6 cm) dia., 5/16 in. (0.79 cm) dia. hole/disk; c) /machined from 3.5 in. (8.9 cm) dia. pressed and sintered powder billet which had been hot extruded at 1800 °C for 3 to 1 reduction; d) 99.98%; e) $\rho_{300}/\rho_4 = 35$; g) density: 19.077 g/cm$^3$.

APPARATUS
a) radial; b) annealed $Pt_{90}$ $Rh_{10}$ - Pt/calibrated at 3 standard melting points.

DATA
a) 323 to 1273 K; b) Table 2 - $\rho$, $\lambda$; c) uncertainty: ±1.5% at 1000 °C.

ANALYSIS
a) results agree with Langmuir, I. and Taylor, J. B., Phys. Rev. Z., 50, 68-87 (1936) and Tye, R. P., Nb, Ta, Mo and W, A. G. Quarrell, Ed., Elsevier Publishing Co., 169-79 (1961) between 300 and 600 K.

[22] Moore, J. P., McElroy, D. L. and Barisoni, M., Thermal Conductivity Measurements Between 78 and 340 K on Aluminum, Iron, Platinum, and Tungsten, Proceedings of the Sixth Thermal Conductivity Conference, Wright-Patterson AFB, Ohio, 737-78 (1966)

PURPOSE
To describe an apparatus which is capable of accurately measuring $\lambda$, $\sigma$, and S for metals between 78 and 340 K.

SPECIMEN
a) 5 to 8 cm long/rod; c) high purity: electron beam melted; d) 98%, radial: 99.98% W; e) high purity (RRR > 400), radial (RRR = 31.4), 98% (RRR = 4.1); f) radial ($\rho_0$ = 0.1593 μΩ·cm), 98% ($\rho_0$ = 1.560 μΩ·cm); g) density (g/cm$^3$): high purity: 19.29, radial: 19.077, 98% = 19.19.

APPARATUS
a) longitudinal; b) chromel-P and constantan thermocouples/from calibrated spools/thermocouples attached to specimen by discharge welding or epoxy, leads thermally grounded to guard cylinder; c) guard cylinder, 5 x 10$^{-7}$ mm of Hg (7 x 10$^{-5}$ Pa) mm vacuum.

DATA
a) high purity: 80 to 300 K, radial: 100 to 300 K; b) Table 4 - $\rho$, $\lambda$ (smoothed values); c) uncertainty: ±1.8%.

[23] Osborn, R. H., Thermal Conductivities of Tungsten and Molybdenum at Incandescent Temperatures, J. Opt. Soc. Am., 31, 428 (1941)

PURPOSE
To determine $\lambda$ of W, Mo in filament form.

SPECIMEN
a) (2.5 to 5.0) x $10^{-3}$ mm dia./wire; c) annealed at 2700 K for 2 h.

APPARATUS
a) direct electrical heating; b) disappearing filament optical pyrometer; c) vacuum sealed pyrex tube.

DATA
a) 1100 to 2000 K; b) Table 1 - $\lambda$, Fig. 3 - $\rho$/data points listed in TPRC data series.

ANALYSIS
a) results agree with Forsythe, W. E., J. Opt. Soc. Am., 24, 114 (1934).

[24] Powell, R. L., Harden, J. L., and Gibson, E. F., Low Temperature Transport Properties of Commercial Metals and Alloys. IV. Reactor Grade Be, Mo, and W, J. Appl. Phys., 31(7), 1221-4 (1960)

PURPOSE
To study the low temperature mechanical and transport properties of several reactor materials.

SPECIMEN
a) 13 mm long; 3.67 mm dia./rod; d) 97.9%; f) $\rho_0$ = 0.16 x $10^{-8}$ $\Omega$·m.

APPARATUS
a) longitudinal; b) Au-Co vs. Cu thermocouples; c) vacuum insulation.

DATA
a) 4 to 70 K; b) figure 1 - $\lambda$, figure 2 - $\rho$, figure 3 - L; d) correction for thermal contraction.

ANALYSIS
a) deNobel, J., Physica, 25, 261 (1957); 23, 349 (1957) values of $\lambda_g$ for single crystal W are three times larger than these results and his values below 20 K show no $T^2$ dependence as expected theoretically.

[25] Powell, R. W. and Tye, R. P., New Measurements on Thermal Conductivity Reference Materials, Int. J. Heat Transfer, 10(5), 581-96 (1967)

PURPOSE
To provide further data on $\lambda$ and $\rho$ of materials suggested for use as standard reference materials.

SPECIMEN
a) 10 cm long; 0.4 cm dia./rod; d) 99.99% W; e) RRR = 150; g) source: Johnson Matthey and Co.

APPARATUS
a) longitudinal, ingot Fe standard used for energy outflow measurements.

DATA
a) run 1: 300 to 700 K, run 2: 450 to 760 K, run 3: 400 to 1000 K;
b) figure 3, Table 6 (smoothed).

ANALYSIS
a) results agree with Laubitz, M. J., Can. J. Phys., 41 (1963) and Flynn, D. R. and Robinson, H. E., private communication by Laubitz, M. J.

[26] Sharma, J. K. N., Heat Conductivities Below 1 K I, Cryogenics, 7(3), 141-56 (1967)

PURPOSE
To determine if the anomalies found in $\lambda$ below 1 K represent a general behavior of metals.

SPECIMEN
a) /wire; b) polycrystalline; g) $\rho_{295}/\rho_{1.5}$ = 30, source: Lamp and Metals Ltd.

APPARATUS
a) longitudinal; b) carbon resistors/calibrated against heat sink temperature for each run.

DATA
a) 0.5 to 1.0 K; b) figure 9 - $\lambda$; c) uncertainty: ±2%; corrected for thermomolecular pressure.

ANALYSIS
a) comparison with Davey, G. and Mendelssohn, K., Phys. Lett., 7, 183 (1963).

[26A] Taylor, R. E., Thermal Properties of Tungsten SRM's 730 and 799. J. Heat Transfer, 100(2), 330-3 (1978)

PURPOSE
To compare λ results on sintered tungsten with previous results on arc-cast tungsten.

SPECIMEN
a) SRM 730, 99.98%; b) sintered; c) RRR = 75, density: 19.23 ± 0.05 g/cm$^3$.

APPARATUS
a) longitudinal.

DATA
a) 1300 to 2600 K; b) Table 3 - λ, ρ, L; c) corrected for thermal expansion; f) uncertainty: ±5% from 300 to 2000 K, ±8% above 2000 K.

ANALYSIS
b) results lie between NBS, TPRC values;
d) $\lambda(w/m\cdot K) = 0.144644 \times 10^{-8} T^3 \pm 0.08$ from 1200 to 3000 K.

[27] Timrot, D. L. and Poletskii, E., Use of Heating by Electron Bombardment to Investigate the Coefficient at Heat Conductivity in High Melting Point Alloys and Compounds, High Temp. (USSR), 1, 147 (1963)

PURPOSE
To study the thermophysical properties of solids at high temperatures.

SPECIMEN
a) /rod; d) 99.9+% W; g) 5 < length/dia. ratio < 6.

APPARATUS
a) electron bombardment; b) optical pyrometer; c) vacuum insulation.

DATA
a) 1200 to 3000 K; b) text (smoothed), figure 3 - λ/data points listed in TPRC data series; c) uncertainty: ±10%.

ANALYSIS
a) comparison with Powell, R. W. and Schofield, F. H., Proc. Phys. Soc., London, 51, 153 (1939); Worthing, A. G., Phys. Rev., 4, 6 (1914); Osborn, R. H., J. Opt. Soc. Am., 31, 428 (1941); Gumenyuk, V. S. and Lebedev, V. V., Fiz. Met. Metalloved., 11, 1 (1961).

[27A] Touloukian, Y. S., Powell, R. W., Ho, C. Y., and Klemens, P. G., Thermophysical Properties of Matter, Volume 1: Thermal Conductivity, Metallic Elements and Alloys, 68-81 (1970)

PURPOSE
To provide an extensive list of data for $\lambda$ of the metallic elements and alloys.

SPECIMEN
d) 99.99+%; f) $\rho_0 = 1.70 \times 10^{-9}$ $\Omega$·cm.

APPARATUS
a) not given.

DATA
a) 0 to 8500 K; b) Figure and Table 63R - $\lambda$, recommended values; c) uncertainty: ±3% near room temperature, ±3 to 8% at other temperatures; e) the values below 1.5 Tm are calculated to fit the experimental data by using n = 2.40, $\alpha' = 2.06 \times 10^{-5}$, and $\beta = 0.0696$.

[28] Trodahl, H. J., The Thermopower of Pure Tungsten Below 9 K, J. Phys. F, 3, 1972-6 (1973)

PURPOSE
To make measurements of S on a pure W crystal in order to identify electron-electron scattering effects.

SPECIMEN
a) 3 cm long; 3 mm dia./rod; b) single crystal; e) RRR = 16300; g) [110] axis along geometric axis, supplied by Materials Research Corp.

APPARATUS
a) longitudinal; b) matched Ge thermometers.

DATA
a) 0 to 9 K; b) figure 1 - $\lambda$.

ANALYSIS
a) comparison with Wagner, D. K., Garland, J. C. and Bowers, R., Phys. Rev. B, 3, 3141 (1971), and White, G. K. and Woods, S. B., Can. J. Phys., 35, 656 (1957).

[29] Van Witzenburg, W. and Laubitz, M. J., Magnetoresistances and the Phonon Conductivity of Metals, Can. J. Phys., 46(17), 1887-94 (1968)

PURPOSE
To measure the magnetoresistances of Cu, Ag, Au, and W.

SPECIMEN
a) 1.6 mm dia./wire; b) annealed in vacuum at 1620 K for 2 h; d) 99.95% W; e) RRR = 46.6; f) $\rho_0$ = 0.11 μΩ·cm; g) source: United Min. Chem. Corp.

APPARATUS
a) longitudinal; b) Pt resistance thermometers; c) radiation shield.

DATA
a) 80 to 150 K; b) Table 4 - λ; c) uncertainty: ±3%; d) correction applied to temperature derived from Pt thermometers.

ANALYSIS
a) compared with Fulkerson, W., private communication (1968); b) concludes that lattice conductivity accounts for 40% at λ for the temperature range investigated.

[30] Wagner, D. K., Lattice Thermal Conductivity and High-Field Electrical and Thermal Magnetoconductivities of Tungsten, Phys. Rev. B, 5, 336-47 (1972)

PURPOSE
To investigate the temperature dependence of  and λ for W in a strong magnetic field to provide further information about low temperature scattering mechanisms.

SPECIMEN
c) specimen spark cut from zone-refined crystal; e) original crystal: $\rho_{299}/\rho_0$ 63000; g) rod axis parallel to [110] direction.

APPARATUS
a) longitudinal, H oriented normal to rod axis along [001] direction; b) matched carbon resistors/calibrated against stardard Ge resistance thermometer; c) adsorbent, vacuum insulation.

DATA
a) 1.8 to 6.5 K; b) figures 1,2 - $H^2/\rho xx$, $H^2/WxxT$ respectively/ρ, H (kG) for runs 7-13 = 2.66, 5.32, 7.98, 10.6, 13.3, 16.0, 18.6.

ANALYSIS
a) results agree with Long, J. R., Phys. Rev. B, 3, 2476 (1971).

[31] Wagner, D. K., Garland, J. C., and Bowers, R., Low Temperature Electrical and Thermal Resistivities of Tungsten, Phys. Rev. B, 3, 3141 (1971)

PURPOSE
To study the temperature dependence of $\rho$ and WT in a number of high purity W single crystals.

SPECIMEN
a) W-3, W-5, W-8: 1.5 mm dia., W-4: 1.0 mm dia., W-7: 3.0 mm dia./rods; b) single crystals; c) electron beam zone melted; f) $\rho_0$ (W-3) = 1.231 x $10^{-10}$ $\Omega$·cm, $\rho_0$ (W-4) = 1.780 x $10^{-10}$ $\Omega$·cm, $\rho_0$ (W-5) = 5.724 x $10^{-10}$ $\Omega$·cm, $\rho_0$ (W-7) = 0.566 x $10^{-10}$ $\Omega$·cm, $\rho_0$ (W-8) = 0.695 x $10^{-10}$ $\Omega$·cm; g) all oriented to [110].

APPARATUS
a) longitudinal; b) carbon resistance thermometers/calibrated against standard Ge resistance thermometer; c) adsorbent, vacuum insulation.

DATA
a) 0 to 6 K/< 30 mK; b) figure 3 - $(WT-\rho_0/L_0)$, figure 2 - $(\rho-\rho_0)$; c) uncertainty: ±1% for 1.5 mm dia., ±8% for 3.0 mm dia.

ANALYSIS
a) L results agree with Bennett, A. J. and Rice, M. J., Phys. Rev., 185, 968 (1969) and Rice, M. J., Phys. Rev. Lett., 20, 1439 (1968), but are significantly below Herring, C.

[32] Wheeler, M. J., Thermal Diffusivity at Incandescent Temperatures by a Modulated Electron Beam Technique, Br. J. Appl. Phys., 16, 365 (1965)

PURPOSE
To assess the performance of an apparatus by means of measuring K and $\lambda$ of Pt, Ta, Mo, W.

SPECIMEN
a) 1.5 mm thick/disk; c) /cut from swaged rod; d) 99.5% W; g) source: General Electric Co., Osram Lamp Works.

APPARATUS
a) periodic heat flow; b) optical pyrometer; c) vacuum insulation.

DATA
a) 1200 to 3000 K; b) Fig. 10/data points listed in TPRC data series; c) uncertainty: ±5%; d) corrected for losses in viewing window of pyrometer, spectral emissivity of specimen.

ANALYSIS
a) $\lambda$ results agree with Vines, R. F. (1941), Malter, L. and Langmuir, D. B., Phys. Rev., 55, 745 (1939), Worthing, A. G., Phys. Rev., 28, 190 (1926), and Worthing, A. G. and Forsythe, W. E., Astrophys. J., 61, 147 (1925).

[33] White, G. K. and Woods, S. B., Low Temperature Resistivity of the Transition Elements: Cobalt, Tungsten, and Rhenium, Can. J. Phys., 35, 656 (1957)

PURPOSE
To report experimental values of $\rho$ and W for Co, W, Rh.

SPECIMEN
a) Wlb: 4 mm dia./rod; c) annealed at 1350 °C for several hours in vacuum, then kept at 600 °C for several more hours.; d) 0.01% Mo, traces Fe, Sl, Cu; f) $\rho_0 = 3.15 \times 10^{-8}$ Ω·cm; g) source: Johnson, Matthey and Co.

APPARATUS
a) longitudinal; b) He gas thermometers; c) radiation shield, thermometers Au plated to reduce radiation transfer.

DATA
a) 2 to 127 K; b) figure 2 - $\lambda$/data listed in TPRC data series; c) uncertainty: ±1%.

ANALYSIS
a) comparison with Rosenberg, H. M., Philos. Trans. Roy. Soc. London, 247, 441 (1955), DeHaas, W. J., and deNobel, J., Physica, 5, 449 (1938), and Kannaluik, W. G., Proc. Roy. Soc. London, Ser. A, 141, 159 (1933).

NBS-114A (REV. 2-8C)

| U.S. DEPT. OF COMM. BIBLIOGRAPHIC DATA SHEET (See instructions) | 1. PUBLICATION OR REPORT NO. NBSIR 84-3007 | 2. Performing Organ. Report No. | 3. Publication Date June 1984 |
|---|---|---|---|

4. TITLE AND SUBTITLE

THERMAL CONDUCTIVITY OF ALUMINUM, COPPER, IRON, AND TUNGSTEN FOR TEMPERATURES FROM 1 K TO THE MELTING POINT

5. AUTHOR(S)

J. G. Hust and A. B. Lankford

6. PERFORMING ORGANIZATION (If joint or other than NBS, see instructions)

NATIONAL BUREAU OF STANDARDS
DEPARTMENT OF COMMERCE
WASHINGTON, D.C. 20234

7. Contract/Grant No.

8. Type of Report & Period Covered

9. SPONSORING ORGANIZATION NAME AND COMPLETE ADDRESS (Street, City, State, ZIP)

10. SUPPLEMENTARY NOTES

☐ Document describes a computer program; SF-185, FIPS Software Summary, is attached.

11. ABSTRACT (A 200-word or less factual summary of most significant information. If document includes a significant bibliography or literature survey, mention it here)

Literature data on the thermal conductivity of commercially pure aluminum, copper, iron, and tungsten specimens have been collected, coded, critically analyzed, and correlated with analytical techniques based on theoretical and empirical equations. The resulting functions are presented and used to generate tables and graphs of thermal conductivity as a function of temperature and residual resistivity ratio (RRR). An annotated bibliography of references is included. Discussions are included on the variations in thermal conductivity caused by chemical impurities, physical defects, size effects, and magnetic fields. Smoothed values are presented for temperatures from 1 K to near the melting point and for a large range of RRR values.

12. KEY WORDS (Six to twelve entries; alphabetical order; capitalize only proper names; and separate key words by semicolons)

aluminum; copper; electrical resistivity; iron; Lorenz ratio; residual resistivity ratio; thermal conductivity; tungsten

13. AVAILABILITY

☒ Unlimited

☐ For Official Distribution. Do Not Release to NTIS

☐ Order From Superintendent of Documents, U.S. Government Printing Office, Washington, D.C. 20402.

☒ Order From National Technical Information Service (NTIS), Springfield, VA. 22161

14. NO. OF PRINTED PAGES 262

15. Price $22.00